Ageing through reproductive death in *Caenorhabditis elegans*

Institute of Healthy Ageing and department of Genetics, Evolution and Environment, University College London

Carina Carla Kern

Genetics and Evolutionary Biology

PhD Thesis

Supervisor: David Gems

November 2020

I, Carina Kern, confirm that the work presented in this thesis is my own. Where information has been derived from other sources, I confirm that this has been indicated in the thesis.

……

Abstract

The nematode worm *Caenorhabditis elegans* has emerged as one of the premier model systems for ageing research. Its use has led to the discovery of many biological mechanisms of ageing conserved across species, including acceleration of ageing by insulin/IGF-1 signalling (IIS) and germline signalling. Ageing in *C. elegans,* however, is unusual in terms of the severity and early onset of senescent pathology, particularly affecting organs involved in reproduction. For example, in post-reproductive hermaphrodites, intestinal biomass is converted into yolk leading to intestinal atrophy and yolk steatosis. While late yolk production has long been viewed as futile, is it possible that it somehow promote fitness? Results in this thesis show that post-reproductive *C. elegans* hermaphrodites vent yolk that can be consumed by larvae, promoting their growth. Thus, post-reproductive mothers can contribute to reproductive fitness by converting their biomass into milk, suggesting that intestinal atrophy is a cost of lactation. This type of massive reproductive effort involving biomass repurposing leading to organ degeneration is characteristic of semelparous organisms (i.e. that exhibit only a single reproductive episode) ranging from monocarpic plants to Pacific salmon where it leads to rapid death (reproductive death). Results also show that lactation occurs in other hermaphroditic *Caenorhabditis* nematode species but not in females. Moreover, the latter do not exhibit intestinal atrophy or steatosis, and are longer lived suggesting that they do not undergo reproductive death. Furthermore, germline ablation strongly increases lifespan in hermaphrodites but not females; similarly, blocking sexual maturation e.g. by gonadectomy can greatly increase lifespan in other organisms that undergo reproductive death. IIS which accelerates *C. elegans* ageing is also shown to promote lactation. These results suggest that *C. elegans* hermaphrodites exhibit reproductive death, suppression of which increases lifespan. This has major implications in terms of what one can learn about human ageing from *C. elegans.*

Impact Statement

Findings in this thesis present an altered picture both of *C. elegans* as a model for ageing research, and of ageing research more broadly. Results demonstrate that lifespan in *C. elegans* is not limited by ageing as occurs in most higher animals, but rather by a form of suicidal reproductive effort leading to early death (reproductive death) that is typical of semelparous organisms such as Pacific salmon. These findings have major implications. *C. elegans* is one of the most commonly used model organisms in ageing research. The great interest in *C. elegans* in the ageing field particularly stems from the discovery around 30 years ago that single gene mutations can dramatically increase its lifespan. Ageing had previously been viewed as a relatively immutable process of passive entropic deterioration; the discovery, however, suggested the existence of central mechanisms governing the entire process of ageing that were responsive to intervention. Ageing is conserved across the animal kingdom, and arguably so too should be the mechanisms governing it. In other words, findings should inform understanding of human ageing, opening up the possibility of intervening in and slowing human ageing: the main cause of disease and death worldwide.

However, if *C. elegans* is semelparous and undergoes reproductive death, as shown here, suppression of this provides a potential explanation for the unusually large magnitude of lifespan increases observed. In certain respects this explains away the mystique of *C. elegans* ageing. Moreover, it argues against the existence of core mechanisms of ageing as a whole in iteroparous organisms amenable to manipulation to produce dramatic deceleration of ageing. Ageing in iteroparous organisms such as humans is often viewed as a completely different process to reproductive death. These results therefore raise the question: Is *C. elegans* an unsuitable model for studying ageing more broadly, like Pacific salmon and other semelparous animals? However, semelparous reproductive death appears to result from grossly exaggerated versions of programmatic mechanisms present in iteroparous species. Thus, the relatively small increases in iteroparous lifespan following interventions similar to those that greatly extend *C. elegans* lifespan reflect suppression of weaker programmatic determinants of ageing that are only a minor subset of the causes of ageing in iteroparous organisms. Arguably, therefore, *C. elegans* is a good model for understanding programmatic mechanisms of ageing that lead to senescent multimorbidity that are universal across metazoan organisms, in a conveniently exaggerated and relatively pure form. Thus, the impact of these results is a transformation in our understanding of *C. elegans* as an ageing model and of ageing more broadly.

Acknowledgements

I am indebted to many people who have helped me throughout my PhD.

Past and present members of the Gems Lab, Institute of Healthy Ageing and collaborators, including: StJohn Townsend, Nancy Hui, Shivangi Srivastava, Hongyuan Wang, Nyi Than, Mike Cao, John Labbadia, Marina Ezcurra, Dominik Maczik, Evgeniy Galimov, Victor Konstantellos, Victoria Tse, Thanet Sornda, Ann Gilliat, Jürg Bähler, Lazaros Foukas, Antoine Salzmann, Graham Taylor, Nigel Rendell, Mark Turmaine, Giovanna Vinti, Kerri Kinghorn, Kuei-Ching Hsiung, Teresa Niccoli, Filipe Cabreiro as well as my second supervisor, Seirian Sumner. Without them this work would have not been possible. They have also provided invaluable advice and friendship during the course of my PhD.

My family and friends who have always encouraged and supported me.

The largest debt of gratitude is owed to my supervisor David Gems. He has been an excellent mentor and friend. His guidance has not only made this a thought provoking and insightful journey, but has also shaped the way I think. Any future achievements in my scientific career will in large part be because I had him as a teacher.

Table of contents

List of figures and tables

CHAPTER 1: INTRODUCTION

CHAPTER 2: METHODS

CHAPTER 3: *C. ELEGANS* PROVIDE MILK FOR THEIR YOUNG

CHAPTER 4: *C. ELEGANS* HERMAPHRODITES UNDERGO SEMELPAROUS REPRODUCTIVE DEATH

Glossary

Adaptive death: Synonymous with programmed organismal death. Here death of an individual is a selected trait, providing a direct benefit in terms of inclusive or group fitness (Lohr et al., 2019).

Androdioecious: Where adults are male or hermaphrodites (as opposed, in the context of this thesis, to male or female).

Antagonistic pleiotropy (AP): Where action of a given gene is both beneficial and detrimental to fitness. If the latter occurs later in life and is therefore subject to weaker selection, such a gene may be favoured by natural selection, and promote ageing (Williams, 1957).

Biological constraint: A property of organisms and/or their ecology that prevents the evolution of traits that would increase fitness. It can occur for example where two or more traits are interlinked in a way that precludes the maximisation of fitness in both at the same time.

Coat-tails hypothesis (New term): This proposes that quasi-programmes more easily evolve in selection shadows created by costly programmes (on their coat-tails).

Costly programme (New term): A biological programme that simultaneously promotes fitness and incurs a cost in terms of pathological changes to tissues or organs where the programme is executed. One form of programmatic mechanism involving hyperfunction by which AP causes senescence (Gems et al., 2020) (cf. quasi-programme).

Disposable soma: Theory proposing that natural selection favors investment of limited resources into reproduction rather than somatic maintenance, accelerating damage accumulation and, therefore, senescence (Kirkwood, 1977).

Gonochoristic: Where adults are male or female (as opposed, in the context of this thesis, to male or hermaphrodite).

Hypofunction: Lack of optimum biological design resulting in pathology due to the absence of a particular function (Maklakov and Chapman, 2019).

Hyperfunction: Where wild-type gene function actively leads to senescent pathology, as opposed to passive random damage or wear and tear (Blagosklonny, 2006).

Iteroparous: Where multiple reproductive cycles can occur over the course of a lifetime.

Non-regulated ageing (New term): That part of the process of senescence not involving plastic programmatic mechanisms and/or under global hormonal control (Gems et al., 2020) (cf. regulated ageing).

Primary constraint (New term): The evolution of trade-offs by AP can be a multi-step process deriving from initial, primary constraints, and then further evolutionary change involving additional, secondary constraints.

Programmed ageing: Senescence caused by a relatively ordered series of biological processes that promotes fitness via inclusive fitness or group fitness.

Programmatic ageing: Where complex biological processes contributes to senescence, but not necessarily to fitness (cf. quasi-programmes, costly programmes).

Protandry: The form of gametogenesis in hermaphroditic organisms where male gametes are formed first and then female gametes. *C. elegans* hermaphrodites generate sperm and then oocytes. Sperm are used for self-fertilisation, and when self sperm stocks are depleted, reproduction ceases.

Quasi-programmed ageing: Senescence caused by a relatively ordered series of biological processes that does not promote fitness; may occur due to futile run-on of wild-type programmes that promote fitness earlier in life (Blagosklonny, 2006).

Regulated ageing (New term): That part of the process of senescence that is under hormonal control (e.g. GH/IIS/mTOR and steroid hormones) and involving programmatic mechanisms (Gems et al., 2020) (cf. non-regulated ageing).

Reproductive death: A form of suicidal reproductive effort found in some semelparous species (e.g. Pacific salmon, monocarpic plants). Here, reproductive maturity triggers the rapid development of lethal pathologies and fast senescence coupled to reproductive success (Finch, 1990b).

Run-on: Futile continuation of gene function or processes in later life, leading to pathology (de la Guardia et al., 2016) (cf. quasi-programme).

Secondary constraint (New term): Secondary constraints influence the shape of the trade-off function (c.f. primary constraint).

Semelparous: Organisms with a single reproductive episode before death. Also used to denote semelparity with reproductive death.

Senescence: The overall process of deterioration with age or the resulting pathological condition (not to be confused with cellular senescence, which is a particular form of cell cycle arrest affecting some vertebrate cell types). Although ageing has several meanings, in the biological context it is usually synonymous with senescence.

Source-to-sink biomass conversion: Resource remobilisation where autophagic processes break down cellular constituents in one tissue/organ to provide resources for another (cf. costly programme).

Yolk milk (New term): Yolk vented by hermaphroditic nematodes into their local vicinity for the purpose of provisioning larvae, in a form of primitive nursing.

Chapter 1: Introduction

1.1 Ageing is pathological

When encountering a disease, a natural question to ask is: is there a cure? By contrast, we accept ageing (i.e. senescence, from the Latin *senex* for old) as a normal and inevitable process that we must all go through. As defined by Alex Comfort, senescence is ‘a decrease in viability and an increase in vulnerability’ and ‘an increasing probability of death with increasing chronological age’ (Comfort, 1979) (for simplicity, from here on ageing will be used

synonymously with senescence, not to be confused with cellular senescence as defined by Leonard Hayflick).

The fact that the very word ‘senescence’ refers to deterioration resulting in death implies that ageing is akin to disease and from a biological perspective senescence appears to be a form of complex disease syndrome. Descriptions of ageing, however, range from ‘part of the natural order’ to ‘wholesome’ (Kass, 1983; Callahan, 1994; Fukuyama, 2002), views rooted in classical (Roman) medical philosophy and inherited via medieval medicine (Gems, 2015), and according to which ageing is not appropriate for medical attention. Is our understanding of ageing stuck in the dark ages? It is easy to see why such views persist. When faced with an inevitable tragedy where the end is known from the beginning, it is comforting to find a purpose in it.

A clearer understanding of whether ageing is pathological will help determine whether intervention is desirable as well as provide invaluable insights into what could be causing ageing. A step towards the former is answering two questions asked by the philosopher Arthur Caplan: Does ageing have a purpose? And: Is it distinct from pathology? [Or put another way, ‘Is disease distinct from ageing?’ Pathology and disease will be used interchangeably for simplicity as precisely defining these terms is the subject of much philosophical debate that lies beyond the scope of this thesis] (Caplan, 1992; Caplan, 2005; Gems, 2015).

1.1.1 Does ageing have a purpose?

Contrary to popular belief ageing is not a conserved characteristic of all life; ageing is neither inevitable nor universal in the animal kingdom and longevity is not immutable. Certain complex organisms are found to show no increase in mortality rate with age, including lobsters, rockfishes, tortoises and mammals like the naked mole-rat (Beltran-Sanchez & Finch, 2018). Still others, like the fresh-water polyp *Hydra vulgaris* (Martínez, 1998), present with no observable signs or symptoms of ageing. Moreover, numerous studies in model organisms have robustly shown that maximum lifespan can be extended through interventions such as dietary restriction. If ageing is not an unavoidable and immutable feature of organisms, is its persistence in the animal kingdom the result of it conferring some evolutionary benefit, i.e. is it an adaptation?

Ageing is maladaptive for the individual undergoing it, and so at face value it does not fit the definition of an evolved trait. Alfred Russel Wallace was the first to propose this by echoing older ideas of the Roman philosopher Lucretius in his De Rerum Natura (On the Nature of Things) (Bailey, 1947). His ideas were supported and developed by the influential biologist August Weismann into a theory of programmed death: the purpose of ageing is to weed out the

weak and worn-out elderly, allowing limited resources to be freed up for the younger and healthier members of the population (Weismann, 1882; Weismann, 1889).

There are two problems with this theory, however. First, as noticed by Weismann himself, this hypothesis seeks to explain the problem of ageing by ageing itself and so entails circular reasoning (Comfort, 1979; Austad, 1997, p.55). The second problem is that the fitness cost of programmed death to individuals is predicted to exceed the inclusive fitness benefits. Long-lived individuals are expected to leave more offspring than short-lived ones; as articulated by the evolutionary biologist Ernst Mayr: 'the object of natural selection is first and foremost the individual' (Mayr, 1997).

Evolutionary biologists now generally reject the view that ageing is an adaptation (Haldane, 1941; Medawar, 1952; Williams, 1957). However, possible exceptions include organisms that exist as compact (viscous) colonies of isogenic individuals where the distinction between an individual and a colony of individuals is blurred (Galimov et al., 2019; Lohr et al., 2019; Gems, et al., 2020). In such organisms, such as the yeast *Saccharomyces cerevisiae*, death could increase inclusive fitness in a manner analogous to programmed cell death in multicellular metazoans. These exceptions aside, ageing is not an adaptation, and has no purpose.

1.1.2 Is ageing distinct from disease?

Here two possibilities are (i) that there is no distinction between ageing and disease; or (ii) that ageing itself is not pathological and is merely associated with an increased risk of diseases like cancer and Alzheimer's, which we should focus on treating without interfering with the central ageing process.

Caplan concluded that (ii) is incorrect, reasoning that the mechanisms proposed to result in ageing are similar to those known to underlie many disease processes (Caplan, 1992; Caplan, 2005). In support of this, treatments that extend lifespan in animal models do so through preventing or delaying pathology, whether that pathology is caused by ageing or by something else. Moreover, an extended lifespan is invariably accompanied by an extended youth-span (Podshivalova, et al., 2017; Kenyon, 2010; Bartke et al., 2013). A common misconception associated with possibility (i) which this disproves is the 'Tithonus error': the fear of living longer while enduring an ever-worsening debilitated and demented state (Williams, 1999; Pletcher, 2002). The name originates from the story of Tithonus in Greek mythology to whom Zeus granted eternal life but, cruelly, not eternal youth. With time the unfortunate Tithonus grew increasingly decrepit but could never die.

To summarise, the conceptual division between ageing-related diseases and an underlying non-pathological ageing process is a false one, and ageing has as little purpose as any disease such as tuberculosis or typhus which we readily treat. From a biological perspective ageing manifests as the accumulation of a set of pathologies with age (Gems, 2014; Kulminski, et al., 2007; Rockwood & and Mitnitski, 2007; Gems, 2015). Some ageing pathologies limit lifespan, such as cancer or cardiovascular disease, and some do not, such as the greying of hair and wrinkling of skin (Gems, 2015). As one is now dealing with the idea of preventing individual pathologies that include the likes of cancer and Alzheimer's disease, the question of intervention has a clear answer: no pathology is desirable and treatment for all senescent pathologies (all ageing) is as right and good as any disease treatment.

1.2 Is ageing one process or many?

Diseases of ageing are highly diverse, differing from one another in terms of tissues affected, severity and progression. Moreover, they appear to different extents and at varying rates in different individuals. Is increasing risk of presentation with time the only factor linking them? This was claimed by Richard Doll and Richard Peto in their essay 'There is no such thing as ageing' (Peto & Doll, 1997). The fact that ageing-associated pathologies tend to arise in the same part of the life span does not prove that they have a common underlying cause which we can term 'ageing'. As they argue: 'If we want to understand the mechanisms by which lung cancer arises we should study these and not the mechanisms of some other age-related phenomenon such as the menopause' (Peto & Doll, 1997).

At the opposite end of the spectrum is the opinion that there could be a central cause of ageing, originating from the fact that certain interventions can cause large increases in both health-span and lifespan in model organisms (Kenyon, 2010; Bartke et al., 2013). For instance, up to a 10-fold increase in lifespan has been achieved in the microbiverous nematode *C. elegans* (Ayyadevara et al., 2008). This has led to the belief that if one were able to intervene in the central ageing process in humans, all ageing-associated diseases could be prevented (Holliday, 1996; Butler, et al., 2008).

To understand how, and if, diverse ageing-associated pathologies arise from central mechanisms, one can find clues in the results of long-lived animal model studies (Gems, 2015). Clue one: lifespan extension is mostly accomplished via the suppression of the activity of biological pathways, achieved by genetic manipulation or use of drugs in mammals (Migliaccio, 1999; Holzenberger, 2003; Harrison, et al., 2009), *C. elegans* (Friedman, 1998; Kenyon, 1993;

Kimura, 1997) and the fruit fly *Drosophila melanogaster* (Tatar, 2001; Bartke, 2001). This tells us that, oddly, the activity of certain normal biological pathways contribute to ageing pathology (Blagosklonny, 2006; Blagosklonny, 2008). Clue two: no intervention causes an indefinite lifespan in the models, i.e. they all die eventually (Blagosklonny, 2008). Clue three: suppression of two or more life-limiting biological pathways can sometimes result in additive effects (Kenyon, 2010).

Together, this implies that: (i) there is no one central mechanism resulting in ageing, and instead (ii) the immediate ageing-pathologies organisms tend to die of originate from the action of a small, finite number of wild-type biological pathways (Gems, 2015). This is reconcilable with the observation by Doll and Peto that: 'some (age-related phenomena) will probably have part or all of their mechanisms of origin in common, but some may not'. Based on these differing views, several alternative models of how ageing mechanisms translate to ageing pathology can be drawn (Figure 1.1, taken from (Gems, 2015)). Based on current knowledge, the most plausible scenario is, arguably, D. Here distinct mechanisms exist causing different senescent pathologies/diseases, but some mechanisms cause multiple pathologies (or multimorbidity), explaining how suppression of a single pathway can lead to a substantial extension of youthspan and lifespan, as is experimentally observed (Gems, 2015).

While a single central ageing process is unlikely, it remains possible that the vast majority of different ageing mechanisms can be understood as resulting from expression of a limited number of broad pathophysiological principles (Gems and Kern, 2021). Similarly, infectious diseases differ greatly in their specific aetiologies, e.g. tuberculosis vs rabies, progression, severity, and symptoms yet all originate from infectious pathogens.

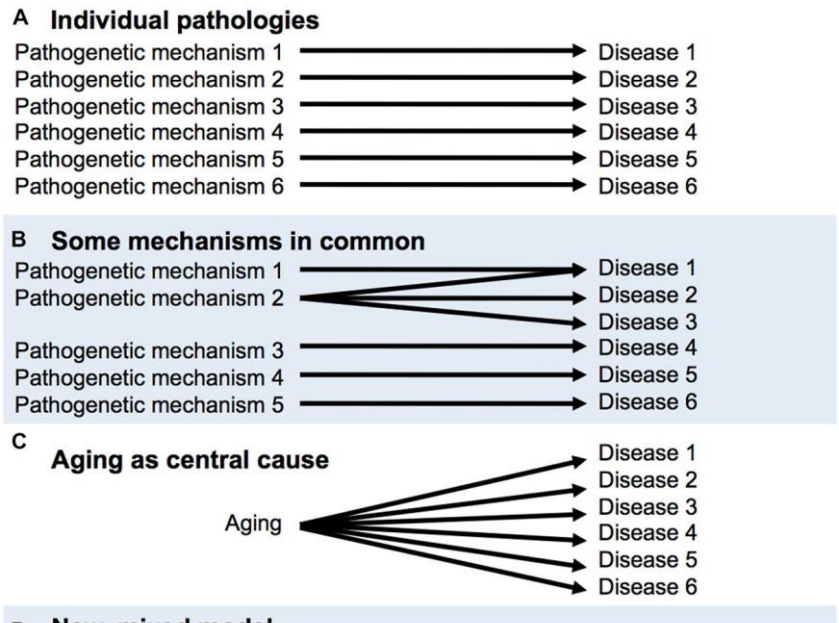

FIGURE 1.1. Ageing as a cause of age-related disease: different models. (A) There is no ageing process, only individual diseases of ageing. **(B)** A few diseases of ageing may have shared mechanisms. **(A,B)** Derived from (Peto and Doll, 1997). **(C)** A central ageing process (e.g. molecular damage accumulation due to inadequate somatic maintenance) causes all diseases of ageing. **(D)** Mixed model, based on recent findings and concepts. Some pathways promote many pathologies (senescent multimorbidity), including a number that limit healthspan and lifespan. But this does not mean that they control the ageing process, only part of it. Arguably, D is more realistic than A-C. Reproduced from (Gems, 2015).

1.3 The need for a simple model to make sense of a complex process

Mechanisms of ageing in humans are masked by our immense complexity, including a great number of specialised and interconnected cells, tissues, organs and systems. Due to this, simple short-lived animal models are invaluable and provide us with the possibility of fully understanding ageing in them. One such commonly used model is the nematode *C. elegans,* which is inexpensive to maintain and easy to study. Understanding the primary causes of ageing in *C. elegans* should help us understand fundamental principles of ageing as an overall process that will aid in unravelling the mysteries of human ageing, and will be the focus of this thesis.

1.3.1 Basic background: *C. elegans* anatomy, reproductive strategy and life cycle

C. elegans has a simple body plan with relatively little compartmentalisation of function (Figure 1.2, taken from (Herndon, et al., 2017)). For example, the function of the liver, gastrointestinal tract, and adipose tissue are all performed by the intestine in the worm (McGhee, 2007). Along with the intestine, the pharynx, gonad and uterus form the main inner organs (Figure 1.2). The different tissues are surrounded by a pseudocoelomic space filled with fluid to keep

them under an internal hydrostatic pressure. The outer body wall consists of the cuticle, hypodermis, excretory system, neurons, and muscles (Figure 1.2).

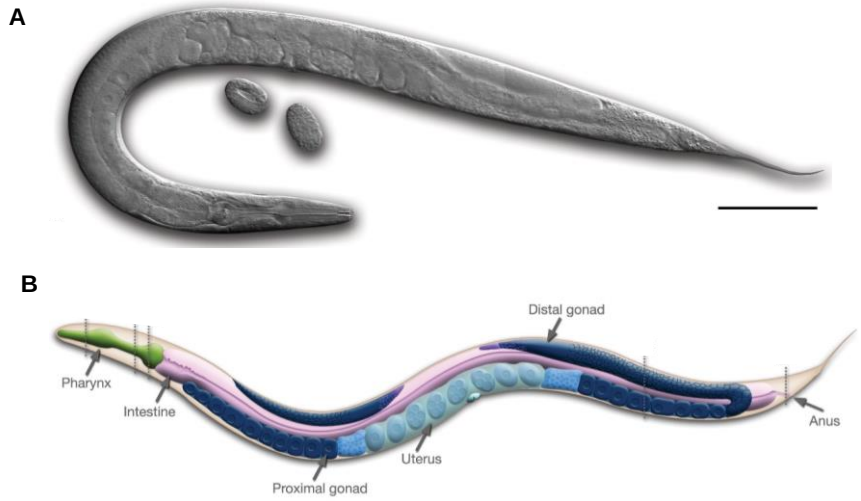

FIGURE 1.2. *C. elegans* anatomy. (A) Nomarski image of an adult hermaphrodite, left lateral side. Scale bar 0.1 mm. Similar to other nematodes, the body is unsegmented, cylindrical in shape and tapered at the ends. **(B)** Schematic showing anatomy of an adult *C. elegans* hermaphrodite, left lateral side. The intestine is composed of 20 large cells arranged around a central lumen with a rectal valve at the end. The pharynx at the top of intestine contains a hard chitin based grinder for both mechanical digestion of bacteria which the worms feed on as well as to prevent live pathogens from entering the intestine. The outer cuticle of the worm is also formed by chitin for protection, secreted by the underlying hypodermis. Body musculature is striated and is attached to this hypodermis forming long longitudinal strips, contraction and relaxation of which allows for the sinusoidal movement of the worm (Riddle, et al., 1997). Muscles in the pharynx, vulva and excretory system are non-striated (Altun & Hall, 2009). The nervous system of the worm consists of a small number of neurons; in the post mitotic adult this is divided into the somatic nervous system made up of 282 neurons and the pharyngeal nervous system containing 20 neurons. Reproduced from (Altun & Hall, 2009).

C. elegans is androdioecious (males and hermaphrodites), primarily existing as protandrous hermaphrodites that make and store sperm prior to switching to egg-laying. The occasional presentation of males in hermaphroditic populations is rationalised as a necessary means to obtain favourable recombinant genotypes (Crnokrak & Barrett, 2002; Lande, et al., 1994) (Figure 1.3, taken from (Altun & Hall, 2009)).

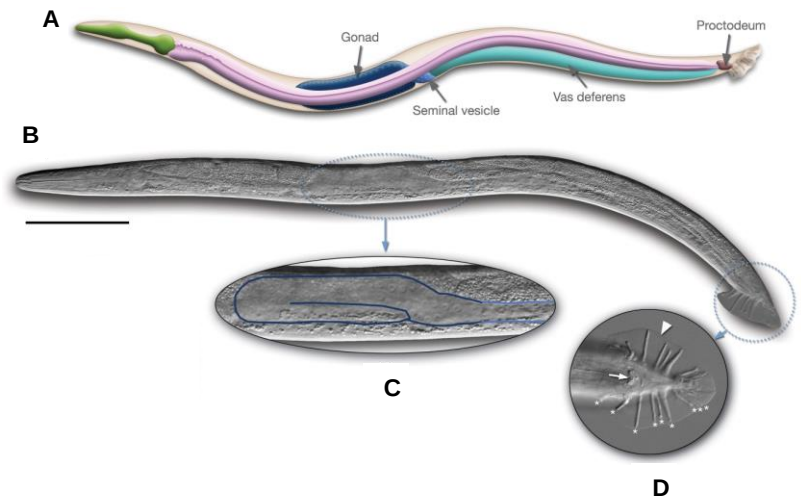

FIGURE 1.3. *C. elegans* male. (A) Schematic drawing of anatomical structures, left lateral side. Males are thinner and shorter, with gonads consisting of a single J-shaped arm. Hermaphrodites contain 5 pairs of autosomal chromosomes and a pair of sex chromosomes (XX), while males contain the same autosomal chromosomes but only have one sex chromosome (XO) arising via X chromosomal nondisjunction at a rate of around 0.01% (Hodgkin, et al., 1979). Although males mate with hermaphrodites to produce a 1:1 ratio of male and hermaphrodite cross-progeny, as additional hermaphrodites are almost always produced by selfing, reproduction is skewed towards hermaphroditism. **(B)** Nomarski image of an adult male, left lateral side. Scale bar 0.1 mm. **(C)** The unilobed distal gonad of the animal in B is shown as enlarged. **(D)** The adult male tail with copulatory apparatus for transfer of sperm at the end, ventral view. Arrow: cloaca; arrowhead: fan. Rays on tail 1-9 are labelled with asterisks. Reproduced from (Altun & Hall, 2009).

The hermaphrodite reproductive system is simple, with a clear delineation between germline cells and the somatic gonad (Figure 1.4, taken from (Lints & Hall, 2009)). One oddity of the system is hermaphrodites can lay as many as 100 excess oocytes, almost as much as the whole biomass of the mother (Ward and Carrel, 1979); sex-allocation theory applied to hermaphrodites predicts that self-fertilizing individuals will invest enough resources into male function (i.e. sperm production) and reproduction to allow for fertilisation of all ova (Charnov, 1982). Given the rare occurrence of males in the wild (reviewed (Schulenburg & Félix, 2017)), the reason for the additional investment into unfertilised oocyte production is an old puzzle.

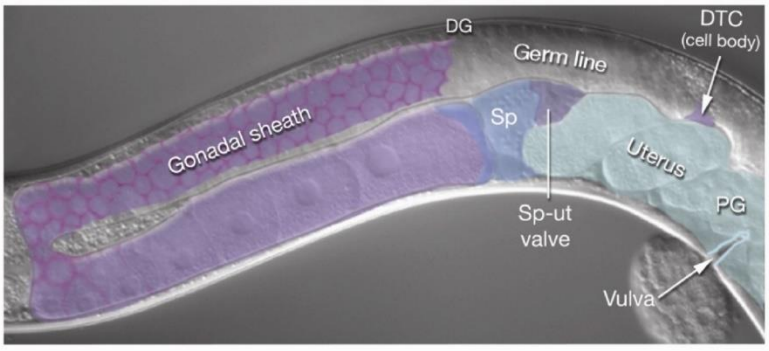

GURE 1.4. *C. elegans* reproductive system. Nomarski image of an adult anterior gonad arm, lateral view. The reproductive system consists of two gonad arms that run along either side of the central intestine. The somatic gonad refers to the non-germ-line component of each arm and is made up of five tissues types: distal tip cells (DTCs) with one large cell located at the start of each gonad arm that act as leader cells for gonadal arm elongation during development as well as promote mitosis and/or inhibit meiosis of the germ cells during development and in the adult, gonadal sheath, spermatheca (Sp) where sperm are made stored for oocyte fertilisation, spermatheca-uterine valve

(Sp-ut), and the uterus. All cells of the somatic gonad are derived from two founder cells, Z1 and Z4, that are present in the L1 gonad primordium. Germ cells are derived from Z2 and Z3 founder cells. In particular, the sheath and DTC play a critical role in the development and organisation of the germ line (Kimble & White, 1981; Hall, et al., 1999). The extent and location of mature somatic gonad tissues are indicated by the colour overlay. Magnification, 400x. PG: posterior gonad; DG: distal gonad. Reproduced from (Lints & Hall, 2009).

The main benefit of hermaphroditism is that it facilitates a rapid boom-and-bust resource depletion strategy to overgrow gonochoristic (male and female) competitors, as individuals do not have to lose valuable time finding mates. Also, self-fertilisation allows every individual in a population of hermaphrodites to bear its own young (unlike with gonochorism) enabling faster population growth (Katju, et al., 2008; Stewart & Phillips, 2002).

Unlike *C. elegans*, the vast majority of other species in the *Caenorhabditis* clade are gonochoristic (for phylogenetic details see Chapter 4). How habitat is associated with choice of reproductive strategy remains largely unresolved as there is currently little empirical data on the relative incidence of androdioecious and gonochoristic species in different habitats (Schulenburg & Félix, 2017; Frézal & Félix, 2015; Félix & Duveau, 2012; Félix, et al., 2014).

A key benefit of *C. elegans* as an ageing model is its short life cycle, with a maximum lifespan of around 30 days (Figure 1.5, taken from (Altun & Hall, 2009)), and observable senescent changes with age. Moreover, *C. elegans* can transition to a long-lived and stress-resistant diapause during the late L1 (larval 1) stage when harsh environmental conditions are sensed (Figure 1.5). The dauer diapause is an alternative L3 stage. Dauers can survive up to four months, well beyond maximum lifespan during normal reproductive development. If conditions become favourable, dauers can develop on to the L4 stage of the lifecycle and continue to adulthood with no negative effect on maximum adult lifespan (Altun & Hall, 2009).

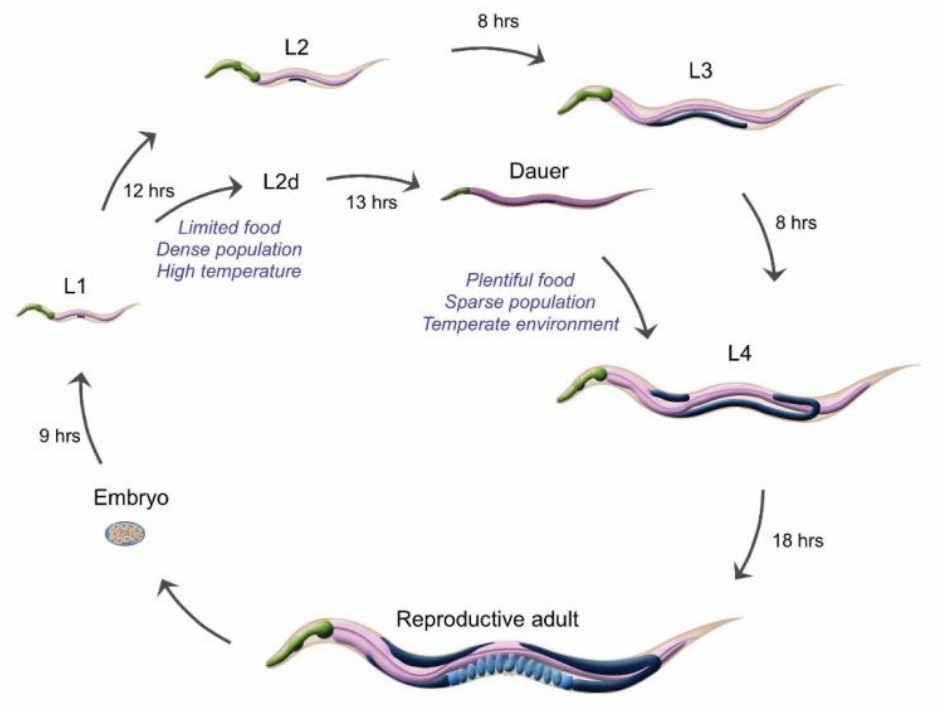

FIGURE 1.5. Life cycle of *C. elegans* (22˚C)**.** Fertilization occurs at 0 min. Numbers along the arrows indicate the length of time the animal spends at each stage. *C. elegans* has a lifespan of around 2-3 weeks at an optimum temperature of around 20˚C for fertility, with development accelerated at higher temperatures and decelerated at lower temperatures consistent with rate of living affects more generally observed in invertebrates (Loeb & Nortrop, 1917; Van Voorhies & Ward, 1999; Leiser, et al., 2011). After hatching, movement to adulthood takes around 3 days, with moulting to 4 larval stages (L1-L4) in between. Dauer larvae are morphologically distinct from larvae that develop in replete conditions: they have a specialised cuticle with alae, are radially constricted and do not feed, possessing a sealed buccal cavity and a radially constricted pharynx that does not pump. Reproduced from (Altun & Hall, 2009).

1.3.2 Development of senescent pathology in *C. elegans*

Major senescent pathologies are observed relatively early in life in *C. elegans* hermaphrodites. Progression of these pathologies is rapid and maximum severity is typically reached by around day 14 of adulthood (c.f. maximum lifespan of 30 days) (Figure 1.6, taken from (Ezcurra, et al., 2018)). The most highly visible pathologies are pharyngeal degeneration, intestinal atrophy, yolk/lipid steatosis, gonad degeneration and uterine tumour formation, each of which will be described in turn. It has been suggested that a major driver of development of severe pathologies in reproduction-linked organs is the futile continuation of wild-type programmes that are beneficial in early adulthood. How this fits into current theories of ageing will be discussed later in this chapter. In contrast to hermaphrodites, males do not exhibit gross senescent pathologies of this sort, apart from pharyngeal degeneration (de la Guardia et al., 2016; Ezcurra et al., 2018; Ezcurra et al., 2020). Also, in the absence of mating or male-male interactions, males are longer lived than hermaphrodites (Gems and Riddle., 2000).

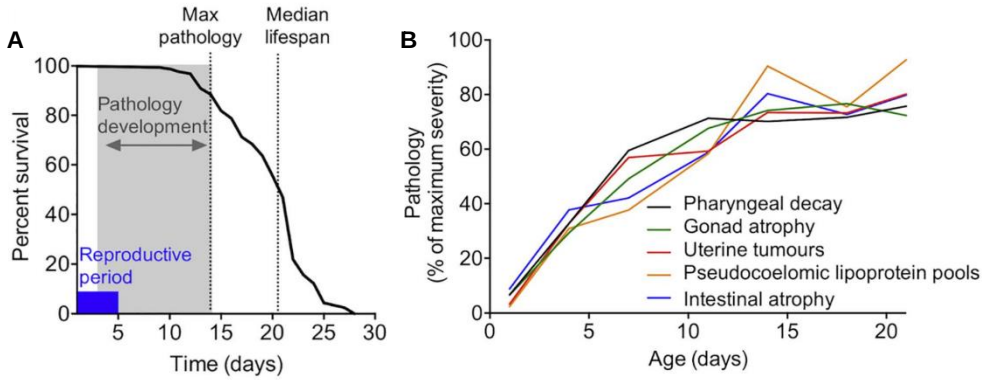

FIGURE 1.6. Senescent pathology development in *C. elegans* with age. (A) Pathologies develop early in life. In relative terms *C. elegans* has an unusually long post-reproductive life, with reproduction ceasing by around day 7 of adulthood (Ezcurra, et al., 2018). **(B)** Senescent pathologies develop in a concerted fashion. Maximum severity is reached by around day 14 of adulthood. Reproduced from (Ezcurra, et al., 2018).

Pharyngeal degeneration appears to result from multiple etiologies, some known and some not. It is characterised by increased presentation of tissue infection, radial muscle degeneration, and atrophy resulting in a ~70% decrease in pharyngeal cross-sectional area with increasing age (Zhao, et al., 2017; Ezcurra, et al., 2018) (Figure 1.7A). Other pathologies discussed here affect organs associated with reproduction. Two pathologies whose development appears coupled to one another are intestine atrophy (Garigan, et al., 2002; McGee, et al., 2011) and ectopic deposition of lipid and vitellogenin-rich yolk, resulting in steatosis (Sornda, et al., 2019; Yi, et al., 2014; McGee, et al., 2011; Garigan, et al., 2002; Herndon, et al., 2002; Chen, et al., 2016) (Figure 1.7B, taken from (Gems et al., 2020)). After sperm depletion, continued yolk production by the intestine is supported by consumption of intestinal biomass in a seemingly futile process, leading to gut atrophy and yolk steatosis (Ezcurra, et al., 2018). Similarly, gonadal degeneration is promoted to a continuation of physiological apoptosis (PA; i.e. programmed cell death and not damage induced), which during reproduction promotes oocyte growth (de la Guardia et al., 2016; Luo & Murphy, 2011; Gumienny, et al., 1999) (Figure 1.7C, taken from (Gems et al., 2020)). Of particular prominence are the tumour-like masses in the uterus, each of which develop from a small number of unfertilised oocytes after sperm depletion (Golden, et al., 2007; Wang, et al., 2018a) (Figure 1.7C). Mirroring mammalian ovarian teratomas (*tera* from Greek for monster, due to the multiple tissue types including skin, hair, and teeth these tumours are associated with in mammals), these are caused by the initiation of futile embryogenetic programmes in unfertilised oocytes (Wang, et al., 2018a; Wang, et al., 2018b). Besides the gut-yolk link, other links between pathologies have been detected. For example, gonad degeneration is positively correlated with

uterine tumour formation such that in worms with tumours that differ in size, the gonad arms with larger tumours show greater gonadal atrophy (Wang, et al., 2018b).

For more details on pathology progression and scoring as well as example Nomarski images, see Chapter 2 Methods. Action of futile continuation of wild-type programmes in senescent pathogenesis in *C. elegans* is consistent with finding that suppression of the activity of wild-type biological pathways that promote growth also promote ageing (Friedman, 1998; Kenyon, 1993; Kimura, 1997).

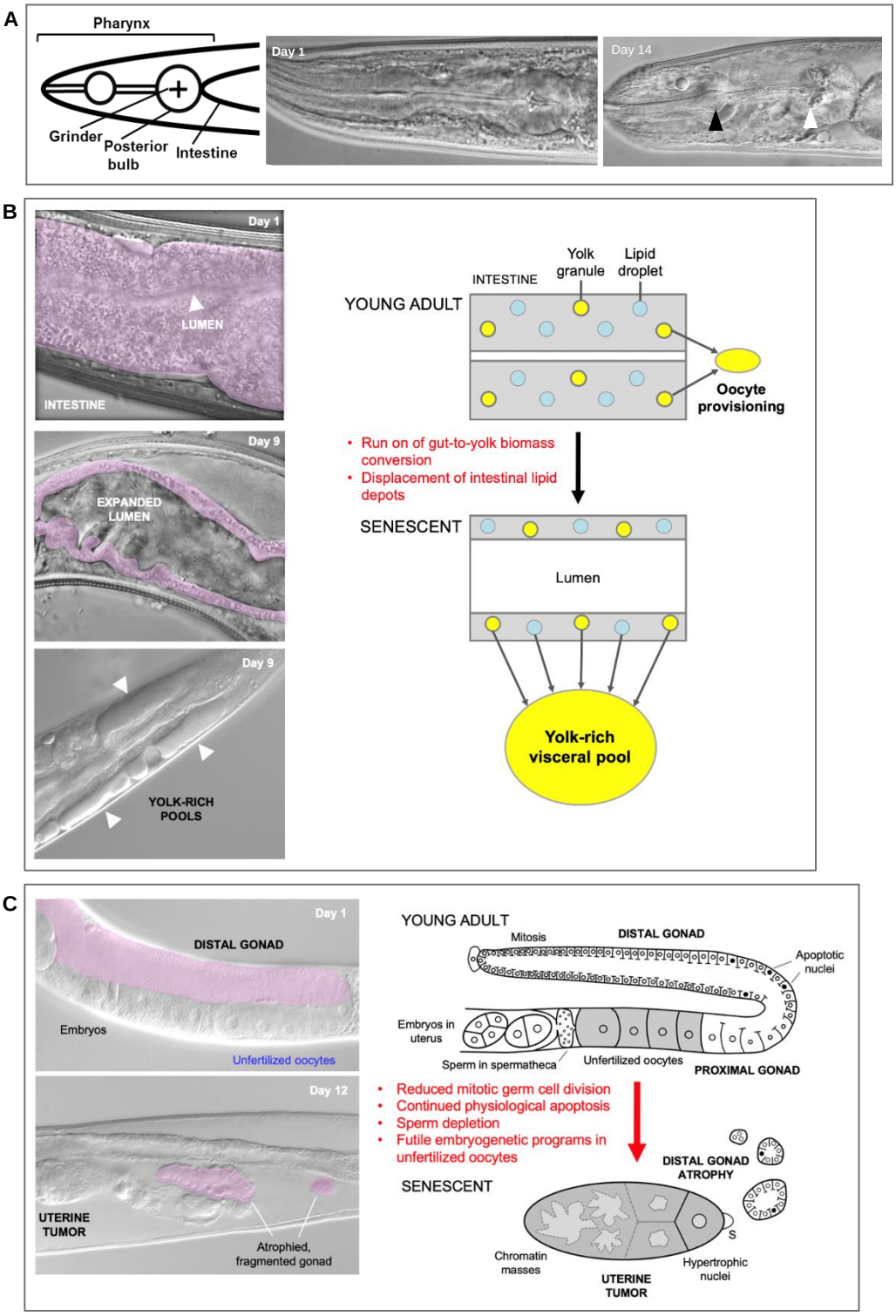

FIGURE 1.7. Major senescent pathologies in *C. elegans* hermaphrodites. (A) Pharyngeal degeneration with age. Visible loss of tissue and radial muscle is seen on day 14, as well as vacuoles (white arrow) and a distended lumen (black arrow) due to the presence of bacteria. **(B)** Left, intestinal atrophy and yolk-rich visceral pool accumulation. Right, hypothesis for etiology of both pathologies: a vitellogenic programme continuation, where remobilisation of intestinal biomass into yolk continues in a futile fashion (Benedetto and Gems, 2019; Ezcurra et al., 2018). **(C)** Distal gonad atrophy and teratoma-like uterine tumor formation. Left: appearance of pathologies under Nomarski microscopy; distal gonad marked in pink. Right: proposed pathophysiology involving futile programme continuation. In the young adult oocytes are generated by proliferation of mitotic germline stem cells which then enter meiosis, and then in most cases undergo PA to generate cytoplasm to fill expanding oocytes (Gumienny et al., 1999; Jaramillo-Lambert et al., 2007; Wolke et al., 2007). Subsequently, declining stem cell division (conceivably adaptive) (Kocsisova et al., 2019) and run-on of PA promotes distal gonad atrophy and fragmentation (de la Guardia et al., 2016). Unfertilised oocytes fail to complete meiosis, enter the uterus and develop into teratoma-like tumors containing massively polyploid chromatin masses (Golden et al., 2007) which appears to result, as in mammalian ovarian teratomas, from futile embryonic programme initiation (Wang et al., 2018a; Wang et al., 2018b). B and C reproduced from (Gems et al., 2020).

1.3.3 Factors influencing *C. elegans* lifespan and conservation in other organisms

Initial work into the genetics of ageing in *C. elegans* was carried out by Michael Klass and Thomas Johnson (Friedman & Johnson, 1988; Johnson & Wood, 1982; Klass, 1977; Klass, 1983) and led on to the identification of many factors affecting ageing: insulin/IGF-1 signalling (IIS), germline signalling, mitochondrial function, loss of protein folding homeostasis, steroid hormones and epigenetic changes (Gems, et al., 2020; Antebi, 2013; Kenyon, 2010; Greer, et al., 2010; Labbadia & Morimoto, 2014; Munkácsy & Rea, 2014). Signalling pathways in *C. elegans* with the greatest effects on lifespan are shown in Figure 1.8, taken from (Aguilaniu, et al., 2016)). Interventions in some of these factors, such as reducing insulin/IGF-1 or mTOR (mechanistic target of rapamycin) signalling and enhancing protein folding homeostasis, were later found to increase lifespan in mammals as well (Bluher, et al., 2003; Holzenberger, et al., 2003; Evans, et al., 2011), though effects on longevity are not as large, proportionally, as in *C. elegans.*

While *C. elegans* has been of great utility to ageing research, special care is required when interpreting results from model organism, particularly invertebrates. *C. elegans* senescence is just one sample of the great diversity in patterns of ageing observed in nature, and the extent to which aetiologies of senescence vary across taxa remains an open question, but it clearly does vary. For instance, *C. elegans* somatic cells are all post-mitotic and also show no sign of cellular senescence (*sensu* Hayflick, referring to irreversible cell cycle arrest with cellular hypertrophy and hypersecretion), unlike in mammals where stem cell exhaustion (Conboy & Rando, 2012; Shaw, et al., 2010) and accumulation of senescent cells (van Deursen, 2014) likely contribute to ageing (Gems, et al., 2020). Severe impairment of antioxidant defence or mitochondrial impairment also enhances lifespan in *C. elegans*, but results in death in mammals (Rea, 2005; Van Raamsdonk & Hekimi, 2009).

To make sense of results, understand why certain wild-type programmes are linked to senescent pathology in *C. elegans*, and translate findings to humans, context is required in the form of realistic theoretical frameworks.

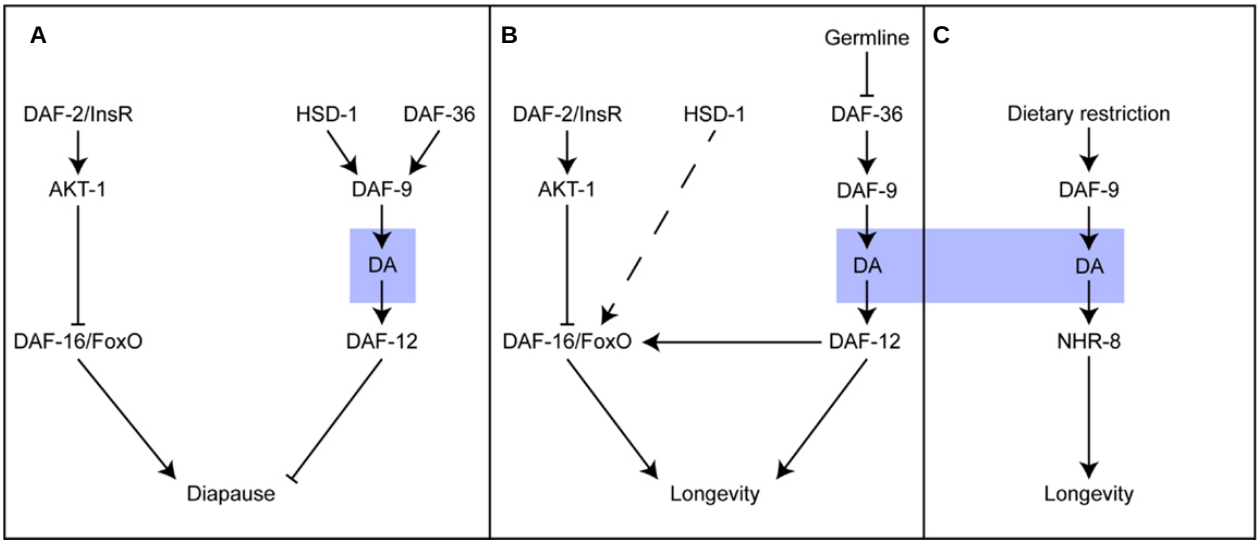

FIGURE 1.8. Longevity pathways in *C. elegans* with the largest effects on lifespan. (A,B) IIS and germline signalling. **(A)** Association with entry into the dauer diapause for comparison. **(B)** IIS and germline signalling in lifespan extension. Increase in lifespan by *daf-2*, insulin and IGF-1 receptor homologue, requires *daf-16* which encodes a member of the FOXO family of forkhead transcription factors (Kenyon, 1993). Insulin-like peptides bind DAF-2 to initiate a phosphorylation cascade which eventually targets DAF-16 preventing it from entering the nucleus (Hertweck, et al., 2004; Paradis & Ruvkun, 1998; Lin, et al., 2001). IIS also controls dauer formation through use of many similar key components including DAF-18/PTEN and DAF-16/FOXO (Hu, 2007; Riddle, et al., 1997). For simplicity, interconnection between the IIS and TOR pathway is not shown. Whether DAF-16 affects longevity independent of TOR is currently not known. Longevity in response to germline ablation works through inhibition of the nuclear hormone receptor (NHR) DAF-12 as well as through the IIS related DAF-16 transcription factor (Hsin & Kenyon, 1999): removal of either DAF-12 or DAF-16 leads to suppression of lifespan extension through germline removal (Hsin & Kenyon, 1999), and germline removal has been shown to increase intestinal nuclear localization of DAF-16 (Lin, et al., 2001). In the absence of germline signalling, enhanced production of the steroid hormone Δ7-dafachronic acid (DA) by DAF-9 (cytochrome P450) binds DAF-12. The presence of the somatic gonad is required for germline removal to cause lifespan extension (Hsin & Kenyon, 1999). **(C)** DR in lifespan extension. DR associated lifespan extension is via DA but interestingly does not involve DAF-12 (as *daf-12(rh61rh411)* null mutants are still long lived on DR), and instead involves another closely related NHR, NHR-8 (Thondamal, et al., 2014). NHR-8 is a homologue of the vertebrate Liver-X and Vitamin-D receptors and is a master regulator of cholesterol homeostasis, affecting cholesterol balance, fatty acid desaturation, apolipoprotein production, and bile acid metabolism. NHR-8's role in longevity determination is not well understood (Magner, et al., 2013). DAF-36: Cholesterol 7-desaturase; HSD-1: orthologous to 3beta-hydroxysteroid dehydrogenase/Delta(5)-Delta(4) isomerases (3beta-HSDs), which are key steroidogenic enzymes. Adapted from (Aguilaniu, et al., 2016).

1.4 Evolutionary theories of ageing: foundations and principles for understanding ageing

Is natural selection unable to work against ageing? What argues against this possibility and requires explanation is the fact that different species have different rates of ageing, or in some cases seemingly no ageing at all, suggesting that the process is countered to different extents (Comfort, 1956; Rose, 1991; Finch, 1994 a). As commented by George Williams: 'It is

remarkable that after a seemingly miraculous feat of morphogenesis, a complex metazoan should be unable to perform the much simpler task of merely maintaining what is already formed' (Williams, 1957). If we can understand why ageing evolved, i.e. the ultimate cause(s) of ageing, this will not only shed light on the proximate mechanisms of ageing but also help us understand which animals are more or less susceptible to different proximate mechanisms. In other words, it will give us the necessary foundations and principles needed to solve ageing.

1.4.1 Theory of Antagonistic Pleiotropy

While ageing likely has no purpose in most cases, it is possible that ageing evolved due its association with traits that have a purpose. Peter Medawar suggested this could occur through gene pleiotropy where one gene influences two or more phenotypic traits (Medawar, 1952). Williams then elaborated upon this and developed it into the now well-established theory of Antagonistic Pleiotropy (AP). AP genes influence at least one beneficial and one harmful trait, hence 'antagonistic'. If the benefit(s) outweigh the cost(s), the gene is selected for and a trade-off is made; the result of many such trade-offs is a major cause of ageing.

When does a benefit outweigh a cost, and so when are AP genes selected for? Two main factors must hold true. First, the cost cannot detract from the organism's propensity to reproduce as differential reproduction is the key to the action of natural selection. Moreover, a clear distinction between offspring and parents must exist. In most complex organisms this is in the form of a germline for reproduction and soma (i.e. the remainder of the body) for self-maintenance, termed the germline-soma barrier or Weismann barrier (Weismann, 1885). An extrapolation is that ageing is not predicted to evolve in organisms that reproduce by simple symmetric division or splitting (Charlesworth, 1994; Ackermann, et al., 2007; Partridge & Barton, 1993). Why does senescence usually present with the chronological passing of time? The answer is the second factor: the force of selection declines with time, as first noted by Ronald Fisher (Fisher, 1930) and then developed by Medawar, Haldane and Williams (Haldane, 1941; Williams, 1957). Regardless of how low mortality is, there will always be a higher chance of surviving to an earlier time point than a later time point, independent of senescence and due to external hazards such as predation, infection and accidents. Earlier benefits will be selected for over costs that present later in life, and so an organism's performance will experience progressively weaker selection with advancing age (see Figure 1.9 for illustration of reproductive decline, taken from (Williams, 1957)).

Notably, it is not essential for the negative effects of AP genes to be restricted to very late in life. Any pleiotropic gene that ensures the survival and reproductive potential of an organism up until its highest reproductive probability where the force of selection is greatest (apex of solid line in Figure 1.9), should, in theory, be selected for even if it confers adverse effects after this point (Williams, 1957). Also, not all costs necessarily contribute to senescence. To do so they must affect physiology. For instance, certain risks like predation, although they may affect life-history optimisation, will not contribute to senescence (Partridge, 1997).

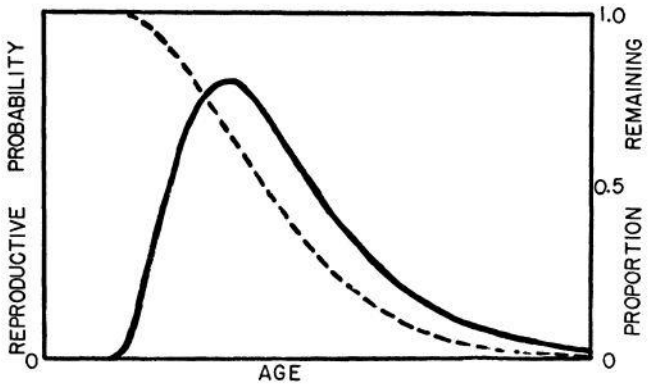

FIGURE 1.9. Relationship between age and probability of reproduction. The solid curve is the reproductive probability distribution (independent of senescence). The dashed curve indicates the proportion of the total reproductive probability that remains after any given age. Reproduced from (Williams, 1957).

1.4.2 The Mutation Accumulation theory

Based on the assumption that natural selection declines with age, Medawar also proposed the Mutation Accumulation (MA) theory (Medawar, 1946; Medawar, 1952). Once selection is sufficiently attenuated late in life, deleterious random mutations with effects restricted to later life will escape the force of selection. Accumulation would then occur through genetic drift as the mutations are passed from one generation to the next, with most animals in the wild either having died or completed the majority of their reproductive output before the effects of these mutations become consequential. Ageing resulting from MA would hypothetically only become apparent when an organism moves to a less hazardous environment where it can survive to more advanced ages, such as under laboratory conditions (Medawar, 1952).

MA, if true, could explain the puzzle of genetic conditions like Huntington's disease, an invariably fatal autosomal dominant neurological disease (Medawar, 1952). If the disease is inherited and always fatal, why has natural selection not resulted in its removal from the gene pool? The likely answer is that the onset of Huntington's disease is some time after the onset reproduction (Haldane, 1941).

1.4.3 Antagonistic Pleiotropy versus Mutation Accumulation

While MA and AP are not mutually exclusive, it is important to determine just how much each process contributes to the evolution of ageing and therefore ageing mechanisms. Contributions of adaptive AP trade-offs are well accepted and supported to the point where they are seen as ubiquitous in ageing biology, unlike non-adaptive MA which is contested (Partridge & Gems, 2002; Hughes & Reynolds, 2005; Moorad & Promislow, 2009). A direct way to test for the action of AP is to identify wild-type alleles that cause senescence and then see if they have pleiotropic beneficial traits expressed early in life (Rose, 1991; Charlesworth, 1994). In other words, is a trade-off is made between early life fitness, such as reproduction or growth, and late-life fitness, such as survival. When such trade-offs have been carefully looked for, they have usually been found (Flatt & Promislow, 2007; Flatt & Schmidt, 2009; Moorad & Promislow, 2009; Austad & Hoffman, 2018).

1.4.4 The Disposable Soma theory

By what mechanisms do pleiotropic genes exert their pathological costs? Williams said relatively little about the proximate mechanisms through which the ultimate mechanism of AP works (Williams, 1957). One possible mechanistic explanation is provided by the Disposable Soma (DS) theory proposed by Tom Kirkwood (Kirkwood, 1977; Kirkwood & Holliday, 1979). This proposes that ageing is the result of optimising limited resource allocation between the disposable soma and indispensable reproduction. The result is an insufficiency in somatic maintenance, leading to pathological unrepaired stochastic damage accumulation which causes ageing. Thus, disposable soma elegantly combines ultimate and proximate accounts of ageing, the latter being the theory that ageing is caused by molecular damage accumulation (Figure 1.10 A, taken from (Gems & de la Guardia, 2013)). In principle, genes determining the trade-off between reproduction and somatic maintenance could exhibit AP, as proposed (Partridge & Gems, 2002). It is worth noting that in a sense all AP theories incorporate the idea of a ‘disposable soma’, given the assumption of a germline-soma barrier where reproductive benefits are favoured over somatic costs (Blagosklonny, 2007).

While conceptually appealing given its simplicity, several problems have been identified with the DS theory. In general, it now appears that stochastic damage accumulation is more a symptom rather than a cause of senescent pathologies (Blagosklonny 2006; Van Raamsdonk and Hekimi 2010; Gems and Partridge 2013; Gems & Doonan, 2009), though there are exceptions such as in the filamentous fungus *Podospora anserina* (Dufour et al., 2000). More specifically,

predictions of resource optimisation have been shown to not hold true. For example, the theory predicts that men should live longer than women because their reproductive investment is less, and this is not the case (Blagosklonny, 2010). It also predicts that decreased resources and so investment into the soma should accelerate ageing, but the intervention of DR robustly increases lifespan in ageing models (Blagosklonny, 2013). A third example is the inhibition of protein biosynthetic genes in *C. elegans*, which the DS theory predicts should decreases lifespan as somatic maintenance is impaired, but here too the intervention robustly increases lifespan. Attempts have been made to reconcile these with DS. For example, Kirkwood argues that women live longer due to increased investment into somatic maintenance (Kirkwood, 2010), the effects of DR are explained using the allocation hypothesis whereby DR leads to diversion of resources from reproduction to somatic maintenance and so allows for an increased lifespan (Holliday, 1989; Kirkwood and Shanley, 2005; Masoro and Austad, 1996), and inhibition of protein biosynthetic genes in *C. elegans* are argued to potentially free up of resources that are then invested in somatic maintenance (Hansen et al., 2007; Hipkiss, 2007). As argued by Mikhail Blagosklonny, more parsimonious predictions are that women should live shorter since they invest more into reproduction, increasing resources for somatic maintenance should increase lifespan, and perturbing somatic maintenance should decrease lifespan (Blagosklonny, 2007; Blagosklonny, 2010).

1.4.5 The hyperfunction theory and quasi-programmes

An alternative AP ultimate/proximate theory proposes that deleterious wild-type gene activity or 'hyperfunction' is a major cause of senescence. This theory is derived from surveys of recent findings and different versions of it were independently proposed by Blagosklonny and João Pedro de Magalhães (Blagosklonny, 2006; Blagosklonny, 2007; Blagosklonny, 2008; Blagosklonny, 2013; de Magalhães & Church, 2005; de Magalhães, 2012). Such pathological gene activity is not an adaptation, rather it is quasi-programmed (Blagosklonny, 2006), a coinage of Blagosklonny's to describe the futile and pathological execution of a biological programme; in other words, programmed in the mechanistic sense but not in the adaptive sense. Another way of expressing this is that while such mechanisms of ageing are not programmed, they are programmatic in nature. This avoids the falsehood of saying that ageing is programmed and, ergo, an adaptation

Why should quasi-programmes exist in the first place? Although Williams never presented a mechanistic explanation for how AP costs could result in senescence, he did briefly describe a

hypothetical example: ‘we might imagine a mutation arising that has a favourable effect on the calcification of bone in the developmental period but which expresses itself in a subsequent somatic environment in the calcification of the connective tissue of arteries’ (here arterial calcification is clearly a pathology) (Williams, 1957). This is based on one of Williams’s assumptions that the pleiotropic nature of certain gene results from them producing ‘different effects in different somatic environments, and that these effects become progressively less controlled by selection with increasing adult age’ as the force of selection declines (Williams, 1957).

In particular, both Blagosklonny and de Magalhães view quasi-programmes as originating from a continuation (i.e. a slow cumulative effect throughout adulthood) of developmental growth including adult developmental processes, such as reproduction, repair/tissue homeostasis and immunological programmes (Gems and Kern, 2021; Blagosklonny, 2006; Blagosklonny, 2007; Blagosklonny, 2008; Blagosklonny, 2013; de Magalhães & Church, 2005; de Magalhães, 2012) (Figure 1.10 B, taken from (Gems & de la Guardia, 2013)). For example, presbyopia (long-sightedness with age) results from the continued growth of the lens during adulthood causing a gradual and futile increase in its thickness (Strenk et al., 2005). Such continuation is unlikely to be precise given the decline in selection (Williams, 1957; Blagosklonny, 2007a), as well as the fact that senescent pathologies often result from multiple aetiologies (Al Anouti et al., 2019; Armstrong, 2013; Glocker et al., 2006; Glyn-Jones et al., 2015; Higashi et al., 2019; Huertas and Palange, 2011). Apart from arising from run-on of adult programmes (primary mechanisms), as in presbyopia, quasi-programmes may also be triggered in later life as secondary drivers of pathogenesis (Gems and Kern, 2021; Kern et al., 2021).

The hyperfunction theory is supported by the strong link between growth-associated pathway suppression, e.g. IIS and mTOR, and lifespan extension (Blagosklonny, 2007; Blagosklonny, 2009). Moreover, this theory predicts accelerated ageing in men due to increased mTOR activity promoting muscle growth in them (Blagosklonny, 2010), as well as the observed lifespan extension from interventions which inhibit growth such as dietary restriction (Figure 1.10 C, taken from (Gems & de la Guardia, 2013) or affect the consequences of sustained growth such as continued protein synthesis (Blagosklonny, 2006; de Magalhães & Church, 2005). As described previously, many ageing pathologies characterised in *C. elegans* are also in line with

programmatic hyperfunction (Figure 1.10 D, taken from (Gems & de la Guardia, 2013) with more recent findings added).

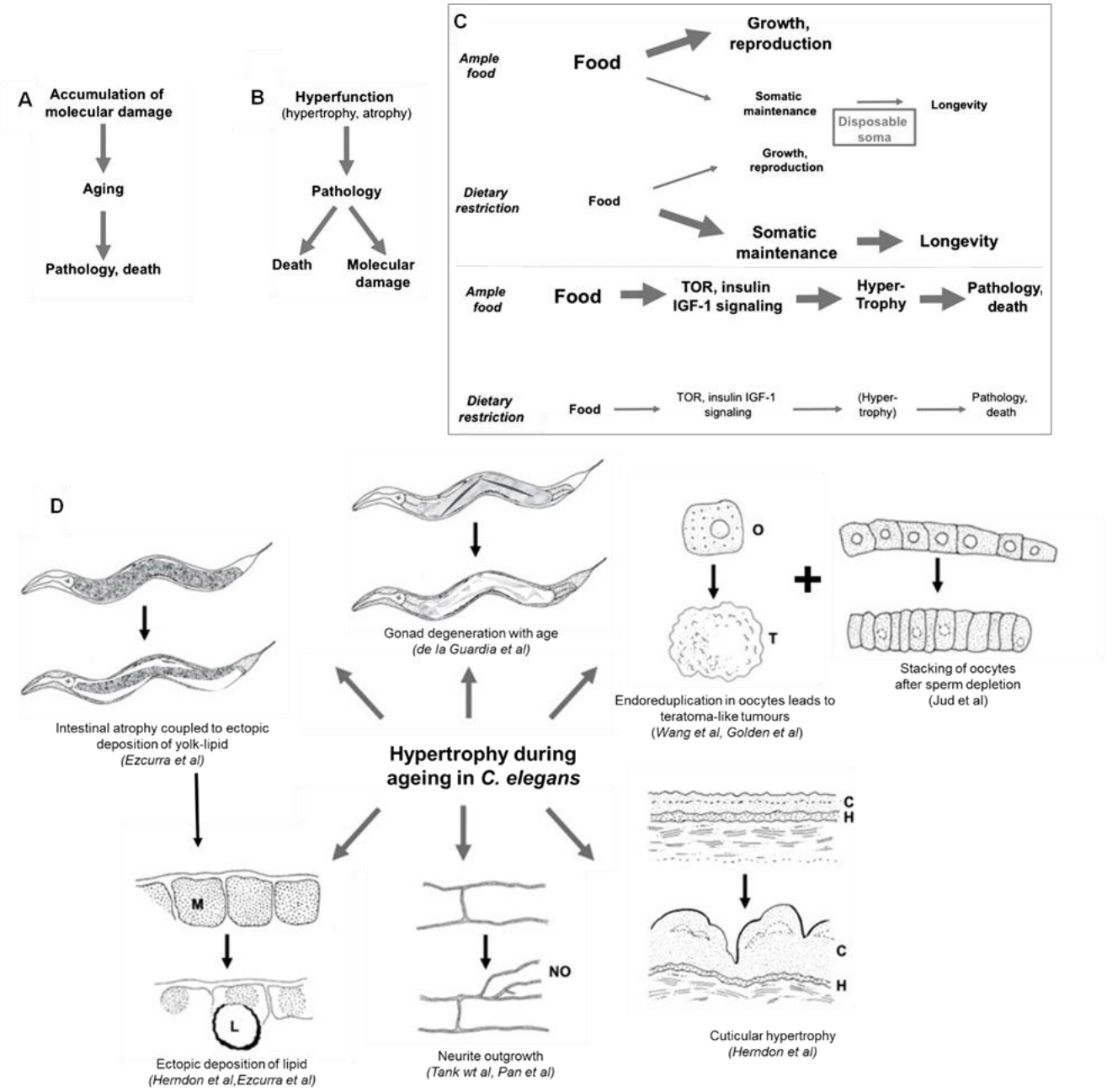

FIGURE 1.10. Ageing as a quasi-programme of development. (A,B) Harmonizing two theories for direct comparison. **(A)** Simplified representation of molecular damage theory (including oxidative damage theory). **(B)** Simplified representation of hyperfunction theory. **(C)** Explanation for effects of dietary restriction in terms of the DS theory and hyperfunction. Top: Disposable soma theory. Bottom: The hyperfunction theory. **(D)** Evidence for hypertrophy during ageing in *C.elegans*. This figure shows seven examples of age change that involve hypertrophy, including some of the major scenescent pathologies discussed previously (c.f. Fig. 7): intestinal atrophy coupled to accumulation and redistribution of lipid-yolk (here in ageing muscle, L, lipid droplet; M, muscle), gonadal degeneration, stacking of oocytes in the gonad post sperm depletion, appearance of intrauterine tumour masses as a consequence of runaway endoreduplication in unfertilised oocytes (O, oocyte; T, tumor), cuticular hypertrophy (C, cuticle; H, hypodermis), and neurite outgrowth (NO, neurite outgrowth). In each part, the young adult worm is shown above and an older worm below (Ezcurra, et al., 2018; Depina, et al., 2011; Garigan, et al., 2002; Golden, et al., 2007; Herndon, et al., 2002; Jud, et al., 2007; McGee, et al., 2011; Tank, et al., 2011; de la Guardia et al., 2016; Wang et al.,

2018a; Wang et al., 2018b). **(A,B,C)** Reproduced from (Gems & de la Guardia, 2013). **(D)** Adapted from (Gems & de la Guardia, 2013) with more recent findings added.

1.4.6 Costs due to evolutionary constraint

Evolutionary constraints may preclude a trait from reaching, shifting away from, or slowing down in its approach to a defined selective optimum and so limit the production of a new phenotype. Selection in the presence of constraints may also result in costs which contribute to senescence. As recently proposed by Luis Acerenza, constraints can be categorised into two main types: (i) selection constraints, which are the result of opposing selection pressures at play; and (ii) organisational constraints, which restrict the production of certain phenotypic variants and are caused by the structure, kinetics, regulation and composition, i.e. overall 'organisation', of an organism (Acerenza, 2016).

This categorical division can also be linked to Richard Lewontin's conception of genotype and phenotype maps (Acerenza, 2016; Lewontin, 1947), which connect the genotype to the phenotype, i.e. connect two differences, one at the genetic level and one at the phenotypic level. Briefly, the average genotype of a population can be viewed as a point in the space of all possible genotypes (G space), and the average phenotype of the same population as a corresponding point in the space of all possible phenotypes (P space). Selection constraints do not restrict the P space (i.e. all possible phenotypes) but rather reduce the accessible P space by limiting the persistence of phenotypic variants (Acerenza, 2016), resulting in costs. On the other hand, organisational constraints restrict the phenotype space and include constraints that have been previously classed as genetic, functional and developmental (Acerenza, 2016; Maynard Smith, et al., 1985; Arnold, 1992; Brakefield & Roskam, 2006). Trade-offs that occur as a consequence of constraints can also be classed according to the constraints involved, i.e. selection vs organisational (Acerenza, 2016).

An example of a selection constraint is provided by the Central American túngara frog *Engystomops pustulosus*. Here males croak to attract females, but doing this also attracts a predator, the fringe-lipped bat *Trachops cirrhosus* (Tuttle & Ryan, 1981). This results in a reduction of the accessible P space, i.e. maximising success at attracting mates, while phenotypically possible, is not selected for because it comes at the cost of being eaten by fringe-lipped bats. An example of an organisation constraint is lactation, which comes at the cost of bone loss. Here there are two linked traits under positive selection, with a coupling mechanism under conflicting selection. This results in the P space being restricted, i.e. not losing bone while optimally producing calcium-rich milk is not a phenotypic possibility.

Organisational constraints can be further divided into those that result from the interconnected nature of biological traits, as in with bone resorption during lactation, and those that result simply from biological impossibility (Acerenza, 2016; Gems and Kern, 2021). For example, although the condensation of two molecules of ethanol to form n-butanol is a highly exergonic reaction, no enzymes have been identified that catalyse it suggesting that an active site capable of this catalysis simply cannot evolve from existing enzymes (Bar-Even et al., 2012).

1.5 The context of life-history evolution

Why does ageing occur at different rates in different species? The evolutionary theory of ageing is embedded in the broader framework of life-history theory, designed to study the diversity of strategies employed by different organisms, especially those affecting reproduction and survival.

1.5.1 Revisiting r- and K-selection and relating it to *r* vs R_0 maximisation

The theory of r- and K-selection was one of the first predictive models for life-history evolution (MacArthur & Wilson, 1967). It is derived from the Verhulst equation (Verhulst, 1838) which describes the self-limiting growth of a biological population. While once popular, the r/K model fell out of favour due to being incorrectly associated with specific sets of life-history traits that were based on erroneous assumptions (Dańko, et al., 2018). Once these are corrected, however, the model is highly useful, particularly due to its simplicity (Dańko, et al., 2018).

Populations can be roughly classified according to whether they are in a state of constant growth, r-selected (r for the 'rate' of growth and therefore rate of reproduction), or whether they are in a steady-state under density-dependent regulation, K-selected (from the German *Kapazitätsgrenzen* meaning capacity limit). If there is no density-dependence for a given population, selection only works on r (rate of growth) to maximise reproductive output and so the best measure of fitness is the 'intrinsic rate of natural increase' (*r*; also called the Malthusian parameter and defined as the difference between birth rate and death rate). A lack of density-dependence usually arises when extrinsic mortality is high, leaving the population in a state of constant growth. Species that maximise *r* favour traits such as rapid development with a small overall size and early maturity (Stearns, 1976, Stearns, 1977).

When density dependence is a factor, a population may either favour *r* maximisation or 'expected lifetime offspring production' (R_0; calculated by multiplying the proportion of females surviving to each age by the average number of offspring produced at each age and then adding

the products from all the age groups). Previous problems with the r/K model were that all K-selected animals were assigned R_0 traits (Dańko, et al., 2018). As a simplification, the greater the relative value of adults in a population the more R_0 is favoured. Therefore, if density-dependence acts uniformly on all age classes the Malthusian parameter (r) still holds (Dańko, et al., 2017; Dańko, et al., 2018)) (mathematically equivalent to no density-dependence). On the other hand, if density-dependence is stage-specific and acts to affect the survival of juveniles more than adults, r is no longer a good fitness measure. Instead, the organism will favour traits such as delayed development, delayed age of maturity and a larger size (Dańko, et al., 2017; Dańko, et al., 2018). R_0 may also be favoured when density dependence has phenotypic effects such as suppressing the birth rate (fertility) to make the population stationary, as again maximising r is not ideal (Charlesworth, 1980; Argasinski & Broom, 2013; Argasinski & Rudnicki, 2017; Dańko, et al., 2017; Dańko, et al., 2018).

In reality, a continuum is predicted to exist between the extremes of populations working to either maximise r or R_0, with most species falling somewhere in between (Dańko, et al., 2017). This is very much a simplification which looks at the main determinants of life history; in reality there exists a wide variety of possible life histories due to several other factors being at play.

1.5.2 Linking r - R_0 maximisation and parity continua: new arguments

One life history trait linked to r vs R_0 maximisation is reproductive strategy (Gadgil & Solbrig, 1972; Stearns, 1976; Stearns, 1977; Dańko, et al., 2018). Consistent with an r vs R_0 continuum, there also exists a continuum of reproductive strategies with semelparity and iteroparity as two extremes (Figure 1.12) (Hughes, 2017; Jones, 1975; Luckinbill, 1979). While Dańko et al. do not specifically consider semelparity and iteroparity when describing the r-R_0 maximisation continuum (built on the r/K model) and life history strategy (Dańko, et al., 2017; Dańko, et al., 2018), parity arguably follows on with it having been previously assigned to the r/K model (Gadgil & Solbrig, 1972) and the enlarged concepts summarised by Stearns (Stearns, 1976; Stearns, 1977).

A semelparous strategy involves one large reproductive burst in life, often suicidal due to the large costs required to facilitate it (reproductive death). Iteroparous animals on the other hand can achieve multiple rounds of reproduction, each round having relatively modest effects on future function and survival. Conditions favouring maximal r will favour a large single reproductive effort as early as possible regardless of cost to maximise exponential growth, and hence favour semelparity (Stearns, 1976; Stearns, 1977). Conditions favouring maximal R_0 will

favour a smaller number of offspring and iteroparity (Stearns, 1976; Stearns, 1977; Dańko, et al., 2018). Relating parity to *r* vs R_0 maximisation is also a simple way to resolve Cole's paradox of semelparity (Schaffer, 1974). This asks: why do all animals not just opt for a semelparous reproductive burst type strategy to maximise exponential growth and colonisation of their habitat? The relative value of adults (which, for example, will be greater if mortality is higher for juveniles than adults) is the main determinant here, as large costs associated with semelparity will affect future adult survival and so lifetime reproductive output (Cole, 1954; Charnov, 1973; Schaffer, 1974).

One could argue that senescence also follows a continuum based on rate, with either rapid, gradual or even seeming 'negligible senescence' observed (Finch, 1994) (Figure 1.12). This continuum is exemplified in the variety of mortality rate doubling times (MRDT) that species exhibit. Mortality rate increases more steeply after the initiation of rapid senescence (Finch, 1994 a) (Figure 1.12) where MRDT is usually around 0.005 to 0.1 years unlike in gradual senescence with around 0.3 to 10 years (Finch, 1994 a) and even 115 years the naked mole rat (Beltran-Sanchez & Finch, 2018) (MRDT for humans is 7-9 years (Finch, 1994 a)). As the onset of senescence can vary, rate of senescence does not necessarily translate to length of lifespan. For example, century plants can live for 10-30 years before rapid senescence through reproductive death is triggered.

Trade-off costs have been used to link *r* maximisation to parity, where the more selection acts to maximise *r*, the more semelparity is favoured even if it comes at greater trade-off costs (Partridge & Sibly, 1991). The consequence of amplified trade-off costs is more rapid senescence (Gems, et al., 2020). Arguably, the same principles can be used as one means to link the more recently proposed existence of a semelparity-iteroparity (Hughes, 2017), *r*-R_0 maximisation (Dańko, et al., 2018) and rate of senescence continuums. The existence of causal links between the continuums is highlighted by the fact that mechanisms operative in semelparous organisms leading to rapid senescence are likely an amplification of processes occurring at lower levels in iteroparous ancestors (Gems, et al., 2020), with semelparity itself likely being a derived trait (Finch, 1994 a).

These are broad generalisations. Animals need not display either one or the other set of life-history traits with a typically associated level of senescence. For example, one might come across an animal species, X, in the wild that falls closer to the *r* end of the *r* -R_0 continuum and favours rapid maturation and early reproduction. Yet X might be iteroparous because although costs are more affordable they are not necessary to facilitate reproduction, i.e. the death rate between reproductive bouts is sufficiently low to allow for iteroparity (Abrams, 1991). One way to more

precisely determine the costs associated with trade-offs and so link the above continuums is through use of trade-off functions. This would also allow us to account for cases like animal X. For further elaboration see Chapter 6, section 6.5.1.

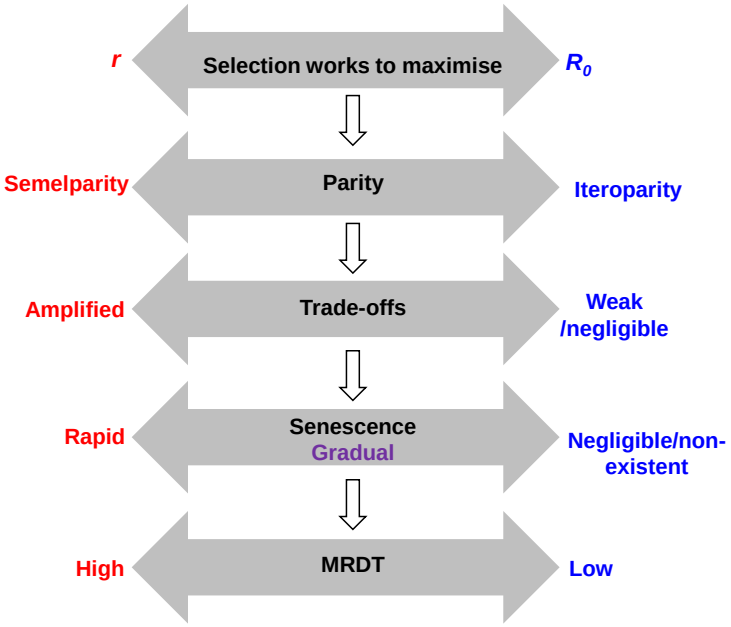

FIGURE 1.12. Tentative model of how the *r-R0*, semelparity-iteroparity and rate of senescence continuums could be linked. When selection works to maximise *r* (Dańko, et al., 2017; Dańko, et al., 2018), a semelparous strategy is favoured. Here costs to continued survival and function are increasing ignored if they are linked to traits that facilitate an early and large reproductive effort (Partridge & Sibly, 1991), i.e. trade-off amplification with higher consequential costs are favoured. The result of amplified trade-off costs is more rapid senescence (Gems, et al., 2020), and a corresponding higher MRDT (Finch, 1994 a). Note: animals with a short lifespan like *Drosophila* and *C. elegans* will inherently have a small MRDT, 0.02-0.04 in both cases, (Finch, 1994 a) making rapid and gradual senescence difficult to distinguish. Likewise, iteroparity and semelparity may be hard to distinguish in short lived organisms (Gems., 2000).

1.5.3 Is *C. elegans* semelparous?

C. elegans is arguably more *r* maximising, with protandrous hermaphroditism itself present to allow a rapid boom-and-bust habitat exploitation strategy (Riddle, et al., 1997). Is it possible that there are terminal investment costs associated with this strategy, i.e. could *C. elegans* be semelparous and undergo reproductive death? Iteroparity and semelparity are hard to distinguish in short lived organisms like *C. elegans* (Gems., 2000). That said, several observations argue against this possibility. For example, many of the gross senescent pathologies observed in *C. elegans* hermaphrodites seem to result from futile continuation of wild-type programmes, i.e. from quasi-programmes (Figure 1.7, 1.10). Moreover, lifespan extension in *C. elegans* can occur, e.g. via reduced IIS (Kenyon et al., 1993) without a reduction in fertility (Larsen, et al., 1995; Gems, et al., 1998; Tissenbaum & Ruvkun, 1998; Dillin, et al., 2002). However, reproductive output consist of more than just fertility, including post-fertility transfers, (Lee, 2003; Austad, 1997;

Lahdenpera, et al., 2004) and it is possible that fecundity benefits of the major observable pathologies in *C. elegans* hermaphrodites are yet to be found. The following chapters identify fecundity benefits coupled to some of these pathologies, and then provide further support for the view that *C. elegans* undergo semelparous reproductive death, suppression of which could explain the unusually large magnitude (in relative terms) of lifespan increases observed in this species.

Chapter 2: Methods

Where new protocols were developed and optimised for the purpose of testing theories in this thesis they are marked as 'new protocols'.

2.1 Culture methods and strains

Maintenance of *C. elegans* and other nematode species was performed using standard protocols (Brenner, 1974). Unless otherwise stated, all strains and species were grown at 20˚C on nematode growth media (NGM) with plates seeded with *E. coli* OP50 to provide a food source. For *C. elegans,* a N2 hermaphrodite stock recently obtained from the Caenorhabditis Genetics Center was used as wild type (N2H) (Zhao et al., 2019). Mutant strains used are described in Wormbase (www.wormbase.org). RT130 *pwIs23 [vit-2::GFP]*, GA1500 *bIs1 [pvit-2::vit-2::GFP + rol-6(su1006)]*, GA1928 *daf-2(e1370)*, DR1296 *daf-2(e1368),* GR1307 *daf-16(mgDf50)*, GA114 *daf-16(mgDf50)*; *daf-2(e1370),* NS3227 *daf-18(nr2037)* and VC20747 *daf-2(gk390525*). GA14 *fog-2(q71),* CB3844 *fem-3(e2006),* GA1928 *daf-2(e1370),* GR1307 *daf-16(mgDf50)*, GA114 *daf-16(mgDf50)*; *daf-2(e1370);* CB4037 *glp-1(e2141)* and SS104 *glp-4(bn2).* Other nematode species used: *C. inopinata* (NK74SC), *C. remanei* (SB146), *C. tropicalis* (JU1373), *C. wallacei* (JU1873), *C. briggsae* (VT847), *C. nigoni* (JU1325), *P. pacificus* (RS2333) and *P. exspectatus* (RS5522). *C. inopinata* alone was initially grown at 25˚C until the L4 stage and then transferred to 20˚C due to its very slow growth rate at 20˚C (Kanzaki et al., 2018). Temperature sensitive mutants (*fem-2, fog-2, glp-1,* and *glp-4)* and accompanying controls were raised at 15˚C until the L4 stage and then shifted to 25˚C, the non-permissive temperature. Other nematode species used: *C. inopinata* (NK74SC), *C. remanei* (SB146), *C. tropicalis* (JU1373), *C. wallacei* (JU1873), *C. briggsae* (VT847), *C. nigoni* (JU1325), *P. pacificus* (RS2333) and *P. exspectatus* (RS5522).

C. elegans maintenance was performed using standard protocols (Brenner 1974). Unless otherwise stated, all species and strains were grown at 20˚C on NGM with plates seeded with *E. coli* OP50 to provide a food source. *C. inopinata* was initially grown at 25˚C until the L4 stage and then transferred to 20˚C due to its very slow growth rate at 20˚C (Kanzaki et al., 2018).

For *Bacillus subtilis* experiments the PY79 strain was used, and wild bacterial isolates (Dirksen et al., 2016) included *Ochrobactrum* MYb71, *Stenotrophomonas* MYb57, and *Achromobacter* MYb9. Bacterial strains were cultured in OP50 medium using standard protocols

(Brenner 1974), with the exception of clones used in RNAi experiments for which lysogeny broth (LB) was used according to standard protocols (Kamath, et al., 2001). RNAi can be induced by feeding in *C. elegans* through cloning a gene of interest into the L4440 vector in *E. coli* HT115 and culturing worms on this. All experiments performed on RNAi used HT115 containing the empty vector L4440 as a control. *E. coli* OP50 expressing red fluorescent protein (OP50-RFP) (Zhao, et al., 2017) was grown in OP50 broth in the presence of 25 μg/ml tetracycline. However, before NGM plates were seeded, OP50-RFP was resuspended in OP50 broth without tetracycline. This was to avoid effects of tetracycline on bacterial pathogenicity that might occur even in the presence of the tetracycline-resistance plasmid. Worms were raised from hatching of alkaline hypochlorite-treated eggs when transferred onto a new bacterial strain.

Unmated hermaphrodites were used unless otherwise stated. For androdioecious species, males were generated from hermaphrodites using a heat shock protocol: hermaphrodites were incubated at 31˚C for 5 hr and then shifted back to 20˚C. This results in a small percentage of males in the F1 generation that are subsequently amplified and maintained via mating with hermaphrodites. When used in experiments, males were cultured at low population density (~ 5 per plate) to reduce deleterious effects of male-male interactions (Gems & Riddle, 2000). For mating, animals were picked at the L4 stage at a ratio of 3:1 males to hermaphrodites/females and left to mature and mate for 24 hr, after which males were removed to prevent excess damage caused by secreted male pheromones or by continual mating (Maures et al., 2014; Woodruff et al., 2014).

2.2 Culture on non-proliferating bacteria

2.2.1 Antibiotic treatment to protect *C. elegans* from infection

80 μl of 500 mM carbenicillin in Milli-Q water was added topically to 10 ml NGM plates (final concentration 4mM) 48 hr after bacterial lawns were seeded to minimise effects of the antibiotic on lawn thickness. Worms were transferred onto plates after 12 hr.

2.2.2 Bacterial UV irradiation to protect *C. elegans* from infection

80 μl of OP50 bacteria was inoculated onto NGM plates and allowed to grow overnight at RT before exposure to UV light (Stratagene UV Stratalinker 2400) for 5 min, 48 hr prior to use to detect and exclude plates with subsequent bacterial growth. Worms were raised from hatching of alkaline hypochlorite-treated eggs on irradiated lawns.

2.3 Microscopy

2.3.1 Slide preparation

Unless otherwise stated, live worms were placed onto 2% agar pads and anaesthetised in a drop of 0.2% levamisole, with coverslips gently placed on top.

2.3.2 Single worm, longitudinal pathology analysis

For experiments where the same worms were imaged using Nomarski microscopy at different time points throughout life, worms on NGM OP50 plates were placed on ice rather than using anaesthesis (Ezcurra, et al., 2018). Within minutes of cooling, worm movement ceased, and animals were transferred to agar pads on microscope slides containing a drop of M9 and coverslips added. Images were taken at 63 x magnification. After imaging, which took no more than a maximum of 3 min, each worm was carefully recovered by pipetting 20 µl of M9 buffer between the top coverslip and the agar pad. The coverslip was then gently removed and the worm picked onto an NGM plate.

2.3.3 Live imaging and video capture of venting behaviour: New protocol

In order to impede worm locomotion and facilitate imaging, polybead microspheres were used. d4 RT130 adults were placed on an NGM plate (no bacteria) in a 15-20 µl drop of 0.1 µm non-fluorescent polybead microspheres (2.5% solids [w/v] aqueous suspension with a coefficient of variance of 15%, 4.55 x 10^{13} particles/ml [Polysciences]). To remove any aggregated particles these were previously filtered through a 0.5 µm pore size syringe filter. A coverslip was then gently placed over the animal to improve image clarity and observations made using a 20x objective (200x magnification) and Nomarski optics. To prevent fluorescence bleaching, Nomarski/GFP (green fluorescent protein) superimposed videoing and imaging were commenced only when movement of the vulval muscles was observed, which often preceded venting or laying of eggs or unfertilised oocytes.

2.3.4 Nomarski and fluorescence imaging

Unless otherwise stated, live worms were placed onto 2% agar pads and anaesthetised in a drop of 0.2% levamisole, with coverslips gently placed on top. Images were captured using one of two microscopes: (i) a Zeiss Axioskop 2 plus microscope with a Hamamatsu ORCA-ER digital camera C4742-95 and Volocity 6.3 software (Macintosh version) for image acquisition; or (ii) an

ApoTome.2 Zeiss microscope with a Hamamatsu digital camera C13440 ORCA-Flash4.0 V3 and Zen software. A constant exposure time was maintained between samples in fluorescence intensity comparisons.

2.3.5 Confocal and airyscan imaging

For this an inverted LSM880 microscope equipped with an Airyscan detector (Carl Zeiss, Jena) was used with a Plan-Aprochromat 63 x 1.4 [numerical aperture (NA)] oil objective with a working distance of 0.19 mm. A 488 nm Argon laser was used for GFP excitation. In confocal mode, emission was recorded via an inbuilt GaAsP (gallium arsenide phosphide) detector. For airyscan, the emission was recorded with the in-built 32-element GaAsP detector. For images showing sample change over time, images were only taken around every 50 min to prevent sample bleaching. In the acquisition of 3D z-series, samples were imaged up to a sample depth of 41 μm, with images of 41 z-planes taken evenly through half of the diameter (dorsoventral) of a worm. Data was processed using Fiji software (NIH), and the 3D Viewer plugin was used for 3D reconstruction.

2.3.6 Reflective confocal microscopy: new protocol

A problem with viewing ingested fluorescent material in the intestinal lumen of L1 larvae is that it is difficult to distinguish it from autofluorescence in intestinal cells (emitted particularly by gut granules). For this reason it is helpful to mark the intestinal luminal using a method other than epifluorescence microscopy. This was achieved by means of a novel approach in *C. elegans*: use of reflective confocal microscopy (RCM). This was optimised to highlight refractive material which we take to be the terminal web that surrounds the intestinal lumen: a dense cytoskeletal network of intermediate filaments at the base of the microvilli, and immediately beneath the apical membrane of instinal cells (McGhee, 2007).

This was performed using an inverted LSM880 microscope (Carl Zeiss, Jena) and a Plan-Aprochromat 63x 1.4 numerical aperture (NA) oil objective with a working distance of 0.19 mm. The main beam splitter was set to T80/R20 with multiphoton laser 405nm excitation. Emission was recorded using an inbuilt GaAsP detector.

2.3.7 Transmission electron microscopy

Nematode sample preparation was based on a standard protocol (Shaham, S. in WormBook 2006 protocol 8). Briefly, animals were washed twice in M9 buffer, placed in fixing solution (2.5%

glutaraldehyde, 1% paraformaldehyde in 0.1 M sucrose, 0.05 M cacodylate) and, to increase staining dye penetration, cut below the pharynx to remove the heads using a 30 G hypodermic needle. They were then rinsed 3 times in 0.2 M cacodylate, fixed in 0.5% OsO_4 and 0.5% $KFe(CN)_6$ in 0.1 M cacodylate on ice and sequentially washed in 0.1 M cacodylate and 0.1 M sodium acetate. Nematodes were then stained in 1% uranyl acetate in 0.1 M sodium acetate (pH 5.2) for 60 min, rinsed 3 times in 0.1 M sodium acetate and then rinsed overnight in Milli-Q water. Samples were then embedded in 3% seaplaque agarose, dehydrated and infiltrated using ethanol and propylene-resin series and then cured at 60˚C for 3 days. Serial 1 μm sections were taken for light microscopy, and, at the posterior half after the uterus, ultra-thin sections were cut at 70–80 nm using a diamond knife on a Reichert ultramicrotome. Sections were collected on formvar-coated 2x1 mm slot grids which allowed low magnification images to be taken without grid bars and stained with lead citrate before being viewed and imaged in a Joel 1010 Transition Electron Microscope (TEM). Images were recorded using a Gatan Orius camera, and obtained using Gatan imaging software.

2.3.8 Ablation of germline precursor cells

Live L1 larvae were mounted on a glass slide on a 5% agar pad with levamisole as anaesthetic. The concentration of levamisole in M9 buffer /Milli-Q water was optimised and maintained among pairs of sibling species: 0.2 mM levamisole in M9 for *C. elegans, C. inopinata, C. tropicalis* and *C. wallacei*; 0.2 mM levamisole in a 1:1 ratio of M9 to Milli-Q water for *C. briggsae* and *C. nigoni* as these species were found to be hypersensitive to salt; and 0.1 mM levamisole in M9 for *P. pacificus* and *P. exspectatus*, as *Pristionchus* larvae survival post recovery from paralysis using levamisole was found to be affected at higher concentrations. Ablations were performed using a Zeiss Axioplan 2 fitted with an Andor MicroPoint laser unit (CE N2 Laser with Ctlr/PSU/IntLk) at 440 nm and Dye Cell 435 nm filter. Germline precursor cells (Z2 and Z3) were identified by morphology and position with Nomarski optics and ablated in newly-hatched L1 animals using a standard protocol (Bargmann & Avery, 1995). Following ablation, larvae were transferred to fresh plates by washing them off with M9 buffer (30 μl) for all the pairs of species except for *C. briggsae* and *C. nigoni* which were recovered in a 1:1 ratio of M9 to Milli-Q water (total 30 μl). All ablated animals were then allowed to recover to day 1 of adulthood and checked under a Nikon SMZ645 microscope for both a lack of egg laying, indicating that the ablation was successful, as well as the presence of a vulva, indicating the Z1 and Z4 cells were intact. For unmated females which do not lay eggs, 15-20 randomly selected worms per condition per trial were checked under Nomarski (10 x air objective and without

immobilisation) on an NGM plate for the presence of a fully developed gonad, and none were found to have one. Mock treatment animals underwent the same manipulations as ablated animals with the exception of being shot with the laser microbeam.

2.4 Protein identification and quantification

2.4.1 Microscopy analysis of fluorescence-labelled YP on NGM plates: new protocol

2.4.1.1 Experimental setup and plate imaging

10 GA1500 L4 larvae were transferred to freshly made 35 mm NGM plates (n = 5 plates per trial; total 50 worms), seeded with 100 µl OP50 24 hr before use to ensure consistent bacterial lawn thickness. Every 24 hr worms were carefully transferred to new plates, with care taken not to disturb the OP50. Worms that bagged (i.e. with internally hatched larvae) or died were replaced with worms that had been maintained for this purpose. Plates with ruptured worms were censored to avoid spillage of internal YP which would confound results. After worms were transferred, 5 superimposed GFP/Nomarski 5 x air objective images were taken of each treated and control plate at random positions across the OP50 lawn to finally cover approximately half the lawn, where worms spend most of their time feeding. For each time point 3 control NGM plates were also treated exactly the same way and imaged, apart from having worms placed on them.

2.4.1.2 Fluorescence quantification

A method was developed to measure relative levels of GFP-labelled protein on NGM plates that have high and varying levels of autofluorescence (background fluorescence), based on NGM thickness, which results in a relatively weak GFP signal to noise ratio. As the protein of interest was observed to be isolated to individual regions on plates, the minimum emission fluorescence of an NGM plate can be used as a an indicator of the true level of background fluorescence, and the range between the minimum and maximum background fluorescence of NGM was found to be near constant (data not shown). By measuring the background autofluorescence of control plates and normalising it to the minimum of treated plates, the maximum background fluorescence of a treated control plate can be estimated and subtracted, as follows (note: fluorescence calculations only refer to the GFP channel):

(i) Images with dust and/or cholesterol crystals (which reduce the minimum emission fluorescence and affect the background fluorescence range) were manually censored (visualised under Nomarski as black dots or black crystals).

(ii) The ratio of minimum and maximum values of fluorescence intensity (FIR) is given by:

$$\rho = \frac{F_{\max}}{F_{\min}}$$

where $F_{\max}$ is the maximum emission fluorescence detected on a plate, and $F_{\min}$ the minimum emission fluorescence detected on a plate (both from background fluorescence; $F_{\min}$ to $F_{\max}$ = background fluorescence range).

(iii) The FIRs were averaged for the three control plates imaged each day to provide a Daily Control Fluorescence Intensity Ratio $\bar{\rho}$ (DCIR). This also takes into account variation in UV lamp output during sample excitation. For each treated plate image, the DCIR was multiplied by the image $F_{\min}$ in order to set a threshold (T) fluorescence level on treated plates below which all fluorescence was considered background fluorescence and ignored.

$$F_T = F_{\min}\,\bar{\rho}$$

(iv) This done, the remaining fluorescence from above the threshold is isolated to ROIs (region of interests) containing GFP-labelled protein, with the fluorescence consisting of both GFP fluorescence as well as background fluorescence. Background fluorescence from these ROIs is then subtracted as follows:

$$F_{\text{GFP}} = -AF_T + \sum_u F_u \qquad A = \text{Pixel count}$$

where $F_{(\text{GFP})}$ is the total fluorescence from GFP on the plate, and F_u is the fluorescence from a given ROI, and $\sum_u F_u$ the total fluorescence from the collection of ROIs remaining on an image after step (iii).

(v) Separation of yolk and oocyte fluorescence was done manually for each image using Volocity 6.3 Acquisition. The free-drawing tool was used to identify oocytes on Nomarski/GFP images by only viewing the Nomarski image. All sum fluorescence within the ROIs was then subtracted from the total calculated in steps (i-iii).

$$F_{\text{Free yolk}} = F_{\text{GFP}} - \sum_u F_{\text{Oocyte}(u)}$$

2.4.1.3 Automating calculations (developed by Antoine Salzmann)

Using the method and calculations provided in (1.4.1.2), steps (ii-iv) in (1.4.1.2) were programmed in Python by Antoine Salzmann to enable quick analyse of many plates in large data sets. For smaller experiments, all steps were performed manually.

2.4.2 Protein gel analysis of YPs

2.4.2.1 Collection of vented YPs on NGM plates: new protocol

100-200 L4 larvae were left on 35 mm plates freshly seeded with 100µl OP50. Worms were transferred every 24 hr with care taken not to disturbing the OP50 lawn. After transferring, a 1 ml solution of 0.001% NP-40 to solubilise yolk (Sharrock et al., 1983) in M9 mixed with a 0.002 mg/ml concentration of BSA (bovine serum albumin) as an external standard was pipetted onto plates, and a small flexible and disposable polystyrene bacterial loop used to sweep up and suspend all surface material in the solution, followed by pipetting into an Eppendorf tube for collection. The addition of BSA both served as a control while loading samples into wells for gel electrophoresis, as well as a control for protein loss (via protein absorption into NGM) or concentration (via M9 alone infiltrating into NGM) during sample collection (BSA is similar in size to YPs, but not so similar that it interferes with YP band detection on gels).

Collected samples were spun at 2600 rpm for 10 min at 4˚C, and the pellet collected as the oocyte fraction, and 500 µl of the supernatant for free yolk analysis. Samples were then lyophilised with 10 µl glycerol, and the remaining pellet solubilised in a solution of 30 µl 4% SDS solution pH 9, 1 ml 1M Tris HCl pH 8, 5 ml Milli-Q water, 10 µl EDTA, and 0.5M 12 mg bromophenol blue (optimised for YPs) by heating 2-4 times (based on the presence of a pellet after treatment) at 95˚C for 5 min while vortexing periodically, and finally centrifuged at 6,000 rpm for 15 min.

All pipetting was performed using LoBind pipette tips and storage was in LoBind Eppendorf tubes to prevent nonpolar residues from attaching to the surface of tubes or tips and so minimising protein loss.

2.4.2.2 Collection of internal (non-vented) YPs

10 worms per condition per treatment were transferred to NGM plates lacking bacteria and allowed to crawl for 30 sec - 1 min to remove surface bacteria. They were then transferred to 25 µl M9 and immediately frozen at -80˚C until used. Samples were added with 25 µL of 2× Laemmli sample buffer (Sigma-Aldrich), incubated at 70˚C and vortexed periodically for 15 min,

and then incubated at 95˚C for 5 min and centrifuged at 6,000 rpm for 15 min.

2.4.2.3 Gel electrophoresis and Coomassie colloidal staining

Sodium dodecyl sulfate–polyacrylamide gel electrophoresis (SDS-PAGE) was performed, using Criterion XT Precast Gels 4–12% Bis-Tris (Invitrogen) and XT MOPS (Invitrogen) as a running buffer (7:1 ratio with Milli-Q water) at 90V. Gels were stained with colloidal Coomassie blue as described (Kang et al., 2014), using 5% aluminum sulphate-(14-18)-hydrate and 2% orthophosphoric acid (85%) to create colloidal particles. Gels were analyzed using ImageQuant LAS 4000 (GE Healthcare). Protein band identification was based on published data (DePina, et al., 2011).

Within lanes, vented YPs were normalised to the BSA that had been added during sample collection as an external standard. For samples of internal YPs, YP bands were normalised to myosin as a standard to account for protein loss during gel loading, as well as to allow for normalisation to worm size when comparing different species.

2.4.3 Mass spectrometry of secretome proteins

2.4.3.1 Sample collection: new protocol

350 fully fed d4 hermaphrodites were picked onto NGM plates lacking OP50 and allowed to crawl for 30 sec - 1 min to remove surface bacteria before being transferred to a 500 µl solution of 0.001% NP-40 in M9 to prevent yolk from sticking to the body walls of animals (Sharrock et al., 1983) in a LoBind Eppendorf. The worms were allowed to vent for 30 min (dry picking worms into a tube took an additional 30 min), with the Eppendorfs lying horizontally to ensure even distribution of YP in the solution and to reduce the risk of worm rupturing. The Eppendorf was then inverted for 1 min and 350 µl of solution decanted from the top of the tube, leaving behind adults which sink to the bottom. After collection, samples were carefully checked for the presence of adult worms. Negligible numbers of unfertilised oocytes were observed, given the short amount of time that worms were left to vent. The tubes with adults remaining were checked thoroughly for adults that had ruptured, which were easy to identify, and if a ruptured worm was found the sample collected from that tube was censored. L3 larvae instead of d4 adults were used for control tubes.

2.4.3.2 Sample running

Independent samples were analysed on a Thermo Scientific™ Q-Exactive Plus Orbitrap mass spectrometer connected to an Ultimate 3000 nanoLC system. Samples were trapped on a Thermo Scientific Acclaim PepMap C18 cartridge (0.3 mm x 5 mm, 5 μm/100 Å) and then chromatographed on a Thermo Scientific Easy-Spray Acclaim PepMap C18 column (75 μm x 15 cm, 3 μm/100Å packing) eluting at 300 nl/min with a 30 min linear gradient of acetonitrile:water:formic acid (5:95:0.1 – 56:44:1 v/v/v). A full MS scan (m/z 135 – 2000 at 70,000 resolution) was acquired with a maximum injection time of 100 ms, and the 10 most intense ions with an intensity threshold 2.0e4 are selected for higher-energy C-trap dissociation (HCD) with a lock mass of m/z 445.12003. The normalised collision energy is 30, with an isolation width of 2 Da and dynamic exclusion of 20 s; singly charged ions were excluded. All chromatography solvents were Optima LCMS grade (Fisher Scientific).

2.5 Lipid staining and quantification

2.5.1 Bodipy staining of lipid

For each time point, vital staining of worms was performed as described (Klapper et al. 2011) using Bodipy 493/503 (488 nm Exc./505-575 nm Em.) (Invitrogen) 1 μg/mL in M9 solution at a final concentration of 6.7 μg/ml, with hermaphrodites incubated in dye for 20 min at RT in darkness. Worms were then transferred to NGM plates (lacking OP50) and allowed to crawl for 3-5 min to remove surface dye, followed by transfer to 35 mm NGM plates (lacking OP50), with 20 worms per plate (n = 1-2 plates per trial), and left to vent for 24 hr. Fluorescence quantification was performed as described in section (1.4.1), with the exception that Nomarski/fluorescence superimposed images were taken of the 5 regions with the most Bodipy fluorescence, which was done due to the lower levels of Bodipy fluorescence relative to YP-GFP fluorescence (likely due to differences in the fluorophores rather than the quantity of vented lipid vs protein). Plates that contained L4 larvae were found to contain no patches of Bodipy fluorescence, indicating that excess surface dye or egested dye did not cause false positive staining.

2.6 Fitness and behavioural assays

2.6.1 Lifespan assays

Animals were maintained at 25-30 worms per plate from the egg stage to minimise

deleterious density-associated effects (Ludewig, et al., 2017) (found to be exacerbated in certain species), and without the addition of FUDR (5-fluoro-2'-deoxyuridine) unless otherwise stated. Mortality was scored every 2-3 days, and all animals transferred every day during the reproductive period, after which transfer was performed every 6-7 days to avoid hypertonic stress due to plate desiccation. Female cohorts were checked carefully from the L4 stage for the presence of males, which shorten female lifespan. Worms were considered to be alive if they were motile or responded to gentle touch with a worm pick. Survival plots show combined lifespan data, with the L4 stage of development taken as day 0. Animals which disappeared from the plate, were accidently killed during handling, dried up on the wall, ruptured or exhibited internal hatching of larvae were recorded as censored. Tests for significant difference between survival curves were performed using JMP software, version 14.0 (SAS Institute, Inc.), with either log-rank test and/or a Cox fit proportional hazard analysis performed.

2.6.2 Brood size and unfertilised oocyte determination

L4 larvae were maintained individually on 35 mm NGM plates with *E. coli* OP50 lawns (n = 10 per trial), and transferred every 24 hr until unfertilised oocyte production ceased, with a minimum of 12 days scored for all worms. For scoring, the open Petri dish was place on an inverted plate bearing a grid of parallel lines, allowing the plate to be efficiently scored with a series of vertical sweeps. Where clumps of oocytes were seen, these were separated using a worm pick, to count individual oocytes. *P. pacificus* and *P. exspectatus* also laid some dead eggs, consistent with previous observations (R.J. Sommer, personal communication), which were discounted.

2.6.3 Pathology scoring

Using Nomarski microscopy, images of senescent pathologies in cohorts of worms (n = 5-10 per time point per condition per trial) were acquired on days 1, 4, 7, 11, 14, 17, 21 and blinded images analysed blind by trained observers using a semi-quantitative scoring system as previously described (Garigan et al. 2002; Riesen et al. 2014 and Ezcurra et al., 2018) to study pathology progression (see Figure 2.1). The scoring protocols were optimised to include all species, not just *C. elegans* as follows:

(i) Pharyngeal atrophy ageing features

a) Absence of radial muscle lines in anterior and posterior bulb

b) Expanded pharyngeal lumen

c) Absence of grinder (except for *Pristionchus*, which does not possess a grinder (Wei et al., 2003))

d) Presence of tissue degeneration vacuoles, caused by bacterial infection or ageing

Scoring:

1. No ageing features
2. One ageing feature
3. Two ageing features
4. Three or more ageing features
5. The pharynx is swollen and full of bacteria, indicating infection as mentioned in (Zhao et al., 2017), or unrecognisable

(ii) Gonadal deterioration

a) Gonad arms do not fill up the body cavity

b) Gonad arms are not mostly touching each other

Scoring

1. No ageing features
2. One ageing feature
3. Two ageing features
4. The gonad arms are fragmented
5. The gonad is unrecognisable

(iii) Uterine tumours

Scoring:

1. Healthy normal uterus of young adult hermaphrodite or female
2. Uterus contains no tumors and may contain unfertilised oocytes and/or few or no fertilised eggs
3. Small tumour present in one or both gonad arms
4. Large tumour(s) present, but do not fill the entire body cavity
5. Massive tumour(s) present, that fill the entire body cavity

Intestinal and PLP scoring was not changed and was performed as previously described (Ezcurra, et al., 2018). Briefly, intestinal atrophy was quantified by measuring the intestinal width near the tail just posterior to the posterior gonad, subtracting the luminal width and

dividing by the body width. Yolk accumulation was measured by dividing the area of yolk pools by the area of the body visible in the field of view through a 63 x objective.

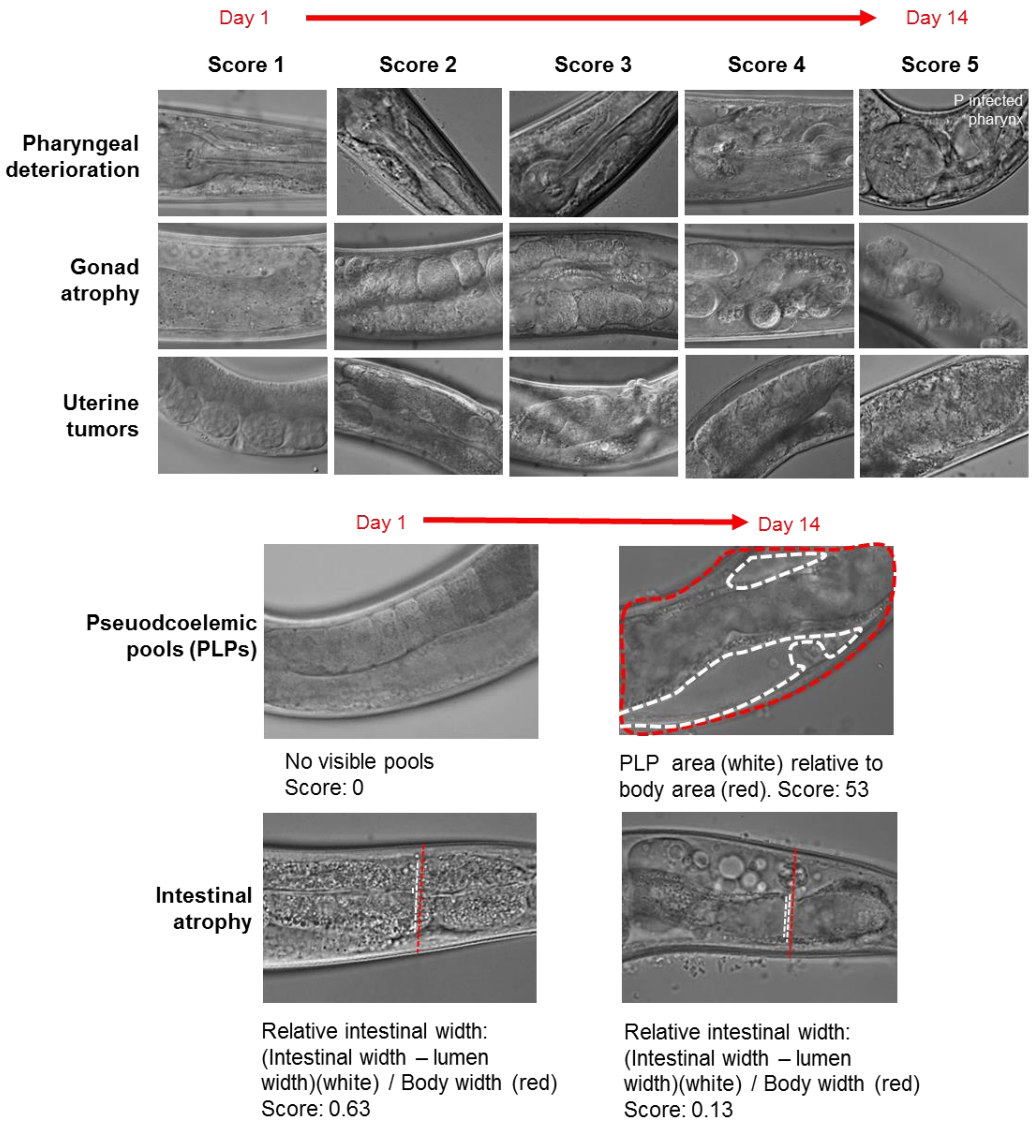

FIGURE 2.1. Pathology measurements. Representative images of pathology scores for *C. elegans* unmated hermaphrodites. Top: Pharyngeal degeneration, gonad atrophy and uterine tumour score (ordinal variables). Bottom: Intestinal atrophy and PLP calculation (continuous variables). Reproduced from (Ezcurra, et al., 2018).

2.6.4 Chemotaxis assay

2.6.4.1 Running and chemotaxis index calculation

The chemotaxis assay was adapted from (Margie, et al., 2013). Briefly, a 5 cm NGM plate was divided into quadrants with test compounds spotted on two opposite quadrants and controls spotted on the two remaining quadrants. Plates were then left for 4 hr (optimised for vented yolk) to form a chemotactic gradient. All spots also contained 4 µl of 0.25M sodium azide as anesthetic.

Next a 2 µl drop containing ~75 arrested L1 larva/µl (obtained through hypochlorite treatment of eggs and then leaving them to hatch in M9) was pipetted at the centre of the plate to a 0.5 cm radius inner circle region of the plate. Animals were excluded from the analysis if they failed to clear the inner circle or were lying on the marked lines. Animals that were located on the edges or walls of the plates were counted as part of the corresponding quadrant. For each experiment, a chemotaxis index (CI) was calculated as:

$$CI = \frac{A - B}{Total\ number\ of\ larvae}$$

where A is the total number of larvae in treated quadrants, and B is the total number of larvae in control quadrants. A + 1.0 score corresponds to maximal attraction, a −1.0 score total repulsion, and results close to 0 indicate a lack of response to the compound.

2.6.4.2 Treatment sample collection: new protocol

For treatments, either an individual d5 heat picked adult was used with controls treated the same way but lacking adult worms, or concentrated secreted proteins from d4 adults were collected as follows.

100 d4 adults were transferred to NGM plates without OP50 and allowed to crawl for 1-3 min to remove surface bacteria and then transferred to a small microwell cell culture plate (Thermo Scientific Nunc 24-well cell-culture multidishes, 1.9 cm^2) containing 500 µl NGM lacking bactopeptone (to prevent tearing of agar) and carbenicillin added topically 24 hr prior at a concentration of 50 mM. This was done by dry picking worms in groups of 30-40 and holding them above the microwell, immediately after which a 10 µl drop of M9 was pipetted onto the pick which gently removed and transferred all worms into the well (no more than 30 µl of M9 was used per well). The worms were then allowed to vent for 24 hr, after which a sterile scalpel was used to cut around the NGM well and transfer it to a 10 ml NGM plate (lacking OP50) right side up. Adults were left for 1 hr to crawl off, after which remaining adults were picked off. The NGM with vented yolk was then cut into quadrants and each was placed as a treated section in a chemotaxis assay. Control sections were treated the same way but either had no worms, or L3 larvae added instead of d4 adults.

2.6.5 Larval growth assay through length measurement

2.6.5.1 Preconditioning of plates with vented yolk milk for larval growth assays: new protocol

30 d4 adults were washed twice in M9 to remove surface bacteria and left to vent for 24 hr on 35 mm NGM plates lacking bactopeptone, with 30 µl of 500 mM carbenicillin in Milli-Q water (plus 4 µl of 500 mM kanamycin in Milli-Q water for RNAi-treated adults as RNAi clones contain a carbenicillin/ampicillin resistance plasmid) added topically 24 hr prior (2-3 plates per trial). Controls had no d4 adults or L3 larvae treated in the same way. Plates with bagging or ruptured worms were censored. Next 200 alkaline hypochlorite-treated eggs were placed on each plate and left for 48 hr to develop, after which larval length was measured.

2.6.5.2 Tests of yolk milk feeding by mothers of their own larvae: new protocol

Shortly after reaching d3 of adulthood, 30 hermaphrodites were washed twice in M9 and placed on 35 mm bactopeptone-less NGM plates (2-3 plates per trial) and left for 24 hr to lay their last eggs. Following this, the adults were either left in situ to vent yolk, removed, or replaced with surrogate worms of the same age. After 48 hr all adults were removed and larval length measured. Plates with bagging or ruptured worms were censored.

2.6.5.3 Larval length measurements

To collect larvae, plates were washed using 500 µl of M9 x 3 times and the collected liquid freeze-thawed (-80˚C) to straighten the larvae. The samples were spun down at 2,000 RPM at 4˚C for 5 min and the pellet along with 500 µl of liquid above it placed on slides for imaging. Volocity 6.3 software (Macintosh version) was then used to measure length.

2.7 Statistical and further computational analysis of data

No statistical methods were used to predetermine sample size. The experiments were not randomised. The investigators were not blinded to allocation during experiments and outcome assessment unless otherwise stated. All statistical tests were performed on raw data using GraphPad Prism 8.0 unless otherwise stated.

2.7.1 Pathology data analysis: New protocol (StJohn Townsend helped with the development of this method)

2.7.1.1 Gradient calculation using generalised linear models

In order to prepare data for modelling, data were pre-processed for the following reasons. Peak pathology level for *C. elegans* is reached by d14, after which pathology levels plateau (Garigan et al. 2002; Riesen et al. 2014; Ezcurra et al., 2018). Thus, pathology data after d14 obscures calculation of gradients representing pathology progression, and only d1-14 were analysed for gradient calculation in order to capture the initial rate of pathology progression. Intestine scores for each combination of species and treatment were normalised to the respective mean intestine score at d1. Therefore, normalised intestine scores represent the change in percentage of intestinal volume, accounting for differences in terms of the ratio of intestinal width to whole body width between species (see 1.6.3). For PLP scores no normalisation was used because percentage of the body cavity containing yolk pools was measured. PLP were analysed as score + 1, in order to ensure all data were positive (a requirement for Gamma regression).

Generalised linear models were applied to the data to test the effect of species, treatment and trial on pathology progression. Interactions terms between these variables were also included. Different model families and link functions were systematically applied to each pathology dataset according to the type of data recorded. For positive, continuous variables (intestine and yolk), pathology scores were modelled as Gaussian and Gamma distributed variables. For ordinal variables (tumour, gonad and pharynx), cumulative link models were applied to the data using the *ordinal* package in R (Christensen, 2019). The following models were selected for each pathology based on minimisation of Akaike information criteria, meaning that these models explained the most variance in pathology progression using the fewest number of terms:

(i) Intestine: Gaussian distributed response variable with inverse link function
(ii) Yolk: Gamma distributed response variable with identity link function
(iii) Tumour, gonad and pharynx: ordinal distributed response variable with log-gamma link function

The vast majority of trial terms were not statistically significant across all pathologies, indicating that differences in pathology progression were reproducible and robust. Hence, trial was not considered further as a variable. In order to compare whether differences in pathology progression between combinations of species and treatment were statistically significant, t-tests were applied explicitly to comparisons of interest using the *multcomp* package in R (Hothorn, et al., 2008).

2.7.1.2 Pathology comparison and relationship to lifespan

In order to compare differences in pathology progression across species and treatments, the gradients from each model were transformed into Z-scores (which describe a value's relationship to the mean of a group of values). This is necessary because the scale of each gradient is different as the scales for each pathology are different. Pathology Z-scores were displayed and compared as heatmaps, using pairwise Euclidean differences to cluster pathologies and species/treatments according to profile similarity.

In order to model the impact of pathology Z-scores on lifespan, linear regression was performed, using the pathology Z-score as the independent variable and the inverse of mean lifespan as the dependent variable. In order to assess the combined impact of all pathologies on lifespan, the median of the pathology Z-scores was used as the independent variable. The Z-scores for all pathologies were found to be statistically significant, and the median pathology Z-score was found to perform better than the individual pathologies.

2.7.2 Bioinformatic analysis of secretome proteins

Proteomes were quantified using MaxQuant 1.6.12.0 (Cox & Mann, 2008) with the default search settings and the *C. elegans* protein database from Uniprot (downloaded on 20 Dec 2019), and downstream analysis was performed using the Proteus package in R (Gierlinski, et al., 2018). Proteins were considered detected in a sample if at least two proteotypic peptides from that protein were detected. Proteins were scored as present in the secretome if present in at least two of the three replicate samples. Proteins were only considered specific to the d4 secretome if not detected in all three L3 control samples.

To approximately quantitate the composition of the secretome, proteins were manually classified according to known functions, and the sum of all peptide intensities across each grouping was used to calculate an approximate relative abundance of each grouping. Significant over-representation of secretome proteins with respect to other datasets was detected using a SuperExactTest (Wang, et al., 2015). To assesses whether the adult secretome showed any distinct patterns of expression in ageing worms or worms with altered IIS (in *daf-2(e1370)* and *daf-16(mu86)* mutants, which are similar to the *daf-16(mgDf50)* mutants used in other experiments here), an existing proteome dataset (Walther, et al., 2015) was used. Proteins were considered upregulated in ageing worms if expression at least doubled from d1 to d17. Proteins were considered IIS-upregulated if expression in d17 wild-type worms was at least twice the expression in d17 *daf-*

2(e1370) worms, normalising for any initial expression differences between d1 wild-type and *daf-2(e1370)* worms. The presence of signal peptides in *C. elegans* proteins was predicted using SignalP 5.0 (Armenteros, et al., 2019). In order to compare the composition of secretome proteins to human milk (D'Alessandro, et al., 2010), cross-species gene set analysis was performed using the XGSA package in R (Djordjevic, et al., 2016), accounting for protein homology mapping between *C. elegans* and humans. Tissue enrichment analysis was performed using the Wormbase tissue enrichment tool (Angeles-Albores et al., 2016) whilst GO term and Interpro term enrichment analysis was performed using DAVID 6.8 (Huang, et al., 2009).

Chapter 3: *C. elegans* provide milk for their young

3.1 Introduction

Investigations of ageing in *C. elegans* have identified interventions which greatly increase lifespan, including removal of the germline (Hsin and Kenyon, 1999), and reduction in insulin/IGF-1 signalling (IIS) (Kenyon, 2010). However, proximate mechanisms of ageing upon which signalling pathways act to accelerate ageing have been difficult to identify. One possible mechanism involves yolk production. In *C. elegans* hermaphrodites, yolk is synthesised by the intestine and transported to oocytes (Kimble, 1983). After depletion of sperm, yolk synthesis continues, supported by autophagy-dependent consumption of intestinal biomass and formation of yolk-rich PLPs (Ezcurra et al., 2018; Garigan et al., 2002; Herndon et al., 2002; Sornda et al., 2019) (Figure 1.7B). Given that yolk production serves no clear purpose in post-reproductive hermaphrodites, this self-destructive process has been interpreted as futile run-on of reproductive function, and is promoted by the *daf-2* IIS receptor (Ezcurra et al., 2018; Herndon et al., 2002) (Figure 1.7B). Here *daf-2* exhibits antagonistic pleiotropy (Williams, 1957), promoting growth, reproduction and pathology, the latter resulting from a futile reproductive programme, or quasi-programme (Blagosklonny, 2006; Ezcurra et al., 2018).

During human ageing, senescent pathologies mainly appear towards the end of life. But *C. elegans* is different: major pathologies develop relatively early, beginning soon after the end of reproduction by selfing (Ezcurra et al., 2018; Garigan et al., 2002; Herndon et al., 2002; Sornda et al., 2019; de la Guardia et al., 2016; Wang et al., 2018) (Figure 1.6). Moreover, in hermaphrodites senescent pathologies are much more extreme than those seen in humans, mice or fruit flies. Not only is there severe intestinal atrophy and yolk steatosis but also gonadal disintegration and the development of large uterine tumours (de la Guardia et al., 2016; Wang et al., 2018) (Figure 1.6,1.7 and 2.1). This is reminiscent of pathology in semelparous organisms that undergo reproductive death (Gems et al., 2020; Finch, 1994a). Moreover, destructive conversion of somatic biomass to support reproduction is a feature of reproductive death (Gems et al., 2020). This suggests the possibility that *C. elegans* might exhibit reproductive death. However, what argues against this interpretation is the seeming futility of the massive, destructive effort by post-reproductive mothers to convert their soma into pools of yolk rich lipid.

Results presented in this chapter imply that this effort is not futile, but instead allows sperm-depleted mothers to continue to contribute to fitness by feeding yolk to their offspring. This and other evidence which will be presented in the next two chapters supports the view that *C. elegans*

exhibit reproductive death, suppression of which leads to large increases in lifespan. This has major implications in terms of the relationship between mechanisms of ageing in *C. elegans* and humans.

3.2 Results

3.2.1 Production of YP170 vitellogenins promotes life-limiting intestinal senescence in *C. elegans*

Three abundant yolk protein species are produced in *C. elegans* to provision oocytes: YP170 (YP: yolk proteins [vitellogenins]) derived from *vit-1–vit-5* which share a high level of sequence similarity (Spieth & Blumenthal, 1985); and YP115 and YP88 derived from *vit-6*. *vit-5* and *vit-6* RNAi have been shown to selectively suppress accumulation of YP170 and YP115/YP88, respectively (Sornda, et al., 2019). Inhibition of YP170 alone via *vit-5* RNAi results in a reciprocal increase in YP115/YP88 levels due to posttranscriptional compensatory mechanisms (Sornda, et al., 2019) and vice versa. Suppression of yolk accumulation by simultaneous knockdown of all YPs via *vit-5,-6* RNAi inhibits intestinal atrophy and modestly extends life span (Ezcurra, et al., 2018).

To test which of the YPs, YP170 or YP115/YP88, are more important for pathogenesis, intestinal atrophy and change in lifespan were measured following knock down of the different YPs via RNAi (Figure 3.1). Consistent with (Ezcurra, et al., 2018), simultaneous knock down of all YPs rescued intestinal atrophy (Figure 3.1A) and increased worm lifespan (significantly in 2 out of 3 trials) (Figure 3.1B). Inhibition of YP170 production alone, despite increasing YP115/YP88 synthesis (Sornda, et al., 2019), also reduced intestinal atrophy (Figure 3.1A) and increased lifespan (significantly in one trial out of 3) (Figure 3.1B) as much as the abrogation of all YPs, consistent with previous observations (Murphy, et al., 2003). In contrast, inhibiting YP115/YP88 production alone accelerated intestinal atrophy (Figure 3.1A) and reduced life span (Figure 3.1B, and Appendix 1 for additional statistics). *vit-6* RNAi lifespan trials showed a consistent decrease, which reached statistical significance in 2 of the 5 trials, suggesting that the effect is small but real. Taken together, these results imply that YP170 production specifically drives intestinal atrophy and this reduces lifespan.

Next PLP accumulation was measured to see if it follows the same pattern given intestinal atrophy is linked to the production of PLPs in the body cavity. Significant PLP change following the pattern of intestinal atrophy was only seen with *vit-5,-6* RNAi knockdown. This suggests that high levels of either YP170 or YP115/YP88 are sufficient to assure normal levels of yolk lipid

production and/or transport into the body cavity. That said, it should also be noted that PLP scoring is likely to be less accurate (see methods section) than intestinal atrophy scoring and, as such, smaller changes in PLP level might not be detected.

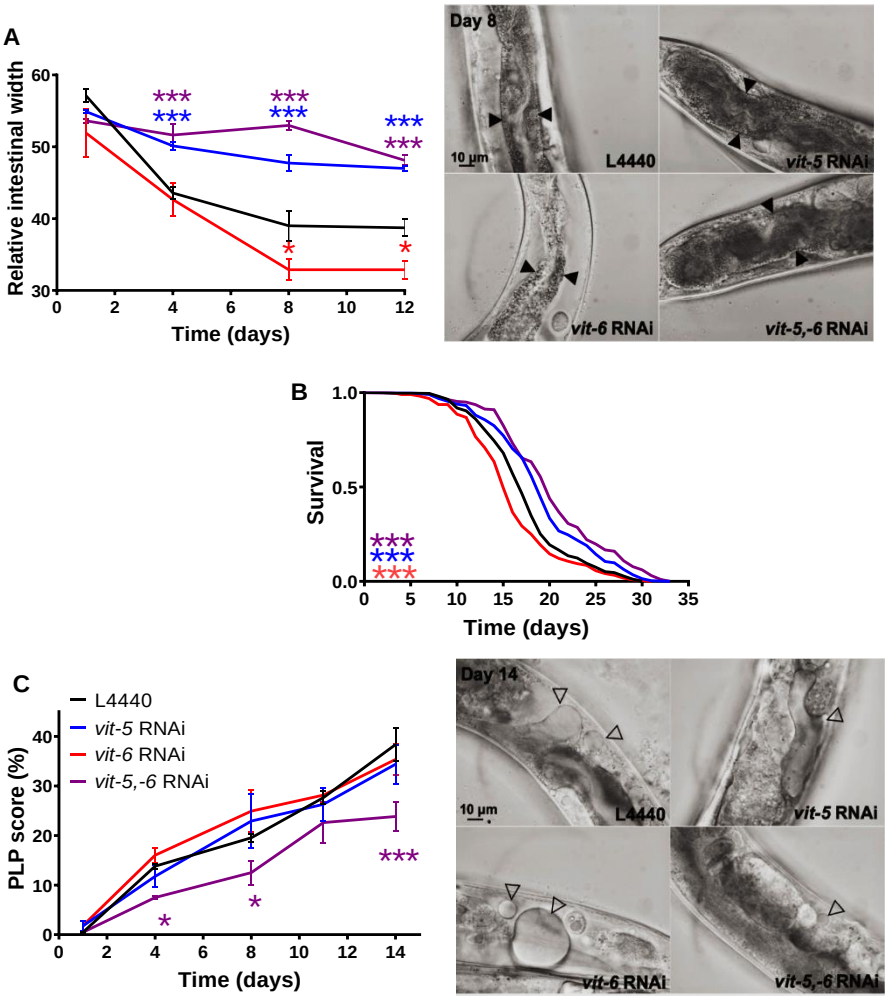

FIGURE 3.1. YP170 production accelerates intestinal atrophy and shortens life span. (A) Effect of *vit* RNAi on intestinal atrophy. Left: Nomarski images. Right: quantitation. **(B)** Effect of *vit* RNAi on life span. Combined lifespans of 3 trials. Cox proportional hazard. For additional statistics see Appendix 1. **(C)** Effect of *vit* RNAi on yolk pool accumulation. Left: Nomarski images. Right: quantitation. **(A,C)** Filled arrowheads: intestine; open arrowheads: PLPs. Data are mean ± s.e.m., age-matched comparison. Scale 10µm. N=3. **P*< 0.05, ****P* < 0.001. Part of the lifespan and pathology data collection was performed by Thanet Sornda. Data in this figure is published (Sornda, et al., 2019).

3.2.2 Post-reproductive *C. elegans* hermaphrodites vent yolk through the vulva

Post-reproductive *C. elegans* hermaphrodites continue to synthesise vitellogenin into late life, and accumulation of PLP is coupled to organismal senescence, including atrophy of the intestine (Ezcurra et al., 2018; Sornda et al., 2019). A question is whether this seemingly futile effort to generate PLPs could somehow promote fitness? After sperm depletion hermaphrodites

lay copious unfertilised oocytes (Ward and Carrel, 1979) (Figure 3.2A,B). We noted the venting of a brownish granular substance during the same period (Figure 3.2A,B). VIT-2::GFP labelled yolk was used to test the idea that this substance was yolk (Hall, et al., 1999). Patches left on plates by hermaphrodites expressing the GFP-tagged vitellogenin (Grant and Hirsh, 1999) were GFP-positive and sometimes associated with unfertilised oocytes which were invariably strongly GFP positive (Figure 3.2A,B).

In terms of timing, quantitation of GFP patches on plates showed that venting of free vitellogenin begins and peaks on d4-6 of adulthood, the same time that unfertilised oocyte production peaks, immediately after cessation of egg-laying, and then continued at lower levels until at least d14 (Figure 3.2C).

Video capture of adults as they crawled on NGM plates confirmed yolk venting through the vulva (Appendix 2 video 1), sometimes along with unfertilised oocytes (Figure 3.2 D,15,16). Airyscan confocal imaging of VIT-2::GFP hermaphrodites showed high levels of free yolk surrounding unfertilised oocytes in the uterus at the age when unfertilised oocytes and yolk patches were deposited on plates (Figure 3.3). By contrast, prior to this when the majority of egg-laying occurs much lower levels of free yolk were seen in the uterus of adults (Figure 3.3) and free yolk was not detected surrounding laid eggs (Appendix 2 video 2). Video capture also confirmed venting of yolk collected in the uterus (Figure 3.4 and Appendix 2 video 1).

Oocytes laid by sperm-depleted mothers also contain vitellogenin and can be easily distinguished on plates using stereomicroscopy. Quantitation of fluorescence from GFP in oocytes relative to free vented yolk revealed twice as much yolk in oocytes at the peak of venting (Figure 3.5A), but the proportion of free vented yolk increased with age until d10, when the ratio was 1:1.

The presence of vented vitellogenin on NGM plates was confirmed using gel electrophoresis. Vented yolk was washed off plates and centrifuged gently to separate unfertilised oocytes (pellet) from free yolk followed by gel electrophoresis and Coomassie colloidal blue staining of the most abundant YP170 band (Figure 3.5A-D). Quantitation of vented free yolk and yolk in unfertilised oocytes using this method defined the same pattern of age changes in vented yolk abundance as fluorometric quantitation of VIT-2::GFP-labelled yolk (Figure 3.5A).

Yolk venting could reflect either an active behaviour or passive leakage, perhaps due to senescence of the vulva. Timing of yolk venting, which coincides with unfertilised oocyte laying (Figure 3.2C), as well as the fact that oocytes and free yolk were often found to be vented together (Figure 3.2A,B, 17A), strongly imply the former. Observations of yolk venting from videos confirm that it is an active process. As with egg-laying or laying of unfertilised oocytes, yolk

venting occurred intermittently and typically in substantial bursts leading to emptying of yolk from the proximal uterus with each burst taking around 5 seconds (Figure 3.4 and Appendix 2 video 1,2). Notably, muscle contraction in the uterus and vulva during yolk venting resembled contraction seen during egg-laying (compare Appendix 2 videos 1 and 2). Thus, venting of free yolk and unfertilised oocytes is an actively regulated process, likely involving the egg-laying neuromuscular and hormonal regulatory system.

PLPs in the body cavity also contain lipid (Hellerer, et al., 2007) which is likely to include yolk lipids, and lipids from intestinal depots released due to gut atrophy (Ezcurra et al., 2018). Staining mothers with the lipid dye Bodipy 493/503 revealed lipid venting that correlated with vented vitellogenin levels (Figure 3.5E). Thus, vented yolk contains substantial amounts of lipid as well as protein.

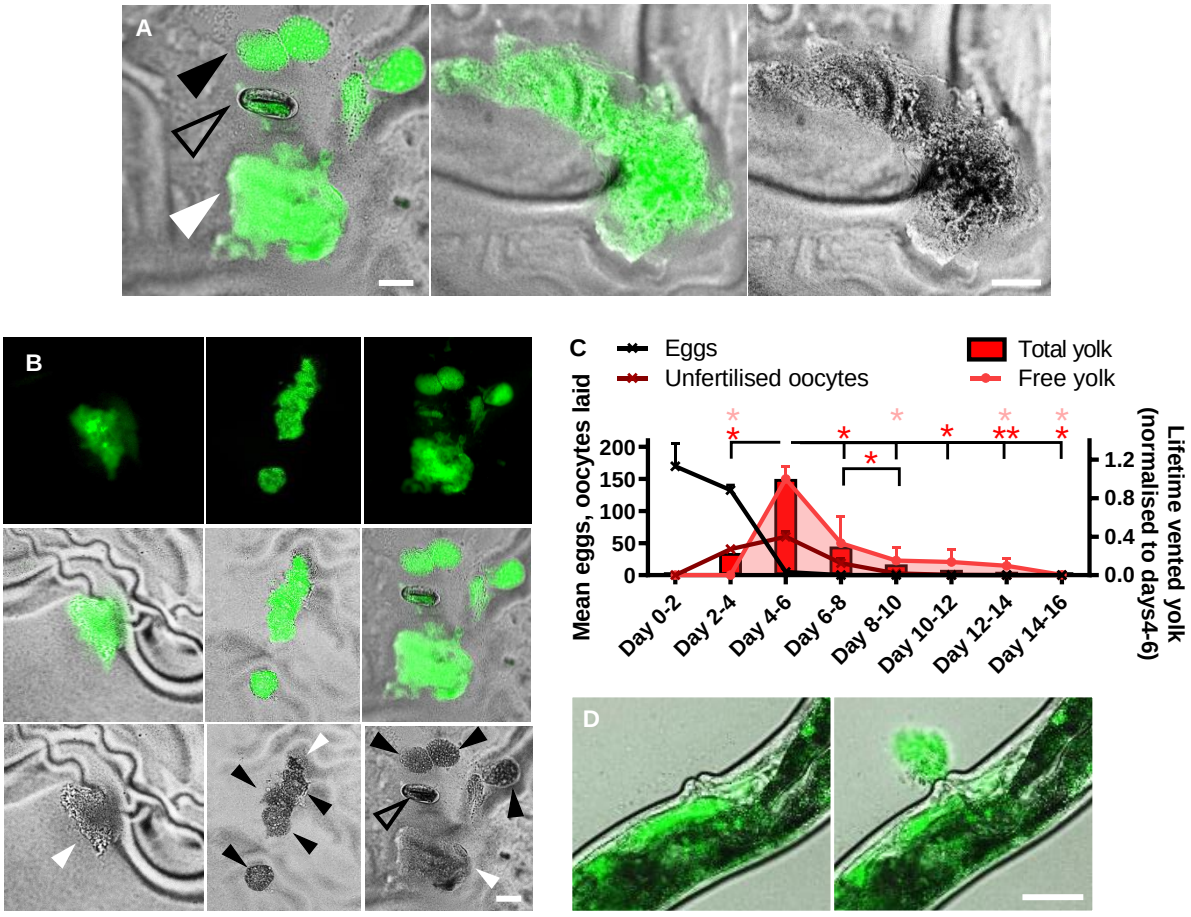

FIGURE 3.2. Yolk venting by adult worms. (A,B) Vented yolk pools and unfertilised oocytes on NGM plates from hermaphrodites on d4 of adulthood, expressing *vit-2::GFP*. **(A)** Left: x200, right: x1000. **(B**) x200. **(C)** Lifetime reproductive schedule, oocyte production, and proportion of total vented yolk (from oocytes + free yolk) and free yolk quantitated from VIT-2::GFP on plates and normalised to d4-6. Mean ± s.e.m. of 3 trials displayed (n=50 per trial for venting and 10 per trial for brood sizes). **P*<0.05, ***P*<0.01 by one-way ANOVA (Tukey correction). **(D)** Live imaging of *VIT-2::GFP* d4 adults with yolk visible in the uterus followed by yolk venting a few seconds later (c.f. Figure 3.4). Scale 50 µm. Antoine Salzmann helped with the microscopy analysis of vented yolk and Mike Cao assisted with the acquisition of some of the venting images.

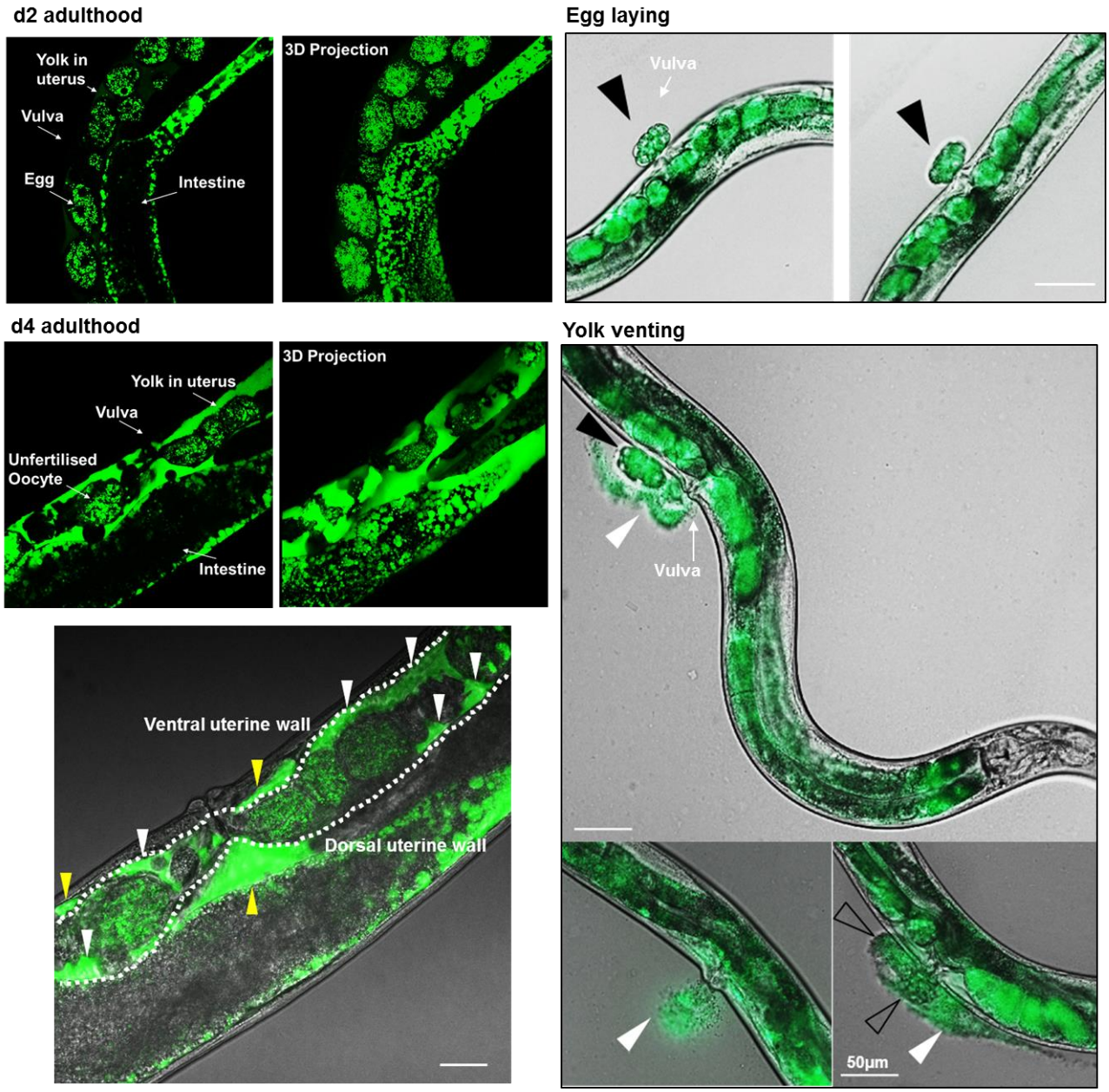

FIGURE 3.3. Yolk venting on d4 of adulthood relative to egg laying on d2. Left: *VIT-2::GFP* d4 adults with internal yolk in the uterus, compared to d2 adults with little/negligible yolk in the uterus. Airyscan confocal and Nomarski images. 3D projection of images of 41 Z-planes taken up to a sample depth of 41 µm through half the width of the same worms. Right: images of venting on d4 and no yolk seen surrounding laid eggs on d2. White arrowheads: vented free yolk and free yolk in the uterus; open arrowheads: unfertilised oocytes, black arrowheads: eggs, yellow arrowheads: yolk in the body cavity. Scale 50 µm.

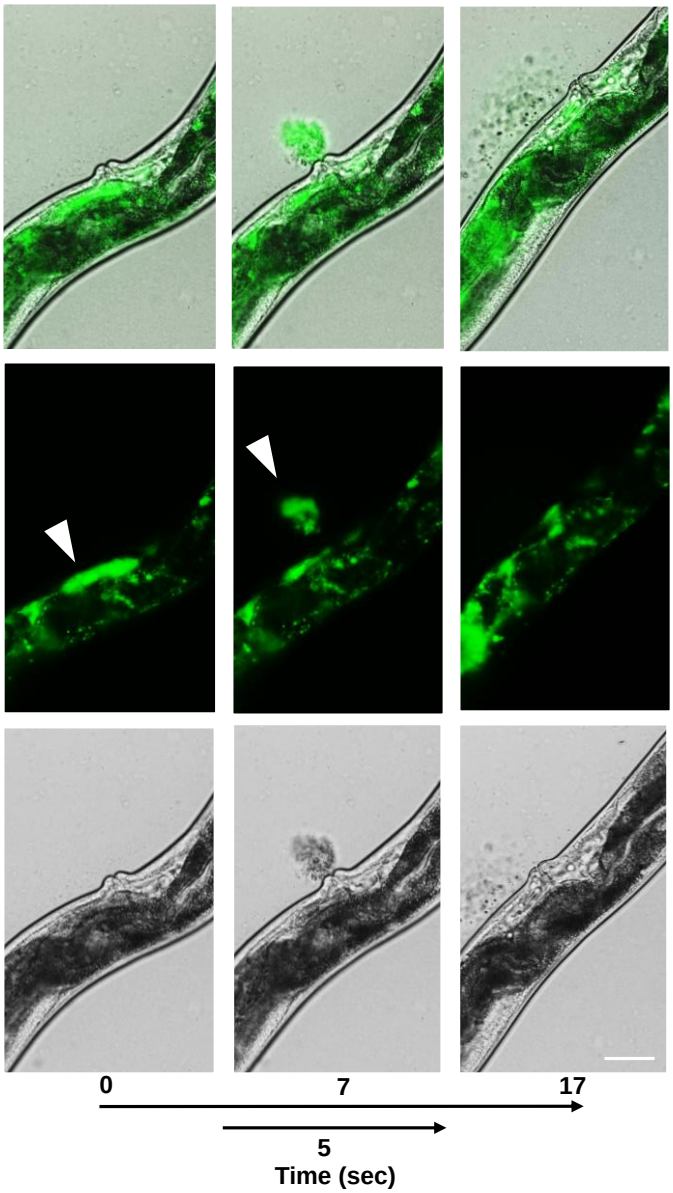

FIGURE 18. Venting time course. Nomarski, GFP and superimposed images. Left: yolk seen in the uterus at time 0 sec, middle: yolk venting at time 7 sec, and right: less yolk in the uterus post venting at time 17 sec. One venting burst takes approximately 5 sec (for full video of yolk venting images are taken from, see Appendix 2 video 1). Scale 50 µm.

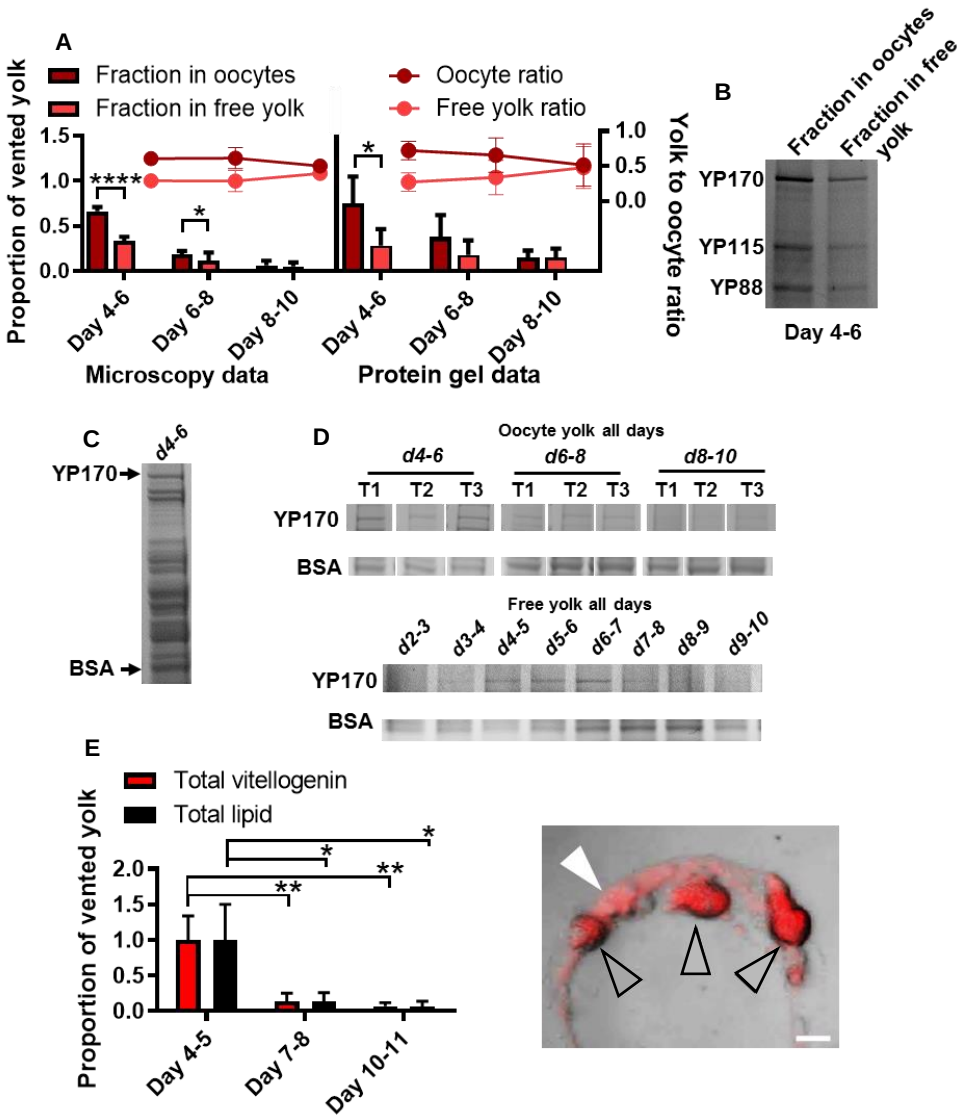

FIGURE 3.5. Vitellogenin in free yolk and oocytes and lipid venting. (A) Relative levels of free yolk vs yolk in unfertilised oocytes. Right: quantitated from VIT-2::GFP fluorescence on plates (n=10 per trial), or from protein gel analysis of YP170 vitellogenin washed from plates (n=100). Data normalised to total yolk on d4-6. Mean ± s.d. of 3 trials displayed. **(B)** Protein gel YP bands after collection from plates on d4-6 (c.f. A). **(C)** Relative position of BSA and YP170 (most abundant YP) on a gel. Other YP bands collected from plates are usually too faint to be observed. **(D)** Gel images of YP170 on all days. **(E)** Lipid venting by adults vital stained with Bodipy 493/503. Right: quantitated *VIT-2::GFP* and vented lipid Bodipy, normalised to d4-6. Left: image of vented lipid and laid oocytes stained with Bodipy. White arrowheads: vented free yolk; and open arrowheads: unfertilised oocytes. Data show mean ± s.e.m of 3 trials. **P*<0.05, ***P*<0.01 by one-way ANOVA for (Bonferroni correction). Scale 50 µm.

3.2.3 Vented yolk supports larval growth

One possibility is that yolk is vented deliberately to support larval growth. Consistent with this, VIT-2::GFP labelled-yolk was visible in the intestinal lumen of L1 larvae after they were left on NGM plates with no food apart from vented yolk for 4 hr (Figure 3.6A). This was visualised using airyscan and superimposed reflective confocal microscopy (RCM) (Figure 3.6A), with RCM being a novel technique in *C. elegans* used to highlight the terminal web that surrounds the

intestinal lumen (Figure 3.6B) and so distinguish fluorescence in the intestinal lumen from surrounding gut granule autofluorescence.

Notably, pre-treatment of *E. coli*-free agar plates with post-reproductive d4 mothers enhanced growth of L1 larvae relative to control (no pre-treatment) plates (Figure 3.6C,D), suggesting larvae can use vented yolk as a food source. As pheromones or other secreted compounds could have resulted in the effect, additional control plates were pre-treated using L3 larvae which likely secrete similar compounds to adults but do not vent yolk (Figure 3.2C; L3 larvae lack a fully formed vulva through which yolk venting occurs and the onset of vitellogenesis is after the L4 stage of development), and similar results were seen (Figure 3.6C,D). To rule out the possibility of the action of other adult-specific secreted compounds or some other effect of maternal presence, mothers were subjected to *vit-5,-6* RNAi which blocks vitellogenin accumulation (Ezcurra et al., 2018) prior to plate preconditioning. This alone was sufficient to completely suppress larval growth conferred by plate pre-treatment with venting mothers (Figure 3.6E).

As mentioned earlier, *vit-5* RNAi suppresses YP170 accumulation, intestinal atrophy and PLP accumulation, but enhances YP115/YP88 accumulation (Figure 3.1) (Sornda et al., 2019). *vit-6* RNAi, on the other hand, does the opposite and worsens intestinal atrophy and PLP accumulation by enhancing YP170 accumulation. This suggests a critical role for YP170 in growth promotion by vented yolk; it predicts that *vit-5* RNAi alone should suppress the benefit of yolk provisioning to larvae, while *vit-6* RNAi should enhance it. This is exactly what was seen, with larvae on plates preconditioned with *vit-6* RNAi adults showing increased length and larvae on plates preconditioned with *vit-5* RNAi showing reduced length relative to the control (Figure 3.6E).

Next, to test whether yolk vented by mothers can directly benefit their own progeny, fully-fed d3 mothers were washed, placed on antibiotic-treated *E. coli*-free plates, and left to lay their last eggs for 24 hr. The mothers were then either left in situ to vent yolk or removed. Removal of mothers reduced growth of their progeny (Figure 3.6F,G). In a further test, after egg-laying, mothers were replaced with surrogate mothers of the same age but treated with *vit-5,-6* RNAi. This alone was sufficient to suppress larval growth conferred by mothers left to vent in situ with larvae (Figures 20F,G). Taken together these results suggests that vented yolk serves a function similar to milk. To indicate this, vented yolk that supports larval growth will be referred to as *yolk milk*.

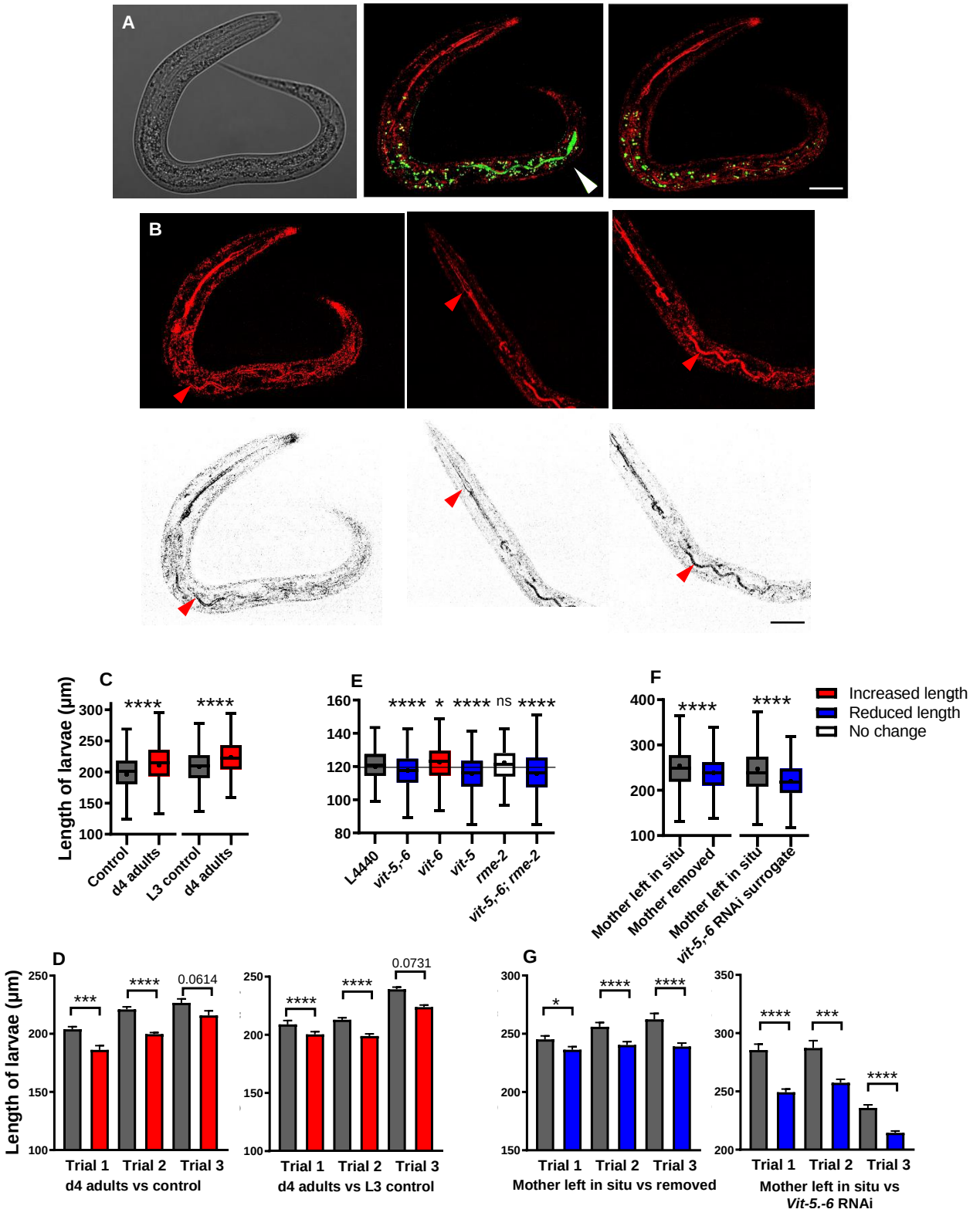

FIGURE 3.6. Vented yolk supports larval growth. (A) Yolk in the intestinal lumen of an L1 larva after it was left on a plate with no food apart from vented yolk for 4 hr. Left: Nomarski microscopy image. Middle: larvae immediately imaged after removal from plates using reflective confocal microscopy (RCM) to highlight the refractive material of the terminal web that surrounds the intestinal lumen (fluorescence filters MBS T80/R20 and 405 nm excitation) (red) and superimposed airyscan image (488 nm excitation) (green) for GFP-labelled yolk. Right: same larva imaged 100 min later showing yolk no longer in the lumen, for comparison. White arrowhead: VIT-2::GFP. Scale bar 20 µm. Fluorescence outside intestinal lumen is from gut granule autofluorescence. **(B)** RCM used to highlight the dense terminal web that surrounds the intestinal lumen (red arrow) (McGhee, 2007) . Top: RCM image. Bottom: RCM image with colour inversion (dark values mapped to light and vice versa, without altering the grey

distribution) to aid visualisation. **(C-G)** Evidence that consumption of vented yolk promotes larval growth, through length measurement of larvae left on plates preconditioned with vented yolk or left with venting mother for 48 hr. Graphs include Tukey box plots of combined data (line at median, + at mean) and individual trial bar graphs (mean ± s.e.m.) (n=200 per trial). All larvae in trials are wild type. Kolmogorov–Smirnov non-parametric test. Red: treatments which increase the dependant variable; blue: that reduce the dependant variable, white: no significant effect, and grey: controls. All larvae in trials are wild type. **(C, D)** Plates preconditioned with venting d4 adults and empty control plates or plates preconditioned with L3 larvae as a control. **(E)** Plates preconditioned with d4 adults treated with combinations of *vit* and *rme-2* RNAi knock down with L4440 control. **(F,G)** Mothers left to lay their last eggs on d3 and left in situ with larvae to provide vented yolk or removed or replaced with *vit-5/6* RNAi knock down surrogates. *P<0.05, *** P <0.0001, **** P <0.0001. Nancy Hui helped with length measurements.

3.2.4 Unfertilised oocytes support larval growth

As described in the introduction, adult hermaphrodites lay over 100 excess oocytes, the overall volume of which exceeds that of the hermaphrodite herself, and this has been noted as oddly wasteful and futile. Findings so far show that the timing of unfertilised oocyte production is similar to that of yolk venting (Figure 3.2C). Moreover, yolk and unfertilised oocytes are often vented together (Figure 3.2A,B, 3.3). Oocytes also contain large amounts of yolk as shown by VIT-2::GFP and confirmed by gel electrophoresis (Figure 3.5A), and at the outset of yolk/oocyte venting, oocytes contain twice as much vitellogenin as free vented yolk (Figure 3.5A). Given that vented yolk (yolk milk) supports larval growth, one possibility is that yolk-filled oocytes also act as a nutrient-rich food source. In support of this possibility, unlike fertilised eggs, unfertilised oocytes lack a chitin shell; moreover, oocytes laid on plates take up the dye trypan blue, implying that the cell membranes are defective which could increase yolk accessibility to larvae (Ward and Carrel, 1979).

In further support, RNAi of the RME-2 yolk receptor, which affects endocytosis of yolk into oocytes and increases internal yolk pools (Ezcurra et al., 2018), in mothers prior to plate preconditioning did not increase significantly affect larval growth (Figure 3.6D). An expectation is that *rme-2* RNAi, by changing the distribution of yolk between oocytes and internal PLPs, should increase the fraction of free vented yolk. If both free yolk and unfertilised oocytes are important for supporting larval growth, however, the decreased level of yolk in oocytes could account for the lack of a significant effect on larval growth following *rme-2* RNAi of mothers.

To establish the extent to which vitellogenin delivered in either form supports larval growth, free yolk and oocyte fractions were separated from conditioned plates on which L1 larvae had or had not been present for 24 hr, and the vitellogenin content assayed (by centrifugation to collect the different fractions, followed by protein gel analysis). The results showed that larval presence causes a significant reduction in vitellogenin from both the oocyte and free yolk fractions (Figure 3.7A), i.e. vitellogenin in both free yolk pools and in unfertilised oocytes is likely consumed by larvae. This provides a possible explanation for the enigma of unfertilised oocyte production: that

they represent an adaptation, aiding delivery of yolk/milk to hungry young larvae (cf. milk and cookies). Thus, laid unfertilised oocytes contain yolk milk.

3.2.5 L1s are attracted to mothers but not to yolk

A function for vented yolk as milk raises the possibility that larvae are attracted to it. However, L1 larvae showed no significant attraction to agar preconditioned with yolk milk from d4 adults relative to untreated agar (Figure 3.7B), but L1 larvae were attracted to adult hermaphrodites on plates; whether this is somehow a function of their yolk milk venting status remains to be explored.

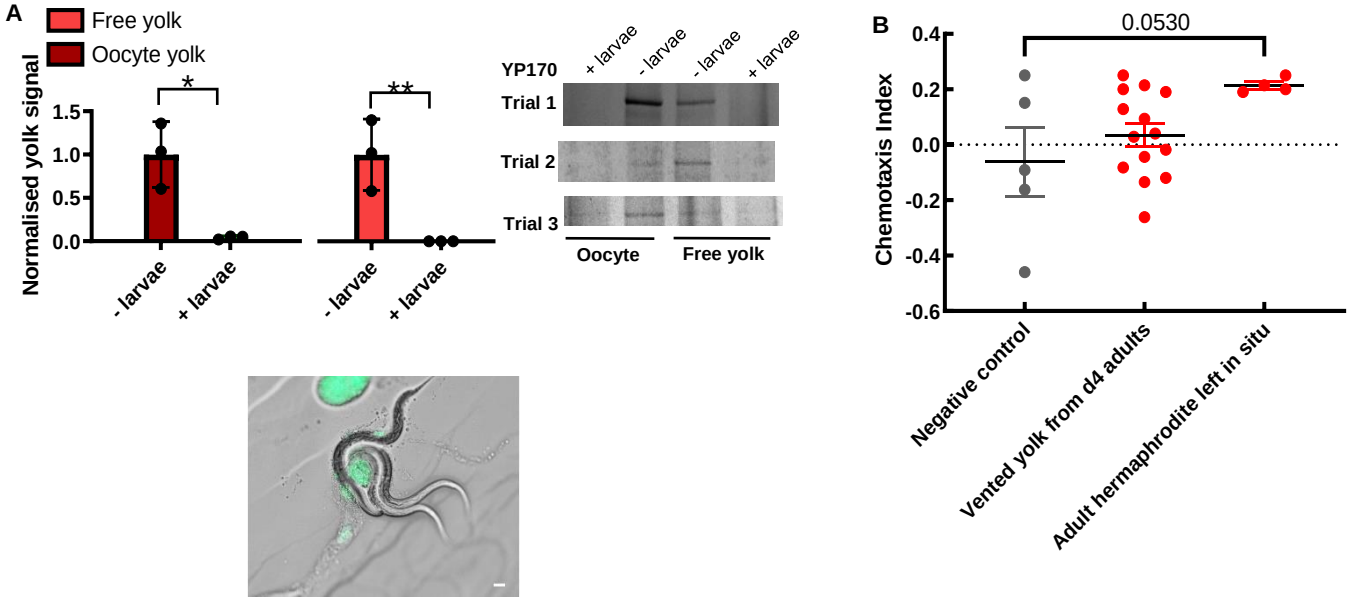

FIGURE 3.7. Larvae consume both free yolk and yolk in oocytes and are weakly attracted to adult mothers. **(A)** Larvae consume vitellogenin in both free yolk and oocyte fractions. Top Right: quantitated levels of YP170 from plates preconditioned with 100 venting d4 adults for 24 hr followed by addition of 200 larvae or no larvae controls for 48 hr and separation of the oocyte and free yolk fraction through centrifuging prior to protein gel electrophoresis. Data show s.d. of 3 trials. t-test, two-tailed. Top Left: protein gel image of YP170 bands from 3 trials. Bottom: Larvae on plates with no food apart from vented yolk **(B)** Larvae are attracted to adult hermaphrodites rather than vented yolk. Data show calculated chemotaxis index of individual trials (each dot represents one trials) with mean ± s.e.m. displayed. One-way ANOVA. *P**<0.05, *P*****<0.01. Victor Konstantellos helped with the running of gels.

3.2.6 Yolk secretion is promoted by insulin/IGF-1 signalling (IIS)

daf-2 insulin/IGF-1 receptor mutants have extended lifespan (Kenyon et al., 1993; Kimura et al., 1997), and reduced vitellogenin synthesis (Depina et al., 2011; Sornda et al., 2019), PLP accumulation (Ezcurra et al., 2018), and laying of unfertilised oocytes (Gems et al., 1998). Thus, IIS promotes ageing and yolk production. One possibility is that IIS promotes post-reproductive yolk production to transfer resources from mothers to offspring via yolk venting. To explore

whether IIS promotes yolk venting, *daf-2(e1370)* and *daf-2(e1368)* mutants with stronger and weaker suppression of pathology, respectively (Ezcurra et al., 2018) were examined. Yolk venting was completely suppressed by both *e1370* and *e1368* (Figure 3.8A). Venting was also increased by the *daf-2(gk390525)* gain-of-function mutation (Tawo et al., 2017) (Figure 3.8A). Effects of *daf-2* on yolk production and lifespan require the *daf-16* FoxO transcription factor (Ezcurra et al., 2018; Kenyon et al., 1993). *daf-16(mgDf50)* restored yolk venting to *daf-2(e1370)* mutants (Figure 3.8A). Moreover, mutation of *daf-18* PTEN phosphatase (Mihaylova et al., 1999; Ogg and Ruvkun; 1998; Rouault, 1999) in mothers, which increases phosphatidylinositol (3,4,5)-trisphosphate (PIP_3) levels, increased yolk venting (Figure 3.8A).

Suppression of unfertilised oocyte production by *daf-2(e1370)* was also *daf-16* dependent, and the number of oocytes laid was dramatically increased (3-5 fold) in *daf-18(nr2037)* and *daf-2(gf)* mutants (Figure 3.8B), underscoring the importance of insulin/IGF-1 and PI3K signalling in unfertilised oocyte production.

Next, effects on the growth of wild-type larvae on plates preconditioned with wild-type or IIS mutant hermaphrodites was tested. Larvae on plates preconditioned with *e1370* d4 adults showed significantly reduced growth relative to plates preconditioned with wild type, and this reduction was *daf-16* dependent (Figure 3.8C): larvae on plates preconditioned with *daf-16(mgDf50)*; *daf-2(e1370)* double mutants showed no reduction in length, and in fact were longer than in the control, suggesting that *daf-16(mgDf50)* increases yolk provisioning for progeny (Figure 3.8C) (not unexpected given *daf-16* unfertilised oocyte production is significantly greater than wild type, with *daf-16* is acting like a mild IIS gain-of-function mutant). Moreover, *daf-18(nr2037)* also increased growth-promoting effects of venting mothers (Figure 3.8C).

To test whether IIS affects the ability of mothers to directly provision vented yolk for their own wild-type progeny, d3 mothers were left on plates to care for their last few young or replaced with *daf-2(e1370)* surrogate mothers of the same age. Larval length measured after 48 hr was found to be significantly greater on plates with wild-type mothers left in situ relative to plates with *daf-2(e1370)* surrogate mothers (Figure 3.8D).

These results imply that IIS promotes *C. elegans* lactation, likely through the promotion of *vit* gene transcription and translation (DePina et al., 2011), gut-to-yolk biomass conversion (Ezcurra et al., 2018) and laying of unfertilised oocytes (Gems et al 1998). This suggests that reduced IIS in *daf-2* mutants reduces late-life contributions to reproductive fitness, revealing a new mode of antagonistic pleiotropy involving this gene.

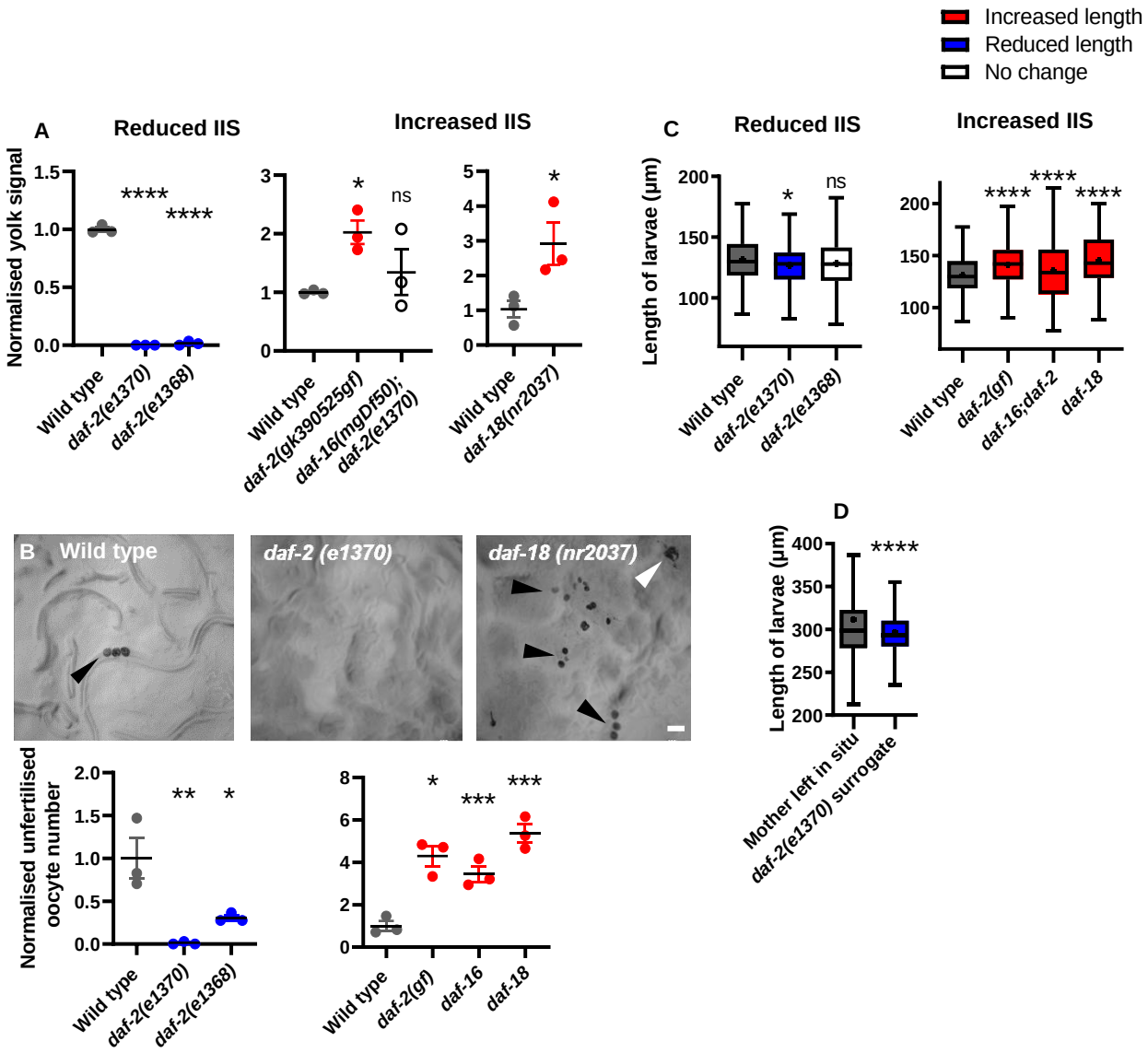

FIGURE 3.8. Yolk venting is promoted by insulin/IGF-1 signalling (IIS). (A) Yolk venting is down-regulated by reduced IIS and up-regulated by increased IIS. Quantitated YP170 band on protein gels. **(B)** Decreased yolk milk provisioning by reduced IIS reduces larval growth on preconditioned plates relative to wild-type, and vice versa for increased IIS. **(C)** Decreased larval growth on plates with *daf-2(e1370)* surrogate mothers. Wild-type mothers were allowed to lay their last eggs and either left in situ or replaced. **(D)** Unfertilised oocyte production is down-regulated by reduced IIS and up-regulated by increased IIS. Bottom: Number laid for 24 hr on d4-6 of adulthood and normalised to wild type. Means ± s.e.m. of 3 trials (n=10 per trial). Top: NGM plates imaged after 15 wild-type, *daf-18(nr2037)* or *daf-2(e1370)* worms were left for 24 hr. White arrowhead: yolk pool. Red: treatments which increase the dependant variable; blue: that reduce dependant variable; white: no effect; and grey: control. **P*<0.05, ***P*<0.01, ****P*<0.0001, *****P*<0.00001; one-way ANOVA or unpaired t-test. Nancy Hui and Serena Mirpuri helped with length measurements.

3.2.7 Proteomic analysis of secretome proteins through mass spectrometry

Findings so far imply that the vitellogenin-rich fluid secreted by sperm-depleted *C. elegans* functions as a milk. To further characterise *C. elegans* yolk milk, secreted proteins were collected from L3 and d4 old hermaphrodites, and subjected to mass spectrometric analysis. The set of protein present in the latter but not the former represents an adult-specific secretome that includes abundant vulvally-vented proteins, and thus approximately represents the vulval secretome

(though it may also include proteins secreted in an adult specific fashion from other orifices, such as the excretory pore and anus, or from the nematode surface). The analysis performed defined a set of 125 proteins (Appendix 3 and Figure 3.9A).

The d4 adult hermaphrodite secretome is expected to include both proteins of likely functional significance (e.g. milk proteins), and random proteins shed from internal organs. To probe the possibility that other components of the vulval secretome are part of worm milk, they were tested to see whether, like vitellogenins, they show an age increase in abundance. Given the strong evidence for IIS promoting gut-to-yolk biomass conversion for the purpose of yolk milk production and the fact that vitellogenin levels increase dramatically with age in an IIS-dependent fashion, another assumption is that the protein constituents of yolk milk will increase with age in an IIS-dependent manner. Focus was therefore on proteins that were a) IIS regulated, b) increase in abundance with age, and c) secreted (possessing a predicted N-terminal signal peptide). For IIS and age upregulation, previously published proteomic data looking at changes from d1 to d17 was used (Walther et al., 2015). For N-signal peptide determination, SignalP 5.0 was used (Almagro Armenteros, et al., 2019). 21 secretome proteins proved to be IIS regulated, 30 up-regulated in old age (defined as more than 1 log2 ratio increased d17/d1), and 28 to contain signal peptides (Table 3.1 and Figure 3.9 A-C, and Figure 3.10). Notably, secretome proteins were significantly enriched for all 3 individual criteria (Figure 3.9D). The analysis also revealed 17 proteins that exhibited all three features, which is 82-fold more than expected by chance alone (Figure 3.9D).

Proteins showing all 3 characteristics included the vitellogenins, which were the most abundant (Figure 3.9C,E and Figure 3.11), as well as 6 transthyretin-related (*ttr*) proteins, TTR-2, -15, -18, -30, -45 and -51. TTRs often function as carrier proteins for lipophilic compounds including lipids; a possibility is that these serve a function similar to lipid carrier proteins that are abundant in mammalian milk. Also present was FAR-3, another predicted lipid-binding protein, that is expressed in the vulva, and FAR-1 and -2 were also present. Other proteins included a cysteine-type endopeptidase inhibitor and a serine endopeptidase inhibitor, CPI-1 and SPI-1, respectively, that likely play a role in worm immunity (Chen, 2019) (Figure 3.9C,E).

In stark contrast to the d4 secretome, few proteins were found to be present in the L3 secretome (i.e. present consistently in two of the 3 samples tested), and in terms of percent abundance, the majority of L3 secretome protein constituents were associated with either the cytoskeleton or protein folding (Figure 3.11). Heat shock proteins are often found in proteome analysis in a non-specific manner, i.e. their presence here could reflect experimental artefact. Moreover, enrichment analysis showed no significant enrichment for IIS upregulated proteins and limited enrichment for age-upregulated proteins (Figure 3.11 B).

A highly abundant neuropeptide like protein, NLP-77 was also identified in the d4 secretome and comprised over 20% of the total secretome. As NLP-77 was detected, albeit in smaller quantities, in control L3 secretome, it was not included in the adult specific secretome (Figure 3.11D). NLP-77 is enriched in body wall musculature, hypodermis, neurons, somatic nervous system, and vulval muscle (based on proteomic studies) and is homologous to the OV-17 antigen secreted in parasitic nematodes including *Onchocerca volvulus* and *Toxocara canis* (OV: *O. volvulus*). The function of OV-17 and NLP-77 is not known.

Tissue enrichment analysis of the d4 and L3 secretomes was also performed, with no significant tissue enrichment detected for the L3 secretome (Figure 3.12A). In contrast, the d4 secretome showed enrichment for intestinal muscle, broadly consistent with intestinal biomass conversion to yolk. Significant enrichment in the d4 secretome was also seen for anal muscle, though this mainly came from proteins that did not show any of the criteria of being IIS regulated, age upregulated or possessing an N-terminal signal peptide (Figure 3.12B). Possibly these are proteins shed via the anus.

To try to gain further insights into possible functions of the vulval secretome, the MS proteome was analysed for enrichments relative to the full worm genome in Gene Ontology Biological Process and Interpro terms using DAVID (Huang et al., 2009) for functional and structural characterisation, respectively (Appendix 4). As expected, this led to several redundant categories, though many were associated with an enrichment for vitellogenin proteins, lipid transport proteins and transthyretin-like proteins, and functions associated with reproduction, embryo development ending in birth or egg hatching, nematode larval development, lipid transport, and determination of adult lifespan (see Appendix 4 for full lists).

Next, the vulval secretome was compared to human breast milk (D'Alessandro, et al., 2010) using the XGSA package in R (Djordjevic et al., 2016). This identified six homologs (Figure 3.12 C) which are present in both proteomes, representing a significant overlap of approximately 10% of the vented yolk proteins which are conserved between *C. elegans* and *H. sapiens* (P=0.00146). However, the fact that many of the conserved proteins identified were associated with protein folding suggests this may be due to proteins that are generally abundant in animal secretions. That said, the presence in human milk of LBP-1, which is associated with lipid transport, suggests a general similarity in terms of lipid carrier function (Figure 3.12 C). Moreover, Interpro term comparison between human milk and the vulval secretome revealed that both contained many categories associated with transporter proteins, including lipid binding proteins (Figure 3.12 D).

Taken together, these findings show that after self-sperm depletion *C. elegans* mothers can enhance growth of their progeny by venting yolk through the vulva. As a means of transferring

resources from mother to after egg-laying, vented yolk serves a function similar to that of mammalian milk. Milk feeding of larvae by mothers is a previously undescribed feature of *C. elegans*, with the results suggesting a new function for the intestine in *C. elegans* hermaphrodites: that of mammary gland.

	Percent intensity in secretome	Protein	Predicted function	Age increase (Log fold change over 1)	IIS upregulated	Signal peptide	Criteria met
P18948	2.51	VIT-6	Vitellogenin-6	8.45	Yes	Yes	3
Q22288	2.23	TTR-15	Transthyretin-like protein 15	4.54	Yes	Yes	3
P05690	1.67	VIT-2	Vitellogenin-2	7.79	Yes	Yes	3
P06125	1.37	VIT-5	Vitellogenin-5	9.28	Yes	Yes	3
P90889	1.12	CELE_F55H12.4	Uncharacterized protein	1.95	Yes	Yes	3
Q2EEM8	1.07	TTR-45	Transthyretin-related family domain	6.90	Yes	Yes	3
P55955	1.03	TTR-16	Transthyretin-like protein 16	1.98		Yes	2
G5EET8	0.84	PUD-1.2	PUD1_2 domain-containing protein	-1.08	Yes		1
Q9N4J2	0.79	VIT-3	Vitellogenin-3	7.65	Yes	Yes	3
Q9NA39	0.78	CCG-1	Conserved cysteine/glycine domain protein	3.23		Yes	2
Q22341	0.73	TTR-30	Transthyretin-related family domain	2.97	Yes	Yes	3
O62289	0.70	TTR-51	Transthyretin-related family domain	7.35	Yes	Yes	3
P52015	0.69	CYN-7	Peptidyl-prolyl cis-trans isomerase 7 (EC 5.2.1.8)	1.05			1
Q9XW17	0.65	CAR-1	Cytokinesis, apoptosis, RNA-associated	2.07			1
Q19478	0.64	FAR-3	Fatty acid/retinol binding protein	7.36	Yes	Yes	3
G5EDZ9	0.55	CPI-1	Cystatin (Cysele1)	7.27	Yes	Yes	3
G5EBF3	0.55	PUD-2.1	Protein up-regulated in *daf-2(gf)*	-0.77	Yes		1
O16462	0.52	GRD-5	Ground-like domain-containing protein	-1.62		Yes	1
Q23683	0.52	CELE_ZK970.7	DUF148 domain-containing protein	6.62	Yes	Yes	3
Q19063	0.50	CELE_E04F6.8	Uncharacterized protein	7.07	Yes	Yes	3
Q20363	0.46	SIP-1	Stress-induced protein 1	6.18	Yes		2
O18089	0.43	CELE_T13F3.6	DUF19 domain-containing protein	1.88		Yes	2
P34500	0.41	TTR-2	Transthyretin-like protein 2	6.56	Yes	Yes	3
P34383	0.34	FAR-2	Fatty-acid and retinol-binding protein 2	2.49		Yes	2
Q19064	0.33	CELE_E04F6.9	Uncharacterized protein	5.00	Yes	Yes	3
O45599	0.31	CBD-1	Chitin-binding domain protein	2.01		Yes	2
O01504	0.28	C37A2.7	60S acidic ribosomal protein P2	-0.51		Yes	1
Q17473	0.28	TTR-18	Transthyretin-related family domain	1.44	Yes	Yes	3
G5EEA8	0.27	NEX-1	Annexin	1.89			1
Q21763	0.23	CELE_R05H5.3	Thioredoxin domain-containing protein	1.60			1
G5ED07	0.21	PDI-3	Protein disulfide-isomerase (EC 5.3.4.1)	-0.05		Yes	1
Q07750	0.20	UNC-60	Actin-depolymerizing factor 1, isoforms a/b	1.07			1
Q17967	0.19	PDI-1	Protein disulfide-isomerase 1 (PDI 1) (EC 5.3.4.1)	-0.17		Yes	1
Q20724	0.19	CELE_F53F4.13	Uncharacterized protein	-0.24	Yes	Yes	2
P27420	0.17	HSP-3	Heat shock 70 kDa protein C	-0.83		Yes	1
P91306	0.16	CEY-2	CSD_1 domain-containing protein	2.11			1
O17687	0.13	NASP-2	SHNi-TPR domain-containing protein	4.85			1
Q21265	0.09	TAG-225	Putative metalloproteinase inhibitor (TIMP-like protein)	2.88	Yes	Yes	3

Classification
- Vitellogenin
- Transthyretin-like
- Lipid binding
- Protein folding
- Ribosomal
- Cytoskeleton
- Unknown
- None of the above

TABLE 3.1. d4 adult specific secretome proteins that are either IIS upregulated, age upregulated or have a predicted N-terminal signal peptide. Significant differences in the distributions were detected using a Kolmogorov-Smirnov test. Nyi Thant helped with mass spec sample collection and StJohn Townsend helped with data analysis.

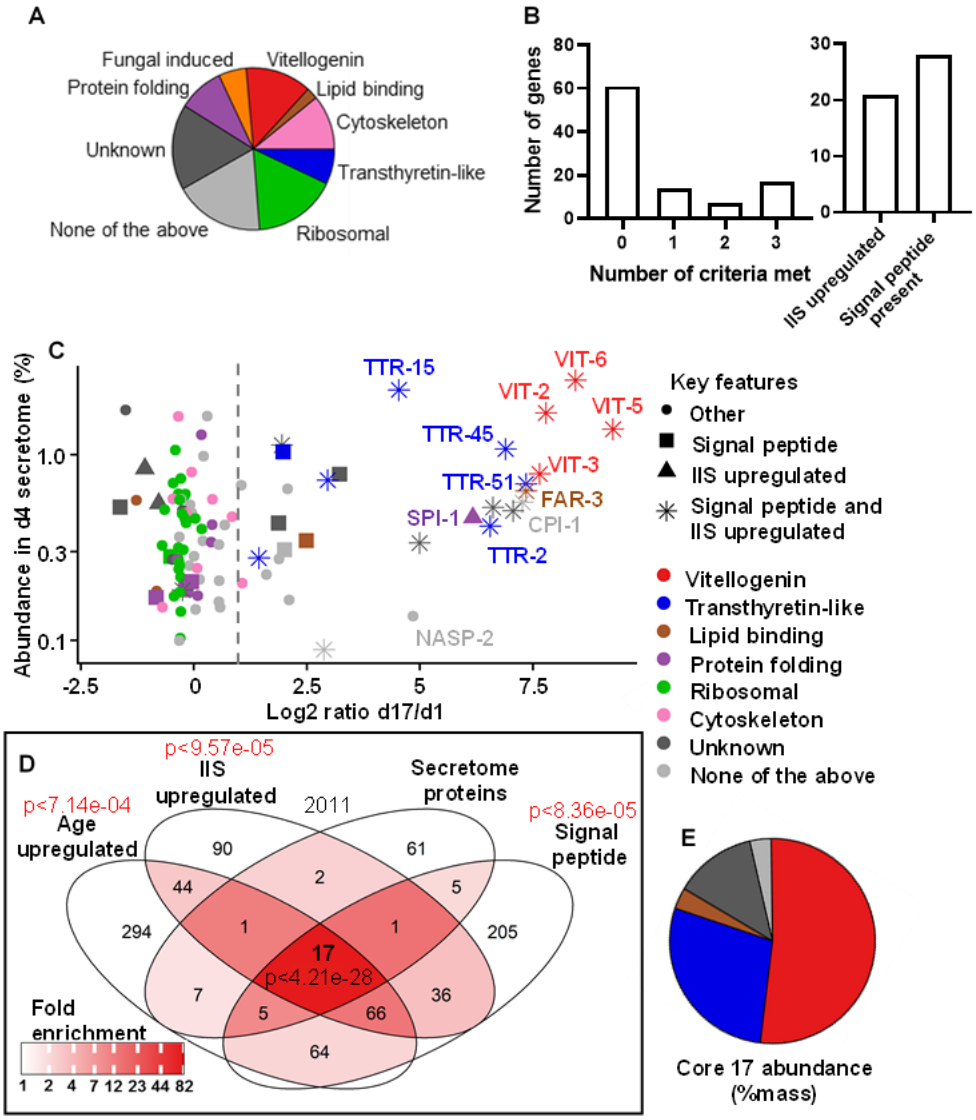

FIGURE 3.9. Proteomic analysis of d4 adult secretome. (A) All proteins detected in the adult-specific d4 secretome. Manual categorisation. **(B)** Number of proteins in adult specific secretome meeting only 1, only 2 or all 3 criteria of being age upregulated, IIS upregulated or possessing an N-terminal signal peptide, and total proteins that meet each requirement (c.f. Table 3.1). **(C)** Relationship between protein abundance in the day 4 adult secretome and increased abundance with age in the overall proteome, from published data for wild-type and *daf-2(e1370)* (Walther et al., 2015). Age upregulated was defined as showing an increase of >log2=1 day 17 vs day 1 (vertical dotted line). Right hand cluster includes many IIS- and age-upregulated secreted proteins. Left hand cluster likely includes proteins shed by tissue breakdown. **(D)** Enrichment analysis of adult-specific secretome proteins relative to all proteins detected in the reference study (Walther et al., 2015). Significant over-representation was detected using a SuperExactTest (Wang, et al., 2015). **(E)** Percentage abundance categorisation of the core 17 proteins in the adult-specific secretome that are IIS upregulated, age upregulated and likely to be secreted (i.e. bear a predicted N-terminal signal peptide).

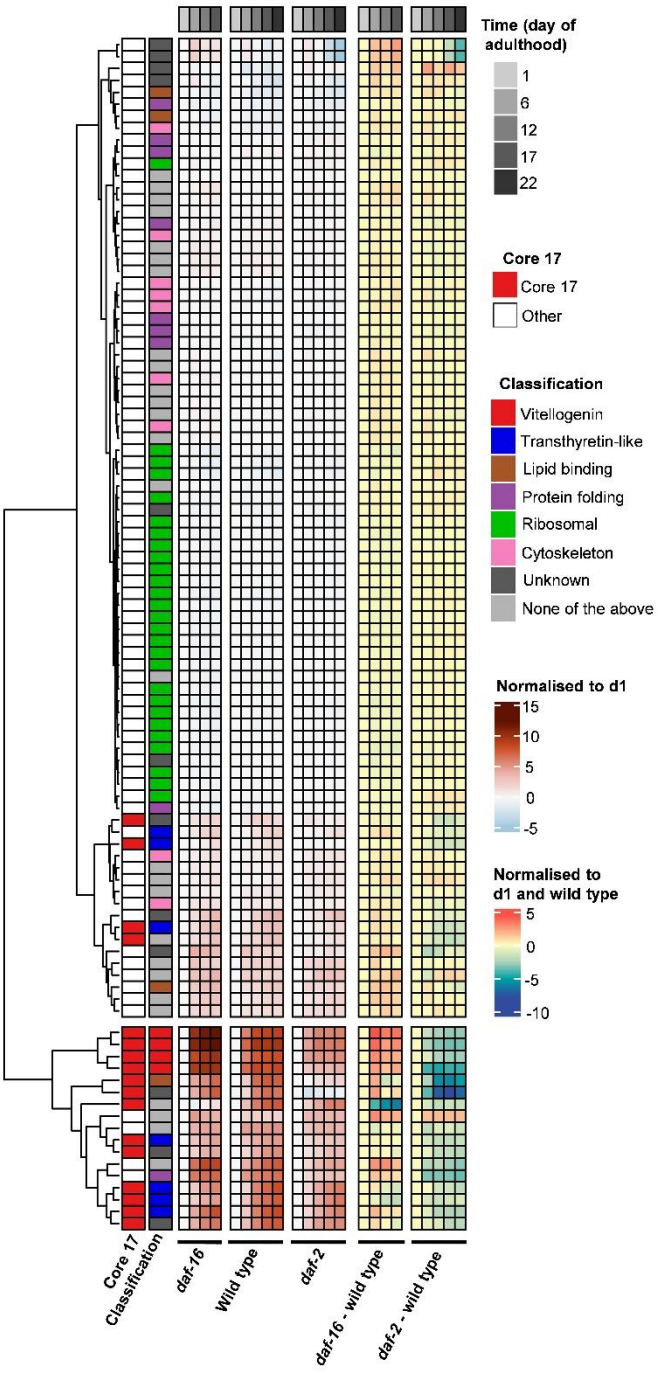

FIGURE 3.10. IIS-regulated proteins in the d4 adult-specific secretome. Adult-specific secretome compared to published data (Walther et al., 2015) for age related changes in wild-type, *daf-2(e1370)* and *daf-16(mu86)* mutants (c.f. Table 3.1 and Figure 3.9).

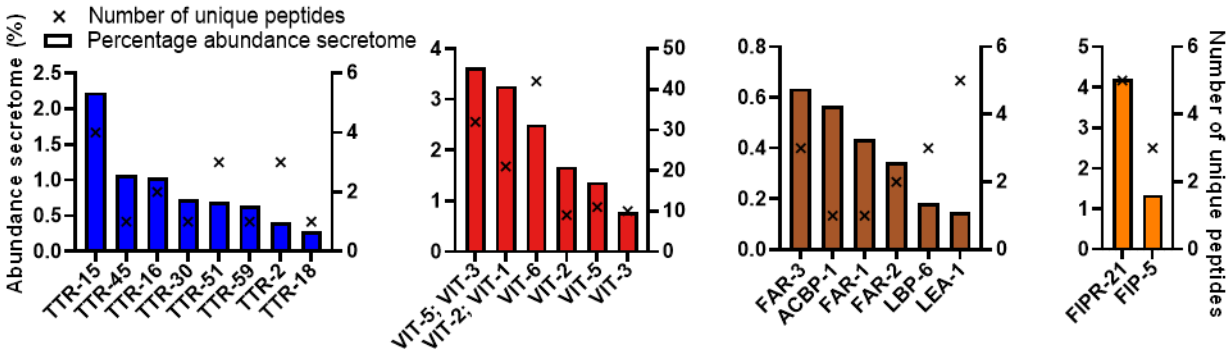

FIGURE 3.10. Proteins of interest in the adult specific d4 secretome. Percentage abundance and unique peptides of all vitellogenins, transthyrethins, fatty acid binding proteins and fungal induced proteins present shown. Fungal-induced proteins were not detected in the internal proteome in a previous study (Walther et al., 2015). The absence of *vit-4* unique peptides is likely an artefact resulting from the high sequence similarity between the vitellogenins: *vit-3* and *-4* have more than 99% sequence similarity to each other (Spieth and Blumenthal, 1985). A few proteotypic peptides were detected for *vit-4*.

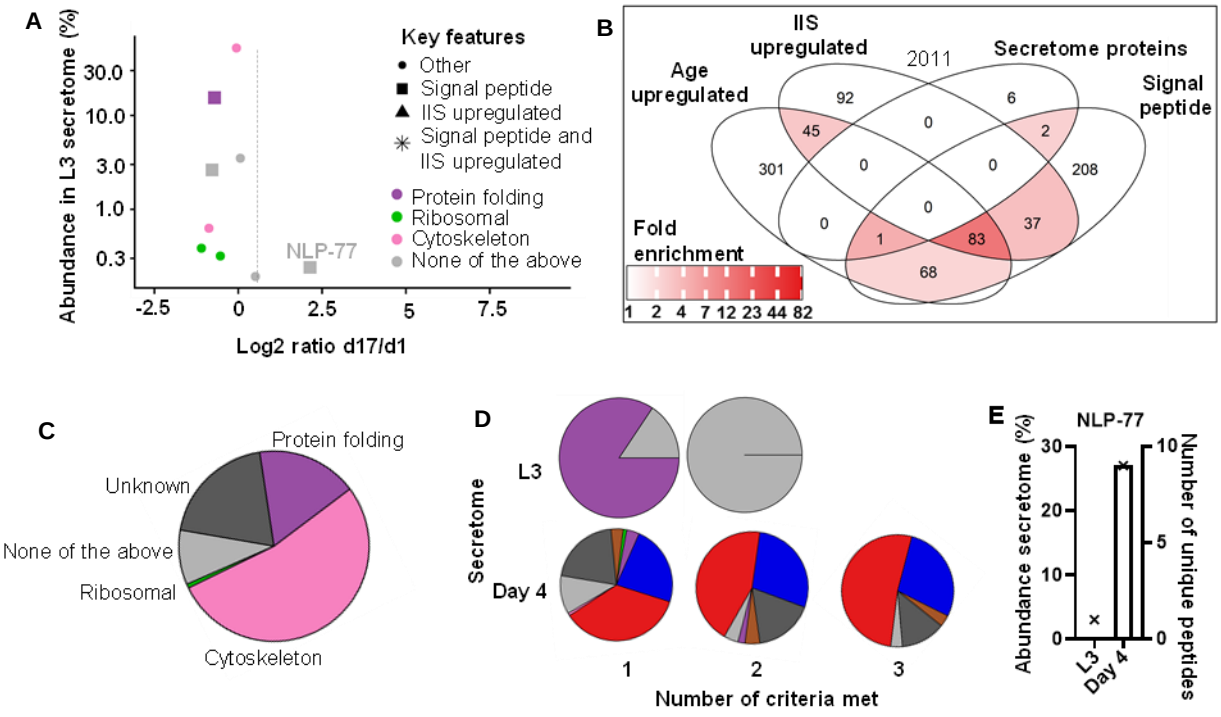

FIGURE 3.11. d4 adult specific proteome and L3 secretome comparison. (A) Few proteins present in the L3 secretome. Protein abundance against internal proteome age associated upregulation displayed by comparison to published data (Walther et al., 2015). **(B)** No significant enrichment of proteins that are IIS upregulated and limited enrichment of age-upregulated proteins in the L3 secretome. Enrichment analysis is relative to all proteins. Significant differences in the distributions were detected using a SuperExactTest (Wang, et al., 2015). **(C)** The L3 secretome primarily consists of cytoskeletal and protein folding associated proteins. Percentage abundance displayed. Manual classification. **(D)** Percentage abundance categorisation of proteins in L3 secretome and adult specific secretome that meet either only 1, only 2 or all 3 criteria of being age upregulated, IIS upregulated or possessing a predicted N-terminal signal peptide. No proteins in the L3 secretome meet all 3 criteria. **(E)** A highly abundant neuropeptide, NLP-77, with unknown function was present in the d4 secretome and also in smaller quantities in the L3 secretome, and therefore was not classified as part of the adult-specific d4 secretome.

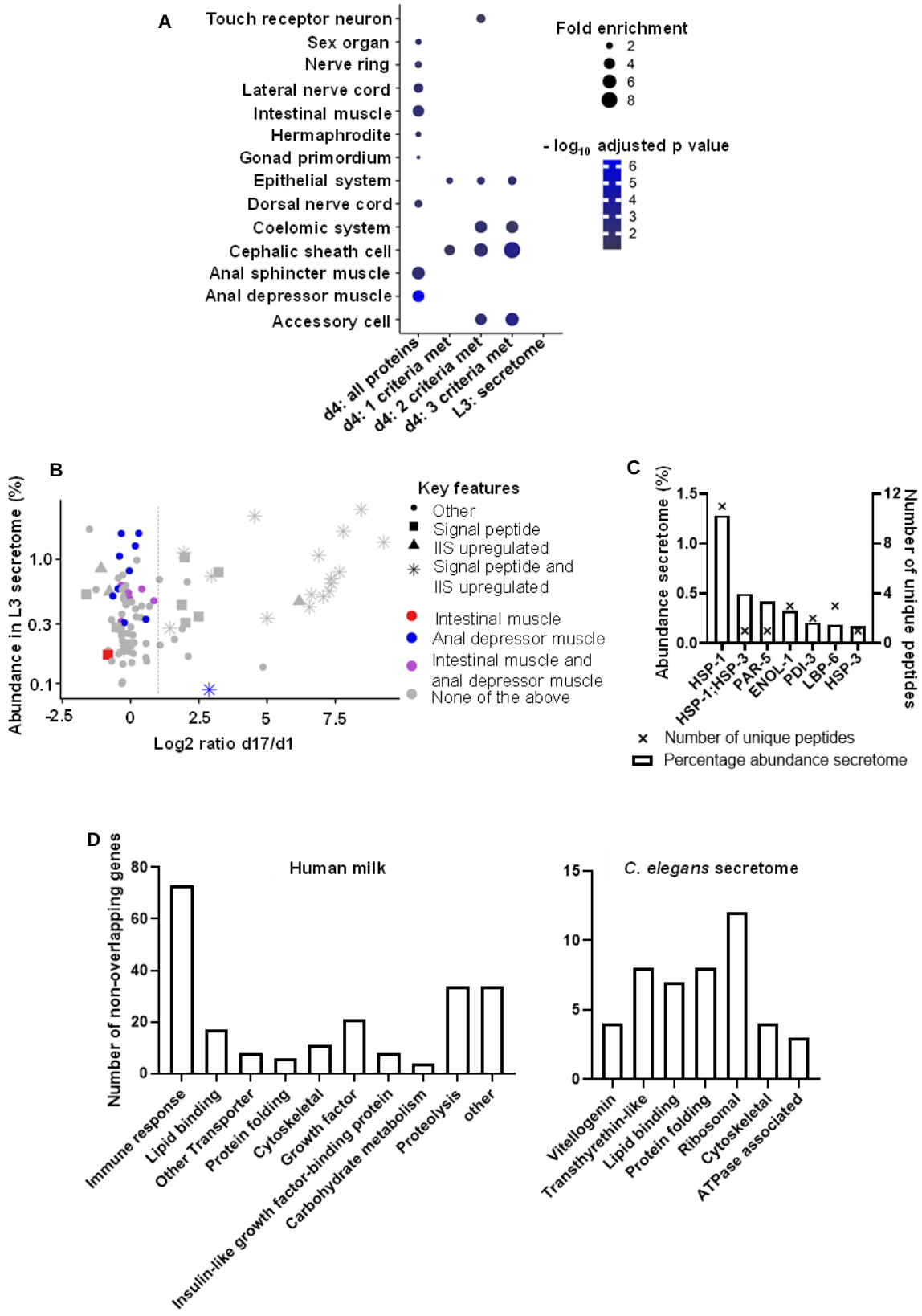

FIGURE 3.12. d4 adult specific secretome tissue enrichment analysis and comparison to the human milk proteome. (A) Tissue enrichment analysis of L3 and adult specific day 4 secretome. All proteins as well as those that met only 1, only 2 or all 3 criteria of being age upregulated, IIS upregulated or possessing a predicted N-terminal signal peptide are displayed. No enrichment was detected for the L3 secretome. Analysis was performed using the

tissue enrichment analysis tool from WormBase (Angeles-Albores et al., 2016). **(B)** Most anal depressor muscle-related proteins are not IIS upregulated, age upregulated or N-terminal signal peptide-containing. **(C)** Conserved proteins in human breast milk and the *C. elegans* day 4 adult specific secretome. Cross-species gene set analysis performed using the XGSA package in R (Djordjevic et al., 2016) accounting for homology mapping between *C. elegans* and humans. Human milk proteome from previously published data (D'Alessandro et al., 2010). Overlap P=0.00146. HSP proteins are frequently present in protein profiles, and the significant P value could be due to their presence. Human homologues include: HSPA8 (heat shock protein family A (Hsp70) member 8); YWHAB (tyrosine 3-monooxygenase/tryptophan 5-monooxygenase activation protein beta); ENO1 (enolase 1); ENO2 (enolase 2); and ENO3 (enolase 3); PDIA3 (protein disulfide isomerase family A member 3); FABP7 (fatty acid binding protein 7); and HSPA5 (heat shock protein family A (Hsp70) member 5). **(D)** Interpro term enrichment analysis relative to the full worm genome for the day 4 adult-specific secretome and comparison to human milk enrichment relative to human genome. Manual categorisation of groups with significant enrichment (cut-off of FDR P<0.05) is displayed to account for redundancy. Number of non-overlapping genes in each category is plotted. For full list of Interpro terms and Gene Ontology Biological Process terms see Appendix 4. Enrichment analysis was performed using Database for Annotation, Visualization and Integrated Discovery (DAVID) (Huang et al., 2009).

2.8 Discussion

3.3.1 Hermaphroditic *Caenorhabditis* produce milk for progeny

This chapter describes a new feature of *C. elegans* life history: hermaphrodites exhibit a form of primitive lactation, with milk feeding of larval kin by mothers. The results show that beginning at the end of egg laying, hermaphrodites vent substantial amounts of liquid rich in vitellogenins and lipid through the vulva and into their local vicinity. Vitellogenin presence in vented yolk was confirmed using three separate methods: (i) protein gel analysis; (ii) GFP labelling of vitellogenin and visualisation under a microscope; and (iii) MS analysis. Lipid presence in vented yolk was shown using the Bodipy lipid stain. Significantly, larvae consumed vented yolk, present either as free pools or within unfertilised oocytes, and this promoted their growth. Yolk consumption was evidenced by the presence of VIT-2::GFP in the lumen of L1 larvae, as well as protein gel analysis showing reductions in the levels of yolk milk, in both free yolk and unfertilised fractions, on plates that had larvae present for 24 hr. The effects of yolk milk on larval growth were robust, with interventions that suppress adult yolk production on preconditioned plates resulting in reduced larval length and vice versa. Moreover, yolk milk vented by mothers was shown to directly benefit their own progeny: replacing wild-type mothers with surrogate mothers in which yolk venting was suppressed reduced larval growth.

MS analysis of vented yolk (as part of the adult specific d4 secretome) further lends support to its function as milk: there was significant enrichment for age-upregulated, IIS-upregulated and putative secreted proteins. IIS is also known to drive conversion of intestinal biomass into yolk (Ezcurra et al., 2018) and was shown here to cause adult hermaphrodites to provide yolk milk for kin. This is in contrast to the L3 secretome which showed limited enrichment for these categories. Notably, many of the proteins in vented yolk have roles associated with transporter proteins, similar to mammalian milk.

Milk feeding also provides a possible explanation for the long-standing enigma of copious laying of unfertilised oocytes (Ward and Carrel, 1979): that such oocytes function as vectors for yolk milk.

Although such maternal care by nematodes might seem surprising, lactation has been described in other invertebrates, including tsetse flies (*Glossina* spp.) (Benoit et al., 2015), the Pacific beetle cockroach *Diploptera punctata* (Marchal et al., 2013) and the pseudoscorpion *Garypus japonicus* (Makioka, 1976). In the latter case, milk generation by the ovaries in *G. japonicus* is coupled to organ atrophy (Figure 3.13), resembling intestinal biomass conversion to yolk in *C. elegans.*

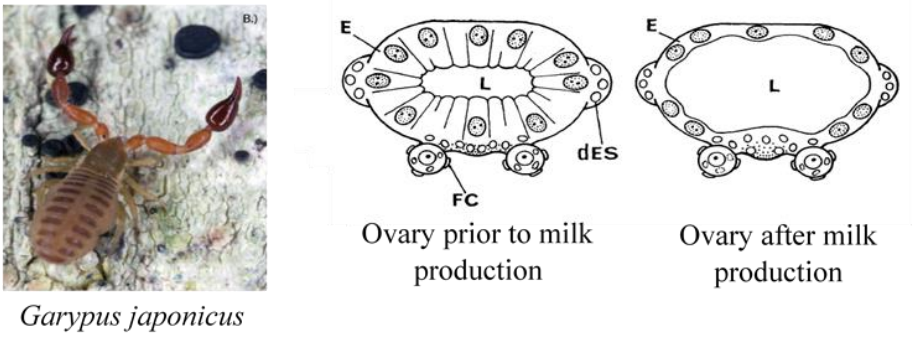

FIGURE 3.13. Atrophy of the ovary associated with milk production, similar to atrophy of the C. elegans intestine. dES : degenerating egg-stalk, E : ovarian epithelium, FC : follicle cell, L : ovarian lumen. Adapted from (Makioka, 1976).

Such behaviour exemplifies the wider phenomenon of trophallaxis, the social transfer of nutrient fluids between individuals, particularly in the context of parental care; trophallaxis encompasses fluid exchanges between social insects as well as mammalian nursing (LeBoeuf, 2017).

3.3.2 Evolutionary explanations for yolk milk feeding in *C. elegans*

In the wild, reproducing *C. elegans* exist mainly as colony-like, high density, largely clonal populations (Lohr et al., 2019; Schulenburg and Félix, 2017). Potentially, it is into this collective that sperm-depleted hermaphrodites vent yolk milk. Hermaphroditism facilitates rapid colonization of new food patches (Schulenburg and Félix, 2017), but protandry leaves mothers unable to contribute to fitness after sperm depletion, an example of a *bauplan*-type trade off (Gould and Lewontin, 1979; Lohr et al., 2019). Although males can mate with hermaphrodites, they are extremely rare in the wild (Schulenburg and Félix, 2017). Moreover, even when hermaphrodites are mated, although the egg laying period is extended, fecundity drops

dramatically with age (Hughes et al., 2007), so continued yolk production with age for the purpose of fertility is not easily justified. Plausibly, late-life yolk milk production is an adaptation to circumvent this block to continued maternal contribution to fitness, here increasing inclusive fitness of the surrounding clonal population. That trophallaxis is often more pronounced in eusocial species (LeBoeuf, 2017) supports an emerging picture of *C. elegans* colonies as lactating superorganisms (Gems et al., 2020).

3.3.3 Births and transfers shape senescence: the relationship between yolk milk production and lifespan

Has post-reproductive yolk milk transfer shaped senescence in *C. elegans*? As explained in the introduction, ageing is thought to evolve partly as the consequence of trade-off costs on physiology, controlled by genes that exhibit antagonistic pleiotropy (AP) i.e. exerting both beneficial and deleterious effects on fitness. If the deleterious effects occur later in life, such AP genes may be favoured by natural selection (Williams, 1957). Previously, post-reproductive yolk production and the pathologies to which it is coupled have been interpreted as futile run-on of reproductive function (Ezcurra et al., 2018; Herndon et al., 2002; Sornda et al., 2019). This is consistent with the AP theory, and recent ideas about its proximate mechanisms in programmatic terms, which argue that futile run-on of biological programmes in later life (or quasi-programmes) can cause senescent pathology (Blagosklonny, 2006; de Magalhaes and Church, 2005; Williams, 1957).

Life history, including senescence, is strongly shaped by reproductive strategy, the main trade-offs of which govern choice between offspring quantity and offspring quality. As a simplification, reproductive strategy can be seen as entailing: (i) the strategy employed to reach the age of reproductive onset, i.e. maturity, (e.g. rapid growth and small body size, or slow growth and a large body size etc.); and (ii), upon reaching maturity, reproductive effort. Only considering birth, i.e. fertility, as reproductive effort (Abrams, 1993; Cichon & Kozlowski, 2000; Cichon, 1997) is insufficient to understand life history evolution (Abrams & Ludwig, 1995; Lee, 2003; Austad, 1997; Lahdenpera, et al., 2004). As stated by Hamilton: “If the organism practises parental care ‘birth’ should be considered to occur, for the purposes of this definition, as the age at which the offspring becomes independent” (Hamilton, 1966). One important form of parental care affecting offspring quality is post-fertility intergenerational transfers, with transfers known to play a large role in either positively or negatively determining adult lifespan (Lee, 2003; Austad, 1997; Lahdenpera, et al., 2004). For example, post reproductive bottle-nose dolphins and pilot

whales survive well past the end of reproduction to breastfeed even their grandchildren (Wachter & Finch, 1997), while death in semelparous *Antechinus* females is usually post-lactation, caused in part by maternal depletion of energy reserves to support the large resource demands of lactation (Fisher & Blomberg, 2011; Braithwaite & Lee, 1979; Green, et al., 1991).

If late-life yolk production in *C. elegans* promotes fitness, then yolk steatosis and intestinal atrophy to which yolk milk production is coupled are not the result of a vitellogenic quasi-program. Instead, intestinal atrophy results from a life history trade-off involving physiological costs associated with a post-fertility transfer (Speakman, 2008). This means that intestinal involution to support yolk-milk production (benefit) in *C. elegans* (Ezcurra et al., 2018) is an active, programmed process (i.e. a programme proper, and not quasi-programmed) of resource reallocation to promote fitness (Figure 3.14). It should be noted though that the trade-off cost of intestinal involution itself is pathological and does not promote fitness. This conclusion suggests a further possibility: that *C. elegans* undergo reproductive death triggered by reproductive maturity and coupled to post-fertility yolk milk production. Suppression of reproductive death might partially explain the unusually high degree of plasticity in lifespan seen in *C. elegans*. This possibility will be explored in the next two chapters.

3.3.4 Insulin/IGF-1 signalling in *C. elegans* regulates ageing through a fecundity trade-off

Although suppression of IIS results in large lifespan extension in *C. elegans*, e.g. via the *daf-2* insulin/IGF-1 receptor (Kenyon et al., 1993), it can do so without reducing fertility (Larsen, et al., 1995; Gems, et al., 1998; Tissenbaum & Ruvkun, 1998; Dillin, et al., 2002), which has even led to the suggestion that the ageing process can be directly regulated (Kenyon, 2011). However, as just described, considering fertility alone as a measure of reproductive effort can be insufficient to give the full picture (Abrams & Ludwig, 1995; Lee, 2003; Austad, 1997; Lahdenpera, et al., 2004). Evidence presented in this chapter shows that IIS enhances venting of both yolk and unfertilised oocytes (Gems et al., 1998) to provision growing larvae. It suggests that suppression of IIS extends *C. elegans* lifespan at least in part through suppression of intestinal atrophy and yolk production (Ezcurra et al., 2018; Garigan et al., 2002; Luo et al., 2010; McGee et al., 2012). This implies that IIS promotes ageing by activating a costly reproduction-associated programme (Figure 3.14), and so suggests a new ultimate-proximate account of the AP action of IIS. Moreover, the likelihood that IIS drives both yolk milk production and ageing (Kenyon et al.,

1993) lends further support to the possibility that *C. elegans* undergo reproductive death, suppression of which results in large increases in lifespan extension.

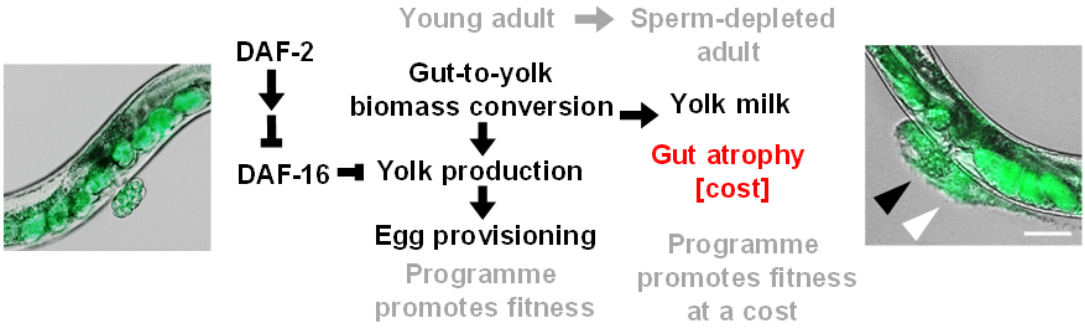

FIGURE 3.14. Model of intestinal conversion to yolk in post sperm-depleted adults, where the benefit of yolk milk comes at the cost of intestinal atrophy. Here IIS promotes self-destructive somatic biomass repurposing, thus promoting senescence in a fashion typical of organisms exhibiting semelparous reproductive death. Scale 50 µm.

3.3.5 Further characterisation of yolk milk feeding

3.3.5.1 Is yolk venting is a regulated active process?

Several results suggest that yolk venting is a regulated active process: (i) timing of yolk venting coincides with unfertilised oocyte laying, with oocytes and free yolk often found to be vented together; (ii) observations of yolk venting from videos shows that, as with egg laying, yolk venting occurs intermittently and typically in substantial bursts leading to emptying of yolk from the proximal uterus, i.e. yolk does not slowly leak out of the uterus; and (iii) muscle contraction in the uterus and vulva during yolk venting resembles contraction seen during egg-laying. While adding further support to the hypothesis that yolk venting is an adaptation, these results also suggest an additional function of the neuromuscular machinery of egg laying: in post-reproductive milk release. It would be interesting to study this further using the many mutations and drugs that have been previously used to dissect the egg laying process (Trent, et al., 1983). For example, one could test to see if, as with egg laying, drugs and chemical agents such as serotonin, quinpirole, chlorpromazine and fluoxetine stimulate yolk venting, while agents such as dopamine or tyramine inhibit it.

3.3.5.2 Could the glyoxylate pathway promote metabolism of ingested yolk in early larvae?

During early larval development, before the metabolic shift that occurs between L1 and L2, the glyoxylate pathway is up-regulated, enabling conversion of acetyl-CoA to glucose via

gluconeogenesis (Wadsworth and Riddle, 1989). One possibility is that this, in part, reflects an adaptation that allows early larvae to synthesise glucose from yolk lipid, thereby enhancing growth. The glyoxylate enzymes isocitrate lyase and malate synthase are encoded by a single gene, *icl-1* (previously known at *gei-7*). *icl-1* is up-regulated in dauers and by *daf-16* (McElwee et al., 2006). To test this, one could monitor the effect of *icl-1* RNAi on growth of L1 larvae on either *E. coli* or vented yolk.

3.3.6 Milk feeding in the wild

How plausible is it that yolk milk production in *C. elegans* and its associated benefits promote fitness in wild populations? This is difficult to assess, but there are some clues. Intestinal biomass conversion to yolk has been shown to be influenced by bacterial pathogenicity, with culture on either antibiotic-treated or UV-irradiated bacterial lawns reducing intestinal atrophy and PLP accumulation (Ezcurra et al., 2020). One means to explore this further would be to culture *C. elegans* on the wild bacterial isolates it is usually associated with (Dirksen, et al., 2016) and then test effects on levels of yolk production.

One feature of many of these wild isolates is that pathogenicity can be influenced by spore formation, with *C. elegans* observed to die very quickly on these strains when spores are present (data not shown). One could test to see if yolk venting is influenced by spore presence, with the assumption that alternative sources of food are even more valuable when the pathogenicity of bacterial strains microbivorous *C. elegans* is associated with increases. Given that *C. elegans* has likely co-evolved with the strains it has been isolated on (Dirksen, et al., 2016) and symbiosis is often a feature co-evolution, a possibility is *C. elegans* may have evolved ways to interact with and condition the bacteria it is associated with. Part of the action of yolk milk may be associated with this. For example, the *C. elegans* intestine which is converted into yolk-milk contains gut granules filled with anthranilic acid (Coburn et al., 2013), and while the function of gut granules remains unresolved, anthranilic acid is known to have antimicrobial properties (Grant, 2013). If it is present in the milk at sufficient levels, anthranilic acid could limit growth of pathogenic strains, or even influence the balance of bacterial species around it to promote its own fitness. A further possibility is that NLP-77 has a similar function associated with altering bacterial populations, especially given it is the homologue of the OV-17 antigen secreted in parasitic nematodes. Note here that parasitic nematodes (and other helminths) secrete a range of proteins that modulate host immunity as a means of avoiding host immune attack (Cooper & Eleftherianos, 2016).

Chapter 4: *C. elegans* hermaphrodites undergo semelparous reproductive death

4.1 Introduction

Ageing in *C. elegans* is unusual in terms of the severity, early onset and rapid rate of progression of senescent pathology with, notably, organs associated with reproduction affected (Figure 1.6) (Ezcurra et al., 2018; Garigan et al., 2002; Herndon et al., 2002). In particular, intestinal biomass is converted into yolk leading to intestinal atrophy and yolk steatosis, and PA in the hermaphrodite germline supports nascent oocyte growth at the cost of gonad atrophy (Ezcurra et al., 2018; Sornda et al., 2019; de la Guardia et al., 2016) (Figure 1.7). This pattern of rapid and severe pathological change affecting organs linked to reproduction (by contrast, the nervous system is relatively well preserved in ageing *C. elegans* (Herndon et al., 2002)) is reminiscent of semelparous organisms that undergo programmed reproductive death. In such organisms, massive translocation of resources at the time of reproduction is coupled to rapid and life-limiting organ degeneration (Young and Augspurger, 1991; Finch, 1990; Gems et al., 2020). For instance, in semelparous salmon severe muscle catabolism is required to generate nutrients to support the effort of swimming upstream for reproduction (Decken, 1992), and in semelparous lampreys muscle and intestinal atrophy is necessary for gonad growth and to sustain swimming (Larsen, 1980).

The last chapter focused on how trophallaxis, the social transfer of nutrient fluids between individuals particularly in the context of parental care (LeBoeuf, 2017), occurs in *C. elegans* through milk venting (free yolk) as well as laying of copious unfertilised oocytes (which act as vectors for yolk milk). This suggests a role for some of the reproduction-associated pathologies observed after self-sperm depletion, where maternal biomass is consumed to produce nutrients in a transferable form for progeny. Moreover, in wild-type males, these pathologies are not seen (de la Guardia et al., 2016; Ezcurra et al., 2018).

Work described in this chapter explores the hypothesis that *C. elegans* experience semelparous reproductive death by using a comparative biology approach. Protandrous hermaphroditism allows *C. elegans* to rapidly colonise new food patches but at the cost of a very short reproductive span (Hodgkin and Barnes, 1991; Schulenburg and Félix, 2017). Arguably, the capacity to convert somatic biomass into milk to feed to offspring allows post-reproductive *C. elegans* to overcome this cost, and promote inclusive fitness. This predicts that among *Caenorhabditis* species, lactation will occur in androdioecious but not gonochoristic species.

Comparing three *Caenorhabditis* sibling species pairs each with hermaphrodites or females, results in this chapter show that lactation and massive early pathology occurs constitutively only in the former. In each species pair hermaphrodites were shorter lived. Moreover, when another well-studied hermaphroditic nematode model, *Pristionchus pacificus*, was tested along with its gonochoristic sibling pair, the same pattern was observed demonstrating that this is not unique to the genus *Caenorhabditis*.

4.2 Results

4.2.1 Yolk venting in *Caenorhabditis* hermaphrodites but not females

One possibility is that the capacity to convert somatic biomass into a vitellogenin-rich soup (or milk) to feed offspring allows sperm-depleted *C. elegans* hermaphrodites to overcome the individual fitness cost of the short reproductive span caused by protandry by promoting inclusive fitness. This predicts that yolk venting will occur in hermaphroditic but not gonochoristic species. To test this, 3 pairs of sibling species in the *Caenorhabditis* genus were compared, where one was hermaphroditic and the other gonochoristic: *C. elegans* vs *C. inopinata*, *C. briggsae* vs *C. nigoni*, and *C. tropicalis* vs *C. wallacei*. These represent 3 independent occurrences of the evolution of hermaphroditism (Cutter et al., 2019) (Figure 4.1 A).

First, yolk venting and yolk accumulation were compared in unmated animals. For each pair of sibling species, copious yolk venting and unfertilised oocyte laying was seen in hermaphrodites and not in females (Figure 4.1 B,C). This suggests that milk feeding may occur in all 3 hermaphroditic species. As in *C. elegans*, vitellogenins accumulated internally to high levels in *C. briggsae* and *C. tropicalis* hermaphrodites, but more modestly in *C. inopinata*, *C. nigoni* and *C. wallacei* females, where accumulation also plateaued at a relatively early time point (Figure 4.2).

Next, hermaphrodites and females of a sibling species pair from the free-living nematode genus *Pristionchus* were compared. YP170 proved to be absent from *Pristionchus* species and instead YP115 and YP88 equivalents were produced in large quantities (Figure 4.2, see especially gel image). This is supported by *P. pacificus* lacking all *vit* genes (*vit-1–vit-5*) apart from *vit-6*, for which two orthologues exist (Dieterich, et al., 2008). Again, *Pristionchus* hermaphrodites but not females showed yolk venting, copious unfertilised oocyte laying and high levels of vitellogenin accumulation in hermaphrodites post sperm-depletion (Figure 4.1 B,C and Figure 4.2). One possibility is that yolk and oocyte venting occurs only after sperm presence followed by depletion, and therefore is absent from unmated females. However, in females mating did not significantly increase yolk venting or laying of unfertilised oocytes after sperm depletion (Figure

4.3). Vented yolk was seen in mated hermaphrodites (Figure 17C) though at much lower levels than in unmated ones, perhaps because more yolk is used to provision oocytes that get fertilised, which are produced in larger numbers. These results support the hypothesis that milk feeding has evolved repeatedly in hermaphroditic nematodes to enable sperm-depleted mothers to continue to contribute to fitness.

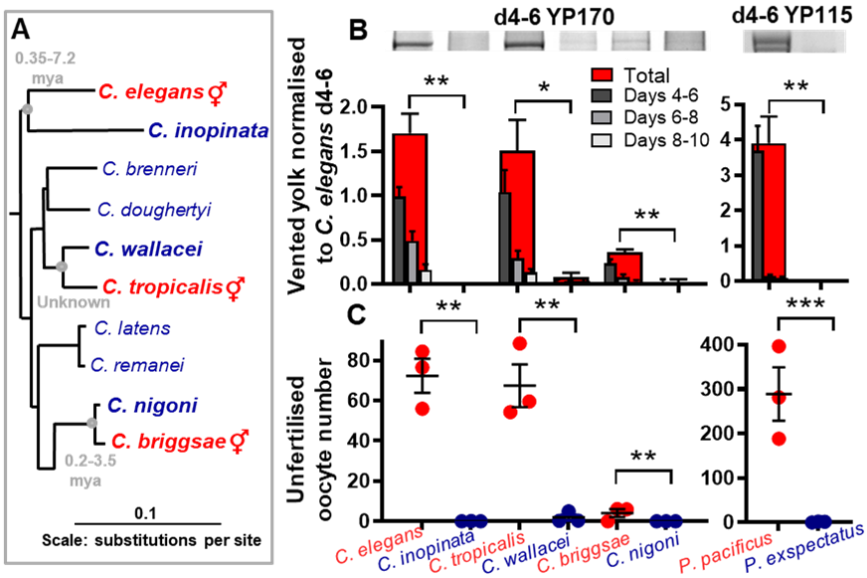

FIGURE 4.1. *Caenorhabditis* hermaphrodites exhibit yolk milk venting. (A) Phylogenetic tree showing androdioecious and gonochoristic *Caenorhabditis* sibling species (Stevens, et al., 2019). Estimates of time since divergence: *C. elegans, C. inopinata* 0.35-7.2 MYA; *C. briggsae, C. nigoni* 0.2-3.5 MYA (Cutter et al., 2019); *C. tropicalis, C. wallacei* still unknown. **(B)** Yolk milk venting present in hermaphrodites but not females (n=100 per trial). Top: major YP at the peak of venting. Bottom: Quantitated data normalised to total yolk on d4-6 in *C. elegans*. **(C)** Unfertilised oocytes are laid by hermaphrodites but not females (n=10 per trial). *Pacificus* species were found to produce a relatively large number of dead eggs during progeny production (easily distinguished from unfertilised oocytes). This is expected for these species (Ralf J. Sommer, personal communication). One-way ANOVA (Bonferroni correction) and one-sample t-test (two-tailed) used based on number of samples being compared. Mean ± s.e.m. of 3 trials displayed. **P*<0.05, ** *P* <0.01,*** *P* <0.001. Females in blue and hermaphrodites in red. Victor Konstantellos helped with running and the analysis of gels and Kavindi Gunaratne and Luis Montemayor helped with brood size counting.

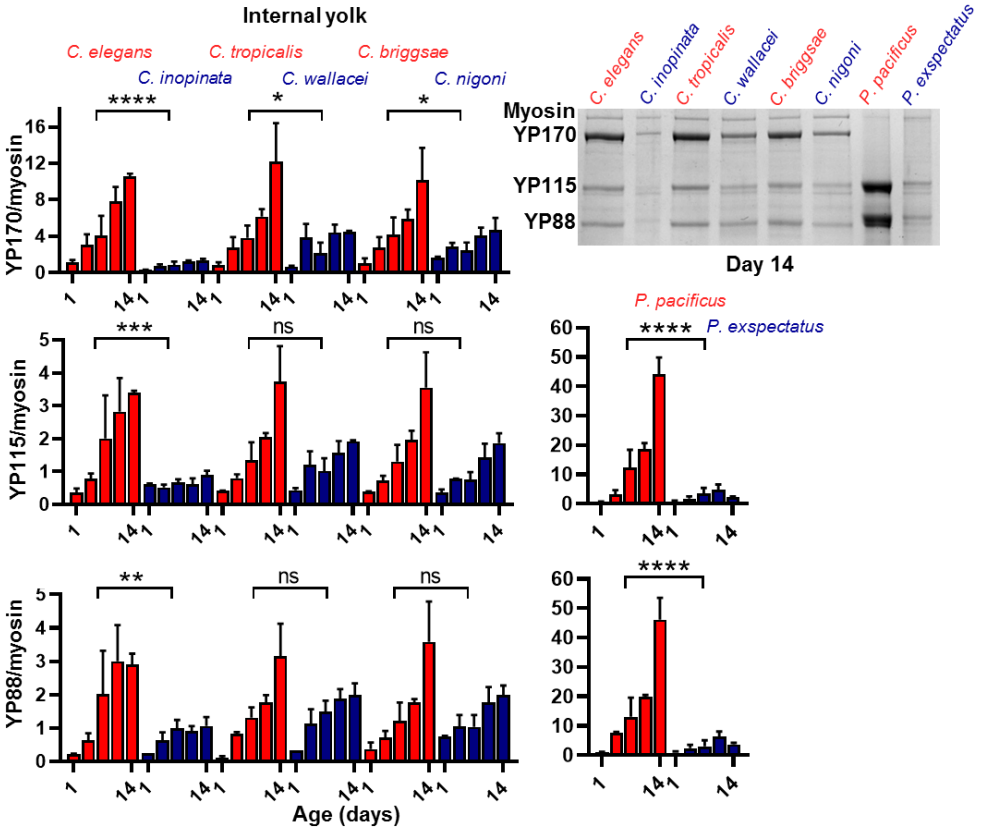

FIGURE 4.2. Greater internal vitellogenin accumulation in hermaphrodites. Greater internal levels of YP170 in *Caenorhabditis* hermaphrodites, and YP115/YP88 in *P. pacificus* hermaphrodites (*Pristionchus* lack YP170). YP bands normalised to myosin to adjust for species differences in body size. Protein gel electrophoresis data with colloidal coomassie blue staining. Mean ± s.e.m. of 3 trials displayed. ANCOVA. * P <0.05, ** P <0.01, *** P <0.0001, **** P <0.00001. Victor Konstantellos helped with the analysis of gels.

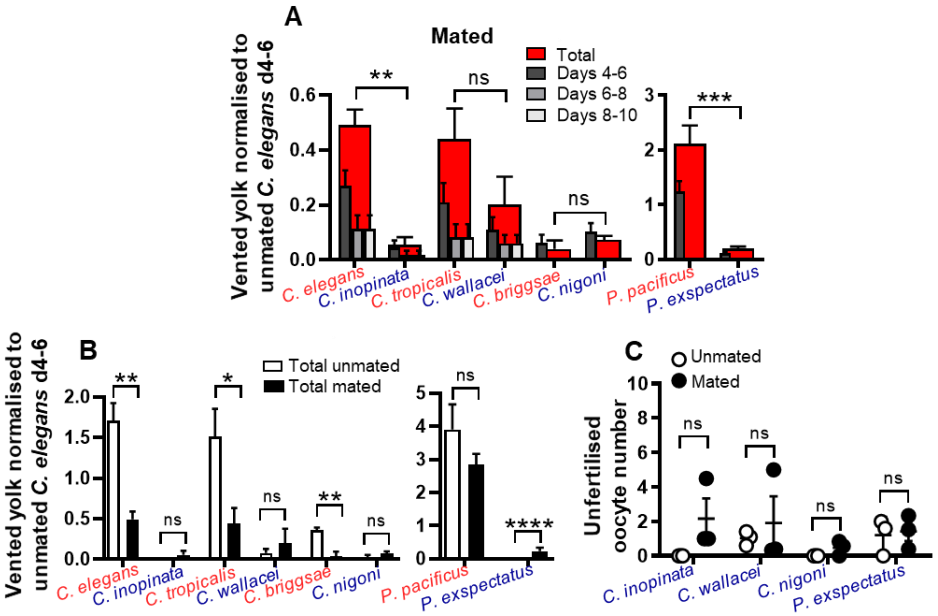

FIGURE 4.3 Mating reduces yolk venting in hermaphrodites while having little effect on yolk venting and unfertilised oocyte production in females. (A,B) Vented YP170 in mated *Caenorhabditis* species and YP115 in mated *Pristionchus* species. Data normalised to unmated *C. elegans* peak venting period of d4-6 (c.f. Figure 4.1B). **(B)** Comparison to unmated data. **(C)** Mating does not significantly increase unfertilised oocyte production in females. Mated *P. exspectatus* produce an especially large number of dead eggs that are easily distinguishes from unfertilised oocytes, and is expected for this species (Ralf J. Sommer, personal communication). One-way ANOVA (Bonferroni correction) and one-sample t-test (two-tailed) used based on number of samples being compared. Mean ± s.e.m. **P*<0.05, ** *P* <0.01,*** *P* <0.001, N=3. Victor Konstantellos helped with the analysis of gels.

4.2.2 Hermaphrodites are shorter lived than females

The working hypothesis is that subsequent to the emergence of hermaphroditism from each gonochoristic ancestor, reproductive death evolved. This predicts that hermaphrodites should be shorter lived than unmated females of their sibling species. To test this, lifespan in the 3 *Caenorhabditis* sibling species pairs is compared. Lifespan was significantly greater in females than in hermaphrodites in all cases apart from between *C. elegans* and *C. inopinata*, the latter as previously reported (Woodruff et al., 2018). *C. elegans* lifespan is limited by infection with the *E. coli* food source (Garigan, et al., 2002; Gems & Riddle, 2000; Zhao et al., 2017). This raises the possibility that *Caenorhabditis* species vary in their susceptibility to *E. coli* infection. Notably, *C. inopinata* is not a terrestrial species but rather dwells within figs on *Ficus septica* trees (Kanzaki et al., 2018), raising the possibility that it might be more susceptible to infection due to lack of natural exposure to a wide array of microbial pathogens. To test this, lifespans of the six species were compared in the presence of the antibiotic carbenicillin to exclude differences in susceptibility to infection. Lifespan was found to be significantly greater in all females when compared to hermaphroditic pairs (Figure 4.4 A, B, and Appendix 1). This suggests that *C.*

inopinata is hyper-susceptible to fatal infection by *E. coli*. Mean lifespans of unmated hermaphrodites on antibiotics were as follows: *C. elegans* (20.1) < *C. tropicalis* (22.5) < *C. briggsae* (23.9). The magnitude of the difference in lifespan between sibling species showed the same ranking: *C. inopinata* (+50%) < *C. wallacei* (+25%) < *C. nigoni* (+21%) (Figure 4.4 C). In a further test *C. inopinata* were cultured on UV-irradiated *E. coli* which is another method to prevent bacterial proliferation and so exclude differences in susceptibility to infection. *C. inopinata* was again found also to be substantially longer lived than *C. elegans* (Figure 4.5 A and Appendix 1).

One problem with drawing conclusions from lifespans of different species of *Caenorhabditis* is that they may differ in terms of their optimal culture temperature. Thus, differences in lifespan at 20˚C could reflect how close or far each species is from its optimal temperature. This is a particular concern with respect to *C. inopinata* which shows optimal growth at a higher temperature; possibly it experiences 20˚C as too cold leading to some form of rate-of-living effect that slows ageing (Kanzaki, et al., 2018; Woodruff et al., 2018). To probe this, lifespans were compared at 25˚C and *C. inopinata* was again found to be longer lived than *C. elegans* (antibiotics present). Thus, greater longevity at 20˚C of *C. inopinata* compared to *C. elegans* does not appears to be due to a temperature effect (Figure 4.5 C and Appendix 1).

Similarly, in the *Pristionchus* sibling species pair, *P. pacificus* and *P. exspectatus*, females were longer lived both with or without antibiotics (+68% with antibiotics) (Figure 4.4 and Appendix 1). This is consistent with a previous report of greater longevity in *Pristionchus* females in general (Weadick and Sommer, 2016). These results support the hypothesis that reproductive death evolved after the appearance of hermaphroditism in both genera, leading to accelerated hermaphrodite ageing rate.

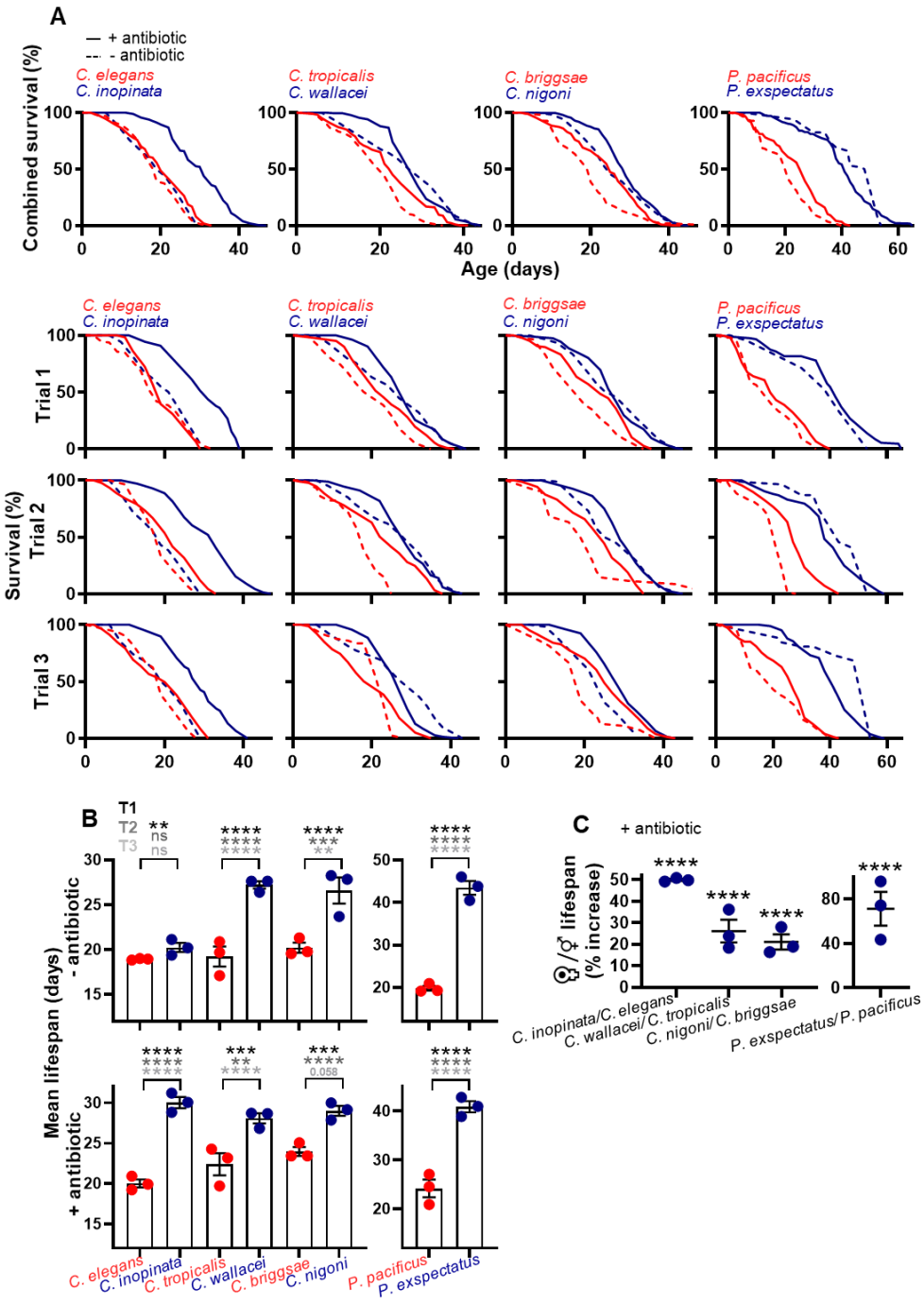

FIGURE 4.4 Hermaphrodites are shorter lived than females. (A,B) Survival data from individual and combined trials of sibling species. In the presence of antibiotics, females are longer lived in all cases. Logrank individual trials. **(C)** Percentage lifespan of females relative to their hermaphrodite sister species pair on antibiotics. Logrank combined data. For additional statistics and sample sizes see Appendix 1. Mean ± s.e.m. of 3 trials. *P<0.05, ** P <0.01,**** P <0.0001, N=3. Shivangi Srivastava helped with the scoring of lifespan assays.

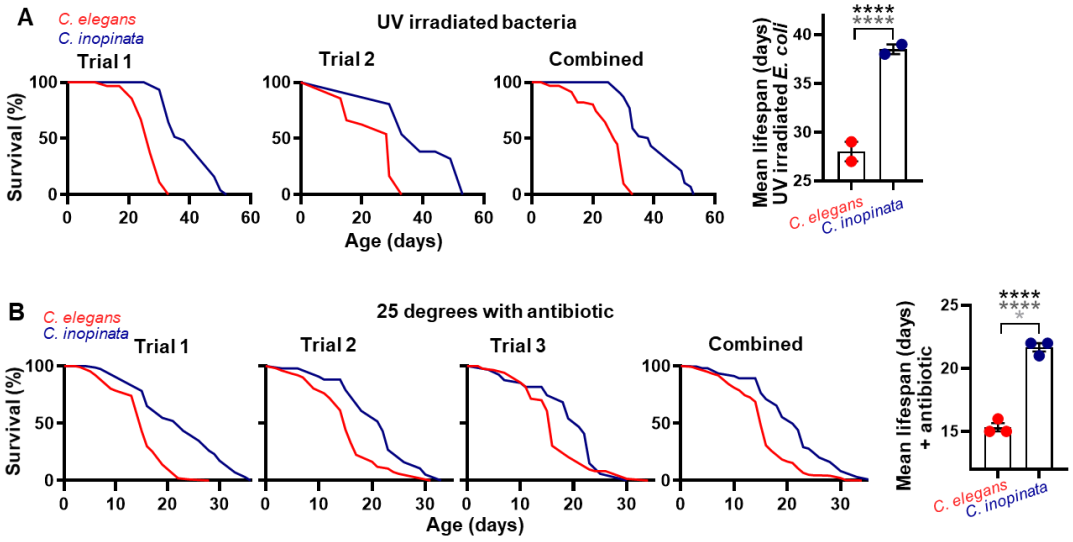

FIGURE 4.5 C. inopinata is hypersensitive to infection. (A) *C. inopinata* is longer-lived than *C. elegans* where both are maintained on UV-irradiated *E. coli*. **(B)** *C. inopinata* is also longer lived than *C. elegans* at 25˚C (with carbenicillin), the optimal culture temperature for the former species. Combined lifespans and individual trials. Logrank individual trials. For additional statistics and sample sizes see Appendix 1. * P <0.05, ** P <0.01,**** P <0.0001. Shivangi Srivastava helped with the scoring of lifespan assays.

4.2.3 Evidence of reproductive death in hermaphrodites but not females

As described, in *C. elegans* destructive somatic biomass repurposing accompanies reproductive effort that is typical of semelparous organisms, ranging from monocarpic plants to Pacific salmon (Gems et al., 2020) (Finch C. , 1994). Visible pathologies in *C. elegans* include uterine tumours, gonadal atrophy, and intestinal atrophy coupled to yolk steatosis as well as pharyngeal deterioration (de la Guardia et al., 2016; Sornda, et al., 2019; Ezcurra et al., 2018; Garigan et al., 2002; Herndon et al., 2002; Wang et al., 2018). It is possible that *C. elegans* hermaphrodites exhibit a form of semelparity in which reproductive maturity triggers a programme of self-destructive reproductive effort leading to rapid death (Gems et al., 2020; Finch, 1994 a). Importantly, production of post-reproductive milk (in the form of free yolk and unfertilised oocytes) provides a possible explanation for the function of such a semelparous programme. If reproductive death is coupled to yolk milk production, this predicts that reproductive death should occur in hermaphrodites but not females, since the latter do not vent yolk milk (Figure 4.1).

To test this, patterns of senescent pathology in the 3 sibling *Caenorhabditis* species pairs were compared. The major senescent pathologies seen in *C. elegans* were also seen in the other two hermaphroditic species, but were largely absent from females (Figure 4.6 and 4.7). Most

notably, intestinal atrophy, PLPs and gonad atrophy were only observed in hermaphrodites (Figure 4.6 and 4.7). Also, notable was a complete absence of uterine tumours in most females with only a small portion presenting with tumours, and also greatly reduced pharyngeal pathology in females. The latter was unexpected, since pharyngeal pathology is not considered to be linked to reproductive effort; these findings suggest that perhaps it is. One possibility is that intestinal atrophy does occur in females, but only in very late life. To probe this, the six species were compared up to day 21, but even at this advanced age, no intestinal atrophy was seen in females (Figure 4.8). Moreover, in the *Pristionchus* sibling species pair, again only the hermaphrodites exhibited pathologies suggestive of reproductive death (Figure 4.9).

The relative severity of major senescent pathology in hermaphrodites differed significantly with the following ranking: *C. elegans*> *C. tropicalis* > *C. briggsae* (Figure 4.6-4.8). This ranking coincides with how long ago the hermaphroditic species is estimated to have evolved from its gonochoristic ancestor for *C. elegans* (0.35-7.2 MYA split) and *C. briggsae* (0.2-3.5 MYA split) (Figure 4.1A) (Cutter et al., 2019). A caveat here is that differences in pathology could to some extent reflect species differences in optimal culture conditions (e.g. temperature, microbiome). This suggests that *C. briggsae* and *C. elegans* could represent early and late stages in the evolution of reproductive death. This is consistent with the existence of a semelparity-iteroparity continuum (Hughes, 2017), where it is hypothesised that mechanisms of senescence operative in semelparous organisms (including plants) and iteroparous ones form an etiological continuum (Gems, et al., 2020), as previously described in Chapter 1.

Notably, in the *Pristionchus* species studied here (*P. pacificus* and *P. exspectatus*) which lack YP170 (Figure 4.2), i.e. the yolk protein coupled to gut atrophy in *C. elegans* (Figure 3.1) (Sornda, et al., 2019), other yolk proteins YP115 and YP88 were found to accumulate as intestinal atrophy and PLP accumulation occurred (Figure 4.2 and 4.9). This could imply that in *Pristionchus* it is YP115/YP88 synthesis rather than YP170 synthesis that is coupled to intestinal atrophy.

4.2.4 Intestinal atrophy in females is induced by mating

It is surprising that such similar pathologies should evolve independently in each of 4 events of the appearance of hermaphroditism. One possibility is that reproductive death is seen in hermaphrodites but not females because only the former are reproducing. To test this mated hermaphrodites/females of the 3 sister species pairs were compared. Mating induced intestinal

atrophy in females, and enhanced it in hermaphrodites, such that all 6 species showed similar levels of atrophy (Figure 4.6-4.9).

Lifespan analysis post mating showed a significant reduction in the lifespans of all females (Figure 4.10 A,B). This reduction was significantly greater than the reduction seen in hermaphroditic sibling species in the pairs, apart from between *C. elegans* and *C. inopinata* (Figure 4.10 C). The latter is not unexpected as antibiotic was not included in these trials, meaning susceptibility to infection in *C. inopinata* could have masked a life-shortening effect of mating.

In *C. elegans*, evolution of hermaphroditism is thought to have begun when females developed the capacity to generate and activate self sperm (Baldi et al., 2009). One possibility is that the appearance of self sperm was sufficient to switch reproductive death from facultative to constitutive. However, spermless *fog-2(q71)* and *fem-2(e2006)* female mutant *C. elegans* showed no detectable reduction in intestinal atrophy, yolk pool accumulation or pharyngeal atrophy (Figure 4.11). Thus, reproductive death in *C. elegans* is not a consequence of reproduction per se, or the presence of self sperm. This and the milder pathology in *C. briggsae* suggest that the evolution of constitutive reproductive death is a complex, multi-step process.

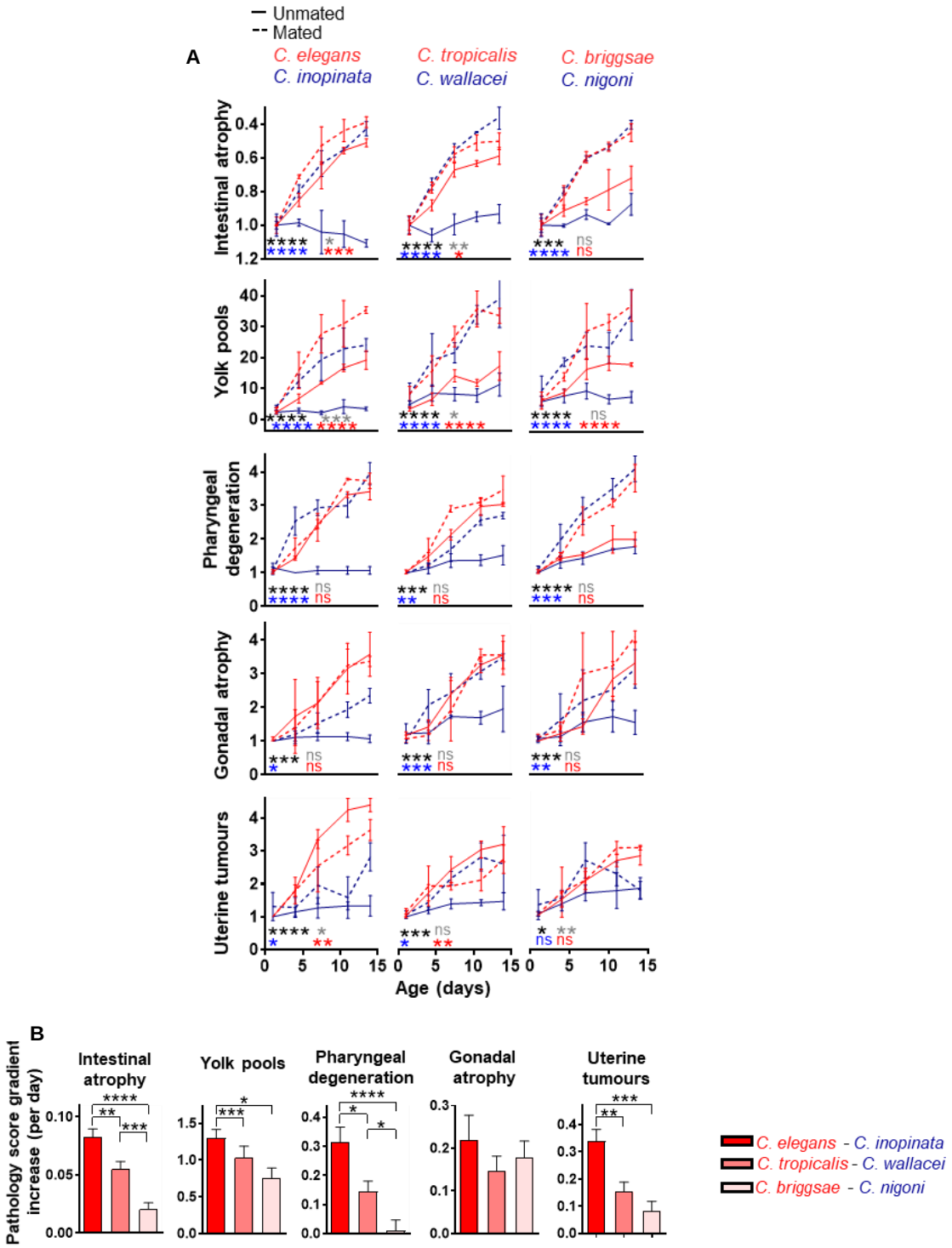

FIGURE 4.6. Reproductive death is constitutive in hermaphrodites and facultative (mating-induced) in females. (A) Severe pathology progression in unmated hermaphrodites and mated animals but not virgin females. Tests for statistical significance: black: hermaphrodites vs females; red: mated vs unmated hermaphrodites; blue: mated vs unmated females; grey: mated hermaphrodites vs mated females. Cumulative Link Model with gamma link function for pharyngeal degeneration, gonadal degeneration and uterine tumours which are scored ordinals. ANCOVA with score normalised to d1 to determine change in percentage of intestinal mass, and ANCOVA with no normalisation for yolk pools. Mean ± s.e.m. of 3 trials displayed (n=10 per time point per trial). **(B)** Bar graphs showing difference in gradient between species pairs, defining the following gradient in difference in severity for most pathologies: *C. elegans* - *C. inopinata* > *C. tropicalis* - *C. wallacei* > *C. briggsae* - *C. nigoni*. Subtraction rather than normalisation is used as gradients are already relative values. * P <0.05, ** P <0.01, *** P <0.0001, **** P <0.00001. StJohn Townsend, Nancy Hui, Victoria Tse and Dominik Maczik helped with parts of the pathology data collection and analysis.

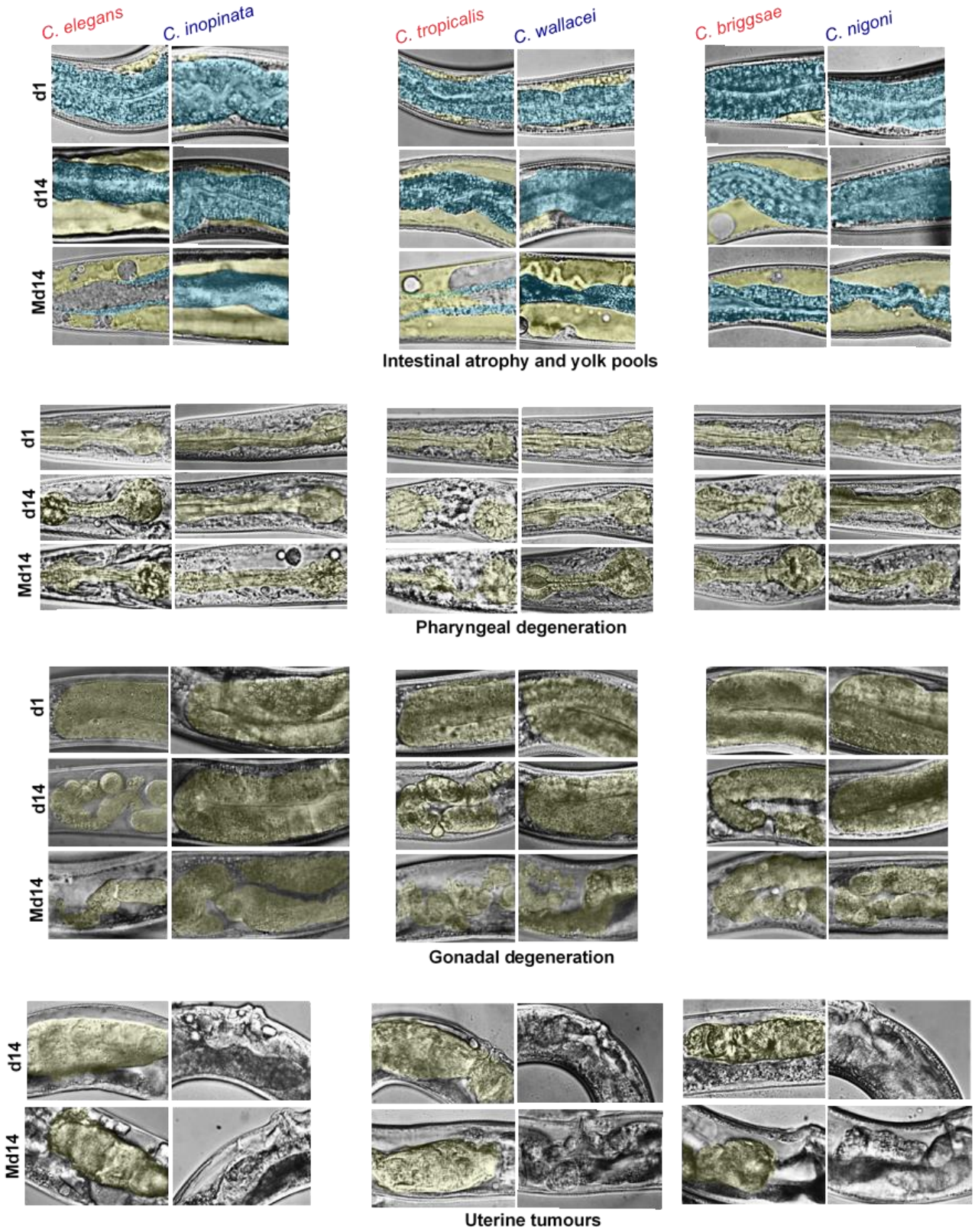

FIGURE 4.7. Representative Nomarski images taken for the purpose of scoring and measuring pathology. Yellow: yolk pools, gonad and tumours, and blue: intestine.

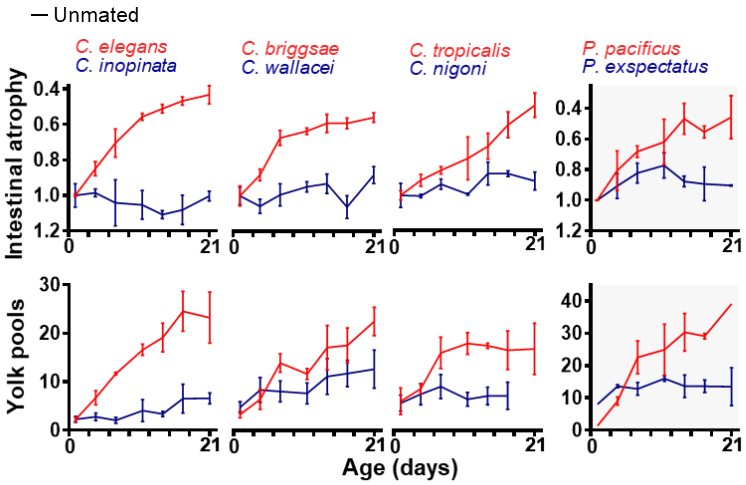

FIGURE 4.8. Pathology scores showing no increase in intestinal atrophy even up to day 21 in unmated females.

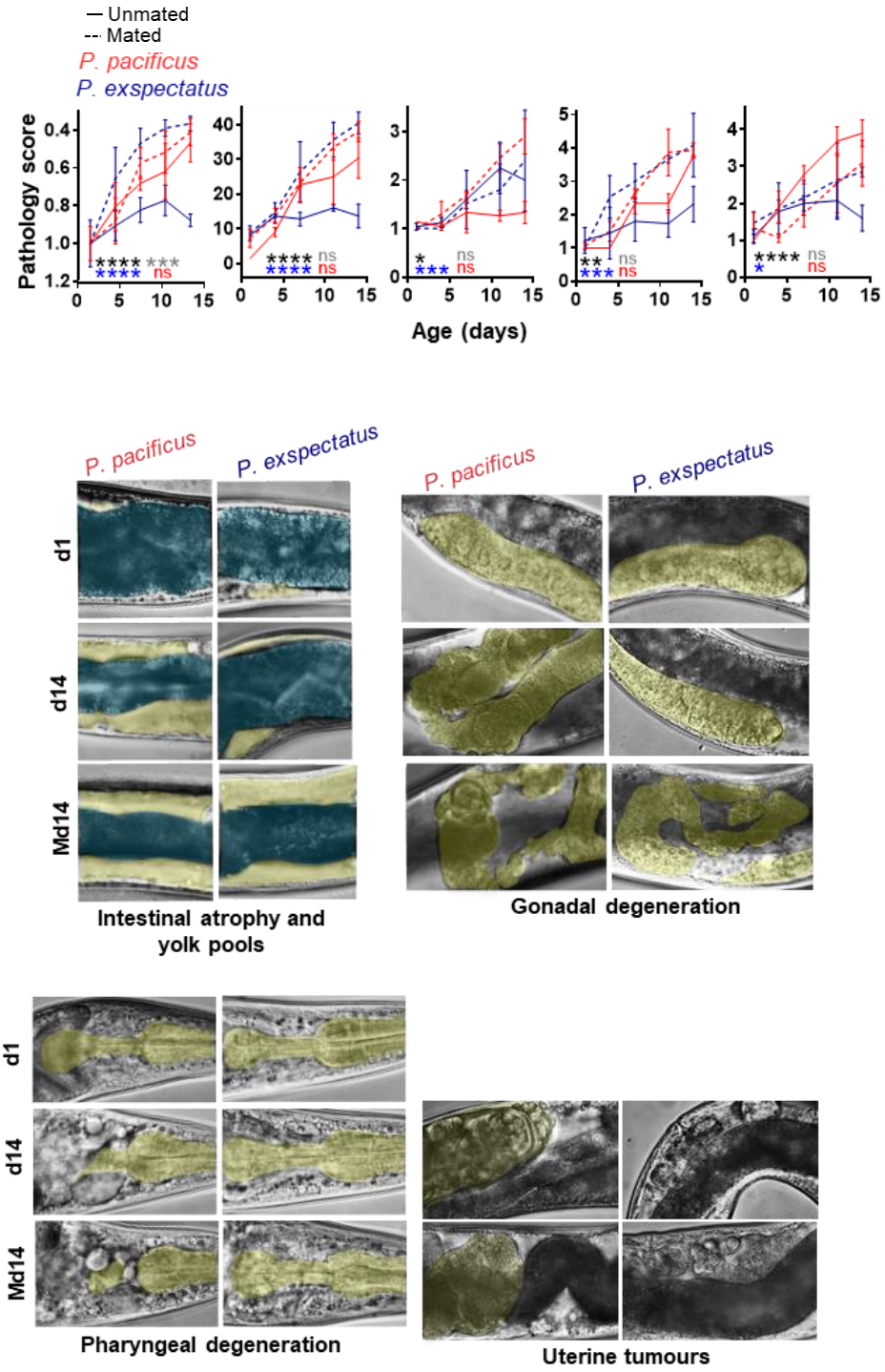

FIGURE 4.9. Evidence of reproductive death in *Pristionchus* hermaphrodites and mating-induced reproductive death in females. Top: Pathology progression through time. Mean ± s.e.m. of 3 trials displayed (n=10 per time point per trial). Tests for statistical significance: black: hermaphrodites vs females; red: mated vs unmated hermaphrodites; blue: mated vs unmated females; grey: mated hermaphrodites vs mated females. P value *<0.05, **<0.01,***<0.001, ****<0.0001. Bottom: Representative Nomarski images taken for the purpose of scoring and measuring pathology. Note position of gonad around the intestine is different in *Pristionchus* species, with the full gonad arm visible in the same plane only after intestinal atrophy.

StJohn Townsend, Nancy Hui, Victoria Tse and Dominik Maczik helped with parts of the pathology data collection and analysis.

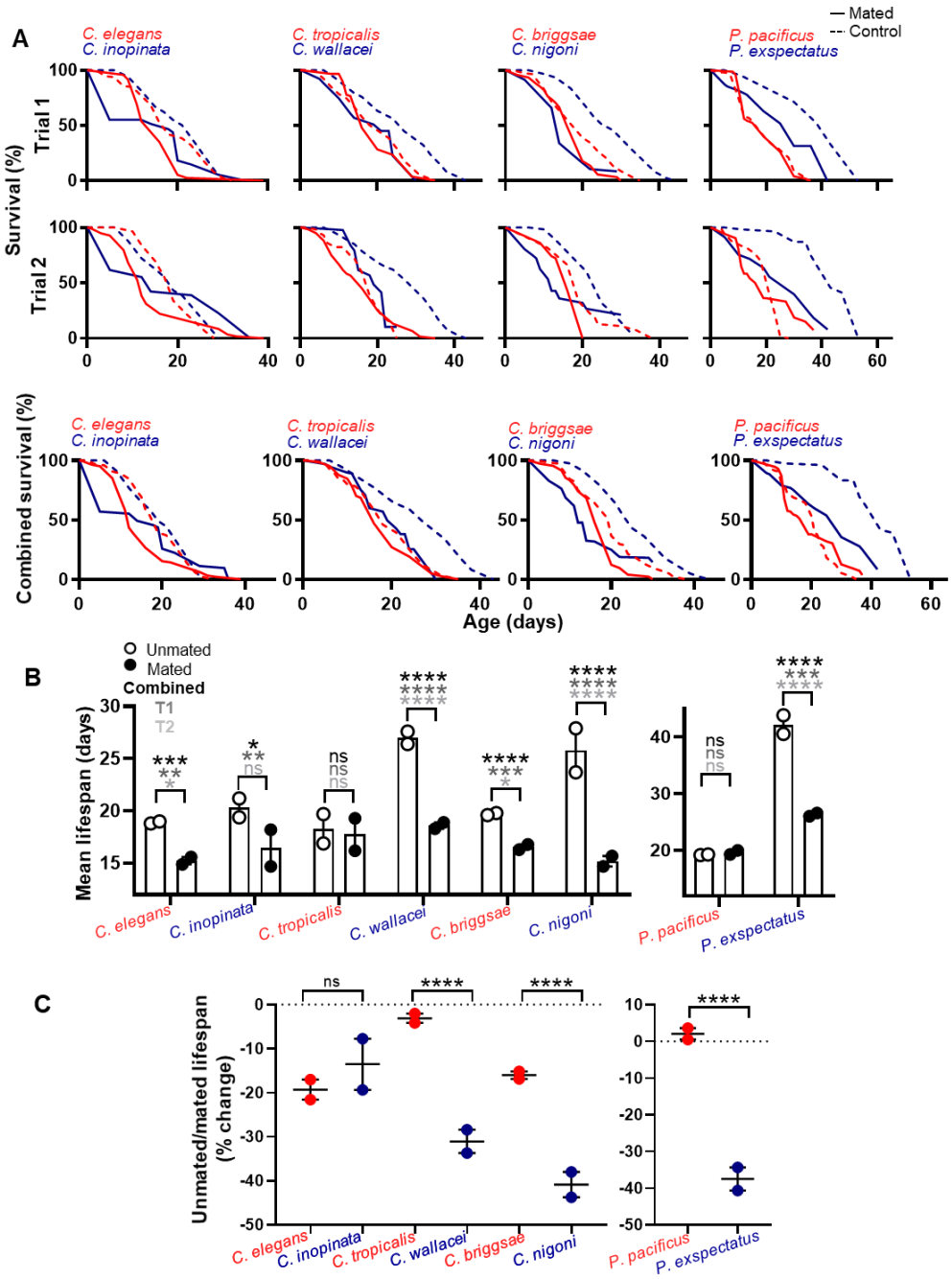

FIGURE 4.10. Mating reduces lifespan in females. **(A,B)** Mating in females significantly reduces lifespan, as previously shown for *C. elegans* (Gems & Riddle, 1996; Shi & Murphy, 2014; Maures, et al., 2014). **(B)** Logrank comparison of mated and unmated animals. **(C)** Cox proportional hazard analysis showing greater effect post mating in most females; the lack of a greater reduction in *C. inopinata* than *C. elegans* could reflect the greater susceptibility of the former to bacterial infection. **(B, C)** Mean ± s.e.m. of 2 trials displayed. For raw lifespan data and details on statistics see Supplementary File 1 and 2, respectively. * P <0.05, ** P <0.01, *** P <0.0001, **** P <0.00001. For additional statistics and sample sizes see Appendix 1. Shivangi Srivastava helped with the scoring of lifespans.

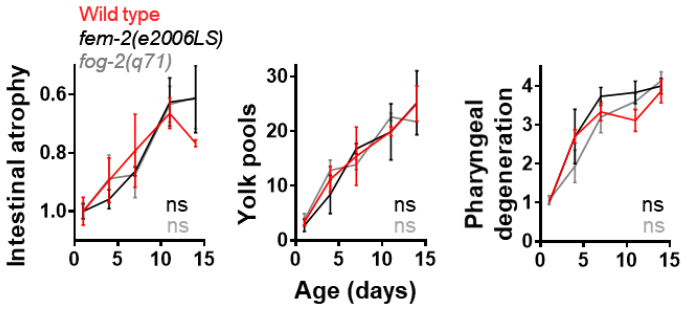

FIGURE 4.11. Reproductive death in *C. elegans* is not a consequence of the presence of self-sperm. Female mutant *C. elegans* show no significant difference in intestinal atrophy, yolk pool accumulation or pharyngeal atrophy (25˚C); it was previously shown that spermlessness accelerates uterine tumour growth which enhances gonad atrophy. (Wang et al., 2018). * *P* <0.05, ** *P* <0.01, *** *P* <0.0001, **** *P* <0.00001. Dominik Maczik helped with the pathology analysis.

4.2.5 The relationship between semelparity associated pathology and lifespan

The working hypothesis here is that reproductive death occurs in hermaphrodites and after mating in females, and shortens lifespan. This predicts: (i) that senescent pathologies in each case should be highly correlated with one another, since they are manifestations of a concerted, programmatic process, and (ii) that severity of pathology will correlate with shorter life.

To analyse the relationship between phylogeny, pathology and mating, hierarchical cluster analysis was performed (Figure 4.12 A). For this a Z-score for each pathology was calculated in order to make comparisons between different pathologies by normalising to the mean severity of the group (i.e. Z-score is measured in terms of standard deviations from the mean, with score 0 indicating that the data point's score is identical to the mean score, +2 representing the most severe pathology in the group and -2 the healthiest animals). This underscored how the difference in pattern of senescent pathology between hermaphrodites and females largely disappeared after mating. Overall all pathologies were found to correlate strongly with one another and developed in a synchronous manner and to approximately the same level of severity in a given individual (Figure 4.12 A). Intestinal atrophy also correlated the strongest with PLP accumulation, which is consistent with gut-to-yolk biomass conversion (Ezcurra, et al., 2018; Sornda, et al., 2019). Pharyngeal deterioration correlated more closely to gonadal degeneration, and the least correlated pathology to the rest were uterine tumours; this is expected given all pathologies are induced to the same or even greater extent in females post mating, apart from uterine tumour formation (see discussion).

To probe whether reproductive death-associated pathologies could be limiting lifespan in the hermaphrodites, median pathology severity (i.e. median of all 5 pathologies) in the different species was compared to the mean lifespan of the species, with antibiotics to avoid confounding effects of infection (Figure 4.12B). The relationship between median Z-score and lifespan followed a consistent pattern of negative correlation. In unmated hermaphrodites, the relationship between pathology and lifespan clearly corresponded to the pathology ranking established above (Figure 4.2, 4.4, 4.6-4.8, 4.10): *C. elegans* > *C. tropicalis* > *C. briggsae* (Figure 4.12 A). Following this relationship leftwards and upwards, the 3 females species cluster together with far lower pathology and longer life, again highlighting the likely presence of a semelparity-iteroparity continuum.

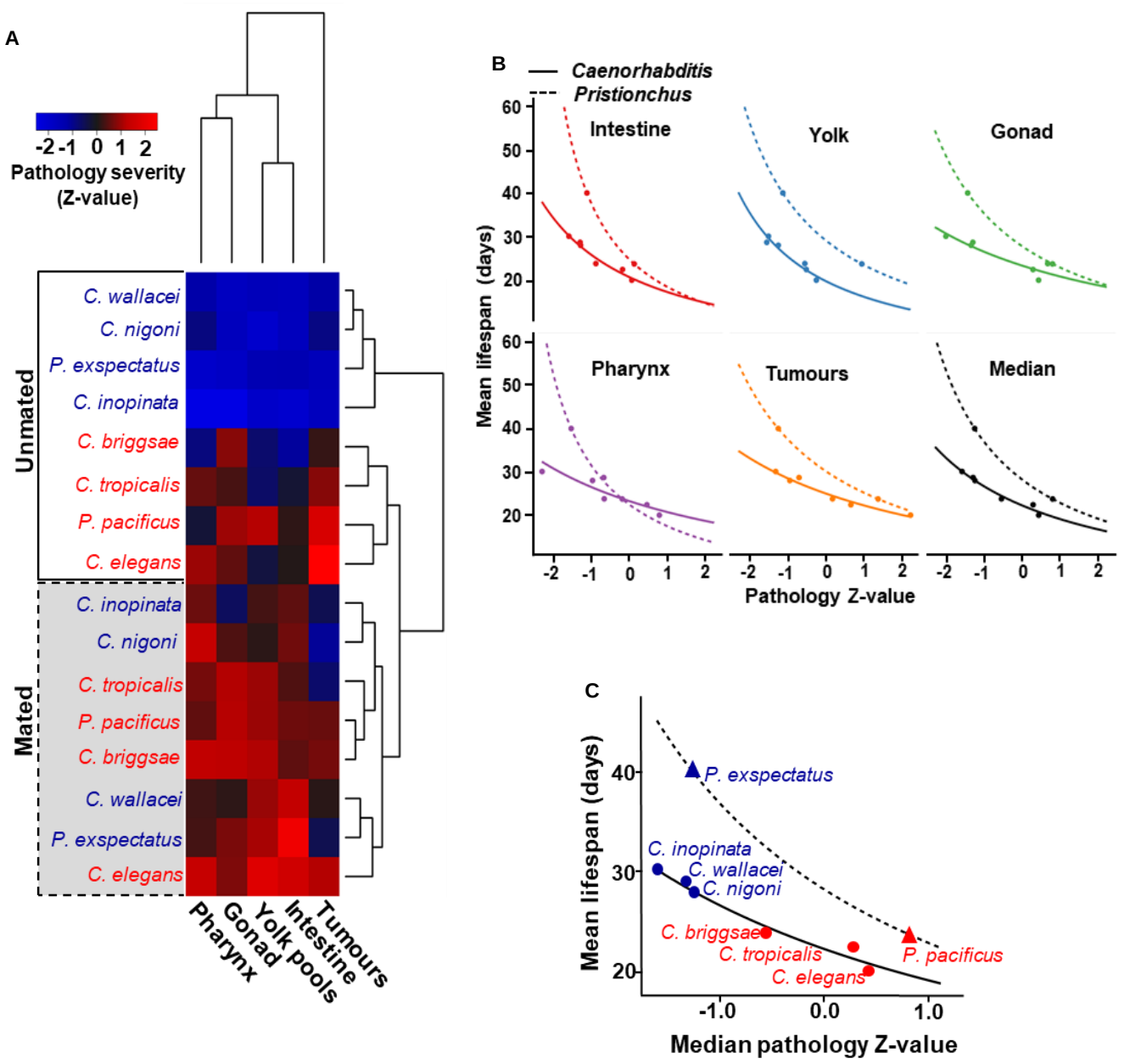

FIGURE 4.12. Level of reproductive death associated pathologies correlate tightly with each other and lifespan. (A) Heat map comparing differences in pathology progression across species and treatments by transforming the calculated gradients of pathology progression into Z-scores (which allows comparison between different pathologies by normalising to the average level of pathology severity, 0, with +2 representing maximum pathology severity in the group and -2 the healthiest animals). Hierarchical clustering based on pair-wise Euclidean distances was used to cluster pathologies and species/treatments according to similarity. **(B,C)** In order to compare each pathology to lifespan, linear regression was performed using the pathology Z-score (numerical value) as the independent variable and the inverse of the lifespan as the dependent variable. In order to assess the combined impact of all pathologies on lifespan, the median of the pathology Z-scores was used as the independent variable. A line of best fit is drawn to connect points for the *Caenorhabditis* species and based on this a hypothetical line is drawn for the *Pristionchus* species. StJohn Townsend helped with the pathology analysis.

4.2.6 TEM ultrastructure changes with age support reproductive death in hermaphrodites but not females

Previous transmission electron microscopy (TEM) studies have shown major degenerative changes in intestinal ultrastructure in *C. elegans* (Herndon et al., 2018) and *C. briggsae* (Rothstein, 1974; Zuckerman, et al., 1971). One possibility is that this is a consequence of semelparous 'programmed' senescence. To explore this further, with emphasis on intestinal senescence, TEM was performed on posterior cross sections from the 3 *Caenorhabditis* sibling species as well as the females *C. inopinata* and *C. wallacei*, examining 1 day old and 14 day old adults. Around 3-5 animals were examined with several sections taken per animal.

As expected, intestinal cross-sectional area was greatly reduced and intestinal lumen often expanded in selfing hermaphrodites but not unmated females, and in all 3 hermaphroditic species dramatic ultrastructural changes were seen similar to those described previously in senescent *C. elegans* (Herndon, et al., 2002) and *C. briggsae* (Epstein, et al., 1972) (Figure 4.13- 4.16, Table 4.1).

Based on the supposition that autophagy-dependent gut-to-yolk biomass conversion promotes atrophy, a prediction is that autophagosomes should be prominent in hermaphrodite intestines. Autophagosomes were identified by reference to previous TEM studies (Herndon, et al., 2018); autophagosomes are recognisable as electron transparent (light) regions bounded by one or more membranes, with some material of fragmented appearance within, sometimes including some highly electron dense puncta (potentially aggregated material, such as lipofuscin). Here it should be stressed that while one can identify structures that are likely to be autophagosomes, identification with complete certainty is difficult, particularly given the structurally chaotic and degenerated nature of the senescent intestine. Autophagosome-like structures were large and abundant in the hermaphrodites but not unmated females (Figure 4.13, 4.15).

Also, notable was the overall reduction in electron density (loss of ground substance) in the intestine, which was severe in *C. elegans*, and notable in *C. tropicalis* but less so in *C. briggsae* and the female species, following the trend of pathology severity *C. elegans* < *C. tropicalis* < *C. briggsae* previously noted (Figure 4.13, 4.16). Loss of ground substance implies a loss of cellular content, consistent with consumption/repurposing of intestinal biomass. In the senescent *C. elegans* intestine, mitochondria were almost absent but in other species remained relatively abundant, particularly near the apical membrane (likely for the purpose of active transport of

nutrients into the intestine). Many mitochondria remained in evidence in ageing *C. tropicalis* and *C. briggsae*, again indicating a lesser degree of degeneration than seen in *C. elegans*.

The ultrastructural changes that are so prominent in senescent *C. elegans* are potentially informative about senescent pathophysiology, including the effects of gut-to-yolk biomass conversion. Unfortunately, there is currently a lack of knowledge of the identity of many ultrastructural features of the senescent intestine. Organelles that are particularly prominent and abundant in the intestine (as shown by Nomarski and epifluorescence microscopy) are lipid droplets, yolk granules and gut granules. Using TEM, lipid droplets (Zhang, 2010) are distinguishable by their electron transparency and being bounded by a single membrane. Yolk granules have been identified in TEM using immuno-gold staining with an anti-vitellogenin antibody (Herndon et al., 2002) and appear as patches of homogenous grey (partial electron transparency). However, in disordered senescent intestines, they can be difficult to distinguish. Gut granules, which are extremely abundant in intestinal cells, are lysosome-related organelles much larger than normal lysosomes, and are of unknown function (Coburn & Gems, 2013). They sometimes contain birefringent material of unknown identify, sometimes anthranilates which causes blue fluorescence under UV light, and sometimes both (Coburn et al 2013; Hermann, et al., 2005). Despite their prominence, gut granules have yet to be identified at the level of ultrastructure (David Hall, Albert Einstein College of Medicine, personal communication), though one hazarded a guess about this (Leung, et al., 1999). Distinguishing lipid droplet, yolk granules and gut granules is further complicated by major differences in appearance of TEMs from different sources, which probably to some extent reflects differences in sample preparation staining.

Certain structures of unknown cytological identity are also a feature of intestinal atrophy in day 14 hermaphrodites, but largely absent in day 1 animals and day 14 females, and include: dark sooty deposits that could be protein or glycogen aggregates with age, dark (highly electron-dense) porous bodies and dark and pale bodies (Figure 4.15, 42, (c.f. Figure 4.6)). Dark porous bodies, with electron-transparent cores were previously seen in senescent *C. briggsae* and interpreted as lipofuscin granules (Epstein, et al., 1972). However, this seems to have been guesswork based on the oxidative damage theory of ageing that predominated at that time.

Deterioration of intestinal microvilli at advanced ages in *C. elegans* was previously noted (McGee, et al., 2011), but a significant difference between hermaphrodites and females was not observed (Figure 4.17). In some areas individual bacteria attach to the base of the microvilli, and may even appear embedded into the villi in a manner suggesting that they may cause local damage (McGee, et al., 2011; Herndon, et al., 2018). With this in mind, one possible reason for

the lack of difference observed between females and hermaphrodites is susceptibility to bacterial infection which may strongly influence microvilli deterioration. This could explain the especially prominent microvilli degeneration seen in *C. inopinata* (Figure 4.17), which is hypersensitive to infection by *E. coli* (Figure 4.4, 4.5).

Another difference in senescent pathology between hermaphrodites and females was also detected. In *C. elegans*, it was previously noted that the cuticle becomes thicker with age, suggesting possible run-on of cuticular biosynthesis across the course of adulthood (Herndon et al., 2018). Age increases in cuticular thickness were found to be less marked in *C. inopinata* (Figure 4.18) than in *C. elegans*. This could imply a link between run-on in cuticular synthesis and semelparity.

Mating *C. inopinata* was found to induce dramatic changes in intestinal ultrastructure as seen in hermaphrodites, including the presence of large masses of amorphous material in the intestine and enlarged pseudocoelom (Figure 4.19), similar to material in *C. elegans* identified using immunogold staining as yolk (Herndon et al., 2018). Loss of ground structure and the presence of structures such as dark porous bodies and sooty deposits were also observed (Figure 4.19). In support of a link between mating and cuticular hypertrophy, mating induced an age increase in cuticular thickness in *C. inopinata* (Figure 4.18). Taken together these findings suggests a possible explanation for how such similar patterns of reproductive death evolved independently in 3 hermaphroditic species: reproductive death is obligate in hermaphrodites and facultative (mating induced) in females. Thus, the evolution of reproductive death in hermaphrodites requires only the activation of semelparity in the absence of mating.

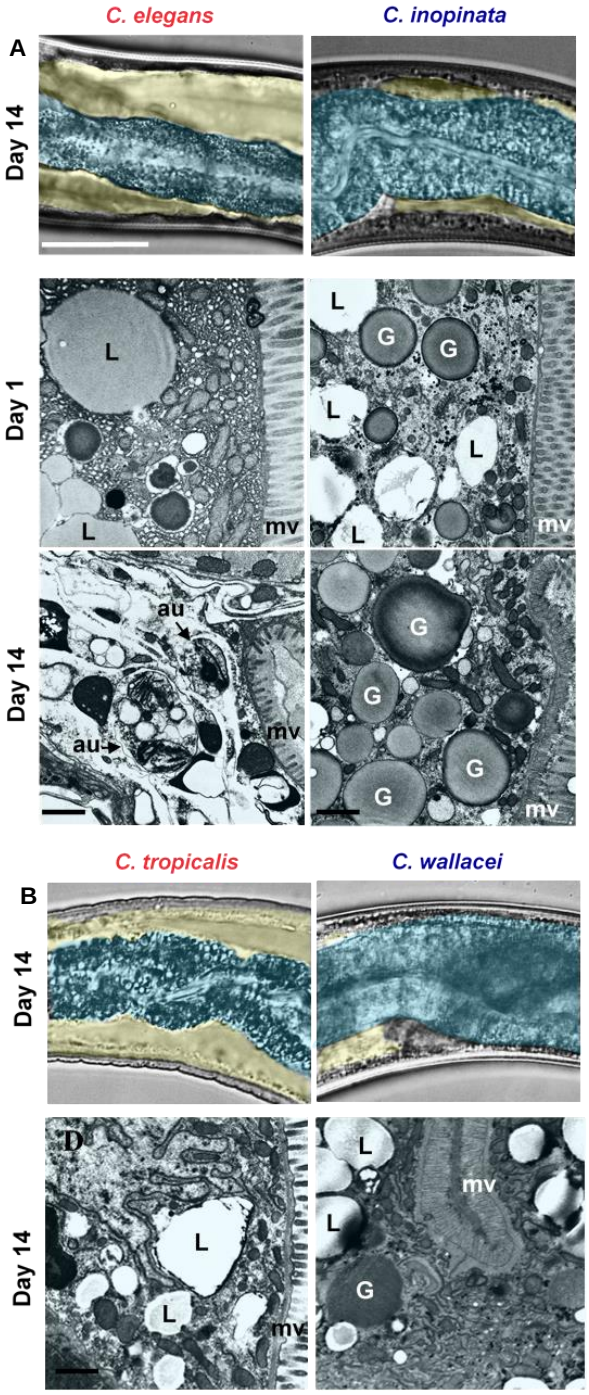

FIGURE 4.13. TEM intestine ultrastructure showing degenerative change in unmated hermaphrodites and little degeneration in unmated females. (A,B) Top: Intestinal atrophy (blue) and yolk pool accumulation (yellow) in ageing hermaphrodites but not females (day 14, unmated). Representative Nomarski images. Scale 25 µm. Bottom: Severe degeneration of intestinal ultrastructure in ageing hermaphrodites but not females (day 14, unmated). Note loss of organelles and ground substance, and presence of autophagosomes. Representative TEM cross-section images through the intestine. mv, microvilli; au, autophagosome-like structure, L, lipid droplets; G, yolk or gut granules (tentative identification). Scale 1 µm (20,000x). The structure of gut granules which are known to be present in the intestine is unknown but possibly many yolk granules and lipid droplets could in fact be anthranilate filled gut granules, with yolk known to stain in different ways, varying in electron density, but generally being darker than what lipid is interpreted to be (personal communication Dave Hall). **(A)** *C. elegans* and *C. inopinata* **(B)** *C. tropicalis* and *C. wallacei*. Mark Turmaine helped with TEM image acquisition.

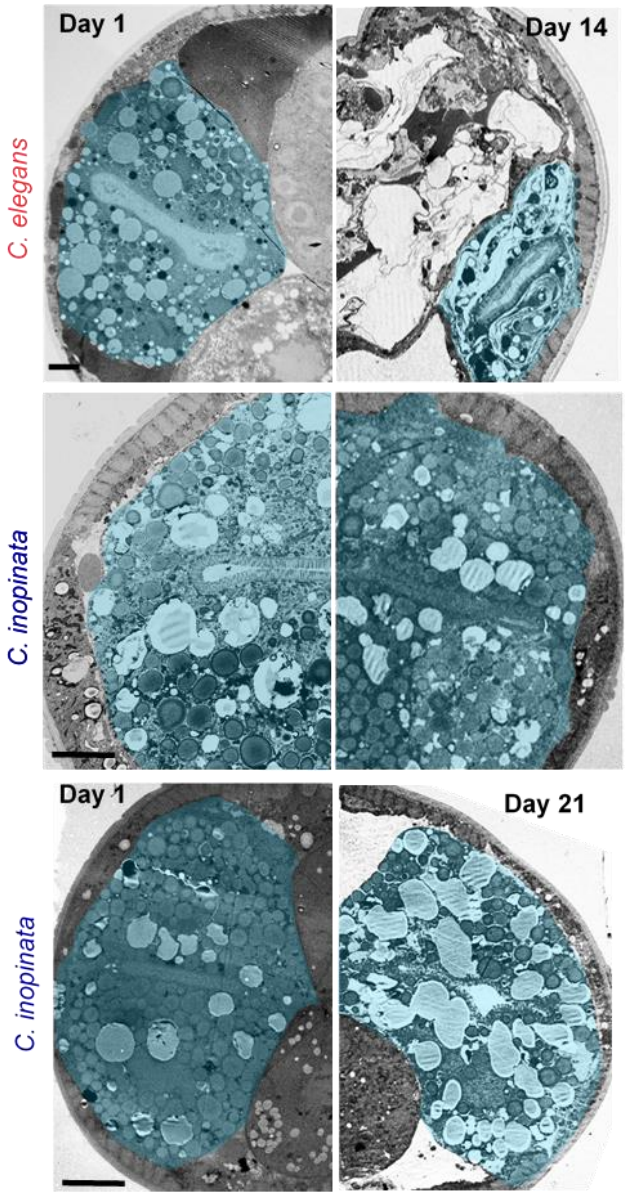

FIGURE 4.14. Low magnification representative TEM showing intestinal atrophy in *C. elegans* with age and little change in intestinal size in *C. inopinata* even by d21. Halves of nematode sibling species pairs are taken from approximately the same region of the animal (between the posterior end of the gonad and anus) to avoid the distorting effects of uterine tumours. Scale 5 µm (5,000x). Mark Turmaine helped with TEM image acquisition.

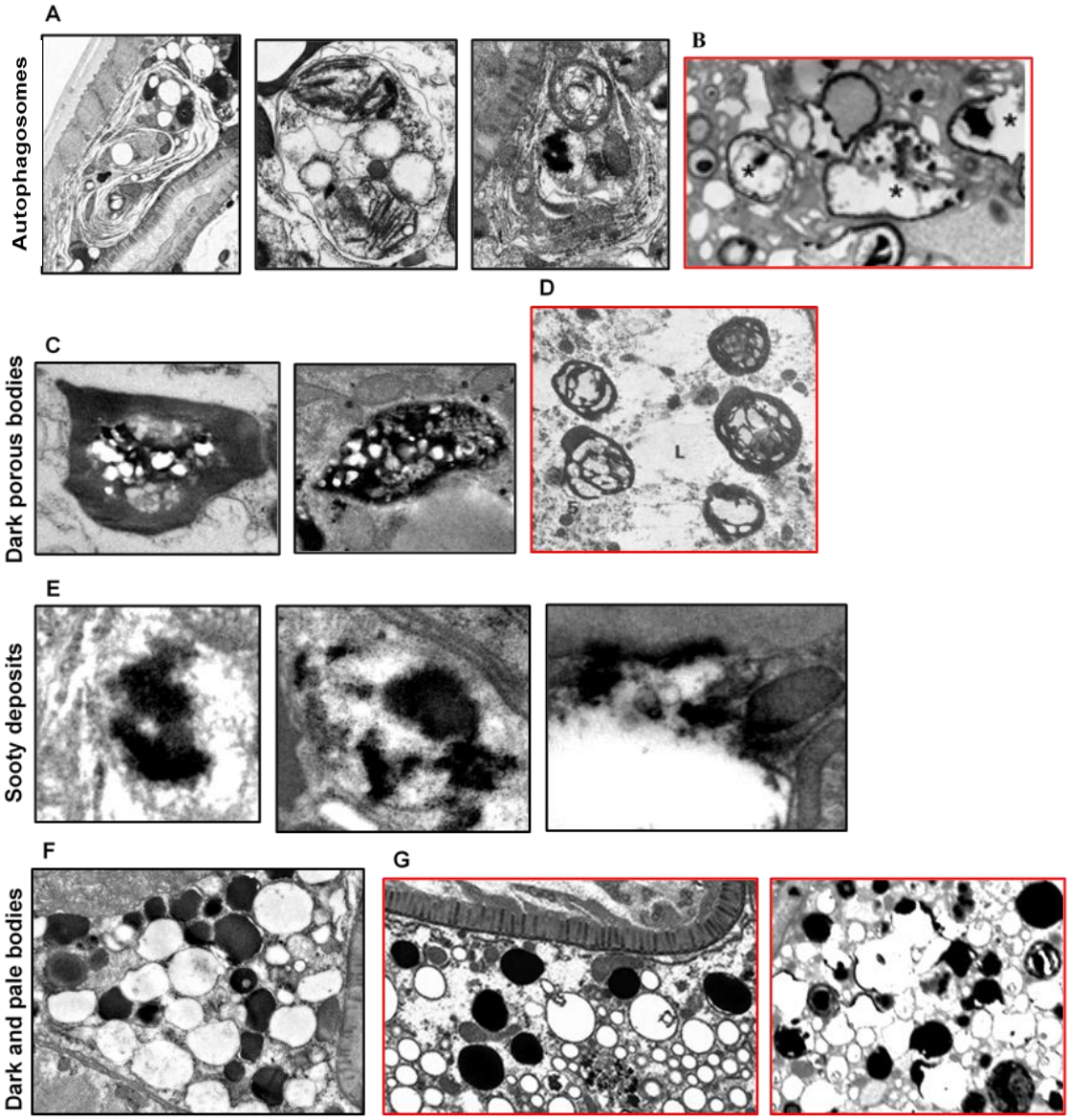

FIGURE 4.15. Bestiary of objects frequently observed in the atrophied intestine of *Caenorhabditis* hermaphrodites. (A) Likely autophagosomes. Left: Containing two spherical objects that are electron dense (black) inside the membrane bound structure; Middle: multilamellar at the bottom; and Right: very large multilamellar autophagosome. **(B)** Autophagosomes identified in (Herndon, et al., 2018) marked with stars. **(C)** Dark porous bodies. Electron dense cortex but internally a combination of electron opaque holes (white) and also very electron dense reticulate material. Possibly old lysosomes full of lipofuscin (c.f. D). **(D)** Examples of objects seen in C from Epstein et al. (1972) in *C. briggsae* in axenic culture. These were interpreted as lipofuscin (without corroboration). **(E)** Sooty deposits. Very electron dense, amorphous, without any clear edge. Looks like an aggregate, possibly of protein or glycogen, with glycogen found to be more evenly distributed and diffuse at earlier time points (c.f. Figure 4.13). **(F, G)** Dark and pale bodies. Pale bodies are usually interpreted as lipid droplets, and dark bodies in one case as gut granules (G) (Herndon, et al., 2018). Lipid droplets usually have a single membrane and gut granules and double membrane, however, the white bodies sometimes appear to have double membranes. Black box: images from TEMs taken in this study; Red box: images from other sources. Mark Turmaine helped with TEM image acquisition.

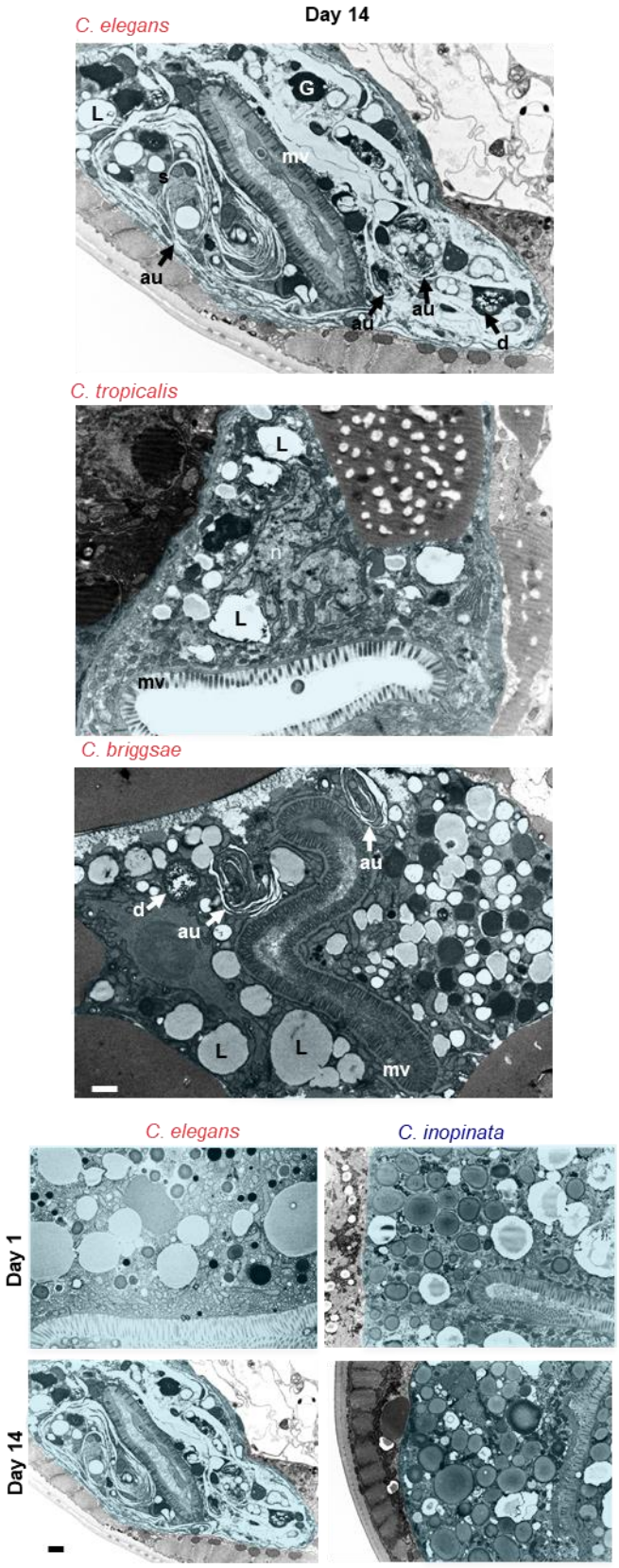

FIGURE 4.16. Hermaphroditic *Caenorhabditis* species showing intestinal degeneration and many of the objects identified in Figure 4.15. Top: *C. elegans, C. tropicalis* and *C. briggsae* hermaphrodites. Dark and pale bodies, sooty deposits, loss of ground structure, dark porous objects and autophagosomes are clearly visible. In addition, large open and empty intestinal lumens, a feature of an ageing intestine (Herndon, et al., 2018), are seen in *C. elegans* and *C. tropicalis* which undergo the most severe levels of reproductive death. The nucleus (n) in *C. tropicalis* and *C. briggsae* have largely lost heterochromatin, similar to what is seen in *C. elegans* around the same time point (Herndon et al., 2018). As images of the nucleus in females at the same time point were not taken, it is not known whether this is likely a conserved feature of ageing in all species or particular to hermaphrodites undergoing reproductive death. Bottom: *C. elegans* and *C. inopinata* on day 1and 14 for comparison at the same magnification. Scale 2µm (x 10,000). Mark Turmaine helped with TEM image acquisition.

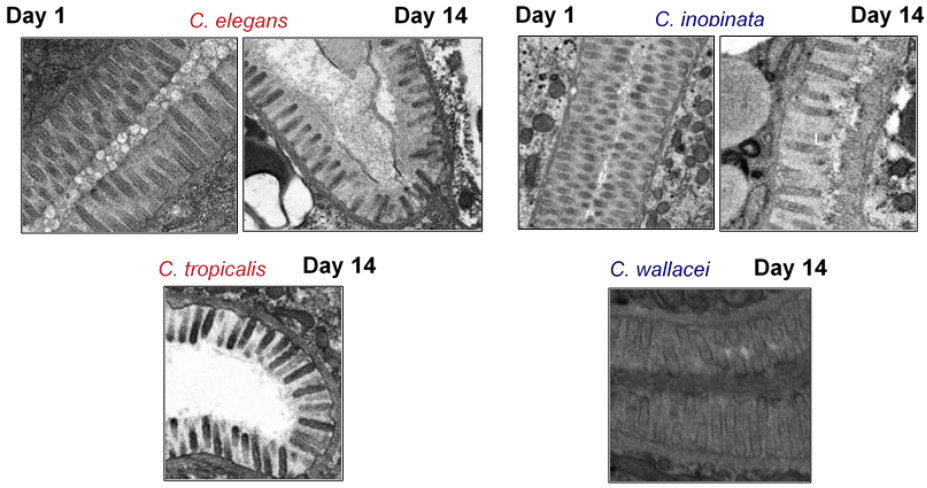

FIGURE 4.17. Degeneration of intestinal microvilli are seen in hermaphrodites and unmated females. This could represent a feature of ageing that is conserved among species regardless of the occurrence of reproductive death or may be the result of susceptibility to bacterial infection given the microvilli are more exposed than internal cellular structures. Mark Turmaine helped with TEM image acquisition.

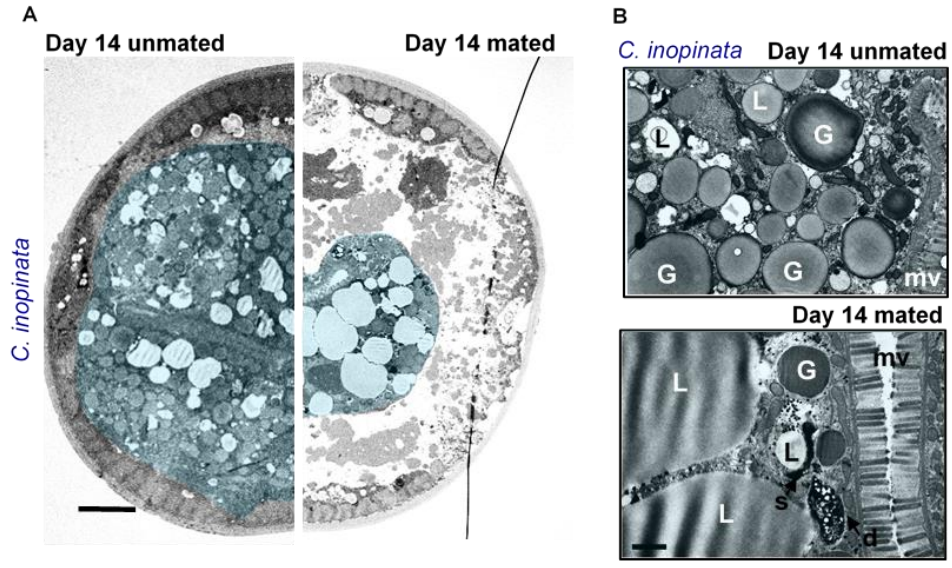

FIGURE 4.18. Intestinal atrophy and ultrastructure degeneration following mating in the female *C. inopinata*. **(A)** Representative TEM cross-section showing a reduction in intestinal size in *C. inopinata* upon mating. Scale 5 µm (5,000x). **(B)** Representative high magnification TEM images showing degenerative ultrastructural changes in the intestine in *C. inopinata* upon mating, with loss of ground structure similar to unmated *C. elegans*, and in contrast to unmated *C. inopinata*, observed (c.f. Figure 4.13). Scale 1 µm (20,000x). Mark Turmaine helped with TEM image acquisition.

Species	Reproductive state	Overall appearance of intestinal cell	Intestinal mitochondria	Intestinal lumen	Major intestinal atrophy	Yolk in body cavity	Body wall muscle deterioration
C. elegans day 14	Hermaphrodite	Degenerated, multiple prominent autophagosomes, major loss of ground substance	Very few	Dilated, full of digestate	Atrophied	+++	+++
C. inopinata day 14	Female	Relatively healthy appearance, few small autophagosomes, ground substance maintained	Many	Closed	Normal	+	Not
C. inopinata day 21	Female	Slight degeneration, few small autophagosomes, slight loss of ground substance, large lipid droplets	Many	Partially dilated	Normal	++	Not/+
C. inopinata mated day 14	Female (mated)	Slight degeneration, few small autophagosomes, slight loss of ground substance, very large lipid droplets	Many	Partially dilated	Atrophied	+++	++/+++
C. tropicalis day 14	Hermaphrodite	Quite degenerated, multiple autophagosomes, little loss of ground substance	Many	Dilated	Atrophied	+++	++?
C. wallacei day 14	Female	Relatively healthy appearance, few small autophagosomes, little loss of ground substance very large lipid droplets	Many	Closed	Normal	+	Not?
C. briggsae day 14	Hermaphrodite	Some degeneration, multiple autophagosomes, ground substance maintained	Many	Closed	Atrophied	++	++?

TABLE 4.1. Summary of TEMs from senescent nematodes, with observations. Most reliable features of hermaphrodites: intestinal atrophy and cell content degeneration, and PLP accumulation. For microvilli degeneration, intestinal lumen dilation and muscle deterioration: *C. elegans* > *C. tropicalis* > *C. briggsae.*

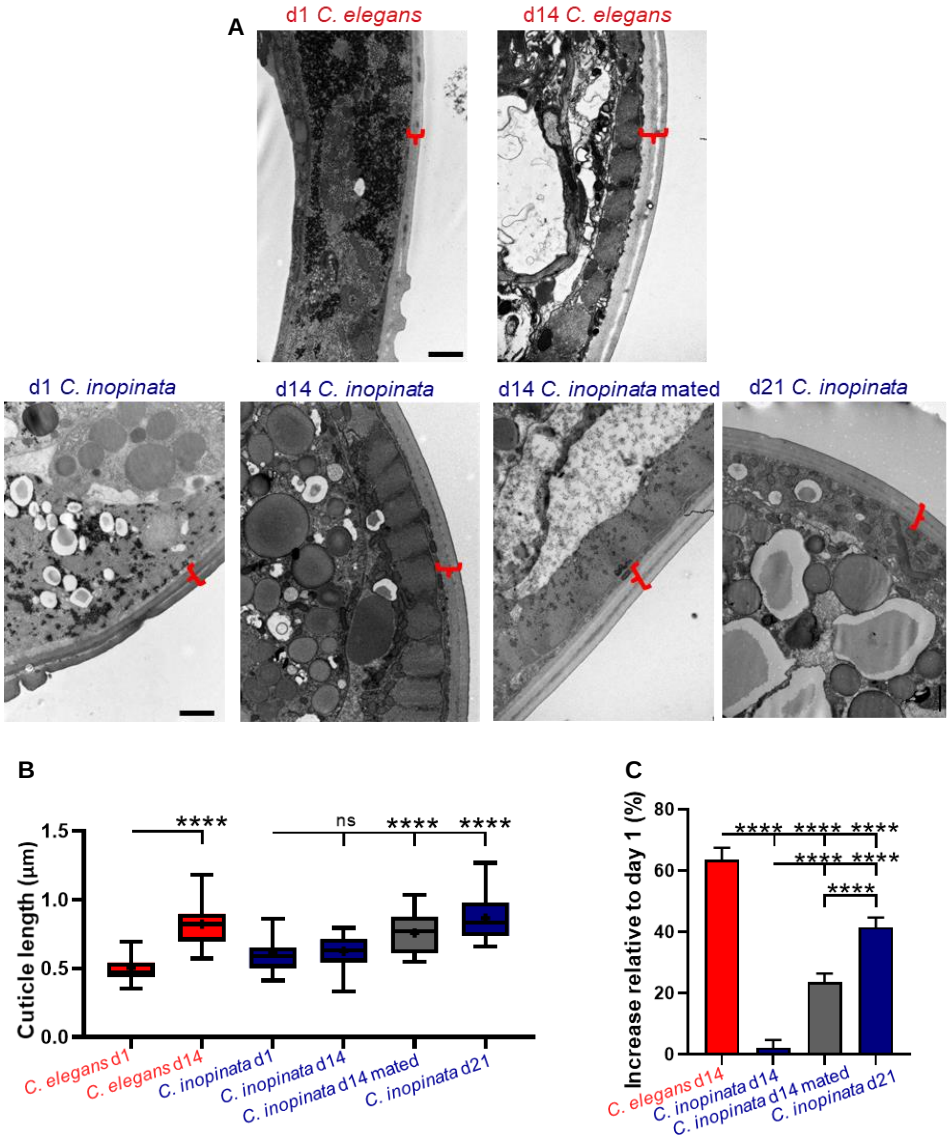

FIGURE 4.19. Cuticular hypertrophy occurs at a slower rate in the female *C. inopinata*, and is worsened by mating. (A) Representative TEM cross-section showing change in cuticular thickness with age in *C. elegans* and *C. inopinata* as well as post mating in *C. inopinata*. Scale 1µm. **(B)** Tukey box plots (line at median, + at mean) of cuticle length (measured at 15 to 25 different places along the cuticle of a worm; n=4 worms per condition). **(C)** Percentage increase relative to day 1 showing change in *C. elegans* by day 14 is even greater than increase in *C. inopinata* by day 21 (c.f. B). Bar graph shows mean ± s.e.m. One-way ANOVA (Bonferroni correction) and one-sample t-test (two-tailed). ***P <0.001,**** P <0.0001.

4.3 Discussion

4.3.1 Evidence in support of reproductive death in *C. elegans*

Iteroparous species exhibiting multiple rounds of reproduction are often longer lived than semelparous species that exhibit a single burst of reproduction (Finch, 1990a), and this may also be true of hermaphroditic nematodes (Gems et al., 2020). Reproductive death (or big bang

reproduction) is an extreme form of semelparity, as seen for example in monocarpic plants, Pacific salmon, and male marsupial mice (e.g. *Antechinus stuartii*) (Finch, 1990a). The very short lifespan of *C. elegans* is consistent with semelparity, although in very short-lived species iteroparity and semelparity are hard to distinguish (Gems et al., 2020; Gems, 2000). That said, a number of observations, many of which are presented in this chapter, point towards sexual maturity triggered-reproductive death in *C. elegans* hermaphrodites:

(i) Early, rapid and synchronous development of major pathological changes in the morphology of organs linked to reproduction are seen in *C. elegans* hermaphrodites (de la Guardia et al., 2016; Garigan et al., 2002; Herndon et al., 2002; McGee et al., 2012; McGee et al., 2011; Ezcurra et al., 2018; Wang et al., 2018) (Figure 2.1,4.6,4.7,4.12A) and this is characteristic of reproductive death (Finch, 1994 a; Gems et al., 2020). The pathologies begins within days of reproductive maturity and involve a level of destructive severity (including massive organ hypertrophy, atrophy and disintegration) that is not typical of senescence in higher animals (Gems et al., 2020).

(ii) *C. elegans* senescent transformation involves destructive source-to-sink type biomass remobilisation to support reproduction that is also characteristic of semelparous animals and plants (reviewed Gems et al., 2020). In particular, gut-to-yolk biomass conversion appears to be part of a suicidal reproductive effort that promotes fitness by feeding trophallactic fluid to larval kin and gonad atrophy facilitates production of unfertilised oocytes that are shown to act as vectors of yolk milk.

(iii) *Caenorhabditis* hermaphrodites that exhibit severe forms of senescent pathology, are shorter lived than (unmated) *Caenorhabditis* females which do not, consistent with reproductive death in the former only.

(iv) *Caenorhabditis* hermaphrodites vent yolk and lay unfertilised oocytes in large numbers, while *Caenorhabditis* unmated and mated females do not

(v) Semelparous senescence occurs earlier in cell compartments or organs that are non-essential for immediate survival and behaviour (e.g. gonad and intestine in *C. elegans*) than in essential organs (e.g. the nervous system in *C. elegans* which remains largely intact with age (Herndon et al., 2002)) (reviewed in Gems et al., 2020). This is because in semelparous organisms that undergo programmed reproductive death, source tissues and organs must be actively dismantled in order to promote function at the sink.

(vi) A common feature of semelparous species is an extended pre-reproductive stage, with death following rapidly after reproductive maturation. For example, eels of the genus *Anguilla* typically spawn and die at 6-12 years of age (Tesch, 1977), and the bamboo *Phyllostachys*

bambusoides flowers and dies after as much as 120 years (Janzen, 1976; Soderstrom and Calderon, 1979). As previously noted (Finch, 1990b)(p.118), *C. elegans* shows this pattern: diapausal dauer larvae can survive for up to 90 days, whereas after recovery from dauer and attainment of adulthood, death occurs within 2-3 weeks (Klass, 1977; Klass and Hirsh, 1976; Gems et al., 2020).

4.3.2 Females do not present with uterine tumours: arguments for uterine tumours as a quasi-programme driven pathology

In contrast to the pathogenic changes coupled to trophallaxis described in the last chapter, fitness promoting processes to which uterine tumour formation is coupled have not been identified, and are difficult to envisage. Thus, like the ovarian teratomas that they resemble, uterine tumours appear to the be result of futile quasi-programmes (Wang et al., 2018). Notably, uterine tumours were present in hermaphrodites but not females (and incidence was not greatly increased in mated females) and followed the pattern of severity *C. elegans* > *C. tropicalis* > *C. briggsae* (Figure 4.6,4.7,4.12A).

How might uterine tumour predisposition evolve in hermaphrodites? A cause of *C. elegans* uterine tumour formation is uncontrolled endoreduplication that occurs in oocytes if they remain unfertilised. In many cell types DNA synthesis in the absence of karyokinesis and cytokinesis is prevented by the G1 and G2 cell cycle checkpoints. However, in a number of species these checkpoints are absent in early embryogenesis. This absence, which promotes embryogenesis also promotes tumour formation. Runaway endomitosis as in unfertilised *C. elegans* oocytes does not occur in unfertilised eggs in *Drosophila* thanks to the presence of an arrest point after meiosis II in the latter, defects in which can result in giant polyploid nuclei within eggs (Doane, 1960) similar to *C. elegans* uterine tumours. Since female *Drosophila* may take some time to be mated, they need to maintain a stock of viable unfertilised eggs, which leads to selection for the post-meiosis II arrest point. By contrast *C. elegans* oocytes are immediately fertilised by self sperm, which arguably should weaken selection for such an arrest point. Moreover, *C. elegans* hermaphrodites are adapted for rapid population growth (Perez et al., 2017; Schulenburg and Félix, 2017), and loss of checkpoints could in principle speed up egg production rate. These arguments are supported by the severity of tumour presentation in the different *Caenorhabditis* hermaphrodites (Figure 4.6,4.7,4.12A) following the same order as the likely time of hermaphroditic species divergence described earlier (Figure 4.1A): *C. elegans* > *C. tropicalis* > *C. briggsae*.

4.3.3 *Pristionchus* species lack YP170 but follow the same pattern of reproductive death: constitutive in hermaphrodites and facultative in females

In *C. elegans,* intestinal involution and yolk milk feeding of progeny is coupled to production of YP170: *vit-5* RNAi which knocks down YP170 production blocks intestinal biomass conversion (Figure 3.1) (Sornda et al., 2019) and growth benefits for yolk milk-fed larvae (Figure 3.6), while *vit-6* RNAi which results in YP115/88 knockdown results in a reciprocal compensatory increase in YP170 production (Figure 3.1) (Sornda et al., 2019) and enhances larval growth benefits from yolk milk feeding (Figure 3.6). This is likely because YP170 is the most abundantly produced yolk protein (Sornda et al., 2019) as well as the most abundantly vented, with the same trend observed in other *Caenorhabditis* hermaphrodites (Figure 4.1,30). In female *Caenorhabditis* species, lifespan reduction as well as intestinal atrophy and PLP accumulation can be induced by mating (Figure 4.6,4.7,4.10). A possible adaptive significance of this change is that females but not hermaphrodites need to await an encounter with a male before commencing reproduction.

Interestingly, although *Pristionchus* species are found to lack YP170, the same pattern is conserved with intestinal atrophy and PLP accumulation occurring constitutively in *P. pacificus* hermaphrodites and induced by mating in *P. exspectatus* females, and instead YP115/88 equivalents likely coupled to these (Figure 4.1,4.2, 4.9, 4.10). Taken together, these results suggest that after the appearance of hermaphroditism in each case, reproductive death independently evolved from being facultative (mating induced) to constitutive by amplification of mechanisms already present in the gonochoristic ancestor (i.e. mechanisms likely predominantly involving YP170 in the *Caenorhabditis* species and YP115/88 equivalents in the *Pristionchus* species).

4.3.4 Context of life history strategy: Is *C. inopinata* more R_0 selected than the other *Caenorhabditis* species tested?

Hermaphroditism in *C. elegans* has been argued to evolve to facilitate a more rapid intrinsic rate of increase and so maximise colonisation of a habitat over gonochoristic competitors (Katju, et al., 2008; Stewart & Phillips, 2002). As described in the introduction, how habitat has determined choice of reproductive strategy remains largely unresolved (Schulenburg and Félix, 2017), though it is likely that hermaphroditism allows colonisation of a greater variety of habitats (not just rotting fruit and stems where these species are predominantly found (Schulenburg and

Félix, 2017)) including those where food sources are more intermittent and scarce like soil (Riddle, et al., 1997). A gonochoristic strategy is argued to be favoured where there is ample food to support mating and several generations prior to food source depletion and dauer dispersal (Riddle, et al., 1997). In this respect, hermaphrodites are arguably more *r* shifted on the *r*-R_0 maximising continuum (Dańko, et al., 2017; Dańko, et al., 2018).

With this in mind, even in relation to other *Caenorhabditis* females-hermaphroditic sibling pairs examined, *C. inopinata* presents with many characteristic of being much more R_0 selected than *C. elegans*. *C. inopinata* has a significantly larger body size and a slower rate of development and growth across a range of temperatures, suggesting a trade-off between body size and developmental timing (Woodruff et al., 2019) (other *Caenorhabditis* species showed relatively little difference in body size and developmental timing when observed at both 20 and 25˚C in this study (data not shown)). What breaks this pattern, however, is that *C. inopinata* has been shown not to reveal any differences in adult lifespan from *C. elegans* (Woodruff et al., 2019). Results presented in this chapter show that *C. inopinata* is hyper-sensitive to infection, and when infection is accounted for, *C. inopinata* is in fact longer lived than both *C. elegans* and other unmated *Caenorhabditis* females examined (Figure 4.4, 4.5). Moreover, unmated *C. inopinata* also shows the least level of pathology (Figure 4.12 A,C). Hyper-sensitivity to infection is not unexpected given the habitat of tree-borne figs that *C. inopinata* was isolated from (Kanzaki et al., 2018). The very different habitat of *C. inopinata* compared to other *Caenorhabditis* species used in this study may also account for its more R_0 maximising associated traits (Kanzaki et al., 2018; Schulenburg and Félix, 2017; Kiontke & Sudhaus, 2006).

Chapter 5: Gonadectomy suppresses reproductive death in *C. elegans*

5.1 Introduction

Do interventions that extend lifespan in *C. elegans* act by suppressing reproductive death (RD)? In most metazoan organisms, both iteroparous and semelparous, reproductive resource transfer is under hormonal control (Gems et al., 2020). Examples include oestrogen-governed calcium transfer from bone via the blood to milk in lactating women (iteroparous), and sex steroid-driven reproductive death in *A. stuartii* and the Pacific salmon *O. nerka* (semelparous), and also abscisic acid-controlled reproductive death in monocarpic (i.e. semelparous) plants. Suppression of the hormonal changes which promote costly reproductive programmes can extend lifespan. This can be achieved by surgical removal of endocrine organs or by behavioural manipulation. In semelparous organisms such interventions typically result in very large and robust increases in lifespan, while in iteroparous organisms their effects are variable, usually modest increases or decreases in lifespan (reviewed in (Gems et al., 2020)). Removal of the germline while leaving an intact somatic gonad in *C. elegans* hermaphrodites results in a large extension of lifespan, of up to 60% (Hsin and Kenyon, 1999). Results described in Chapter 4 raise the possibility that this is due to suppression of reproductive death.

Reduced insulin/IGF-1 signaling (IIS) can also greatly increase *C. elegans* lifespan; the largest increases in *C. elegans* (from a single intervention) have been observed in mutants defective in the *daf-2* insulin/IGF-1 receptor and the *age-1* phosphatidyinositol 3-kinase (PI3K) catalytic subunit (Kenyon, 2010; Ayyadevara et al., 2008). Although reduced IIS can increase lifespan in iteroparous species, the effects are considerably smaller. For example, reduction of PI3K via mutation increases median lifespan by up to ~10-fold in *C. elegans* but only ~1.07-fold and ~1.02-fold in *Drosophila* and mice, respectively (Ayyadevara et al., 2008; Foukas et al., 2013; Slack et al., 2011). In the previous two chapters, IIS was shown to promote yolk milk production, which is coupled to RD-associated pathology. This, again, raises the possibility that reducing IIS increases *C. elegans* lifespan by suppressing reproductive death, at least in part.
In this chapter I explore the possibility that germline ablation increases *C. elegans* lifespan by suppressing reproductive death. In this way, gonadectomy in *O. nerka* before spawning can increase maximum lifespan from 4.8 years to up to 8.5 years (Robertson, 1961) and removal of flowers prior to pollination can increase lifespan in soybean (*Glycine max*) from 119 to 179 days

(Leopold et al., 1959) (see Table 5.1 for comparison of lifespan extension through interventions which suppress reproductive death in semelparous and iteroparous organisms). By comparing three *Caenorhabditis* sibling species pairs with either hermaphrodites or females, I describe how only in hermaphrodites does germline removal markedly increase lifespan, and how this involves suppression of RD-associated pathology. Moreover, when the severity of ageing pathology is plotted against lifespan, a strong negative correlation is observed, in a pattern consistent with an continuum between semelparity and iteroparity (Hughes, 2017). The latter has important implications for the relevance of the biology of ageing in *C. elegans* to that in iteroparous species (e.g. most mammals).

5. 2 Results

5.2.1 Germline removal extends lifespans in hermaphrodites much more than in females

To begin to explore the possibility that germline ablation suppresses reproductive death in *C. elegans*, the effect on lifespan of germline ablation on ageing in the 3 *Caenorhabditis* sibling species pairs was compared. In each case, hermaphrodites exhibited much larger increases in lifespan than females (Figure 5.1 and Appendix 1). Large increases in lifespan were seen in hermaphrodites of *C. elegans* (combined data of 3 trials: +108%, p>0.0001), *C. tropicalis* (+87%, p>0.0001) and *C. briggsae* (+80%, p>0.0001) (Figure 5.1 and Appendix 1). By contrast, only modest increases were seen in females of *C. inopinata* (+30%, p>0.0001), *C. wallacei* (+18%, p>0.0001) and *C. nigoni* (+13%, p>0.05) (Figure 5.1 and Appendix 1).

Testing of the *Pristionchus* sibling species pair yielding similar results: *P. pacificus* hermaphrodites showed a large increase (+64%, p>0.0001) consistent with previous observations (Hsin and Kenyon, 1999) and *P. exspectatus* females a much smaller increase (+12%, p> 0.002). This suggests that this pattern of effects of germline removal may be typical of nematodes in the order Rhabditida to which the genera *Caenorhabditis* and *Pristionchus* both belong (Figure 5.2). This implies that the shorter lifespan of hermaphrodites relative to females in each case is germline dependent, i.e. that shorter lifespan has repeatedly evolved in hermaphrodites in a way that involves germline-dependent mechanisms.

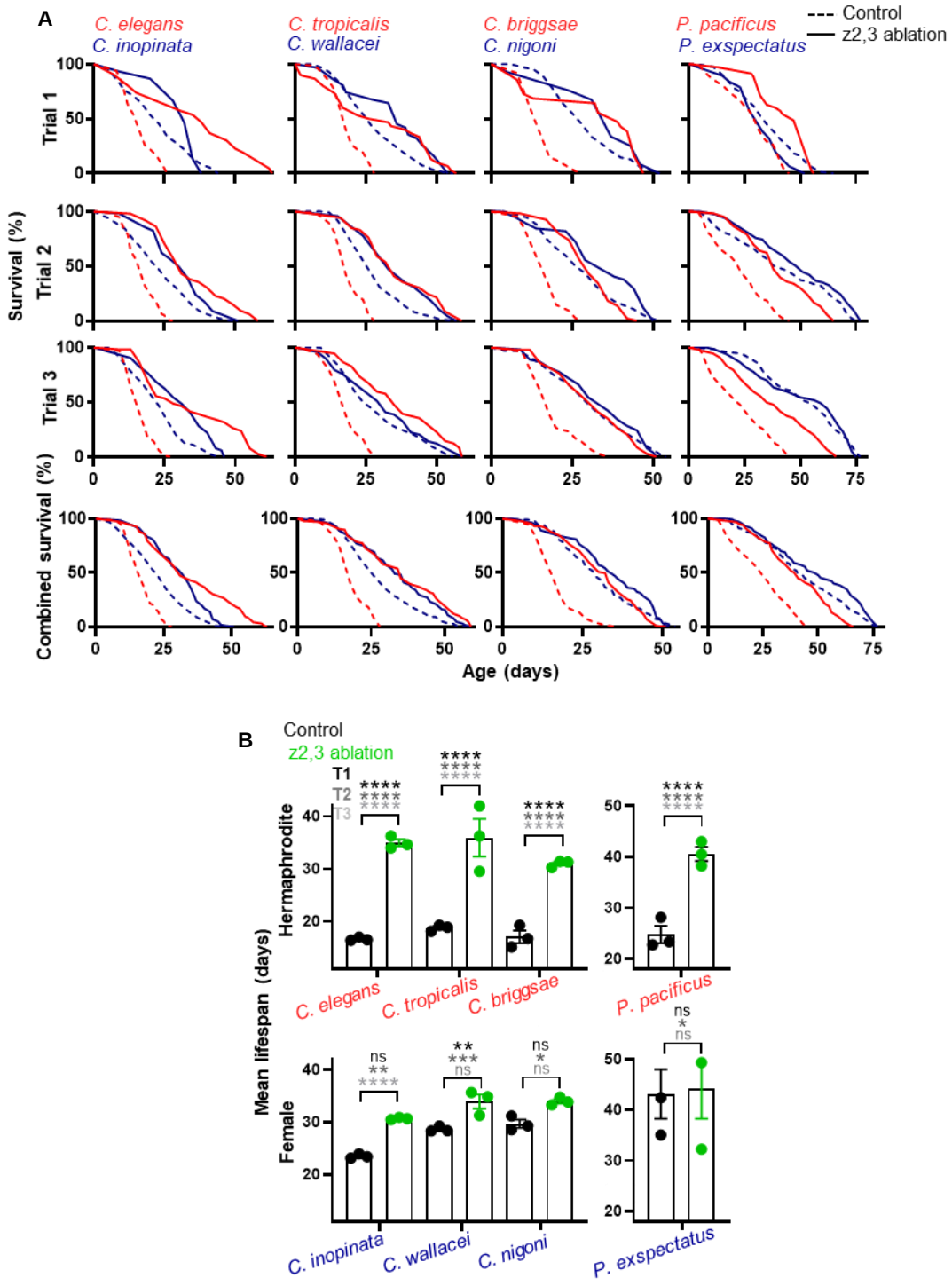

FIGURE 5.1. Germline ablation greatly extends lifespan in hermaphrodites but not females. (A,B) Combined lifespans and individual trials of sibling species showing lifespan extension post z2,3 ablation (i.e. germline ablation) only has a large effect in *Caenorhabditis* and *Pristionchus* hermaphrodites. Logrank tests for individual trials. Mean ± s.e.m. of 3 trials displayed. * P <0.05, ** P <0.01, *** P <0.0001, **** P <0.00001. For additional statistics and sample sizes see Appendix 1. Shivangi Srivastava help with the scoring of lifespans and germline ablation.

Table 5.1. Magnitude of increases in lifespan after gonadectomy or behavioral interventions that prevent reproductive death. It is notable that the magnitude of reported experimentally-induced increases in lifespan, expressed in terms of proportional increase in lifespan, are generally greater in semelparous than iteroparous organisms. Reproduced from (Gems et al., 2020).

C. elegans							
+	Hermaphrodite	Germline ablation (laser)	20˚C, agar plates	19.4 d	31.8 d	+63.9	(Hsin and Kenyon, 1999)
daf-2(e1370)	Hermaphrodite	Germline ablation (laser)	20˚C, agar plates	43.2 d	75.7 d	+75.2	(Hsin and Kenyon, 1999)
+	Hermaphrodite	Germline ablation (laser)	20˚C, monoxenic liquid	16.8 d	35.0 d	+108	(McCulloch, 2003)
daf-2(e1368), daf-2 RNAi	Hermaphrodite	Germline ablation (laser)	20˚C, agar plates	51.0 d	124.1 d	+143	(Arantes-Oliveira et al., 2003)
***Caenorhabditis* species**							
C. elegans	Hermaphrodite	Germline ablation (laser)	20˚C, agar plates	16.7 d	35 d	+109.4	Figure 5.1
C. inopinata	Female	Germline ablation (laser)	20˚C, agar plates	23.5 d	30.7 d	+30.6	Figure 5.1
C. tropicalis	Hermaphrodite	Germline ablation (laser)	20˚C, agar plates	18.8 d	35.9 d	+91	Figure 5.1
C. wallacei	Female	Germline ablation (laser)	20˚C, agar plates	28.7 d	33.9 d	+18.5	Figure 5.1
C. briggsae	Hermaphrodite	Germline ablation (laser)	20˚C, agar plates	17.1 d	31 d	+81.5	Figure 5.1
C. nigoni	Female	Germline ablation (laser)	20˚C, agar plates	29.7 d	34 d	+14.5	Figure 5.1
***Pristionchus* species**							
P. pacificus	Hermaphrodite	Germline ablation (laser)	20˚C, agar plates	24.7 d	40.5 d	+64	Figure 5.1
P. exspectatus	Female	Germline ablation (laser)	20˚C, agar plates	43.1 d	44.3 d	+2.7	Figure 5.1
Semelparous (with reproductive death)							
Glycine max (soy bean)	Monoecious	Flower removal		119 d	179 d	+50.4	(Leopold et al., 1959)
O. hummelincki (octopus)	Female	Optic gland removal		51 d	277 d	+443	(Wodinsky, 1977)
A. anguila (eel)	Unknown	Prevention of sea run	Fresh water	*9 y*[2]	55 y	+511	(Tesch, 1977)
A. anguila (eel)	Unknown	Prevention of sea run	Fresh water	*9 y*[2]	88 y	+877	(Vladykov, 1956)
O. nerka (salmon)	Both sexes	Castration		4.8 y	8.5 y	+77.0	(Robertson, 1961)
A. stuarti (marsupial)	Male	Lab capture prior to mating		1 y	3 y	+200	(Olsen, 1971)
Iteroparous							
D. subobscura	Female	*grandchildless* mutation	20˚C, virgin	58.7 d[3]	67.6 d[3]	+15.1[4]	(Maynard Smith, 1958)
D. melanogaster	Female	*germ cell-less* mutation	25˚C, virgin	*44 d*	*38 d*	-13.6	(Barnes et al., 2006)
D. melanogaster	Female	*tudor* mutation	25˚C, virgin	*71 d*	*57 d*	-19.7	(Barnes et al., 2006)
D. melanogaster	Female	*bag of marbles* over-expression	25˚C	*32,28 d*	*42 d*	+31.3, 50.0	(Flatt et al., 2008)
D. melanogaster	Male	*bag of marbles* over-expression	25˚C	*38,36 d*	*46 d*	+21.0, 27.8	(Flatt et al., 2008)

R. microptera (grasshopper)	Female	Ovariectomy	28˚C	*167 d*	*205 d*	+22.7	(Hatle et al., 2008)
R. microptera (grasshopper)	Female	Ovariectomy	32˚C, 24˚C	*245 d*	*285 d*	+16.3	(Drewry et al., 2011)
M. musculus (mouse)	Female	Ovariectomy before puberty	CBA/J	599 d	540 d	-9.8	(Cargill et al., 2003)
R. norwegicus (rat)	Male	Castration at birth	Inbred Lewis	454 d	521 d	+14.7	(Talbert and Hamilton, 1965)
R. norwegicus (rat)	Male	Castration just before puberty	Osborne-Mendel Yale	615 d	651 d	+5.8	(Asdell et al., 1967)
R. norwegicus (rat)	Female	Ovariectomy just before puberty	Osborne-Mendel Yale	742 d	669 d	-9.8	(Asdell et al., 1967)
R. norwegicus (rat)	Male	Castration just before puberty	Norway albino	727 d	817 d	+21.7	(Drori and Folman, 1976)
F. catus (cat)	Male	Castration		4.9 y	8.2 y	+67.3	(Hamilton et al., 1969)
F. catus (cat)	Female	Spayed		6.8 y	8.4 y	+23.5	(Hamilton et al., 1969)
F. catus (cat)	Both sexes	Gonadectomy		*11.0 y*	*15.0 y*	+36.3	(O'Neill et al., 2015)
C. lupus familiaris (dog)	Both sexes	Gonadectomy		7.9 y	9.4 y	+18.9	(Hoffman et al., 2013)
H. sapiens	Male	Castration		*55.7 y*	*69.3 y*	+24.4	(Hamilton and Mestler, 1969)
H. sapiens	Female	Oophorectomy		*65.2 y*	*65.2 y*	+0	(Hamilton and Mestler, 1969)
H. sapiens	Male	Castration		50.9 y	70.0 y	+37.5	(Min et al., 2012)
H. sapiens	Male	Castration		55.6 y	70.0 y	+25.8	(Min et al., 2012)

[1] Mean lifespan (median lifespan, italics; maximum lifespan, underlined). d, days. y, years.
[2] Eels normally live 6-12 y; the median value is taken here.
[3] Life expectancy at age 10 days.
[4] It might be significant that the strain of *D. subobscura* used in this study mated only once, in contrast to *D. melanogaster* which can remate multiple times (Partridge and Sibly, 1991).

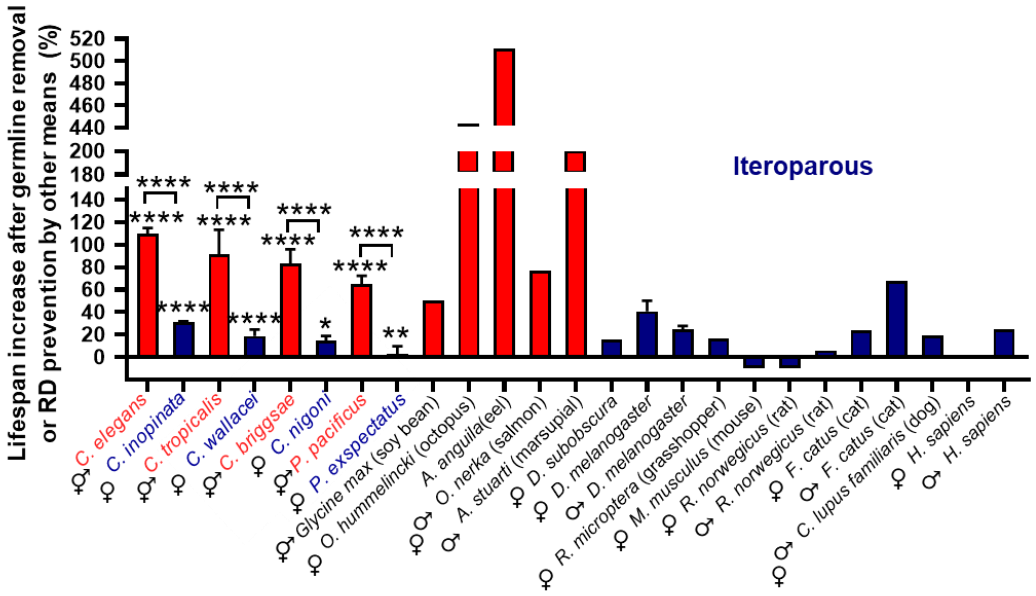

FIGURE 5.2. Large magnitude of lifespan increase following prevention of reproductive death in hermaphrodites mimics other semelparous species. Germline ablation is shown to strongly increases lifespan in hermaphrodites but not female nematode species (c.f. Figure 5.1). Similarly, blocking reproductive death in semelparous species strongly increases lifespan, while gonadectomy in iteroparous species overall does not. For *Caenorhabditis* and *Pristionchus* species, mean ± s.e.m. of 3 trials is shown (stars, logrank test for ablated vs control animals, and Cox proportional hazard test to compare effect in hermaphrodites vs females). Values for other species are taken from a recent review (Gems et al., 2020); c.f. Table 5.1 from the same review); for multiple studies of the same species, only references with both male and female data are included, and for *A. anguila* (eel) data from the most recent source (Tesch, 1977) (see Table 5.1). For additional statistics see Appendix 1. * P <0.05, ** P <0.01,**** P <0.0001.

5.2.2 Germline removal suppresses reproductive death-like pathologies

Prevention of reproductive maturity in semelparous organisms extends lifespan by preventing the massive pathology preceding reproductive death (Gems et al., 2020). For example, in *O. nerka*, as in *C. elegans* hermaphrodites, a range of severe, deteriorative pathologies rapidly develop, affecting the liver, kidney, spleen, heart, thymus and digestive tract (Finch, 1990b; Robertson et al., 1961). These changes can be blocked by castration before spawning (Robertson, 1961). If germline removal extends hermaphrodite lifespan by suppressing reproductive death, then it should suppress reproductive death-like pathologies in hermaphrodites. In all 3 androdioecious species, germline removal strongly suppressed hermaphrodite intestinal atrophy (Figure 5.3A, B). In young adults, germline ablation increased yolk pool (PLP) levels (Figure 5.3A, B). This likely reflects the absence of egg laying, which is a route for yolk efflux (Sornda et al., 2019). Notably, yolk pool levels showed little subsequent increase with age, consistent with reduced gut-to-yolk biomass conversion (Figure 5.3A, B). Gonad atrophy is not scored because germline removal affects the gonad. Tumours were not present in ablated animals (Figure 5.3A, B

and 5.4) as germline removal prevents oocyte formation, and remnant unfertilised oocytes in the gonad post sperm-depletion result in tumours through futile endoreduplication in them (Wand et al., 2018). Interestingly, pharyngeal atrophy was also blocked by germline removal adding further support to this pathology being linked to reproductive death (Figure 5.3A, B and 5.4).

Similar results, but with a weaker effects, were seen in *glp-1(e2141)* and *glp-4(bn2)* mutants with reduced germline development consistent with these mutants constituting a weaker intervention than germline removal via z2,3 cell ablation (Figure 5.3 C).

It is also known that effects of germline removal in *C. elegans* are dependant on the presence of the somatic gonad, as removal of the somatic gonad through z1-4 ablation abrogates the lifespan extension seen in z2,3 ablated animals, and this effect requires DAF-2 insulin/IGF-1 receptor activity. A possibility is that removal of the somatic gonad reduces lifespan by affecting RD-associated pathology. In line with this, z1-4 ablation in *C. elegans* resulted in pharyngeal deterioration and intestinal atrophy similar to wild-type, as well as an associated increase in PLP levels with age (Figure 5.4). Taken together these results support the view that germline removal in *C. elegans*, like gonadectomy in semelparous salmon, increases lifespan by preventing reproductive death, and that this effect is dependent on the presence of the somatic gonad.

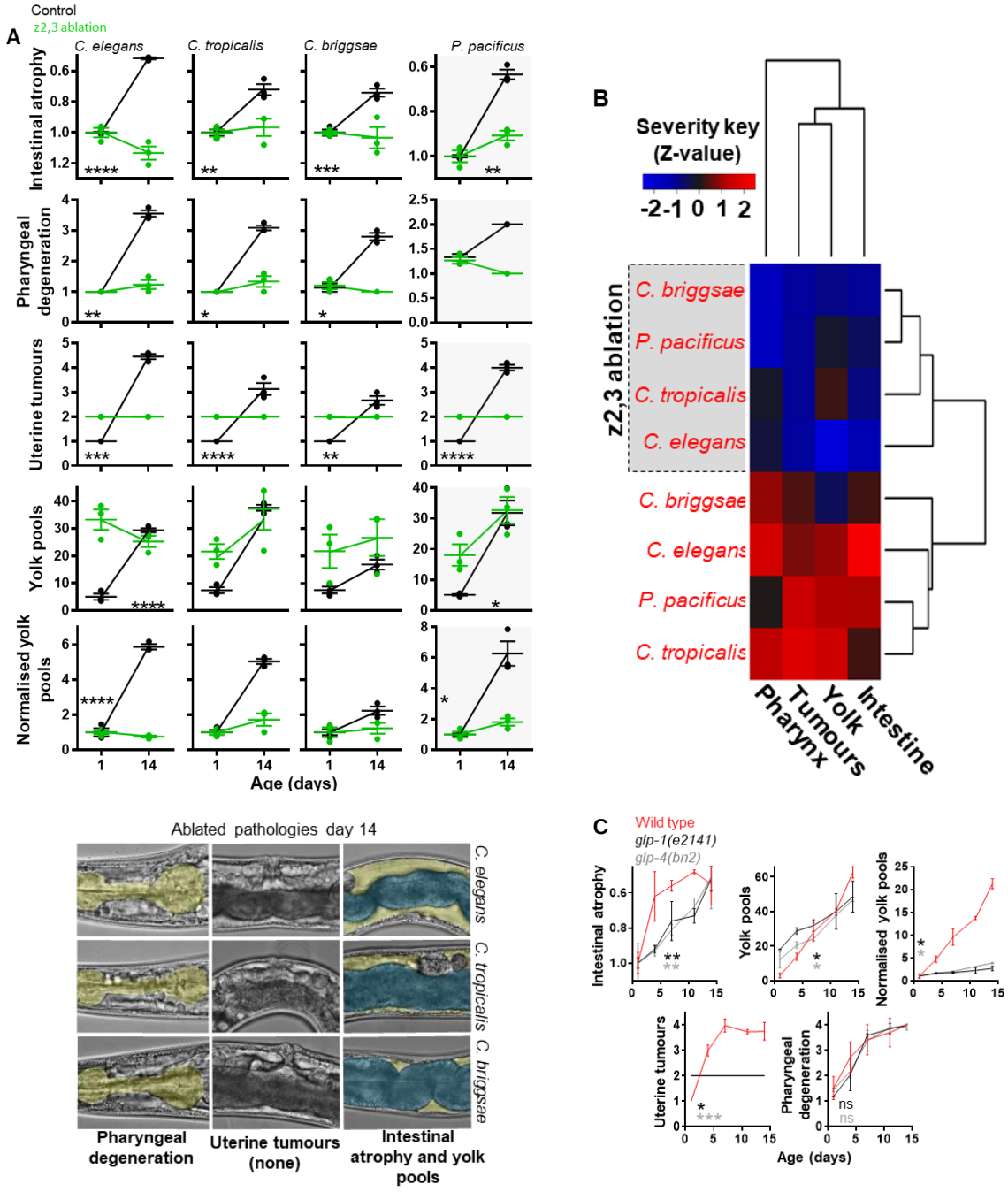

FIGURE 5.3. Germline ablation suppresses RD-associated pathologies in hermaphrodites. (A,B) Pathology progression in hermaphrodites is suppressed following z2,3 ablation. **(A)** Top: Line graphs of pathology change with age. Yolk pools are also displayed normalised to d1 to highlight the lack of increase with age; the high d1 value is likely attributed to the lack of eggs which are a sink for yolk (n=5-10 per time point). Uterine tumours are not present in germline ablated animals as they arise from unfertilised oocytes (score 2= uterus contains no tumors and may contain few or no fertilised eggs; see methods section for details). Bottom: Representative Nomarski microscopy images taken for the purpose of scoring pathologies (c.f. Figure 4.6, 4.7). **(B)** Heat map comparing differences in pathology progression across species and treatments by transforming the calculated gradients of pathology progression into Z-scores. Hierarchical clustering based on pair-wise Euclidean distances was used to cluster pathologies and species/treatments according to similarity. **(C)** Pathology progression in *C. elegans* germline-deficient mutants showing a reduction in most RD-associated pathologies (25˚C). Note that suppression of germline development is not complete in these mutants, in contrast to laser ablated animals, which may account for the weaker suppression of RD-associated pathologies. Mean ± s.e.m. of 3 trials displayed. * P <0.05, ** P <0.01, *** P <0.0001, **** P <0.00001. StJohn Townsend, Shivangi Srivastava and Dominik Maczik helped with parts of the pathology data collection and analysis. Marina Ezcurra collected the data in C.

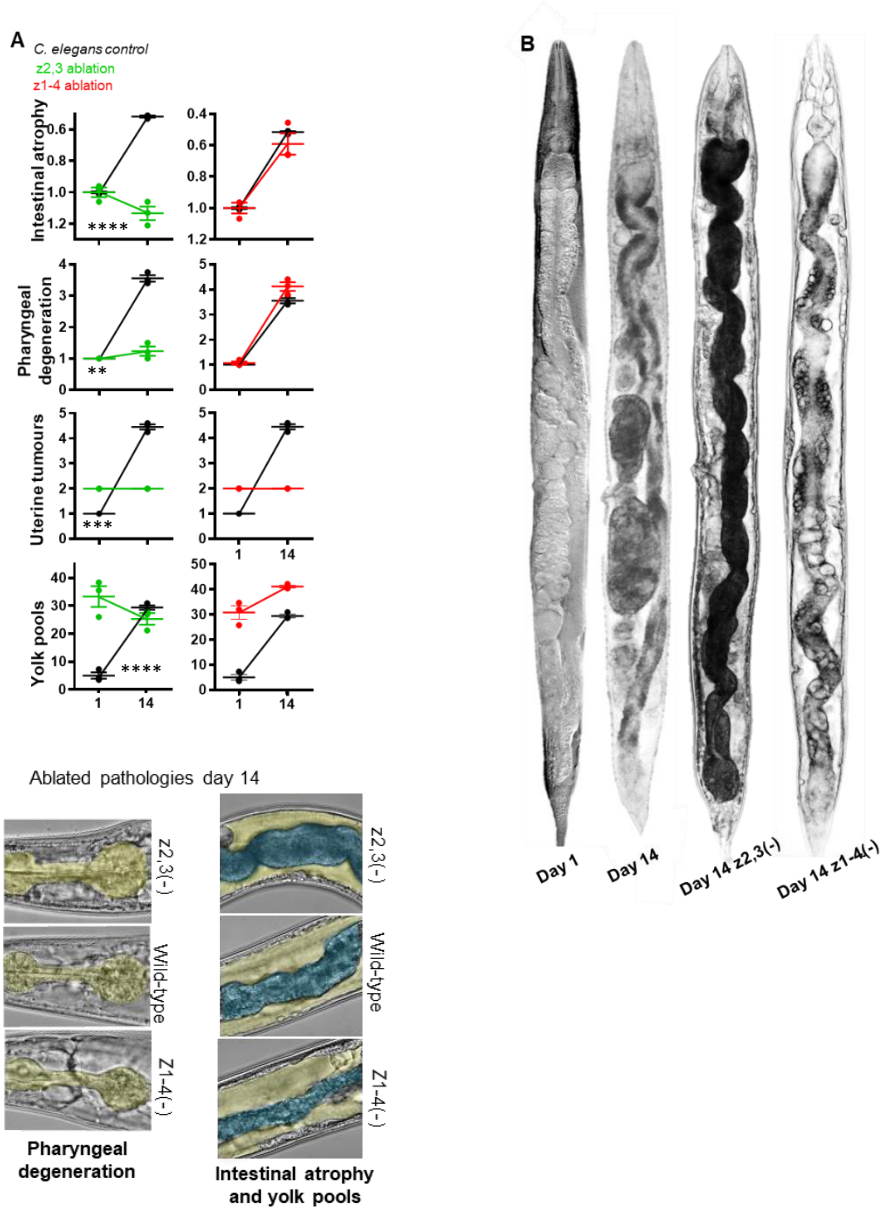

FIGURE 5.4. An intact somatic gonad is required for germline removal to suppress RD-associated pathology. **(A)** Top: Pathology progression following z1-4 ablation (i.e. full gonad removal) shows no difference to wild-type. z2,3(-) and z1-4(-) data were collected together with the same control and are comparable. Bottom: Representative Nomarski microscopy images taken for the purpose of scoring pathologies (c.f. Figure 4.6,4.7,5.3). **(B)** Nomarski images of full worms showing intestinal atrophy in wild-type and z1-4(-) is similar and much worse when compared to z2,3(-) animals. Images have been straightened using the straighten tool in ImageJ.

5.2.3 Reduced insulin/IGF-1 signaling suppress reproductive death associated pathologies

Reduction of IIS, as in *daf-2* insulin/IGF-1 receptor mutants, greatly increases *C. elegans* lifespan, and this effect is dependent upon the DAF-16 FoxO transcription factor (Kenyon et al., 1993; Kimura et al., 1997; Lin et al., 1997; Ogg et al., 1997). In Chapter 3 wild-type IIS was

shown to promote yolk and oocyte venting which are linked to reproductive death. One possibility is that IIS increases lifespan by blocking development of RD-associated pathology. Previous studies have noted some suppression by reduced *daf-2* signaling of several senescent pathologies, including gonadal and pharyngeal deterioration (Garigan et al., 2002), neurite outgrowths (Tank et al., 2011), intestinal atrophy and yolk accumulation (Depina et al., 2011; Ezcurra et al., 2018), and weaker effects on intra-uterine chromatin mass formation (Golden et al., 2007). In line with these previous studies, pathology analysis revealed strong suppression of all RD-associated pathologies in a *daf-16*-dependent manner, but only very weak effects on uterine tumour formation (which, as previously argued, is likely quasi-programme driven (see Chapter 3 discussion)) (Figure 5.5).

However, certain observations are not consistent with the idea that reduced IIS extends lifespan by blocking reproductive death. For example, germline ablation increases lifespan in *daf-2* mutants, seemingly more so than in wild type (+~140% vs +~60%). One possibility is that the two pathways, IIS and germline signalling, act to some extent in parallel to promote reproductive death, while also impacting lifespan via additional pathway-specific mechanisms. Given that germline ablation abrogates tumour formation, while IIS has little effect on the formation of tumours, a possibility is that germline removal partly increase lifespan in IIS mutants by suppressing tumour formation. If true, this could also partly explain why *daf-2* males are longer lived than *daf-2* hermaphrodites. Tumour formation in *C. elegans* can be inhibited by the drug FUDR (5-fluorodeoxyuridine) to suppress DNA synthesis, but this does not increase lifespan in wild type (Riesen et al., 2014), likely because other, RD-associated pathologies limit lifespan in wild-type worms. Notably, treatment with FUDR was found to markedly increase lifespan in both *daf-2(e1370)* and *daf-2(el368)* mutants but not (as previously shown) in wild type (Figure 5.6). This suggests that old *daf-2* mutants die to some extent from tumours, and that extension of *daf-2* mutant lifespan by germline ablation might be due to suppression of tumour formation. Absence of tumours was confirmed in all FUDR-treated worms (data not shown).

5.2.4 A continuum between semelparity and iteroparity

As described earlier, it has been argued that semelparous and iteroparous life histories are not wholly distinct phenomena but rather represent a continuum (Hughes, 2017; Gems et al., 2020). This is consistent with the observed gradient between presence and absence of RD-associated pathology and lifespan in unmated animals in the *Caenorhabditis* genus. Here one sees a gradient of declining pathology and increasing lifespan *C. elegans*> *C. tropicalis* > *C. briggsae*

in the unmated hermaphrodites and then still longer lifespan and no RD-associated pathology in females. The gradient in hermaphrodites coincides with hermaphroditic species divergence times for *C. elegans* (0.35-7.2 MYA split) and *C. briggsae* (0.2-3.5 MYA split) (divergence time of *C. tropicalis* is unknown) (Figure 4.1A) (Cutter et al., 2019). If interventions such as germline removal, IIS, or suppression of yolk protein production (i.e. *vit* gene transcription and translation) increase *C. elegans* lifespan by suppressing RD-associated pathology, this predicts that they will fall somewhere along this continuum based on the extent of their effect on RD-associated pathology and hence lifespan. In line with this, *vit-5*, *vit-6* and *vit-5,-6* RNAi treated worms (with L4440 control), as well as z2,3 ablated hermaphrodites and IIS mutants *daf-2, daf-16* and *daf-2; daf-16* were found to fall on the continuum (Figure 5.7), with *daf-2 C. elegans* and z2,3 ablated hermaphrodites equivalent to unmated females in terms of their pathology level and lifespan, in line with the large effects of these interventions on lifespan.

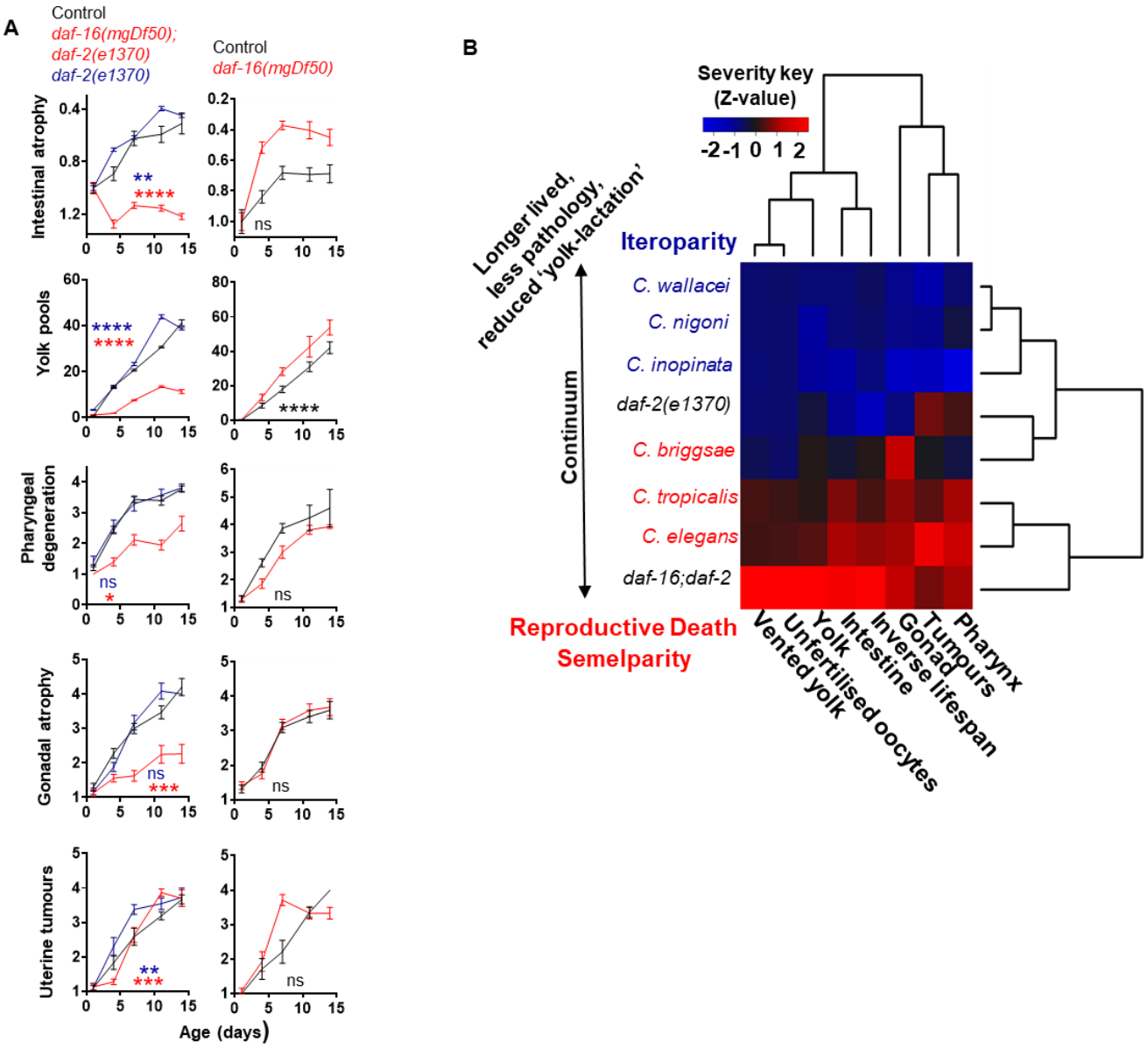

FIGURE 5.5. Reproductive death is promoted by insulin/IGF-1 signalling (IIS). (A) Pathology progression is suppressed in *daf-2(e1370)* mutants, and this is *daf-16* dependant. Mean ± s.e.m. of 3 trials displayed (n=10 per time point per trial). * P <0.05, ** P <0.01, *** P <0.0001, **** P <0.00001. **(B)** Lifespan, RD-associated pathologies and yolk-lactation (yolk venting and unfertilised oocyte production) follow a continuum with *daf-2* behaving like unmated females and *daf-16; daf-2* mutants like unmated hermaphrodites. Heat map comparing differences in pathology progression, lifespan, yolk venting and oocyte production across species and treatments by transforming the calculated gradients of pathology progression into Z-scores. Hierarchical clustering based on pair-wise Euclidean distances was used to cluster pathologies and species/treatments according to similarity (yolk venting and oocyte data is from chapter 3). Pathology data for IIS mutants in A and B from Marina Ezcurra.

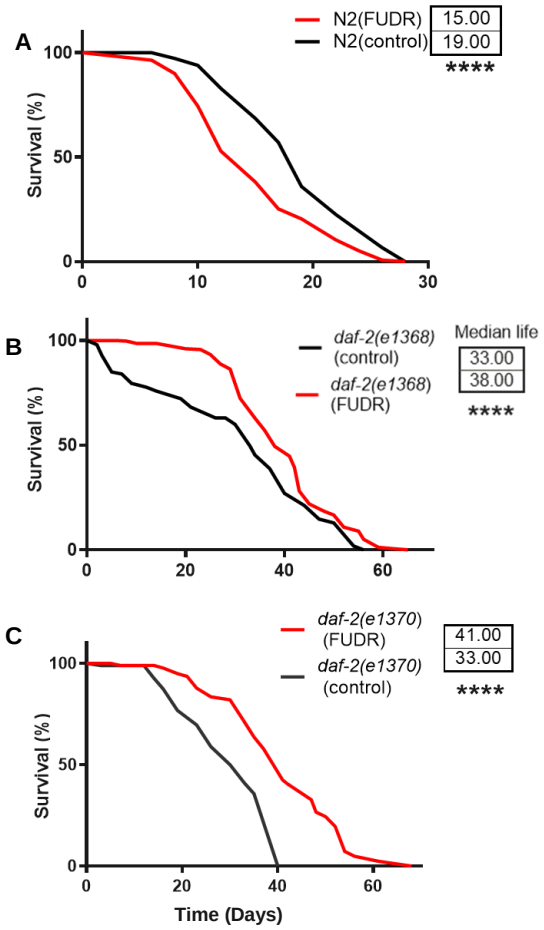

FIGURE 5.6. Suppression of tumours increases lifespan in *daf-2* mutants but not wild type. (A,B,C) All graphs are comparable with trials performed together. Combined data of 3 trials displayed. For additional statistics and sample sizes see Appendix 1. Cox proportional hazard test to compare effect in *daf-2* vs wild type (N2). **** *P* <0.0001. Shivangi Srivastava helped with scoring lifespans.

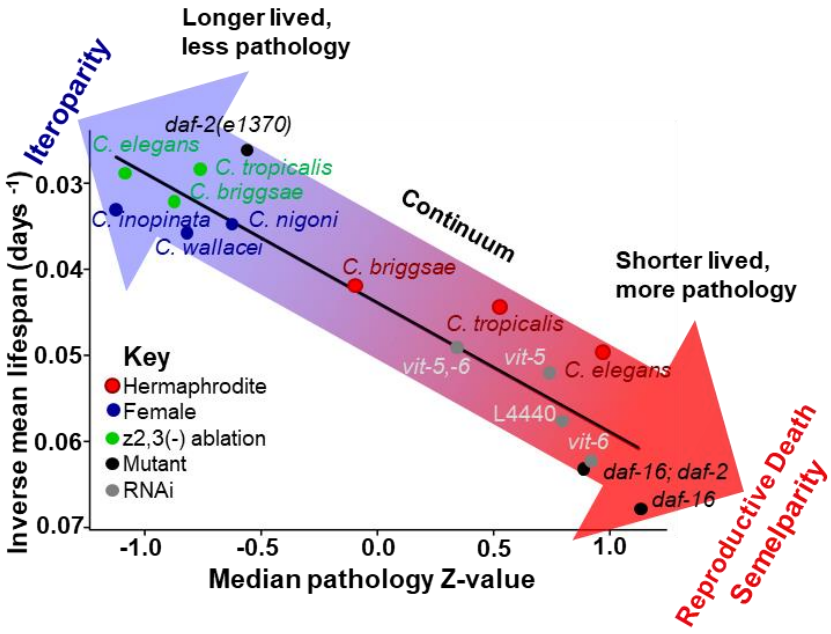

FIGURE 5.7. RD-associated pathologies and lifespan correlate, exemplifying the existence of a semelparity-iteroparity continuum. X axis, median pathology Z-score. Y axis, mean lifespan (unmated, antibiotic treated). Line of best fit in black. For raw pathology data used see (Figure 3.1,4.6,5.3,5.5). For lifespan data used see (Appendix 1). Mutant lifespan data taken from (Bansal et al., 2014).

5.3 Discussion

5.3.1 Signals from the germline trigger constitutive reproductive death in hermaphrodites leading to shorter lifespan

Do signals from the germline trigger constitutive reproductive death in hermaphrodites leading to their shorter lifespan? Results in this chapter support this hypothesis. Germline ablation caused large increases in hermaphrodite lifespan but not female lifespan and abrogated the greater lifespan of females (Figure 5.1). Moreover, increases in lifespan of a large magnitude upon suppression of reproductive death is characteristic of semelparous species (Figure 5.2, Table 5.1). Furthermore, germline ablation suppressed intestinal atrophy in all four hermaphroditic species (Figure 5.3), and the DAF-16/FoxO transcription factor was required for the suppression of intestinal atrophy in *C. elegans* (Ezcurra et al., 2018), as it is for suppression of ageing by germline removal (Hsin and Kenyon, 1999). Further evidence for this hypothesis includes the fact that the striking senescent changes in anatomy seen in hermaphrodites are largely absent from males (de la Guardia et al., 2016; Ezcurra et al., 2018; Ezcurra et al., 2020), suggesting that they do not undergo reproductive death. Consistent with this, a study of individually cultured nematodes in monoxenic liquid culture found that germline ablation by laser microsurgery

increased lifespan in wild-type hermaphrodites but not males (McCulloch, 2003). However, in another study, germline removal increased lifespan in *unc-50(e306)* (orthologue of human unc-50 inner nuclear membrane RNA binding protein) males (Arantes-Oliveira et al., 2002); the reason for the different results of these two studies remains unclear.

This evidence, together with results from the previous two chapters and other findings in support of *C. elegans* undergoing semelparous reproductive death are summarised in Table 5.2.

TABLE 5.2. Features of *C. elegans* consistent with semelparous reproductive death.

1) *C. elegans* hermaphrodites exhibit early, massive pathology affecting organs linked to reproduction.

2) Gut-to-yolk biomass conversion appears to be part of a suicidal reproductive effort that promotes fitness by feeding trophallactic fluid to larval kin.

3) Blocking hermaphrodite reproductive maturation (e.g. by germline ablation) suppresses development of such pathologies, and leads to increases in lifespan of a large magnitude.

4) Germline removal in wild-type males, which do not exhibit semelparity-like pathology, does not increase lifespan.

5) *Caenorhabditis* hermaphrodites, which exhibit senescent transformation, are shorter lived than (unmated) *Caenorhabditis* females, which do not, consistent with reproductive death in the former only.

6) *Caenorhabditis* hermaphrodites vent yolk and lay unfertilized oocytes in large numbers, while *Caenorhabditis* unmated and mated females do not.

7) Germline removal in unmated *Caenorhabditis* females, which do not exhibit semelparity-like pathology, produces much smaller increases in lifespan than in *Caenorhabditis* hermaphrodites.

8) Germline removal removes the difference in lifespan between *Caenorhabditis* females and hermaphrodites.

9) *C. elegans* senescent transformation involves source-to-sink type resource remobilization, as seen in semelparous animals and plants.

10) Autophagic processes that enable biomass conversion and resource remobilization contribute to senescent pathogenesis in semelparous organisms (particularly plants).

11) Semelparous senescence occurs earlier in cell compartments or organs that are non-essential for survival and behavior (gonad, intestine) than in essential organs (e.g. the nervous system).

12) Semelparous species often have an extended pre-reproductive stage, followed by a very brief reproductive stage (c.f. the dauer stage in *C. elegans*).

5.3.2 Does reduced insulin/IGF-1 signalling extend lifespan through suppression of reproductive death?

Three key pieces of evidence suggest that IIS reduction increase lifespan in *C. elegans* by suppressing of reproductive death:

(i) IIS mutants show RD-associated pathology suppression (Ezcurra et al., 2018; Garigan et al., 2002; Luo et al., 2010; McGee et al., 2012) (Figure 5.5) and greatly reduced vitellogenesis (Depina et al., 2011; Ezcurra et al., 2018; McElwee et al., 2003; Murphy et al., 2003).

(ii) IIS mutants show greatly reduced venting of yolk milk and laying of oocytes (yolk milk vectors) (Figure 5.5) to which RD-associated pathologies are coupled.

(iii) Effects on lifespan of both *daf-2* and germline removal require the DAF-16 FoxO transcription factor (Hsin and Kenyon, 1999; Kenyon et al., 1993) and in both cases its action in the intestine is important (Libina et al., 2003; Lin et al., 2001).

However, as described earlier, two facts do not easily fit this hypothesis.

(iv) Germline ablation increases lifespan in *daf-2* mutants (Arantes-Oliveira et al., 2002; Hsin and Kenyon, 1999).

(v) Mutation of *daf-2* increases lifespan in males (Gems and Riddle, 2000; Hotzi et al., 2018; McCulloch and Gems, 2007) though they appear not to exhibit reproductive death.

One possible explanation for (iv) is that uterine tumours limit life in *daf-2* mutant hermaphrodites. Mutation of daf-2 suppresses uterine tumour formation only weakly (Figure 5.5) and blocking tumour formation increases lifespan in *daf-2* mutants but not wild type (Figure 5.6).

5.3.3 Evolved traits accompanying reproductive death that could be a feature of *C. elegans* ageing

5.3.3.1 Adaptive death

Evolutionary theory predicts that adaptive death can evolve more readily in the presence of semelparity, as seen in Pacific salmon (reviewed in Galimov and Gems, 2020). This is because accelerated death post-reproduction in a semelparous organisms involves negigible individual fitness costs. A recent study of simulations of an *in silico* model of *C. elegans* on limited food patches used yield per colony of dauer dispersal forms as a measure of colony fitness (Galimov and Gems, 2020). The behaviour of this model supported the view that under certain conditions shorter adult lifespan can enhance colony fitness by reducing non-productive adult food

consumption and increasing food availability for larvae, especially given the clonal nature of *C. elegans* colonies (Galimov and Gems, 2020).

5.3.3.2 Aphagy: Is pharyngeal atrophy in *C. elegans* programmed aphagy?

Aphagy, the inability of an organism to feed due to anatomical deficiencies, is referred to by Finch as an example of 'rapid senescence' as well as 'inarguably programmed senescence' (Finch, 1994 a). Observed primarily in invertebrates such as mayflies and certain moths post metamorphosis, aphagy greatly limits natural lifespan but also brings two main benefits: it removes the risk associated with food foraging, as seen in mayflies (Finch, 1994b). This is especially the case if risk is so high that it creates a convex trade-off function (Abrams, 1991; Abrams, 1993) (also see Chapter 6 section 6.5.2). A further possibility is that reduces non-productive adult food consumption to increase food availability for larvae. The latter describes consumer sacrifice adaptive death, as may occur in *C. elegans* (Galimov and Gems, 2020a).
As with adaptive death, aphagy has been found to evolve in combination with semelparity, e.g. seen in the marine polychaete annelid *Nereis diversicolor,* mayflies and also Pacific salmon (Finch, 1994a; Finch, 1994 b; Golding & Yuwono, 1994; Kukalovd-Peck, 1985; Hane and Robertson, 1959), as survival after reproduction does not contribute to individual fitness in semelparous species. Moreover, in some cases interventions which suppress reproductive death suppress aphagy. For example, upon reaching maturity *N. diversicolor* stops feeding and undergoes reproductive death that is under neuroendocrine control (Golding & Yuwono, 1994). When reproductive death is blocked by preventing spawning by implanting cerebral ganglia from young, immature donors into the body cavity of adult hosts, and the worms begin to feed again (Golding & Yuwono, 1994; Finch, 1994 b).

While *C. elegans* do not stop feeding immediately upon reaching reproductive maturity, they do show progressive pharyngeal atrophy which correlates with a decline in pharyngeal pumping rate, a measure of food consumption; pumping declines rapidly from day 2 of adulthood and ceases by around day 12, while pharyngeal pathology begins from day 1 and peaks between days 12-14 (data from independent studies, with experinments looking at pharyngeal atrophy alongside decline in pumping rate yet to be done) (Chow, et al., 2006; Croll, et al., 1977; Hosono, et al., 1980; Huang, et al., 2004; Zhao, et al., 2017; Ezcurra, et al., 2018). Moreover, pharyngeal atrophy follows the same patterns of presentation as other RD-associated pathologies: constitutively present in hermaphrodites and induced in mating by females (Figure 4.6,4.7) as well as being suppressed by germline removal (Figure 5.3), with its suppression dependent on the

presence of the somatic gonad (Figure 5.4). Together, these results suggest that pharyngeal atrophy is connected to reproductive death in *C. elegans* and, taken together with findings from computer modelling supporting the benefits of reduced food consumption (Galimov and Gems, 2020), suggests that pharyngeal atrophy could represent programmed (i.e adaptive) aphagy.

5.3.3.3 Loss of regenerative capability

Another trait linked to semelparity is loss of regenerative capacity (Finch, 1994 b). For example, when *N. diversicolor* is in its immature sedentary stage it is able to regenerate ablated segments and this is lost upon reaching maturity. However, if reproductive death is blocked through implanting cerebral ganglia from young individuals as described earlier, the worms can recover their regenerative capacity as well (Golding & Yuwono, 1994).

C. elegans cells are post mitotic, but are capable of repair and regeneration (Vibert, et al., 2018). It would be interesting to test whether regenerative capacity and repair is linked to pathways which accelerate ageing through reproductive death pathology in *C. elegans*, and if regeneration capability is unequal across different tissues. An expectation is that regenerative capability and repair will be downregulated in source cells for biomass repurposing, e.g. the intestine undergoing biomass conversion would be expected to have little regenerative capacity unlike for instance neurons that remain relatively well preserved.

5.3.4 Implication of *C. elegans* being semelparous

Reproductive death is often viewed as distinct from senescence in iteroparous organisms such as humans. However, explanation is required if similar pathways, such as IIS and germline signalling, are affecting lifespan in semelparous *C. elegans* undergoing reproductive death and other iteroparous models studied with merely differences in the magnitude of the effects. Based on these results in this and the last two chapters, as well as recent theories of ageing (Blagosklonny, 2006; de Magalhaes and Church, 2005; Maklakov and Chapman, 2019; Gems et al., 2020), one possible explanation is that semelparity represents an extreme, derived form of programmatic mechanisms of ageing that to a smaller extent contribute to ageing more widely (Gems et al., 2020). This explains the smaller and more condition-dependent effects on lifespan from the same interventions in iteroparous animals. It also implies the existence of a continuum of programmatic mechanisms of ageing between semelparous and iteroparous organisms, with such mechanisms amplified in semelparous organisms. Thus, despite the presence of reproductive death, ageing mechanisms in *C. elegans* may be informative about ageing in iteroparous species

(e.g. humans). The next chapter focuses and elaborates upon this, and builds upon existing theories of ageing.

Chapter 6: Discussion

6.1 Introduction

Humans do not undergo reproductive death but results presented in this thesis support the view that *C. elegans* does. What does this say about the value of *C. elegans* as a laboratory model to understand ageing? Caleb Finch said of semelparous dasyurid marsupials: “Their escape from ‘natural death’ under optimum conditions and their capacity to more than double their natural lifespan caution against overemphasizing lifespan and mortality rates as a basic index of cellular ‘ageing’.” (Finch, 1994a, p. 95). Does this warning now also apply to *C. elegans,* a model organism that has been used extensively over the last four decades for ageing research? The discussion that follow will argue not.

6.2 Costly programmes as conserved causes of senescence

What are the mechanisms operative in semelparous organisms and how do they fit the current evolutionary framework? As described in the introduction, in theory all trade-offs that facilitate an early and large reproductive effort should be amplified in semelparous organisms (Partridge & Sibly, 1991), with the associated costs of these amplified trade-offs on physiology (Partridge, 1997) resulting in rapid senescence (Gems et al., 2020; Gems and Kern, 2021) (Figure 1.12). That being said, not all trade-off costs are inherently unavoidable; some costs arise as a consequence of the decline in the force of selection. For example, quasi-programmes are the result of a lack of selection against futile programmes later in life (Blagosklonny, 2006). Our new understanding of senescent pathophysiology in *C. elegans* provides insight into the specific primary mechanisms governing semelparous reproductive death. Many of the major senescent pathologies in *C. elegans* are indirect physiological costs (Speakman, 2008) of programmes actively selected for, e.g. yolk milk feeding of larvae coupled to the cost of intestinal atrophy and PLP steatosis. While this does fit the definition of an AP trade-off, it does not conform to Blagosklonny's definition of a quasi-programme (futile programme continuation) as its action is not futile. However, there are similarities. In both cases pathology primarily results from hyperfunction rather than loss of function, and more specifically in both cases programmatic processes are involved, i.e. involving action of complex wild-type functions (e.g. anabolic, catabolic) leading to pathology; use of the term “programmatic” is intended to indicate complex and concerted biological functions, but to leave open the question of whether such functions

promote fitness or not. Programmes that promote fitness and as such are actively selected for even though they come at a cost can be termed *costly programmes* (Gems et al., 2020).

A broad difference between these two cases is the relative timing of benefits and costs. The Blagosklonny and de Magalhães accounts (Blagosklonny, 2006; de Magalhães & Church, 2005; de Magalhães, 2012) describe a programme that promotes fitness in early life and becomes harmful later in life as a quasi-programme (Blagosklonny, 2006). By contrast in the case of intestinal atrophy coupled to yolk production, where the costly programme is selected for due to the benefit of yolk milk production, benefit and harm are generated simultaneously (Gems and Kern, 2021).

What determines the timing of costs? Consideration of the relationship between AP trade-offs and constraints can help to answer this question. Quasi-programmes arise in the absence of constraints through a decline in the force of selection with programme action at the time of this decline being futile (Figure 6.1) (Gems and Kern 2021). As detailed earlier, constraints can be divided into those that are selective and those that are organisational (Acerenza, 2016). Trade-offs that occur as a consequence of constraints can also be broadly classified into two groups according to which of these two forms of constraint are involved (Acerenza, 2016). Costly programmes arise from interconnection-type organisational constraints where two linked traits, one beneficial and one deleterious, are under conflicting selection (Figure 6.1) (Gems and Kern 2021). As a result, costly programme benefits and costs arise simultaneously.

Biological constraint in the absence of AP may also result in pathological costs. Notably, the capacity for evolutionary change to achieve optimal biological design tends to be over-estimated (Gould and Lewontin, 1979). For example, it was recently argued that lack of optimum design could result in senescent pathology simply through the absence of a function; to contrast with the concept of hyperfunction, this was termed “hypofunction” (Maklakov and Chapman, 2019). Most observable examples hypofunction occur as a result of phenotypic insufficiency, i.e. lack of sustainability in a function (Gems and Kern, 2021). For example, in primate oogenesis a finite stock of oocytes is formed prior to birth, whose quality in later adulthood is assured by increasing rates of follicular atresia; the human menopause appears to have evolved due to the impossibility of extending reproductive span in women due, as it were, to a design weakness in the ovary. Here hypofunction is manifest as absence of iterogametogenesis (which is present in men).

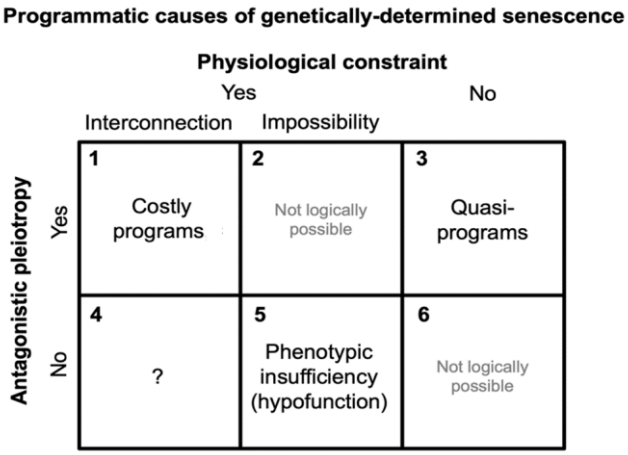

FIGURE 6.1. Common physiological constraint-derived and constraint independent mechanisms of ageing and their overlap with AP: tentative model. Physiological constraints are viewed as either based on the interconnectedness of traits (e.g. clutch size vs egg size) or simple impossibility (see introduction for details). Reproduced from (Gems and Kern, 2021).

6.3 Costly programmes and context of a semelparity-iteroparity continuum

The likelihood that costly programmes are weakly active in iteroparous organisms is supported by the following considerations. First, costly programmes are the primary proximate senescent mechanisms operative in semelparous organisms. And second, semelparity and iteroparity follow a continuum (Hughes, 2017), based on the extent to which selection works to maximise *r* vs R_0 and so affects trade-off costs (Figure 1.12). In line with this likelihood, inhibiting insulin/IGF-1 signalling and germline removal suppresses reproductive death and greatly extends lifespan in *C. elegans*, but can also extend lifespan to a small extent in iteroparous organisms (Gems et al., 2020). This also fits the view that semelparous aetiologies evolved through amplification of mechanisms operative in iteroparous ancestors (Gems et al., 2020; Finch, 1994a).

This view predicts that pathology occurring in semelparous organisms should resemble those seen in a more modest form in iteroparous organisms. In fact, many of the pathological changes that occur rapidly in spawning salmon, one of the best studied organisms known to undergo reproductive death, also occur in later life in much longer-lived salmon in which reproductive death has been suppressed by gonadectomy (Robertson and Wexler, 1962). Thus, reproductive death resembles accelerated ageing. Moreover, many pathologies, including thymic involution (Allard and Duan, 2011), amyloid deposits in multiple regions of the brain (Maldonado et al., 2002; Maldonado et al., 2000), and endothelial cell hyper-proliferation (Farrell, 2002;

Robertson et al., 1961) reminiscent of coronary artery disease (House and Benditt, 1981; Robertson et al., 1961), are observed in both iteroparous mammals and semelparous Pacific salmon (reviewed in Gems et al., 2020).

Notably, one broad difference between semelparous aetiologies and the iteroparous aetiologies from which they evolved is that while the former are irreversible and life-limiting, the latter can be reversible. For example, intestinal atrophy in adult *C. elegans* hermaphrodites or spawning lampreys undergoing reproductive death appears to be irreversible, whereas in iteroparous mammals loss of muscle during starvation or of bone during lactation is reversible (Speakman, 2008; Gems et al., 2020) (Figure 6.2). Plausibly, then, both *C. elegans* reproductive death and mammalian ageing involve quasi-programmes and costly programmes (Figure 6.2). This means that understanding *C. elegans* ageing should provide fundamental insights into elements of the pathophysiology of human senescence.

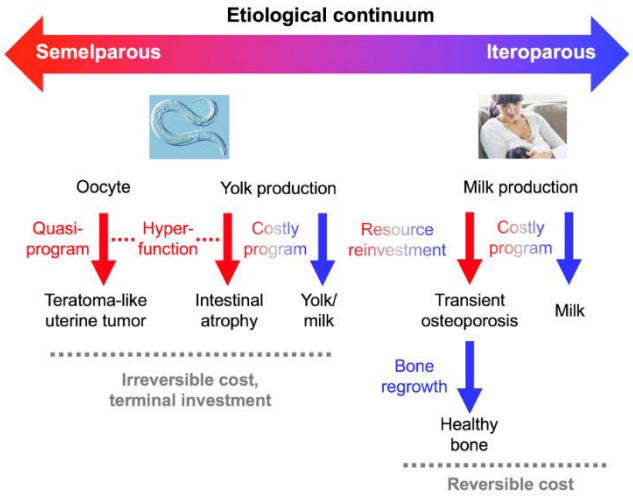

FIGURE 6.2. Programmatic mechanisms of ageing in semelparous and iteroparous organisms: conceptual model. Programmatic mechanisms here include costly programmes and quasi-programmes. The amplification of costly programmes during reproductive death suggests that quasi-programmes may play a relatively greater role in iteroparous ageing. Reproduced from (Gems et al., 2020).

6.4 Quasi-programmes as conserved causes of senescence: links between constraint-derived and constraint-independent mechanisms

Pathology in *C. elegans* also involves quasi-programmes, as seen from the development of teratoma-like uterine tumours (Wang et al., 2018a; Wang et al., 2018b) (see chapter 4 discussion). Notably, across the *Caenorhabditis* genus tumours are seen to follow

the same pattern of presentation as other RD-associated pathologies: i.e. presentation is worse in hermaphrodites compared to females, and in hermaphrodites severity ranking is *C. elegans* > *C. tropicalis* > *C. briggsae* (Figure 4.6,4.7,4.12). In other words, tumour presentation follows the pattern of the semelparity-iteroparity continuum (see especially Figure 4.12B). This begs the question: why would an amplified mechanism that is, as far as can be seen, constraint-independent follow the semelparity-iteroparity continuum?

6.4.1 Costly programmes may cast an early selection shadow: new theory

Constraint-related evolution of ageing is not solely dependent upon the decline in the force of selection. Costly-programmes are, in fact, expected when selection is strong given their association with positive traits actively selected for. Deleterious senescent consequences of costly programmes, by affecting future function and survival, are expected to accelerate the decline in the force of selection. If strong enough, this will result in an earlier selection shadow being cast; this is more likely to occur towards the semelparous (*r* maximising) end of the spectrum (Figure 1.12). For example, the costly programme trade-off of calcium movement from bone to milk previously described has minimal and transient consequences in humans but is pathological enough to affects lifespan in *Antechinus* females (Fisher & Blomberg, 2011; Braithwaite & Lee, 1979; Green, et al., 1991). This in turn will influence other senescent mechanisms that are sensitive to the decline in the force of selection. This points to a causal link in evolutionary mechanisms between costly programmes (and, more generally, constraint-derived mechanisms that are more likely to be operative early in life) and more constraint-independent mechanisms of ageing, such as quasi-programmes, MA, molecular damage etc. (Figure 6.3). As each senescent mechanism in turn will deepen the selection shadow further, this predicts the possible occurrence of an evolutionary cascade of selection shadows, with costly-programmes at the apex (Figure 6.3).

6.4.2 Quasi-programmes may evolve on the coat-tails of costly programmes: new theory

Given that quasi-programmes involve the futile continuation of gene action that is pathological and not switched off, another plausible evolutionary causal link between costly and quasi-programmes is that many quasi-programmes could emerge as the futile continuation of costly programmes. In other words, a given programmatic mechanism of ageing may, with advancing age, change from a costly programme to a quasi-programme. This, along with the effects of costly programmes on the decline in the force of selection,

likely result in quasi-programmes often riding on the evolutionary coat-tails of costly programmes.

In such cases, selection for genes that promote costly programmes is inadvertent selection for genes that result in quasi-programmes later in life. Thus, these genes would have two pleiotropic programmatic costs: costly- and quasi-programme costs. For example, gut-to-yolk biomass conversion in *C. elegans* might have evolved to support lactation, but then run-on in a futile and pathogenic manner after it has ceased to contribute to fitness. Notably, this would mean that the inhibition of many costly programmes and quasi-programmes can be achieved through the same interventions.

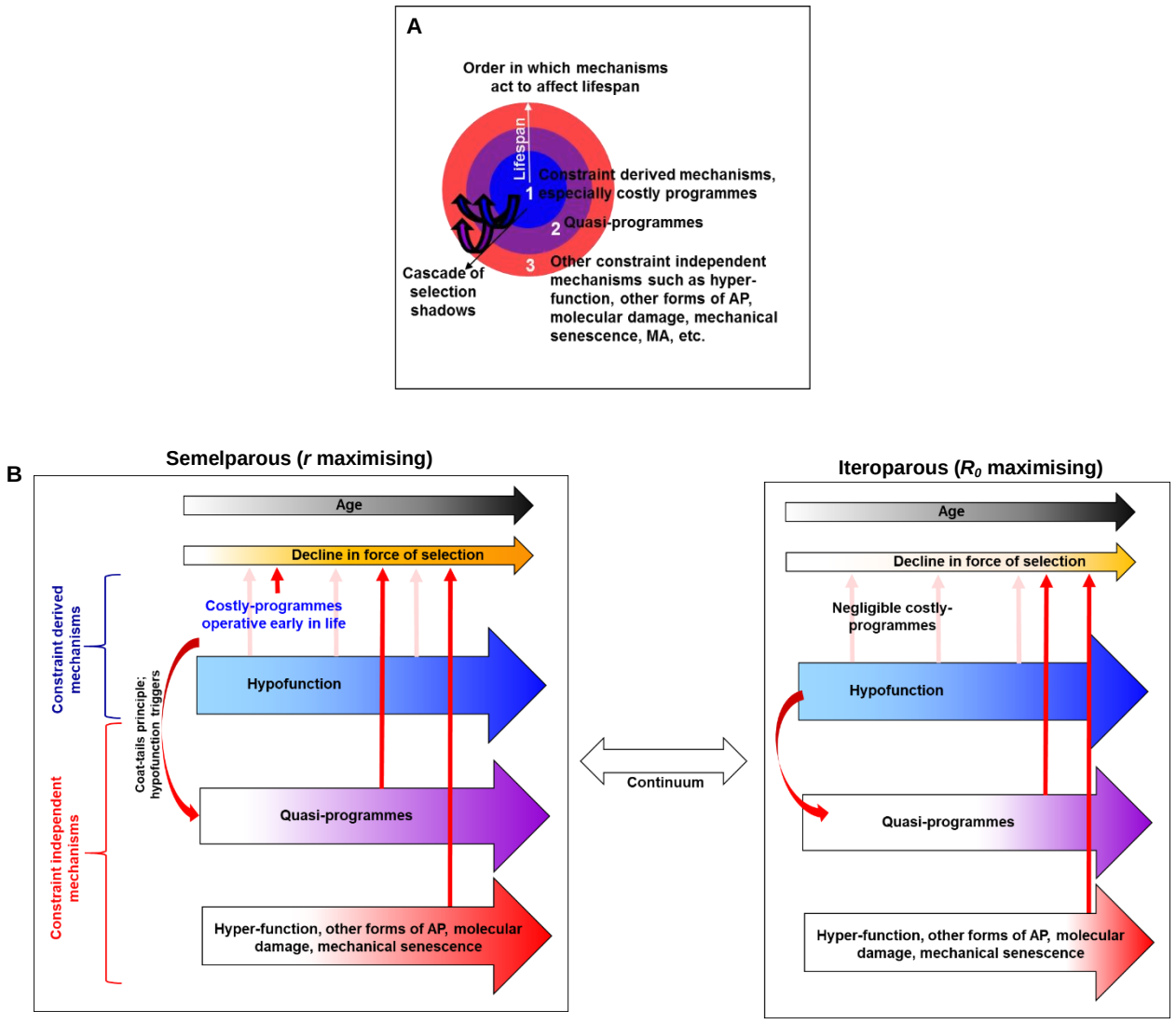

FIGURE 6.3. Costly programmes play a pivotal role in the evolution of ageing: hypothetical new scheme. **(A,B)** Order in which proximate mechanisms work to influence ageing and one another through effects on the force of selection. **(B)** Costly programmes will influence other ageing mechanisms through effects on the force of selection. Broad distinction between constraint-derived and constraint-independent mechanisms shown. Costs of costly programmes are operative early in life as they occur simultaneously with benefits actively selected for. Hypofunction (Maklakov and Chapman, 2019) may also be operative early in life when selection is strong due to dependence on constraints, though as selection weakens with time, the likelihood of hypofunction being

operative will increase. Many quasi-programmes will evolve on the coat-tails of costly programmes, as well as be triggered by hypofunction.

A more detailed picture can be produced by linking this understanding with John Speakman's conceptualisation of physiological costs, as applied by him to reproductive costs (Speakman, 2008) (Figure 6.4). According to his scheme, reproductive costs are either direct, as when required for achieving a reproductive outcome; or they are indirect, as when they are the consequence of a reproductive outcome. Indirect costs are further categorised into those that are either obligatory or compensatory. Costly programmes and associated quasi-programmes can likewise be distinguished (Figure 6.4). An example of a direct cost is organ remodelling to facilitate increased nutrient uptake, as in calcium uptake by the gut during lactation in rats (Speakman, 2008). An obligatory indirect cost is osteoporosis due to calcium repurposing from bone to breast milk in humans, or biomass repurposing from intestinal tissue to yolk milk in *C. elegans*. Compensatory costs involve processes such as reduced investment in some other aspect of physiology to maximise a reproductive benefit, e.g. reducing thermogenesis or physical activity (Speakman, 2008).

While both Blagosklonny and de Magalhães view quasi-programmes in particular as originating from a continuation of developmental growth, including adult developmental processes (Gems and Kern, 2021; Blagosklonny, 2006; Blagosklonny, 2007; Blagosklonny, 2008; Blagosklonny, 2013; de Magalhães & Church, 2005; de Magalhães, 2012), reproductive death in *C. elegans* draws attention to programmes also specifically operative only during reproduction. As such, a distinction can be made between the two (Figure 6.4). For example, while gut-to-yolk biomass conversion appears to occur as a costly programme in hermaphrodites and mated female *Caenorhabditis*, it appears to play little role in ageing in unmated females (Figure 4.6,4.7,4.12). This distinction is also useful when comparing different sexes, such as male *C. elegans* that appear more like unmated females in terms of RD pathologies (de la Guardia et al., 2016; Ezcurra et al., 2018; Ezcurra et al., 2020).

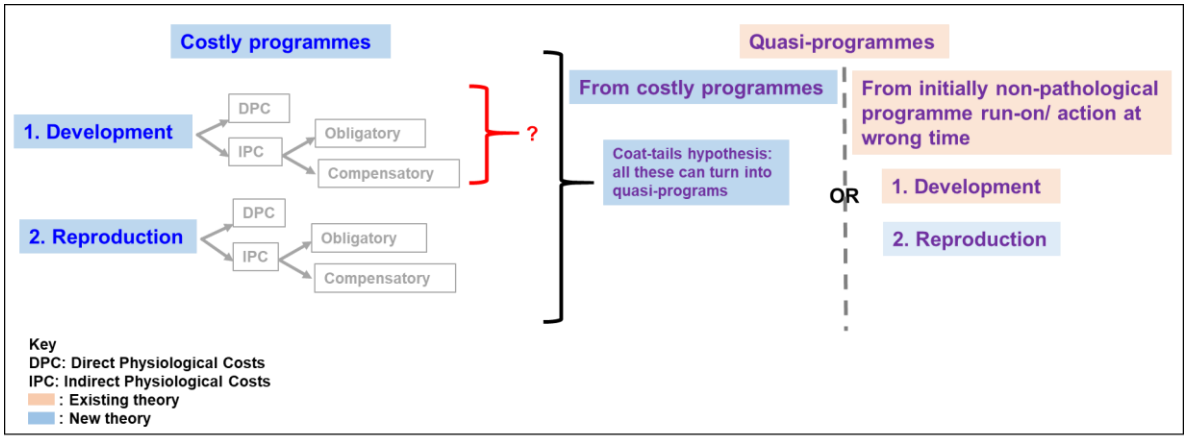

FIGURE 6.4. Overview of old and new programmatic theory: tentative new scheme. As a broad distinction, costly programmes can be divided into those which affect development, including adult developmental processes such as repair/tissue homeostasis and immunological programmes, and those which are only operative during reproduction. Both types of costly programmes may lead to quasi-programmes. Direct physiological costs (DPC) and indirect physiological costs (IPC) are added as an extension of terminology from (Speakman, 2008). To what extent costly-programmes are associated with developmental processes remains largely unexplored. Grey: theory developed by Mikhail Blagosklonny and João Pedro de Magalhães (Blagosklonny, 2008; Blagosklonny, 2013; de Magalhães & Church, 2005; de Magalhães, 2012). Blue: New theory from work presented here and (Gems et al., 2020) (Gems and Kern, 2021). Blue font: Costly programme associated. Purple font: Quasi-programme associated.

Other links between constraint derived and constraint independent mechanisms likely also exist. For example, hypofunction (Maklakov and Chapman, 2019) may exert some of its deleterious consequence through acting as quasi-programme triggers (Figure 6.3). This is seen during menopause where oocyte depletion results in a decline in oestrogen levels which triggers futile osteoclast-mediated bone resorption associated with osteoporosis (Lobo, et al., 2014; Santoro, et al., 2015).

6.5 A unifying theory: parity, trade-off functions, programmatic mechanisms and constraint dependence

6.5.1 Linking trade-off functions to parity using *r* vs R_0 maximisation: new theory

Trade-off trait-fitness relationships can be graphically represented. For simplicity, one can focus on two extreme scenarios of various possibilities: (i) a concave (downward bent) function relating survival to fecundity which represents a situation where even an intermediate value of a reproductive trait come at a large cost; and (ii) a convex (upward bent curve) function where very large gain is achievable prior to costs being realised (Figure 6.5 A). A linear relationship/ function lies in the middle of the two extremes (Figure 6.5 A).

Trade-off functions have been put into the context of parity through use of optimisation theory (Partridge & Sibly, 1991), where adaptation is understood through assigning pay-offs to the different options available to an organism and then deducing the optimal solution which allows for maximum fitness. This is done through superimposing trade-off functions with fitness contours (Figure 6.5 B, adapted from (Partridge & Sibly, 1991)). Fitness contours connect points where the function has the same particular value of fitness (i.e. reproductive output). As shown in Figure 6.5 B, these lines connect points along which *r* is constant (Partridge & Sibly, 1991). For animals that favour R_0 maximisation and R_0 traits (Kozłowski, 1993; Mylius & Diekmann, 1995; Dańko, et al., 2018; Dańko, et al., 2017), arguably this must be corrected to fitness contours connecting points where R_0 is constant. The intercept (yellow X in Figure 6.5 B) between the trade-off function and the highest superimposed fitness contour represents the optimal trade-off (Partridge & Sibly, 1991). A semelparous (more *r* maximising) animal will have different fitness contours to an iteroparous animal as benefit vs cost optimisation is different, leading to a different intercept on the trade-off function (Partridge & Sibly, 1991) (as just discussed, in light of the existence of an *r*-R_0 continuum, arguably fitness contours should be changed to those that maximise R_0 in more iteroparous animals (Dańko, et al., 2018; Dańko, et al., 2017)). Additionally, a strong and important concave function itself will favour a semelparous strategy (Figure 6.5 B) as terminal costs leave the organism no other choice (Partridge & Sibly, 1991). If a given trade-off varies in curvature over its range, multiple optima may be possible which in turn may contribute to diversity of strategy (Partridge & Sibly, 1991).

6.5.2 Context of a 'continuum' between *r*-R_0 and semelparity-iteroparity: new theory

While semelparity and iteroparity are viewed as distinct life history modes in (Partridge & Sibly, 1991) with different fitness contours and so different intercepts, more plausible there exists an *r* vs R_0 (Dańko, et al., 2017) continuum and a semelparity-iteroparity continuum (Hughes, 2017). This implies that a range of gradations in fitness contours will exist according to where the organism is situated on the *r* vs R_0 and semelparity-iteroparity continuums. The more semelparous an organism is, i.e. more *r* shifted on the *r* vs R_0 continuum, the more intercepts on trade-off functions will be shifted to allow for large costs to facilitate as large and early a reproductive output as possible (Figure 6.5 C).

Moreover, based on the idea of a continuum between *r* vs R_0 maximisation fitness contours, strong concave trade-off costs, by influencing *r* vs R_0 maximisation themselves (through effects on adult survival), will arguably influence all trade-off fitness contours. This will result in the intercepts on other trade-off functions being affected and shifted (Figure 6.5 C).

One feature of semelparity is plasticity of strategy as previously described (Finch, 1994 a). Such plasticity may be in part achievable through the animal simply changing the intercept on trade-offs.

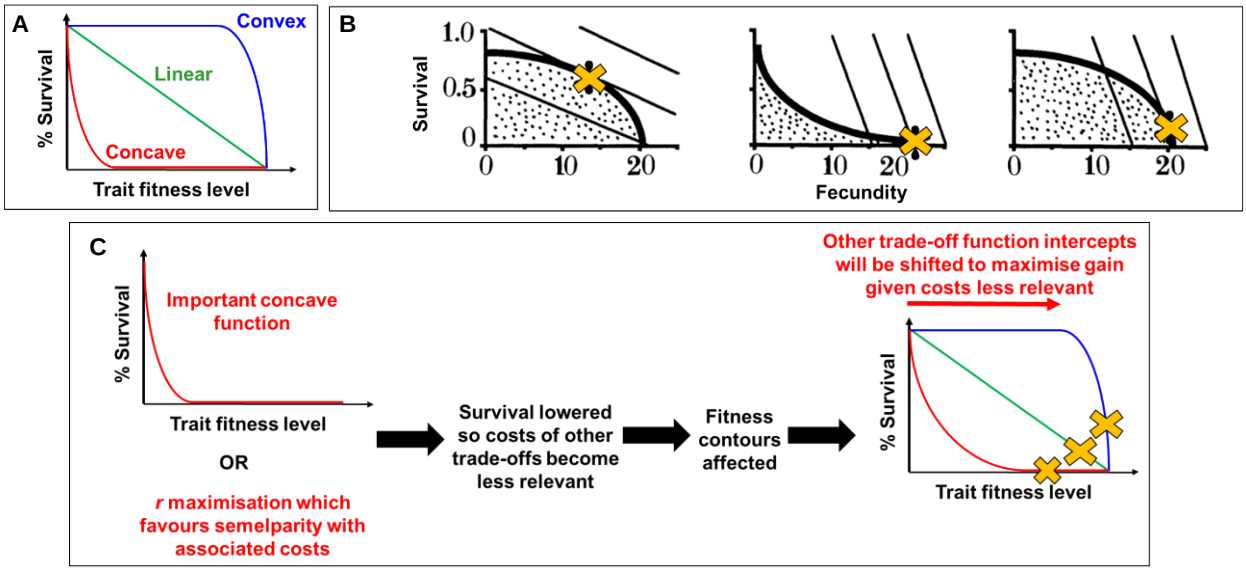

FIGURE 6.5. Linking trade-off functions and *r* vs *R0* maximisation: tentative new model. (A) Representation of various trade-off functions, with a continuum of possibilities lying between an extreme convex and an extreme concave function. Option sets available to the organism (c.f. dots in B, i.e. the space below the trade-off curve for each function) are not highlighted as organisms are likely to opt for the highest survival and reproductive possibility, i.e. the outermost part that is shown by the trade-off curve line. **(B)** Fitness contours (straight lines) superimposed onto the trade-off function to predict the choice of reproductive strategy of the organism. Reproduced and simplified from (Partridge & Sibly, 1991). Fitness contours in the diagram connect lines where *r* (Malthusian parameter) is the same (Partridge & Sibly, 1991), but based on (Dańko, et al., 2017; Dańko, et al., 2018) this should arguably be changed in organisms where selection works to maximise R_0 to connect lines where R_0 is the same (i.e. R_0 is the better measure of fitness in these organisms). The intercept (yellow cross) shows where the animal will sit on the trade-off function, i.e. the optimal trade-off leading to the highest *r* or R_0. An iteroparous animal will favour intermediate costs and benefits, as seen by the intercept on the left convex function. A semelparous, *r*-maximising animal will favour maximum costs and benefits regardless of function shape, represented by the intercept on the convex function on the right. A strong concave function itself will favour a semelparous strategy given the unavoidable costs associated with even a little trait fitness benefit. **(C)** Either a strong concave function or selection acting to maximise *r* will affect the intercepts on all trade-off functions.

6.5.3 Primary and secondary constraints: new theory

To more clearly describe the relationship between trade-off functions and biological constraints I propose using the terms *primary constraints* and *secondary constraints* (Figure 6.6A). Here, if the trade-off is based on an underlying constraint, e.g. costly-programmes, then that constraint is the primary one. This is the case, for example, with calcium transfer from bone to breast milk or intestinal biomass conversion to yolk milk, as is also likely true for many costly programmes. In each case trade-offs arise from a primary organisation constraint where two traits are interconnected and there is a coupling mechanism under conflicting selection. By contrast, secondary constraints influence the shape of the trade-off function. By doing so, secondary constraints may also influence the intercept on the trade-off function through effects on fitness contours, as previously discussed (Figure 6.5B,C, 6.6). An example of a secondary constraint involves the sand cricket *Gryllus firmus*, where a trade-off between fecundity and flight capability is found to be partially determined by the secondary constraint of body size (Roff, et al., 2002). Selection may act on any of these constraints, primary or secondary.

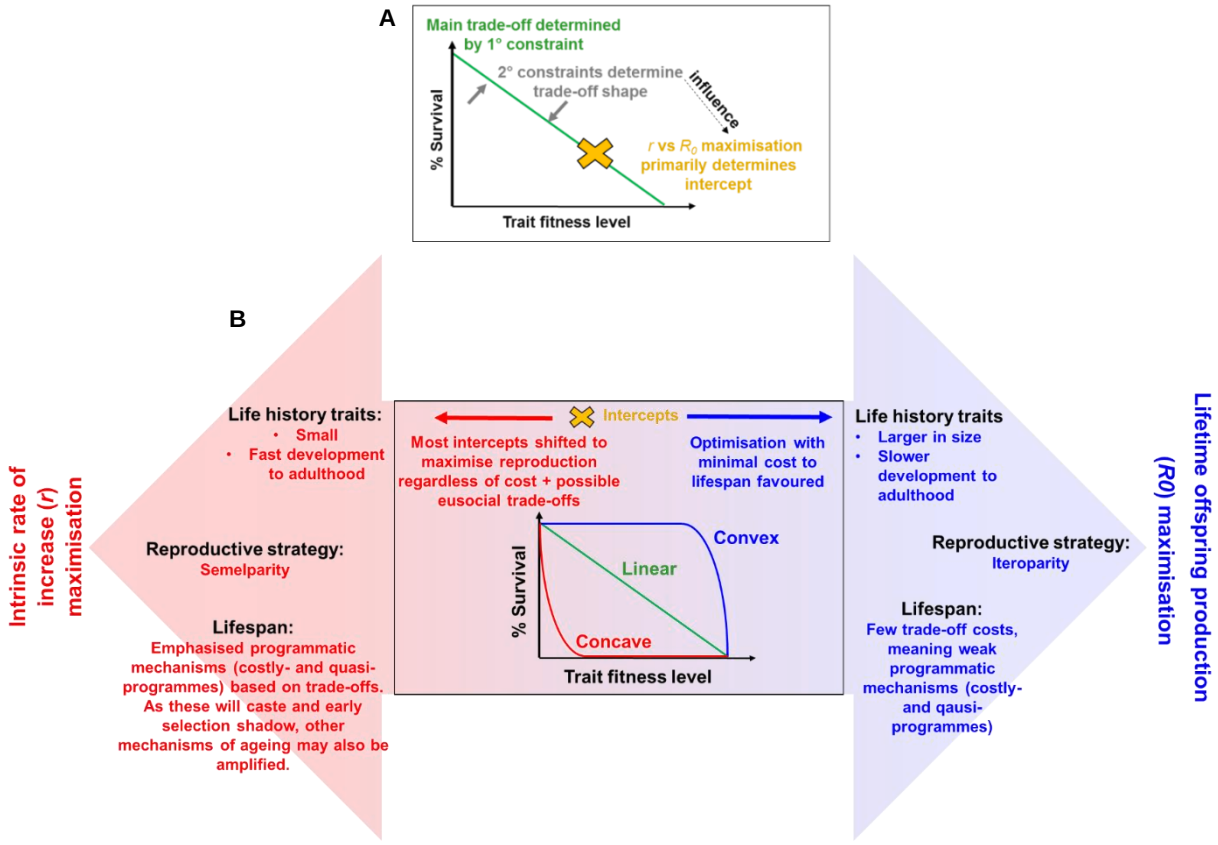

FIGURE 6.6. Unifying trade-off functions, constraints and *r* vs *R0* maximisation: tentative new scheme. **(A)** Primary and secondary constraints and trade-off functions. Only a linear trade-off function is shown for simplicity (the trade-off function may have any shape). If the trade-off arises as a consequence of a constraint, that constraint is termed the primary. Secondary constraints affect the shape of the trade-off function and in

doing so may influence the intercept (yellow cross), which is dependent on fitness contours. **(B)** Combining trade-off functions with *r* vs R_0 maximisation, and life-history traits including reproductive strategy and lifespan. Animals that work to maximise *r* will favour *r*-associated traits and arguably semelparity, and animals that favour R_0 maximisation and R_0 traits and iteroparity (Kozłowski, 1993; Mylius & Diekmann, 1995; Dańko, et al., 2018; Dańko, et al., 2017), with parity following on from the *r* vs R_0 maximisation continuum (Dańko, et al., 2017; Dańko, et al., 2018) as it was previously assigned to the r/K model that the *r* vs R_0 maximisation continuum is built from (Gadgil & Solbrig, 1972; Stearns, 1976; Stearns, 1977). By superimposing fitness contours onto trade-off functions (Partridge & Sibly, 1991) and accounting for the *r* vs R_0 maximisation continuum (Dańko, et al., 2017; Dańko, et al., 2018), one can combine *r* vs R_0 maximisation, parity and the position of trade-off function intercepts into one hypothetical model. Here, the more an organism works to maximise *r* over R_0, the more trade-off function intercepts are shifted to allow for an early and large semelparous reproductive episode regardless of costs, and vice versa for iteroparous organisms that favour lifetime offspring production. That said, large costs are not always a requirement of a large reproductive effort; trade-off function shape is an important determinant, where more concave trade-offs result in larger costs for a given fitness benefit. A strong vital concave trade-off itself will favour a semelparous strategy (Partridge & Sibly, 1991) due to unavoidable early costs, and in doing so will affect the intercepts of other trade-off functions (Figure 6.5 B,C), i.e. secondary constraints may influence trade-off intercepts (see A).

One implication here is that although quasi-programmes do not have a primary constraint, quasi-programme trade-off fitness-cost relationships can be altered by selection acting on secondary constraints. Take for instance quasi-programmed run-on resulting in presbyopia with age (Strenk et al., 2005) where a trade-off occurs between lens growth and poor vision due to long-sightedness. Given that the optical performance of the human eye is the result of contributions and interactions between the lens and several other ocular tissues, e.g. the cornea, sclera, ciliary body and zonules, changes to any of these will affect the trade-off function. Trade-offs are therefore best viewed as multi-factorial rather than simply bivariate relationships (Figure 6.6).

6.5.4 Secondary constraints may result in the same trade-off having different functions in different organisms: new theory

Variation in secondary constraints result in the same trade-off having different functions (i.e. curve shapes) in different organisms (Figure 6.7). Consequently, this may result in the same ageing mechanism having different costs in different organisms. Given that precisely defining trade-off curve shapes is difficult due to a lack of empirical data, reliable identification of an example here is difficult. However, a possible example is the costly programme trade-off of calcium movement from bone to milk in the little brown bat *Myotis lucifugus*, which is very long lived (maximum lifespan, at least 34 yr) relative to most similarly sized small terrestrial mammals. Here different secondary constraints are likely the cause of disproportionate costs during lactation (Figure 6.7), with calcium demand particularly stressful and resulting in significant structural changes and evident osteoporosis in the bones of lactating female *M. lucifugus* (Kwiecinski et al. 1987; Barclay, 1994). It is

possible that it is in order to cope with these costs that *M. lucifugus* have relatively small broods compared to terrestrial mammals (Barclay, 1994). Three of the main secondary constraints determining this in *M. lucifugus* are as follows. (i) Low levels of dietary calcium due both to the prey the bats consume and their inability to obtain calcium from more sources due to their mode of foraging and prey detection (Barclay, 1994) making calcium loss from bones more costly. (ii) The fact that their young have greater calcium demands as they need to reach 70–80% of adult size to withstand the stress of flight (Hood, et al., 2011) unlike most terrestrial mammals of similar size that are nutritionally independent when they reach about 40% of their adult size (Barclay, 1994). And (iii) the need for fully calcified wing bones in bats (both for lactating mothers, which affects their foraging capability before and after lactation as it determines what level of calcium loss from bones is pathological, and for offspring (c.f. point ii)) to likely withstand the unique torsion and shear forces placed on them during flight (Swartz, et al., 1992) (Figure 6.7).

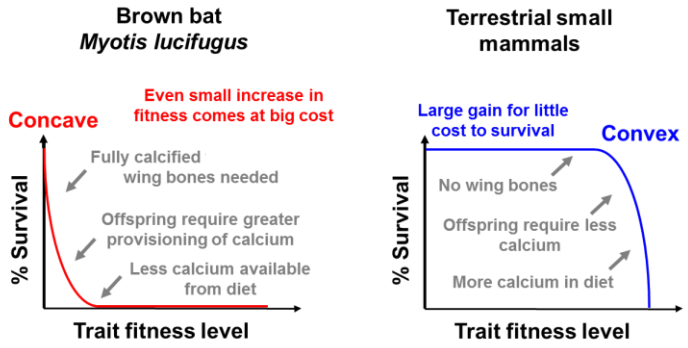

FIGURE 6.7. Secondary constraints: Hypothetical trade-off functions associated with calcium movement from bone to milk in brown bats *Myotis lucifugus* and small terrestrial mammals. Based on the small number of offspring produced, deleterious consequences of bone loss during lactation, and secondary constraints likely associated with calcium movement from bone to milk in *M. lucifugus*, it is likely that the trade-off is more concave than in terrestrial mammals. As depicted here, the trade-off functions are likely an exaggeration, with the animals realistically lying somewhere in between, where *M. lucifugus* is shifted more towards the concave end. Note: precisely defining trade-off curve shapes is difficult as in most cases there is not enough empirical data to measure the shapes of option sets (c.f. Figure 6.5).

6.5.5 Uncoupling AP trade-offs through removal of secondary constraints: new theory

Based on the above, it should be possible in principle to completely break AP trade-offs by removing secondary constraints and so allow an organism to realise its physiological maximum investment into reproduction without cost. There are known examples of trade-off uncoupling (Flatt & Partridge, 2018), e.g. in *Drosophila* where a fertility-lifespan trade-off

can be uncoupled through placement in an artificially benign laboratory environment with a food source that is overall dietary restricted (not calorie rich) but high in essential amino acids (Grandison, et al., 2009).

Another way to uncouple trade-offs is to move the trade-off to a higher level of organisation, i.e. allow for a eusocial trade-off to occur (Flatt & Partridge, 2018). Arguably programmed or adaptive death is one such eusocial trade-off, where in highly clonal individuals (e.g. sphecid wasps, thrips, bark beetles, shrimps, naked mole-rats and aphids) inclusive fitness benefits outweigh any benefit forgone by certain individuals as discussed previously. Other examples here are biomass sacrifice during semelparous reproductive death (Gems, et al., 2020), as well as various forms of inclusive fitness benefit provided by programmed adaptive death (Lohr et al., 2019).

6.5.6 Greater levels of extrinsic mortality may accelerate senescence even close to the *r* end of the continuum due to costly programmes: new theory

Any extrinsic factor that affects the gradient of the decline in the force of selection favours the evolution of increased senescence rate. It has long been assumed that the most important determinant of this decline is extrinsic mortality. As every slope is relative (i.e. the steepness of the slope is determined by the ratio of the 'vertical change' to the 'horizontal change' between (any) two distinct points on the line), uniform changes across the slope where the population is affected as a whole (i.e. age-independent changes), will not affect the gradient (Hamilton, 1966; Taylor, et al., 1974; Abrams, 1993; Charlesworth, 1994; Caswell, 2007; Moorad & Promislow, 2008; Wensink, et al., 2017; Dańko, et al., 2018). When density dependence is a factor, high extrinsic mortality will reduce population density and thus weaken density dependence effects (Dańko, et al., 2017; Dańko, et al., 2018). A simple extrapolation, therefore, is that when R_0 is maximised, extrinsic mortality plays a significant role in shaping life histories and increases the rate of senescence (Figure 6.7) (Dańko, et al., 2017; Dańko, et al., 2018).

On the other hand, it has been argued that extrinsic mortality can be neglected close to *r*-edge of the *r*-R_0 continuum, where effects of extrinsic mortality will act uniformly across the population (Dańko, et al., 2018). One observation from linking the various continuums, i.e. the *r*-R_0, semelparity-iteroparity and rate of senescence continuums (Figure 1.12, 6.6B), is that senescence is likely to be earlier and amplified in more *r*-maximising populations with,

as just argued, possibly even an early selection shadow cast (Figure 6.2). This would result in extrinsic mortality having unequal effects on survival across the population, as older individuals will be more susceptible. In other words, it is likely that there will be greater age-dependence effects closer to the *r* edge of the continuum (ignoring here other possible forms of condition-dependence that are likely to be more case specific). These unequal effects in turn will further favour *r* maximisation when extrinsic mortality is increased, as costs will become more affordable (Figure 6.8).

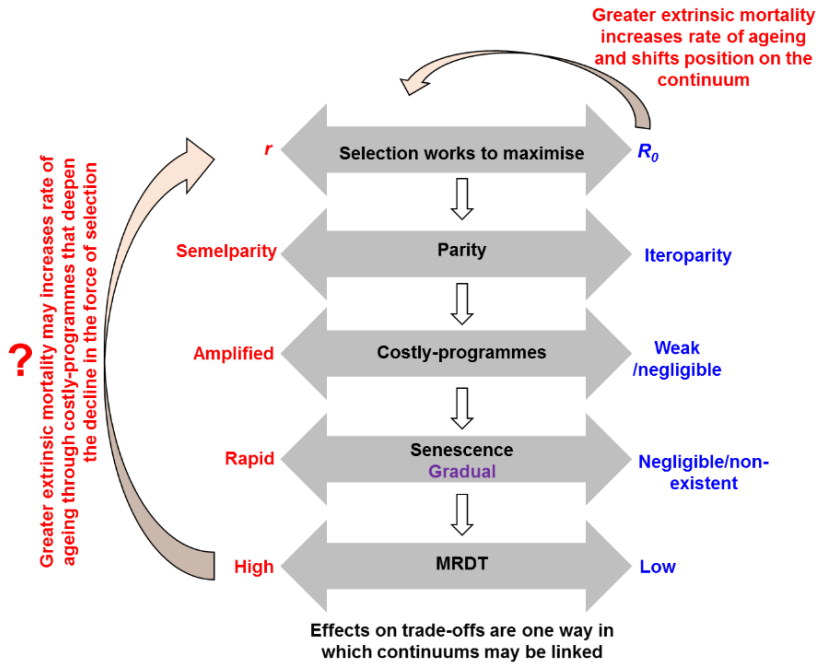

FIGURE 6.8. Links between the *r* -*R0*, semelparity-iteroparity, and rate of senescence continuums and extrinsic mortality: tentative new model. Interplay between different continuums through effects on trade-offs, primarily those that are constraint derived, i.e. costly-programmes. Increasing extrinsic mortality closer to the R_0 end of the continuum will result in more rapid senescence (i.e. push the organism closer to the *r*-end of the continuum) (Dańko, et al., 2017). Due to costly-programmes (and more shifted trade-off intercepts in general (c.f. Figure 6.5)) affecting the decline in the force of selection through deleterious costs, increasing extrinsic mortality closer to the *r* maximising end of the r-R_0 continuum arguably may also result in more rapid senescence. (c.f. Figure 1.12).

6.6 Regulated vs non-regulated mechanisms of ageing

Should a distinction be made between reproductive death and ageing (i.e. senescent death)? As argued above, programmatic mechanisms operative in reproductive death are a part of ageing, and emphasised more towards the semelparous end of the continuum. To argue that programmatic mechanisms are not a part of ageing is akin to arguing that organisms which die from IIS-, mTOR- or GH-mediated pathologies do not die from ageing either, insofar as they involve programmatic mechanisms. That being said, the reproductive death vs ageing distinction does have useful explanatory power (Gems et al., 2020). If death due to programmatic pathophysiologies is

prevented, lifespan is extended but it is not indefinite. Why is this? As argued at the start of this thesis, ageing is unlikely the result of one central underlying mechanism (Figure 1.1) (Gems., 2015). Rather, many mechanisms of ageing likely exist, with certain core mechanisms causing many pathologies of ageing such that suppression of even single pathways leads to significant lifespan extension, as is experimentally observed (Gems, 2015). Reproductive death is one such core mechanism that results in multiple pathologies. Once suppressed, e.g. via gonadectomy as in *C. elegans*, long-lived individuals die of other mechanism of ageing (Figure 1.1, 6.9). This illustrates a general rule about ageing which is that when one life-limiting pathology is removed, other pathologies become life-limiting (de Magalhães, 2012; Gems et al., 2020).

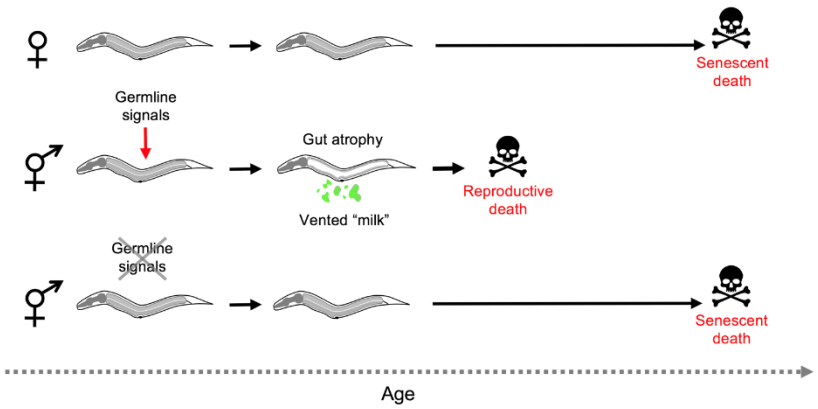

FIGURE 6.9. Ageing and death in Caenorhabditis females and hermaphrodites: simplified working model. In the absence of mating only hermaphrodites exhibit reproductive death, and this is triggered during reproductive maturation by signals from the germline. Removal of the germline by laser microsurgery blocks reproductive death, and markedly extends lifespan in hermaphrodites, removing the difference in lifespan between hermaphrodites and females. Germline ablation only modestly increases female lifespan (not depicted) (Figure 5.2). Reproduced from (Gems et al., 2020).

What limits lifespan when programmatic causes of senescence are prevented in iteroparous organisms? A new view of ageing (Gems et al., 2020), retaining one element of the reproductive death vs ageing distinction can be used to answer this. Here senescent aetiologies are divided into two classes (Gems et al., 2020). First, *regulated ageing*, which is a relatively plastic component under hormonal control (e.g. GH/IIS/mTOR and steroid hormones in animals, abscisic acid and gibberellins in plants) and largely involving hyperfunction and programmatic mechanisms (such as costly programmes and quasi-programmes). Second, *non-regulated ageing*, which is a relatively unalterable (non plastic; i.e. relatively immutable except through evolutionary change) component involving a wider range of aetiologies, including AP affecting many genes through various mechanisms such as mechanical senescence and molecular damage (Figure 6.10; c.f. 6.3).

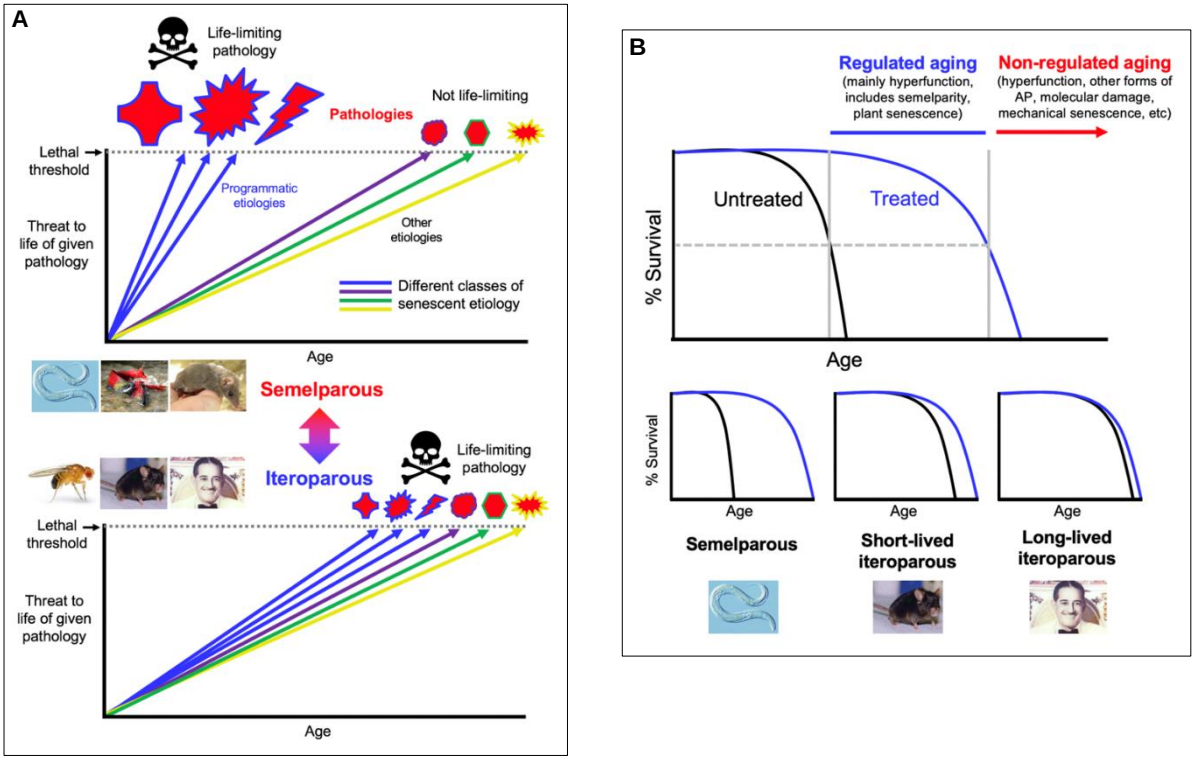

FIGURE 6.10. Ageing in semelparous and iteroparous organisms: conceptual models (A) Difference in senescent pathogenesis in semelparous and iteroparous organisms. The figure shows the degree of harmfulness of a range of pathologies with different types of aetiology (indicated by different colours). Top, reproductive death. Here exaggeration of programmatic mechanisms leads to rapid development of gross pathologies leading to death. Bottom, typical animal senescence (iteroparous species). Here many more types of aetiology contribute to life-limiting pathology, to which programmatic aetiologies contribute to some degree, and senescence is more multifactorial. Preventing programmatic pathophysiology that causes reproductive death causes very large increases in lifespan, giving a false impression that the entire ageing process has been suppressed. **(B)** Regulated and non-regulated ageing. When regulated ageing is suppressed, lifespan is limited by non-regulated ageing, which is far less plastic. Interventions with conserved effects on lifespan (e.g. reduced IIS) in iteroparous organisms have larger effects in shorter-lived species, perhaps because shorter-lived species tend to have higher levels of regulated ageing. Reproduced from (Gems et al., 2020).

6.7 Concluding remarks

Given that reproductive death occurs in *C. elegans* hermaphrodites but not humans, is *C. elegans* still a good model to study ageing more broadly? The discovery of *C. elegans* mutants with large increases in lifespan implied the existence of mechanisms controlling ageing as a whole. Combined with the notion that somatic maintenance is a powerful determinant of ageing (Kirkwood and Rose, 1991), this suggested that similar plasticity might exist in humans, affecting the entire ageing process, and providing a target for future interventions to decelerate ageing. Findings in this thesis, sadly, argue against this possibility. However, understanding *C. elegans* ageing remains an important objective on the path to understanding ageing in general, and has

been highly informative. For example, in the past a sharp distinction was made between true ageing, caused by stochastic damage accumulation, and programmed ageing as observed in Pacific salmon. In *C. elegans* stochastic damage does not appear to play a major role in ageing, whereas programme-like processes do (Raamsdonk et al., 2010, Gems and Partridge 2013), including both costly reproductive programmes and quasi-programmes (Gems et al., 2020). Both of the latter are promoted by pathways such as IIS and germline signalling, which also have effects (though weaker) on lifespan in higher animals. This suggests intertwined roles of programmes, quasi-programmed and stochastic damage in animal ageing. Therefore, arguably *C. elegans* remains an excellent model for understanding how programme-like processes lead to senescent multimorbidity.

Bibliography

Abrams, P., 1991. Life history and the relationship between food availability and foraging effort. Ecol. 72, 1242–1252.

Abrams, P. A., 1993. Does increased mortality favour the evolution of more rapid senescence? Evol. 47, 877-887.

Acerenza, L., 2016. Constraints, trade-offs and the currency of fitness. J Mol Evol. 82, 117–127.

Ackermann, M., Chao, L., Bergstrom, C. et al., 2007. On the evolutionary origin of aging. Aging Cell. 6, 235–44.

Aguilaniu, H., Fabrizio, P., Witting, M., 2016. The role of dafachronic acid signaling in development and longevity in caenorhabditis elegans: digging deeper using cutting-edge analytical chemistry. Front Endo. 7, 12.

Almagro Armenteros, J.J., Tsirigos, K.D., Sønderby, C.K., et al., 2019. SignalP 5.0 improves signal peptide predictions using deep neural networks. Nat. Biotech. 37, 420–423.

Altun, Z., Hall, D., 2009. Handbook of C. elegans anatomy. WormAtlas.

Angeles-Albores, D., Lee, R., Chan, J., et al., 2016. Tissue enrichment analysis for C. elegans genomics. BMC Bioinfo. 17, 366.

Antebi, A., 2013. Steroid regulation of C. elegans diapause, developmental timing, and longevity. Curr Top Dev Biol. 105, 181-212.

Argasinski, K., Broom, M., 2013. The nest site lottery: How selectively neutral density dependent growth suppression induces frequency dependent selection. Theo Pop. Bio. 90, 82–90.

Argasinski, K., Rudnicki, R., 2017. Nest site lottery revisited: Towards a mechanistic model of population growth suppressed by the availability of nest sites. J Theo Bio. 420, 279–289.

Arking, R., 1998. Biology of aging, 2nd ed. Sunderland, MA: Sinauer Assoc.

Armenteros, A., Tsirigos, K., Sønderby, C. et al., 2019. SignalP 5.0 improves signal peptide predictions using deep neural networks. Nat Biotechnol. 37, 420–423.

Arnold, S., 1992. Constraints on phenotypic evolution. Am Nat. 140, 85–107

Austad, S., 1997. Why We Age. New York, NY: John Wiley.

Austad, S. N., Hoffman, J., 2018. Is antagonistic pleiotropy ubiquitous in aging biology? Evol Med Public Heal. 1, 287-294.

Ayyadevara, S., Alla, R., Thaden, J.J., Shmookler Reis, R.J., 2008. Remarkable longevity and stress resistance of nematode PI3K-null mutants. Aging Cell. 7, 13-22.

Bailey, C., 1947. Titi Lucreti Cari De Rerum Natura. Volume 3, Oxford, UK: Clarendon Press.

Baird, S.E., Sutherlin, M.E., Emmons, S.W., 1992. Reproductive isolation in Rhabditidae (Nematoda: Secernentea); mechanisms that isolate six species of three genera. Evol. 46, 585-594.

Baldi, C., Cho, S., Ellis, R.E., 2009. Mutations in two independent pathways are sufficient to create hermaphroditic nematodes. Science. 326, 1002-1005.

Bansal, A., Kwon, E., Conte, D.J., Liu, H., Gilchrist, M., MacNeil, L., Tissenbaum, H., 2014. Transcriptional regulation of Caenorhabditis elegans FOXO/DAF-16 modulates lifespan. Longev. Healthspan. 3, 5.

Barclay, R., 1994. Constraints on reproduction by flying vertebrates: Energy and calcium. Americ Nat. 144, 1021-1031.

Bargmann, C.I., Avery, L., 1995. Laser killing of cells in Caenorhabditis elegans. Methods Cell Biol. 48, 225.

Bartke, A., 2001. Mutations prolong life in flies: implications for aging in mammals. Trends Endocrinol Metab. 12, 233-234.

Beltran-Sanchez, H., Finch, C., 2018. Age is just a number. Elife.

Benoit, J., Attardo, G., Baumann, A., et al., 2015. Adenotrophic viviparity in tsetse flies: potential for population control and as an insect model for lactation. Annu Rev Entomol. 60, 351–371.

Bennett, D., 1987. Immune-based erosive inflammatory joint disease of the dog: canine rheumatoid arthritis. Clinical, radiological and laboratory investigations J. Small Anim Pract. 28, 779-797.

Blagosklonny, M., 2009. TOR-driven aging: Speeding car without brakes, Cell Cycle. 8, 4055-4059.

Blagosklonny, M. V., 2006. Aging and immortality: quasi-programmed senescence and its pharmacologic inhibition. Cell Cycle. 5, 2087–2102.

Blagosklonny, M. V., 2007. Paradoxes of aging. Cell Cycle. 6, 2997-3003.

Blagosklonny, M. V., 2008. Aging: ROS or TOR. Cell Cycle. 7, 3344–3354.

Blagosklonny, M. V., 2010. Why the disposable soma theory cannot explain why women live longer and why we age. Aging. 2, 884–887.

Blagosklonny, M. V., 2012. Answering the ultimate question “What is the Proximal Cause of Aging?” Aging. 4, 861–877.

Blagosklonny, M. V., 2013. MTOR-driven quasi-programmed aging as a disposable soma theory: blind watchmaker vs. intelligent designer. Cell Cycle. 12, 1842–1847.

Bluher, M., Kahn, B., Kahn, C., 2003. Extended longevity in mice lacking the insulin receptor in adipose tissue. Science. 299, 572-574.

Borash, D. J., Rose, M. R., Mueller, L. D., 2007. Mutation accumulation affects male virility in Drosophila selected for later reproduction. Physiol Biochem Zool. 80, 461–472.

Braithwaite, R., Lee, A., 1979. A mammalian example of semelparity. Amer Nat. 113, 151–155.

Brakefield, P., Roskam, J., 2006. Exploring evolutionary constraints is a task for an integrative evolutionary biology. Am Nat. 168, 4–13.

Brenner, S., 1974. The genetics of Caenorhabditis elegans. Genet. 77, 71-94.

Butler, R. et al., 2008. New model of health promotion and disease prevention for the 21st century. BMJ. 337, a399.

Callahan, D., 1994. Aging and the goals of medicine. Hastings Cent Rep. 24, 39–41.

Canetti, D., Rendell, N.B., Gilbertson, J.A., et al., 2020. Diagnostic amyloid proteomics: experience of the UK National Amyloidosis Centre. Clin Chem Lab Med. 58, 948-957.

Caplan, A., 1992. “Is aging a disease?,” in If I were a rich man could I buy a pancreas?, ed. A. Caplan (Bloomington: Indiana University Press), 195–209.
Caplan, A., 2005. Death as an unnatural process. Why is it wrong to seek a cure for aging? EMBO Rep. 6, 72–75.
Carbone, M. A. et al., 2006. Phenotypic variation andnatural selection at Catsup, a pleiotropic quantitative trait gene in Drosphila. Curr Biol. 16, 912–91.
Caswell, H., 2007. Extrinsic mortality and the evolution of senescence. Trends Ecol Evol. 22, 173–4.
Charlesworth, B., 1994. Evolution in Age-structured Populations. Cambridge Univ. Press, Cambridge, UK.
Charlesworth, B. A., 1980. Evolution in age-structured populations. Cambridge Univ. Press, Cambridge, UK.
Charnov, E. L,. Schaffer, W.M., 1973. Life-history consequences of natural selection: Cole's result revisited. Americ Nat. 107, 791–793.
Charnov, E. L., 1982. The Theory of Sex Allocation. Princeton, NJ: Princeton University Press.
Charnov, E. L., 1993. Life History Invariants: Some Explorations of Symmetry in Evolutionary Ecology. Oxford University Press, Oxford.
Christensen, R.H.B., 2019. Regression Models for Ordinal Data [R package ordinal version 2019.12-10].
Coburn, C., Gems, D., 2013. The mysterious case of the C. elegans gut granule: death fluorescence, anthranilic acid and the kynurenine pathway. Front Genet. 4, 151.
Cole, L., 1954. The population consequences of life history phenomena. Quart Rev Bio. 29, 103–137.
Comfort, A., 1979. The Biology of Senescence, 3rd Edn Edinburgh and London: Churchill Livingstone.
Conboy, I., Rando, T., 2012. Heterochronic parabiosis for the study of the effects of aging on stem cells and their niches. Cell Cycle. 11, 2260–2267.
Cox, J., Mann, M., 2008. MaxQuant enables high peptide identification rates, individualized p.p.b.-range mass accuracies and proteome-wide protein quantification. Nat Biotech. 26, 1367-1372.
Crnokrak, P., Barrett, S. C. H., 2002. Perspective: Purging the genetic load: A review of the experimental evidence. Evol. 56, 2347–2358.
Curtsinger, J. W., Khazaeli, A. A., 2002. Lifespan, QTLs, age-specificity, and pleiotropy in Drosophila. Mech Ageing Dev. 123, 81–93.
Cutter, A.D., Morran, L.T., Phillips, P.C., 2019. Males, outcrossing, and sexual selection in Caenorhabditis nematodes. Genet. 213, 27-57.
D'Alessandro, A., Scaloni, A., Zolla, L., 2010. Human milk proteins: an interactomics and updated functional overview. J Proteome Res. 9, 3339-3373.
Dańko, M., Burger, O., Argasiński, K., et al., 2018. Extrinsic Mortality Can Shape Life-History Traits, Including Senescence. Evol Biol. 45, 395–404.
Dańko, M. J., Burger, O., Kozłowski, J., 2017. Density-dependence interacts with extrinsic mortality in shaping life histories. PLoS ONE. 12, e0186661.

de la Guardia, Y., Gilliat, A.F., Hellberg, J.,et al., 2016. Run-on of germline apoptosis promotes gonad senescence in C. elegans. Oncotarget. 7, 39082-39096.
de Luca, M., Roshina, N. V., Geiger-Thornsberry, G. L., 2003. Dopa decarboxylase (Ddc) affects variation in Drosophila longevity. Nat Genet. 34, 429–433.
de Magalhães, J., 2012. Programmatic features of aging originating in development: aging mechanisms beyond molecular damage? FASEB J. 26, 4821–4826.
de Magalhães, J., Church, G., 2005. Genomes optimize reproduction: aging as a consequence of the developmental program. Physiol. 20, 252–259.
de Magalhães, J. P., Toussaint, O., 2002. "The evolution of mammalian aging." Exp Gerontol. 37, 769-775.
Depina, A., Iser, W., Park, S., 2011. Regulation of Caenorhabditis elegans vitellogenesis by DAF-2/IIS through separable transcriptional and posttranscriptional mechanisms. BMC Physiol. 11, 11.
Dieterich, C. et al., 2008. The Pristionchus pacificus genome provides a unique perspective on nematode lifestyle and parasitism. Nat Genet. 40, 1193-1198.
Djordjevic, D., Kusumi, K., Ho, J., 2016. XGSA: A statistical method for cross-species gene set analysis. Bioinformat. 32, i620-i628.
Epstein, J., Himmelhoch, S., Gershon, D., 1972. Studies on aging in nematodes III. Electronmicroscopical studies on age-associated cellular damage. Mech Ageing Develop. 1, 245-255.
Escobar, J. S., Jarne, P., Charmantier, A., David, P., 2008. Outbreeding alleviates senescence in hermaphroditic snails as expected from the mutation-accumulation theory. Curr Biol. 18, 906–910.
Evans, D., Kapahi, P., Hsueh, W.-C., Kockel, L., 2011. TOR signaling never gets old: aging, longevity and TORC1 activity. Ageing Res Rev. 10, 225–237.
Ezcurra, M. et al., 2018. C. elegans eats its own intestine to make yolk leading to multiple senescent pathologies. Curr Biol. 28, 2544-2556.
Fabian, D., Flatt, T., 2011. The evolution of aging. Nature Education Knowledge, 3,9.
Félix, M., Braendle, C., Cutter, A. D., 2014. A streamlined system for species diagnosis in Caenorhabditis (Nematoda: Rhabditidae) with name designations for 15 distinct biological species. PLoS.
Félix, M., Duveau, F., 2012. Population dynamics and habitat sharing of natural populations of Caenorhabditis elegans and C. briggsae. BMC Biol. 10, 59.
Finch, C.E., 1994 a. Longevity, Senescence and the Genome. Chicago, IL: University of Chicago Press. pp. 206–247.
Finch, C.E., 1994 b. Latent capacities for gametogenic cycling in the semelparous invertebrate Nereis. Proc Nat Ac Sci USA. 91, p.11769.
Fisher, D., Blomberg, S., 2011. Costs of Reproduction and Terminal Investment by Females in a Semelparous Marsupial. PLoS ONE. 6, e15226.
Fisher, R. A., 1930. The Genetical Theory of Natural Selection. Oxford, UK: Clarendon Press.
Flatt, T., Partridge, L., 2018. Horizons in the evolution of aging. BMC Biol.16, 93.
Flatt, T., Promislow, D. E. L., 2007. Physiology: Still pondering an age-old question. Science. 318, 1255–1256.

Flatt, T., Schmidt, P. S., 2009. Integrating evolutionary and molecular genetics of aging. Biochimica et Biophysica Acta. 1790, 951–962.

Foukas, L., Bilanges, B., Bettedi, L., Pearce, W., Ali, K., Sancho, S., Withers, D., Vanhaesebroeck, B., 2013. Long-term p110alpha PI3K inactivation exerts a beneficial effect on metabolism. EMBO Mol. Med. 5, 563–571.

Fox, C. W. et al., 2006. The genetic architecture of life span and mortality rates: gender and species differences in inbreeding load of two seed-feeding beetles. Genet. 174, 763-773.

Fox, C. W., Stillwell, R. C., 2009. Environmental effects on sex differences in the genetic load for adult lifespan in a seed-feeding beetle. Heredity. 103, 62–72.

Frézal, L., Félix, M., 2015. C. elegans outside the Petri dish. Elife. 4, e05849.

Friedman, D., Johnson, T., 1988. A mutation in the age-1 gene in Caenorhabditis elegans lengthens life and reduces hermaphrodite fertility. Genet. 118, 75-86.

Friedman, D. J. T., 1998. Three mutants that extend both the mean and maximum life span of the nematode, Caenorhabditis elegans, define the age-1 gene. J Gerontol. 43, 102-109.

Fukuyama, F., 2002. Our Posthuman Future: The Consequences of the Biotechnology Revolution. London: Profile Books.

Gadgil, M., Solbrig, O., 1972. The concept of r- and K-selection: evidence from wild flowers and some theoretical considerations. Am Nat. 106, 14-31.

Galimov, E., Lohr, J., Gems, D., 2019. When and how can death be an adaptation? Biochem (Moscow). 84, 1433-1437.

Galimov, E.R., Gems, D., 2020a. Death happy: Adaptive death and its evolution by kin selection in organisms with colonial ecology. Philos Trans R Soc B. In press.

Galimov, E.R., Gems, D., 2020b. Shorter life and reduced fecundity can increase colony fitness in virtual C. elegans. Aging Cell 19, e13141.

Garigan, D., Hsu, A., Fraser, A., et al., 2002. Genetic analysis of tissue aging in Caenorhabditis elegans: a role for heat-shock factor and bacterial proliferation. Genet. 161, 1101-1112.

Gems, D., 2000. Longevity and ageing in parasitic and free-living nematodes. Biogeron. 1, 289-307.

Gems, D., 2014. What is an anti-aging treatment? Exp Gerontol. 58, 14–18.

Gems, D., 2015. The aging-disease false dichotomy: understanding senescence as pathology. Front Genet. 6, 212.

Gems, D., de la Guardia, Y., 2013. Alternative Perspectives on Aging in Caenorhabditis elegans: Reactive Oxygen Species or Hyperfunction? Antioxid Redox Signal. 19, 321–29.

Gems D, Kern CC (2021). Understanding aging: How does antagonistic pleiotropy work? In preparation.

Gems, D., Kern, C., Nour, J., Ezcurra, E., 2020. C. elegans hermaphrodites undergo semelparous reproductive death. Preprints, 2020110019.

Gems, D., Partridge, L., 2013. Genetics of longevity in model organisms: debates and paradigm shifts. Annu Rev Physiol. 75, 621–644.

Gems, D., Riddle, D. L., 1996. Longevity in Caenorhabditis elegans reduced by mating but not gamete production. Nature. 379, 723-725.

Gems, D., Riddle, D.L., 2000. Genetic, behavioral and environmental determinants of male longevity in Caenorhabditis elegans. Genet. 154, 1597-1610.
Gems, D., Sutton, A.J., Sundermeyer, M.L., etv al., 1998. Two pleiotropic classes of daf-2 mutation affect larval arrest, adult behavior, reproduction and longevity in Caenorhabditis elegans. Genet. 150, 129-155.
Gierlinski, M., Gastaldello, F., Cole, C., et al., 2018. Proteus: an R package for downstream analysis of MaxQuant output. BioRxiv, 416511.
Giles, J., Szklo, M., Post, W. et al., 2009. Coronary arterial calcification in rheumatoid arthritis: comparison with the Multi-Ethnic Study of Atherosclerosis. Arthritis Res Ther. 11, 36.
Golden, T., Beckman, K., Lee, A., 2007. Dramatic age-related changes in nuclear and genome copy number in the nematode Caenorhabditis elegans. Aging Cell. 6, 179–188.
Gong, Y. T. J. N., Woodruff, R. C., 2006. Effect of deleterious mutations on life span in Drosophila melanogaster. J Gerontol A Biol Sci Med Sci. 61, 1246– 1252.
Goodman, D., 1987. Retinoids and retinol-binding proteins. Harvey Lect. 81, 111–132.
Gould, S.J., Lewontin, R.C., 1979. The spandrels of San Marco and the Panglossian paradigm: a critique of the adaptationist programme. Proc R Soc Lond B. 205, 581-598.
Grandison, R., Piper, M., Partridge, L., 2009. Amino-acid imbalance explains extension of lifespan by dietary restriction in Drosophila. Nature. 462, 1061–5.
Grant, B., Hirsh, D., 1999. Receptor-mediated endocytosis in the Caenorhabditis elegans oocyte. Mol Biol Cell. 10, 4311-4326.
Green, B., Newgrain, K., Catling, P., Turner, G., 1991. Patterns of prey consumption and energy use in a small carnivorous marsupial, Antechinus stuartii. Aust J Zoolo. 39, 539–547.
Greer, E. et al., 2010. Members of the H3K4 trimethylation complex regulate lifespan in a germline-dependent manner in C. elegans. Nature. 466, 383-387.
Haldane, J. B. S., 1941. New Paths in Genetics. London: Allen and Unwin.
Hall, D. H. et al., 1999. Ultrastructural features of the adult hermaphrodite gonad of Caenorhabditis elegans: relations between the germ line and soma. Dev Biol. 21.
Hamilton, W., 1966. The moulding of senescence by natural selection. J Theor Biol. 12, 12-45.
Harman, D., 1956. Aging: a theory based on free radical and radiation chemistry. J Gerontol. 11, 298-300.
Harrison, D., Strong, R., Sharp, Z., 2009. Rapamycin fed late in life extends lifespan in genetically heterogeneous mice. Nature. 460, 392-395.
Herndon, L., Schmeissner, P., Dudaronek, J., 2002. Stochastic and genetic factors influence tissue-specific decline in ageing C. elegans. Nature. 419, 808–814.
Herndon, L., Wolkow, C., Hall, D., 2018. The aging intestine. In WormAtlas.
Hertweck, M., Göbel, C., Baumeister, R., 2004. C. elegans SGK-1 is the critical component in the Akt/PKB kinase complex to control stress response and life span. Dev Cell. 6, 577–588.

Hodgkin, J., Barnes, T.M., 1991. More is not better: brood size and population growth in a self-fertilizing nematode. Proc R Soc Lond. B 246, 19-24.
Holliday, R., 1996. The urgency of research on ageing. Bioessays. 18, 89-90.
Holzenberger, M. et al., 2003. IGF-1 receptor regulates lifespan and resistance to oxidative stress in mice. Nature. 421, 182-187.
Hood, W., Oftedal, O., Kunz, T.H., 2011. Is tissue maturation necessary for flight? Changes in body composition during postnatal development in the big brown bat. J Comp Physiol B. 181, 423-35.
Hothorn, T., Bretz, F., Westfall, P., 2008. Simultaneous inference in general parametric models. Biometrical J.: J. Math. Methods Biosci. 50, 346-363.
Hsin, H., Kenyon, C., 1999. Signals from the reproductive system regulate the lifespan of C. elegans. Nature. 399, 362-366.
Huang, D., Sherman, B., Lempicki, R., 2009. Systematic and integrative analysis of large gene lists using DAVID bioinformatics resources. Nat Protoc. 4, 44-57.
Hughes, K., 2010. Mutation and the evolution of ageing: from biometrics to system genetics. Phil Trans R Soc. B3651273–1279.
Hughes, K., Alipaz, J., Drnevich, J., Reynolds, R., 2002. A test of evolutionary theories of aging. Proc Natl Acad Sci USA. 99, 14286–14291.
Hughes, K. A., Reynolds, R. M., 2005. Evolutionary and mechanistic theories of aging. Annu Rev Entomol. 50, 421-445.
Hughes, P., 2017. Between semelparity and iteroparity: Empirical evidence for a continuum of modes of parity. Ecol Evol. 7, 8232-8261.
Innes, J., Clegg, P., 2010. Comparative rheumatology: what can be learnt from naturally occurring musculoskeletal disorders in domestic animals?, Rheumatolo. 49, 1030–1039.
Johnson, T., Wood, W., 1982. Genetic analysis of life-span in Caenorhabditis elegans. Proc Natl Acad Sci USA. 79, 6603-6607.
Jones, J., 1975. The r-K-selection continuum. Am Nat. 110, 320-323.
Jud, M. et al., 2007. Conservation of large foci formation in arrested oocytes of Caenorhabditis nematodes. Dev Genes Evol. 217, 221–226.
Kang, D., Gho, S.G., Suh, M., Kang, C., 2002. Highly sensitive and fast protein detection with coomassie brilliant blue in sodium dodecyl sulfate-polyacrylamide gel electrophoresis. Bull Korean Chem Soc. 11, 1511-1512.
Kanzaki, N., Tsai, I., Tanaka, R., et al., 2018. Biology and genome of a newly discovered sibling species of Caenorhabditis elegans. Nat Commun. 9, 3216.
Kass, L., 1983. The case for mortality. Am Scholar. 52, 173–191.
Katju, V., LaBeau, M., Lipinski, J., Bergthorsson, U., 2008. Sex change by gene conversion in a Caenorhabditis elegans fog-2 mutant. Genet. 180, 669–672.
Keller, L. F., Reid, J. M., Arcese, P., 2008. Testing evolutionary models of senescence in a natural population: age and inbreeding effects on fitness components in song sparrows. Proc R Soc B. 275, 597–604.
Kelly, J., 2008. Testing the rare-alleles model of quantitative variation by artificial selection. Genetica. 132, 187-98.
Kenyon, C., 2010. The genetics of ageing. Nature. 464, 504-512.

Kenyon, C., Chang, J., Gensch, E., et al., Tabtiang, R., 1993. A C. elegans mutant that lives twice as long as wild type. Nature. 366, 461-464.
Kimble, J., White, J., 1981. On the control of germ cell development in Caenorhabditis elegans. Dev Biol. 81, 208-219.
Kimura, K. D., Tissenbaum, H. A., Liu, Y., ., Ruvkun, G., 1997. daf-2, an insulin receptor-like gene that regulates longevity and diapause in Caenorhabditis elegans. Science. 277, 942-946.
Kiontke, K., Félix, M.-A., Ailion, M., et al., 2011. A phylogeny and molecular barcodes for Caenorhabditis, with numerous new species from rotting fruits. BMC Evol Biol. 11, 339.
Kiontke, K., Sudhaus, W., 2006. Ecology of Caenorhabditis species. WormBook. The C. elegans Research Community, WormBook.
Kirkwood, T.B.L., Rose, M.R., 1991. Evolution of senescence: late survival sacrificed for reproduction. Philos Trans R Soc. B 332, 15-24.
Kirkwood, T. B., 1977. Evolution of ageing. Nature. 270, 301–304.
Kirkwood, T., Holliday, R., 1979. The evolution of ageing and longevity. Proc R Soc Lond B Biol Sci. 205, 531-546.
Klapper, M., Ehmke, M., Palgunow, D., et al., 2011. Fluorescence-based fixative and vital staining of lipid droplets in Caenorhabditis elegans reveal fat stores using microscopy and flow cytometry approaches. J Lipid Res. 52, 1281-1293.
Klass, M., 1977. Aging in the nematode Caenorhabditis elegans: major biological and environmental factors influencing life span. Mech Ageing Develop. 6, 413-429.
Klass, M., 1983. A method for the isolation of longevity mutants in the nematode Caenorhabditis elegans and initial results. Mech Ageing Develop. 22, 279-286.
Kozłowski, J., 1993. Measuring fitness in life history studies. Trends in Ecol Evol. 8, 84–85.
Kulminski, A. et al., 2007. Accelerated accumulation of health deficits as a characteristic of aging. Exp Gerontol. 42, 963–970.
Labbadia, J., Morimoto, R., 2014. Proteostasis and longevity: when does aging really begin? Prime Rep. 6, 7.
Lande, R., Schemske, D. W., Schultz, S. T., 1994. High inbreeding depression, selective interference among loci, and the threshold selfing rate for purging recessive lethal mutations. Evol. 48, 965–978.
LeBoeuf, A., 2017. Trophallaxis. Curr Biol. 27, R1299-R1300.
Leips, J., Gilligan, P., Mackay, T. R. C., 2006. Quantitative trait loci with age-specific effects on fecundity in Drosophila melanogaster. Genet. 172, 1595–1605.
Leiser, S., Begun, A., Kaeberlein, M., 2011. HIF-1 modulates longevity and healthspan in a temperature-dependent manner. Aging Cell. 10, 318-26.
Leopold, A.C., Niedergang-Kamien, E., Janick, J., 1959. Experimental modification of plant senescence. Plant Physiol. 34, 570-573.
Lesser, K. J., Paiusi, I. C., Leips, J., 2006. Genetic variation in age-specific immune response in Drosophila melanogaster. Aging Cell. 5, 293–295.
Lewontin, R., 1947. The Genetic Basis of Evolutionary Change (Columbia Biological Series). Columbia: Columbia University Press.

Lin, K., Hsin, H., Libina, N., Kenyon, C., 2001. Regulation of the Caenorhabditis elegans longevity protein DAF-16 by insulin/IGF-1 and germline signaling. Nat Genet. 28, 139–145.
Lints, R., Hall, D., 2009. Reproductive system, somatic gonad. In WormAtlas.
Lobo, R., Davis, S., De Villiers, et al., 2014. Prevention of diseases after menopause. Climacteric. 17, 540-56.
Loeb, J., Nortrop, J., 1917. What determined the duration of life in metazoa? Proc Acad Sci USA. 5, 382–386.
Lohr, J., Galimov, E.R., Gems, D., 2019. Does senescence promote fitness in Caenorhabditis elegans by causing death? Ageing Res Rev. 50, 58-71.
Luckinbill, L., 1979. Selection and the r/K continuum in experimental populations of protozoa. Am Nat. 113, 427-437.
Ludewig, A.H., Gimond, C., Judkins, J.C., et al., 2017. Larval crowding accelerates C. elegans development and reduces lifespan. PLOS Genet. 13, e1006717.
MacArthur, R., Wilson, E., 1967. Monographs in Population Biology. vol. 1. Princeton University Press. The theory of island biogeography.
Macdonald, S., Long, A., 2007. Joint estimates of quantitative trait locus effect and frequency using synthetic recombinant populations of Drosophila melanogaster. Genet. 176, 1261-81.
Maklakov, A. and Chapman, T., 2019. Evolution of ageing as a tangle of trade-offs: energy versus function. Proc Biol Sci. 286, 20191604.
Marchal, E., Hult, E., Huang, J.,et al., 2013. Diploptera punctata as a model for studying the endocrinology of arthropod reproduction and development. Gen Comp Endocrinol. 188, 85–93.
Margie, O., Palmer, C., Chin-Sang, I., 2013. C. elegans chemotaxis assay. J Vis Exp, e50069.
Martínez, D., 1998. Mortality patterns suggest lack of senescence in hydra. Exp Gerontol. 33, 217–225.
Maures, T., Booth, L., Benayoun, B., 2014. Males shorten the life span of C. elegans hermaphrodites via secreted compounds. Science. 343, 541-544.
Maynard Smith, J., Burian, R., Kauffman, S., et al., 1985. Developmental constraints and evolution. Q Rev Biol. 60, 265–287.
Mayr, E., 1997. The objects of selection. Proc Natl Acad Sci USA. 94, 2091–2094.
McCulloch, D., 2003. Sex differences in ageing in the nematode Caenorhabditis elegans, Department of Biology. University College London, London.
McGee, M., Weber, D., Day, N., Vitelli, C., et al., 2011. Loss of intestinal nuclei and intestinal integrity in aging C. elegans. Aging Cell. 10, 699–710.
McGhee, J., 2007. The C. elegans intestine, in: Community, T.C.e.R. (Ed.), WormBook.
Medawar, P. B., 1952. An Unsolved Problem Of Biology. London: H. K. Lewis.
Migliaccio, E., Giorgio, M., Mele, S., et al., 1999. The p66 shc adaptor protein controls oxidative stress response and life span in mammals. Nature, 402, 309-313.
Mihaylova, V., Borland, C., Manjarrez, L., et al., 1999. The PTEN tumor suppressor homolog in Caenorhabditis elegans regulates longevity and dauer formation in an insulin receptor-like signaling pathway. Proc Natl Acad Sci U S A 96, 7427-7432.

Miller, R. A. et al., 2005. T cells in aging mice: genetic, developmental, and biochemical analyses. Immunol Rev. 205, 94–103.
Moorad, J. A., Promislow, D. E. L., 2008. A theory of agedependent mutation and senescence. Genet. 179, 2061–2073.
Moorad, J. A., Promislow, D. E. L., 2009. What can genetic variation tell us about the evolution of senescence? Proc R Soc B Bio Sci. 276, 2271–2278.
Munkácsy, E., Rea, S., 2014. The paradox of mitochondrial dysfunction and extended longevity. Exp Gerontol. 56, 221-233.
Murphy, C., McCarroll, S., Bargmann, C. et al., 2003. Genes that act downstream of DAF-16 to influence the lifespan of Caenorhabditis elegans. Nature. 424, 277–283.
Mylius, S. D., Diekmann, O., 1995. On evolutionarily stable life histories, optimization and the need to be specific about density dependence. Oikos. 74, 218–224.
Nelson, F., Riddle, D., 1984. Functional study of the Caenorhabditis elegans secretory-excretory system using laser microsurgery. J Exp Zool. 231, 45-56.
Nesse, R. M., 1988. Life table tests of evolutionary theories of senescence. Exp Gerontol. 23, 445-453.
Nussey, D. et al., 2013. Senescence in natural populations of animals: widespread evidence and its implications for bio-gerontology. Ageing Res Rev. 12, 214-25.
Nuzhdin, S. V., Pasyukova, E. G., Dilda, C. L., et al., 1997. Sex-specific quantitative trait loci affecting longevity in Drosophila melanogaster. Proc Nat Aca Sci. 94, 9734-9739.
Paradis, S., Ruvkun, G., 1998. Caenorhabditis elegans Akt/PKB transduces insulin receptor-like signals from AGE-1 PI3 kinase to the DAF-16 transcription factor. Genes Dev. 12, 2488–2498.
Partridge, L., 1997. Between Zeus and the Salmon: The Biodemography of Longevity. Washington (DC): National Academies Press (US); 5, Evolutionary Biology and Age-Related Mortality.
Partridge, L., Barton, N., 1993. Optimality, mutation and the evolution of ageing. Nature. 362, 305–11.
Partridge, L., Gems, D., 2002 a. Mechanisms of ageing: public or private? Nat Rev Genet. 3, 165–175.
Partridge, L., Gems, D., 2002 b. The evolution of longevity. Curr Biol. 12, 544-546.
Partridge, L., Sibly, R., 1991. Constraints in the evolution of life histories. Phil Trans R Soc Lond. 3323–13.
Peto, R., Doll, R., 1997. There is no such thing as aging. BMJ. 315, 1030-2.
Pletcher, S., 2002. Mitigating the tithonus error: genetic analysis of mortality phenotypes. Sci Aging Knowledge Environ. 18, pe14.
Podshivalova, K., Kerr, R., Kenyon, C., 2017. How a Mutation that Slows Aging Can Also Disproportionately Extend End-of-Life Decrepitude. Cell Rep. 19, 441–450.
Rea, S., 2005. Metabolism in the Caenorhabditis elegans Mit mutants. Exp Gerontol. 40, 841-849.
Riesen, M., Feyst, I., Rattanavirotkul, N., et al., 2014. MDL-1, a growth- and tumor-suppressor, slows aging and prevents germline hyperplasia and hypertrophy in C. elegans. Aging 6, 98-117.

Reynolds, R. M. et al., 2007. Age specificity of inbreeding load in Drosophila melanogaster and implications for the evolution of late life mortality plateaus. Genetics. 177, 5.
Rheumatic Clinical Slide Collection on Diseases, 1997. American College of Rheumatology.
Riddle, D. L., Blumenthal, T., et al., 1997. C. elegans II. 2nd edition. Cold Spring Harbor (NY): Cold Spring Harbor Laboratory Press. Section III, Life History And Evolution.
Robertson, O.H., 1961. Prolongation of the life span of kokanee salmon (Oncorhynchus nerka kennerlyi) by castration before the beginning of gonad development. Proc Natl Acad Sci USA. 47, 609-621.
Rockwood, K., Mitnitski, A., 2007. Frailty in relation to the accumulation of deficits. J Gerontol. 62A, 722–727.
Roff, D., Mostowy, S., Fairbairn, D., 2002. The evolution of trade-offs: testing predictions on response to selection and environmental variation. Evol. 56, 84-95.
Rose, M. R., 1991. Evolutionary Biology of Aging. New York, NY: Oxford University Press.
Santoro, N., Epperson, C., Mathews, S., 2015. Menopausal Symptoms and Their Management. Endocrinol Metab Clin North Am. 44, 497–515.
Schaffer, W., 1974. Selection for optimal life histories: The effects of age structure. Ecol. 55, 291–303.
Schulenburg, H., Félix, M., 2017. The Natural Biotic Environment of Caenorhabditis elegans. Genet. 206, 55-86.
Shaham, S., 2006. WormBook: Methods in Cell Biology, in: The C. elegans Research Community, (Ed.), WormBook.
Sharrock, W., 1983. Yolk proteins of Caenorhabditis elegans. Dev Biol. 96, 182-188.
Shaw, A. et al., 2010. Aging of the innate immune system. Curr Opin Immunol. 22, 507–513.
Shi, C., Murphy, C., 2014. Mating induces shrinking and death in Caenorhabditis mothers. Science. 343, 536-540.
Slack, C., Giannakou, M.E., Foley, A., Goss, M., et al., 2011. dFOXO-independent effects of reduced insulin-like signaling in Drosophila. Aging Cell. 10, 735-748.
Smolen, J., Aletaha, D., Barton, A., 2018. Rheumatoid arthritis. Nat Rev Dis Primers. 4, 18001.
Sornda, T., Ezcurra, M., Kern, C., et al., 2019. Production of YP170 vitellogenins promotes intestinal senescence in C. elegans. J Gerontol. A 74, 1180-1188.
Speakman, J.R., 2008. The physiological costs of reproduction in small mammals. Philos Trans R Soc B. 363, 375-398.
Spencer, C. C., Promislow, D. E., 2002. Biologists finally horn in on senescence in the wild. Sci Aging Knowledge Environ. 47, pe19.
Spieth, J., Blumenthal, T., 1985. The Caenorhabditis elegans vitellogenin gene family includes a gene encoding a distantly related protein. Mol Cell Biol. 5, 2495-2501.
Stearns, S., 1976. Life-history tactics: a review of the ideas. Q Rev Biol. 51, 3-47.
Stearns, S., 1977. The evolution of life history traits: a critique of the theory and a review of the data. Ann Rev Ecol Sys. 8, 145-171.
Stearns, S., 1992. The evolution of life histories. Oxford University Press.
Stewart, D., Phillips, P., 2002. Selection and maintenance of androdioecy in Caenorhabditis elegans. Genet. 160, 975–982.

Stevens, L., Félix, M., Beltran, T., et al, 2019. Comparative genomics of 10 new Caenorhabditis species. Evol Lett. 3, 217-236.
Suh, Y. et al., 2008. Functionally significant insulin-like growth factor I receptor mutations in centenarians. Proc Natl Acad Sci USA. 105, 3438–3442.
Swartz, S. M., Bennett, M. B., Carrier, D. R., 1992. Wing bone stresses in free flying bats and the evolution of skeletal design for flight. Nature. 359, 726-729.
Swindell, W. R., Bouzat, J. L., 2006. Inbreeding depression and male survivorship in Drosophila: implications for senescence theory. Genet. 172, 317–327.
Tank, E., Rodgers, K., Kenyon, C., 2011. Spontaneous age related neurite branching in Caenorhabditis elegans. J Neurosci. 31, 9279–9288.
Tatar, M., Kopelman, A., Epstein, D., et al., 2001. A mutant Drosophila insulin receptor homolog that extends life-span and impairs neuroendocrine function. Science. 292, 107-110.
Taylor, H. M., Gourley, R. S., Lawrence, C. E., Kaplan, R. S., 1974. Natural selection of life history attributes: An analytical approach. Theor Pop Bio. 5, 104–122.
Tesch, F.W., 1977. The Eel. Chapman and Hall, London.
Turbill, C., Ruf, T., 2010. Senescence is more important in the natural lives of long- than short-lived mammals. PLoS One. 5, e12019.
Tuttle, M. D., Ryan, M., 1981. Bat predation and the evolution of frog vocalizations in the neotropics. Science, Wash. 214, 677-678.
Van Deursen, J., 2014. The role of senescent cells in ageing. Nature. 509, 439-46.
Van Raamsdonk, J., Hekimi, S., 2009. Deletion of the mitochondrial superoxide dismutase sod-2 extends lifespan in Caenorhabditis elegans. PLoS Genet. 5, e1000361.
Van Voorhies, W., Ward, S., 1999. Genetic and environmental conditions that increase longevity in Caenorhabditis elegans decrease metabolic rate. Proc Natl Acad Sci USA. 96, 11399-403.
Verhulst, P., 1838. Notice sur la loi que la population pursuit dans son accroissement. Corresp Math Phys. 10, 113–121.
Vibert, L., Daulny, A., Jarriault, S., 2018. Wound healing, cellular regeneration and plasticity: the elegans way. Int J Dev Biol. 62, 491-505.
Vijg, J., Kennedy, B., 2016. The Essence of Aging. Gerontol. 62, 381-385.
Wahlin, B., Meedt, T., Jonsson, F., et al., 2016. Coronary Artery Calcification Is Related to Inflammation in Rheumatoid Arthritis: A Long-Term Follow-Up Study. BioMed Res Int.
Walther, D., Kasturi, P., Zheng, M., et al., 2015. Widespread proteome remodeling and aggregation in aging C. elegans. Cell. 161, 919-932.
Wang, H., Zhang, Z., Gems, D., 2018a. Monsters in the uterus: teratoma-like tumors in senescent C. elegans result from a parthenogenetic quasi-program Aging. 10, 1188-1189.
Wang, H., Zhao, Y., Ezcurra, M.,et al., 2018b. A parthenogenetic quasi-program causes teratoma-like tumors during aging in wild-type C. elegans. NPJ Aging Mech Disease. 4, 6.
Wang, M., Zhao, Y., Zhang, B., 2015. Efficient test and visualization of multi-set intersections. Sci Rep. 5, 16923.

Ward, S., Carrel, J.S., 1979. Fertilization and sperm competition in the nematode Caenorhabditis elegans. Dev Biol. 73, 304-321.
Weadick, C.J., Sommer, R.J., 2016. Mating system transitions drive life span evolution in Pristionchus nematodes. Am Nat. 187, 517-531.
Wei, J.Z., Hale, K., Carta, L., et al., 2003. Bacillus thuringiensis crystal proteins that target nematodes. Proc Natl Acad Sci. U S A 100, 2760-2765.
Weismann, A., 1882. Uber die Dauer des Lebens. Jena, Germany: Verlag von Gustav Fisher.
Weismann, A., 1885. The Continuity of the Germ-Plasm as the Foundation of a Theory of Heredity. (Translated and edited by Edward B. Poulton, Selmar Schönland,and Arthur E. Shipley in Essays upon Heredity and Kindred Biological Problems, Oxford: Clarendon Press. 1891, 163-256).
Weismann, A., 1889. Wallace AR. The action of natural selection in producing old age, decay and death [A note by Wallace written "some time between 1865 and 1870."]. In: Weismann A. Essays Upon Heredity and Kindred Biological Problems. Oxford: Clarendon Press.
Wensink, M. J., Caswell, H., Baudisch, A., 2017. The rarity of survival to old age does not drive the evolution of senescence. Evol Bio. 44, 5–10.
Williams, G., 1999. The 1999 Crafoord Prize lectures. The Tithonus error in modern gerontology. Q Rev Biol. 74, 405-15.
Williams, G. C., 1957. Pleiotropy, natural selection and the evolution of senescence. Evol. 11, 398–411.
Woeber, K.A., Ingbar, S.H., 1968. The contribution of thyroxinebinding prealbumin to the binding of thyroxine in human serum, as assessed by immunoadsorption. J Clin Invest. 47, 1710–1721.
Woodruff, G. C., Knauss, C. M., Maugel, T. K., Haag, E. S., 2014. Mating damages the cuticle of C. elegans hermaphrodites. PLoS One. 9, e104456.
Woodruff, G.C., Johnson, E., Phillips, P.C., 2018. A large close relative of C. elegans is slow-developing but not long-lived. bioRxiv dx.doi.org/10.1101/426254.
Wullschleger, S., Loewith, R., Hall, M., 2006. TOR signaling in growth and metabolism. Cell. 124, 471–484.
Wullschleger, S., Loewith, R., Hall, M. N., 2006. TOR signaling in growth and metabolism. Cell. 124, 471-84.
Zhao, Y., Gilliat, A.F., Ziehm, M., et al., 2017. Two forms of death in aging Caenorhabditis elegans. Nat Commun. 8, 15458.
Zhao, Y., Wang, H., Poole, R.J., et al., 2019. A fln-2 mutation affects lethal pathology and lifespan in C. elegans. Nat Commun. 10, 5087.
Zimniak, P., 2008. Detoxification reactions: relevance to aging. Ageing research reviews 7, 281–300.

Appendix 1: Summary statistics for lifespan analyses

Strain/ conditions		Number of deaths/ censored[1]	Mean [median] lifespan (days)	% change vs control	*p* vs. control Logrank	% change vs *vit-5* RNAi	*p* vs *vit-5* RNAi (log rank)
C. elegans L4440 (RNAi control)	C	436/58	17.4 [17]				
	1	98/2	18.4 [17]				
	2	98/2	18.4 [17]				
	3	96/4	17.3 [18]				
	4	67/27	15.5 [16]				
	5	77/23	16.6 [16]				
C. elegans *vit-5* RNAi	C	286/14	19.2 [19]	+10.4 [+12]	<0.0001		
	1	98/2	19.2 [19]	+4.4 [+12]	0.1764		
	2	97/3	19.6 [20]	+6.3 [+18]	0.0903		
	3	91/9	18.8 [19]	+8.7 [+6]	0.0414		
C. elegans *vit-6* RNAi	C	462/39	16.0 [15]	-8.2 [-12]	<0.0001	-16.9 [-21]	<0.0001
	1	97/3	16.6 [16]	-9.7 [-6]	0.1535	-13.5 [-16]	0.0110
	2	96/4	17.1 [16]	-7.1 [-6]	0.0649	-12.6 [-20]	0.0006
	3	88/12	16.4 [16]	-5.2 [-11]	0.8286	-12.8 [-16]	0.0662
	4	91/10	14.7 [15]	-5.3 [-6]	0.0446		
	5	90/10	15.0 [15]	-9.5 [-6]	<0.0001		
C. elegans *vit-5,-6* RNAi	C	295/5	20.4 [20]	+17.4 [+18]	<0.0001	+6.3 [+5]	0.0031
	1	99/1	22.0 [22]	+19.4 [+29]	<0.0001	+14.3 [+16]	0.0006
	2	98/2	19.7 [20]	+6.6 [+18]	0.0943	+0.2 [0]	0.959
	3	98/2	19.7 [20]	+13.6 [+11]	0.0014	+4.5 [+5]	0.2195

Table 1. *C. elegans* lifespan after *vit* RNAi treatment. C is combined (pooled) data from all trials, with numbers of individual trials also shown. Part of the data was collected by Thanet Sornda. Data published in (Sornda et al., 2019).

antibiotic and control 20℃		Number		Lifespan (days)		%change treatment	%change ♀ vs ♂	Logrank	Cox PH Prob>ChiSq
		death	censored	mean	median				
	C	219	27	20.14	20.00	6.08	49.92	♂T vs ♂ 0.0049	<.0001
C. elegans antibiotic	1	55	9	19.93	19.00	5.75	50.82	♂T vs ♂ 0.8516	<.0001
	2	92	5	20.92	22.00	10.34	49.12	♂T vs ♂ 0.0012	<.0001
	3	72	13	19.25	20.00	1.22	49.75	♂T vs ♂ 0.1069	0.0087
	C	216	31	18.99	19.00		6.79	♂ vs ♀ 0.0057	
C. elegans control	1	112	7	18.85	18.00		12.22	♂ vs ♀ 0.1287	
	2	54	11	18.96	19.00		2.26	♂ vs ♀ 0.1192	
	3	50	13	19.02	19.00		6.25	♂ vs ♀ 0.0491	
	C	172	111	30.20	31.00	48.92		♀T vs ♀ < 0.0001	
C. inopinata antibiotic	1	51	39	30.06	31.00	42.12		♀T vs ♀ < 0.0001	
	2	71	9	31.20	33.00	60.89		♀T vs ♀ < 0.0001	
	3	50	63	28.83	29.00	42.65		♀T vs ♀ < 0.0001	
	C	130	96	20.28	20.00			♂T vs ♀T < 0.0001	
C. inopinata control	1	41	32	21.15	24.00			♂T vs ♀T < 0.0001	
	2	43	32	19.39	19.00			♂T vs ♀T < 0.0001	
	3	46	32	20.21	21.00			♂T vs ♀T < 0.0001	
	C	264	22	22.55	23.00	15.71	24.75	♂T vs ♂ < 0.0001	<.0001
C. tropicalis antibiotic	1	95	10	24.28	23.00	23.20	18.34	♂T vs ♂ 0.0003	0.0559
	2	91	5	23.17	25.00	35.46	23.73	♂T vs ♂ < 0.0001	<.0001
	3	78	7	19.71	23.00	-5.72	36.14	♂T vs ♂ 0.4462	0.0226
	C	162	43	19.49	21.00		39.54	♂ vs ♀ < 0.0001	
C. tropicalis control	1	78	7	19.71	23.00		33.97	♂ vs ♀ < 0.0001	
	2	44	16	17.11	18.00		61.59	♂ vs ♀ < 0.0001	
	3	40	20	20.90	23.00		32.19	♂ vs ♀ < 0.0001	
	C	230	72	28.13	27.00	3.44		♀T vs ♀ 0.1461	
C. wallacei antibiotic	1	82	25	28.73	28.00	8.82		♀T vs ♀ 0.6742	
	2	78	22	28.67	29.00	3.72		♀T vs ♀ 0.7144	
	3	70	25	26.83	27.00	-2.91		♀T vs ♀ 0.0038	
	C	240	49	27.19	27.00			♂T vs ♀T < 0.0001	
C. wallacei control	1	87	10	26.40	27.00			♂T vs ♀T 0.0006	
	2	77	20	27.64	32.00			♂T vs ♀T 0.0010	
	3	76	19	27.63	32.00			♂T vs ♀T < 0.0001	
	C	273	29	23.91	25.00	20.33	20.52	♂T vs ♂ 0.0049	0.0165
C. briggsae antibiotic	1	107	9	23.44	24.00	18.53	18.92	♂T vs ♂ 0.0007	0.0056
	2	86	6	23.43	25.00	9.88	28.01	♂T vs ♂ 0.1113	0.8878
	3	80	14	25.07	25.00	28.06	16.33	♂T vs ♂ 0.0002	0.629
	C	190	34	19.87	20.00		35.53	♂ vs ♀ < 0.0001	
C. briggsae control	1	96	20	19.78	24.00		40.80	♂ vs ♀ < 0.0001	
	2	40	14	21.32	19.00		32.56	♂ vs ♀ 0.0023	
	3	54	0	19.57	19.00		21.02	♂ vs ♀ 0.0165	
	C	268	49	28.82	29.00	7.00		♀T vs ♀ 0.228	
C. nigoni antibiotic	1	116	10	27.87	28.00	0.11		♀T vs ♀ 0.5663	
	2	74	21	29.99	29.00	6.11		♀T vs ♀ 0.4993	
	3	78	18	29.16	225.00	23.10		♀T vs ♀ < 0.0001	
	C	227	46	26.93	25.00			♂T vs ♀T < 0.0001	
C. nigoni control	1	90	11	27.84	28.00			♂T vs ♀T 0.0004	
	2	76	21	28.26	28.00			♂T vs ♀T < 0.0001	
	3	61	14	23.69	23.00			♂T vs ♀T 0.0582	
	C	232	26	23.86	27.00	18.71	68.22	♂T vs ♂ < 0.0001	<.0001
P. pacificus antibiotic	1	92	7	20.93	19.00	9.12	95.85	♂T vs ♂ 0.1019	0.7063
	2	68	6	27.12	27.00	40.36	43.54	♂T vs ♂ < 0.0001	<.0001
	3	72	13	24.59	27.00	17.48	74.23	♂T vs ♂ 0.0674	0.018
	C	274	65	20.10	20.00		120.37	♂ vs ♀ < 0.0001	
P. pacificus control	1	93	12	19.18	20.00		111.05	♂ vs ♀ < 0.0001	
	2	79	41	19.32	21.00		126.81	♂ vs ♀ < 0.0001	
	3	102	12	20.93	20.00		119.88	♂ vs ♀ < 0.0001	
	C	271	46	40.14	41.00	-9.38		♀T vs ♀ 0.0111	
P. exspectatus antibiotic	1	110	11	40.99	42.00	1.26		♀T vs ♀ 0.5208	
	2	81	11	38.92	38.00	-11.17		♀T vs ♀ 0.1355	
	3	105	24	42.85	45.00	-6.91		♀T vs ♀ 0.0017	
	C	73	58	44.29	53.00			♂T vs ♀T < 0.0001	
P. exspectatus control	1	21	11	40.48	43.00			♂T vs ♀T < 0.0001	
	2	29	44	43.82	43.00			♂T vs ♀T < 0.0001	
	3	22	3	46.02	53.00			♂T vs ♀T < 0.0001	

antibiotic and control 25℃		Number		Lifespan (days)		%change ♀ vs ♂	Logrank	Cox PH Prob>ChiSq
		death	censored	mean	median			
C. elegans	C	268	66	15.57	15.00	-25.76	♂T vs ♀T < 0.0001	0.0407
	1	110	32	15.09	15.00	-33.72	♂T vs ♀T < 0.0001	
	2	83	22	15.30	15.00	-27.64	♂T vs ♀T < 0.0001	
	3	75	12	16.53	16.00	-13.35	♂T vs ♀T 0.0198	
C. inopinata	C	176	60	20.97	22.00			
	1	75	13	22.76	22.00			
	2	27	27	21.15	22.00			
	3	74	20	19.08	21.00			

UV irradiated bacteria 20℃		Number		Lifespan (days)		%change ♀ vs ♂	Logrank	Cox PH Prob>ChiSq
		death	censored	mean	median			
C. elegans	C	46	27	25.65	28.00	-35.14	♂T vs ♀T < 0.0001	<.0001
	1	24	18	27.54	27.00	-31.01	♂T vs ♀T < 0.0001	
	2	22	9	23.77	29.00	-40.75	♂T vs ♀T < 0.0001	
C. inopinata	C	43	27	39.55	35.00			
	1	30	20	39.92	38.00			
	2	13	7	40.12	33.00			

Table 2. Female sibling species are longer lived than hermaphrodites when bacterial pathogenicity is accounted for. C is combined data from all trials, and T is treatment (antibiotic carbenicillin vs control).

Mated vs control 20℃		Number		lifespan(days)		%change treatment	%change ♀ vs ♂	Logrank	Cox PH Prob>ChiSq
		death	censored	mean	median				
	C	123	24	15.01	12.00	-20.72	5.58	♂T vs ♂ 0.0004	0.8463
C. elegans mated	1	41	8	15.62	16.00	-17.14	-5.89	♂T vs ♂ 0.0017	0.5995
	2	82	16	14.91	12.00	-21.36	21.82	♂T vs ♂ 0.0194	0.1326
	C	166	18	18.93	18.00		7.19	♂ vs ♀ 0.0455	
C. elegans control	1	112	7	18.85	18.00		12.22	♂ vs ♀ 0.1287	
	2	54	11	18.96	19.00		2.26	♂ vs ♀ 0.1192	
	C	105	16	15.84	14.00	-21.91		♀T vs ♀ 0.0213	
C. inopinata mated	1	74	13	14.70	18.00	-30.51		♀T vs ♀ 0.0012	
	2	31	3	18.17	14.00	-6.31		♀T vs ♀ 0.6203	
	C	84	64	20.29	19.00			♂T vs ♀T 0.1954	
C. inopinata control	1	41	32	21.15	24.00			♂T vs ♀T 0.6610	
	2	43	32	19.39	19.00			♂T vs ♀T 0.1117	
	C	144	7	18.07	16.00	-3.54	10.64	♂T vs ♂ 0.7607	<.0001
C. tropicalis mated	1	83	7	19.31	16.00	-2.00	-2.33	♂T vs ♂ 0.8952	0.0069
	2	61	0	16.20	16.00	-4.12	13.16	♂T vs ♂ 0.9253	0.0017
	C	123	22	18.73	18.00		44.13	♂ vs ♀ < 0.0001	
C. tropicalis control	1	78	7	19.71	23.00		33.97	♂ vs ♀ < 0.0001	
	2	45	15	16.89	18.00		63.63	♂ vs ♀ < 0.0001	
	C	83	55	19.99	19.00	-25.96		♀T vs ♀ < 0.0001	
C. wallacei mated	1	30	21	18.86	21.00	-28.56		♀T vs ♀ 0.0048	
	2	53	34	18.33	19.00	-33.69		♀T vs ♀ < 0.0001	
	C	164	30	27.00	27.00			♂T vs ♀T 0.0441	
C. wallacei control	1	87	10	26.40	27.00			♂T vs ♀T 0.5469	
	2	77	20	27.64	32.00			♂T vs ♀T 0.0185	
	C	180	1	16.62	16.00	-15.34	-12.04	♂T vs ♂ < 0.0001	<.0001
C. briggsae mated	1	123	0	16.78	16.00	-15.14	-6.17	♂T vs ♂ 0.0004	<.0001
	2	57	1	16.27	16.00	-16.90	-9.41	♂T vs ♂ 0.0159	0.1378
	C	150	20	19.63	20.00		33.53	♂ vs ♀ < 0.0001	
C. briggsae control	1	96	20	19.78	20.00		40.86	♂ vs ♀ < 0.0001	
	2	54	0	19.57	19.00		21.02	♂ vs ♀ 0.0165	
	C	161	66	14.62	12.00	-44.23		♀T vs ♀ < 0.0001	
C. nigoni mated	1	43	4	15.74	14.00	-43.48		♀T vs ♀ < 0.0001	
	2	118	62	14.74	12.00	-37.80		♀T vs ♀ < 0.0001	
	C	151	26	26.22	25.00			♂T vs ♀T 0.0746	
C. nigoni control	1	90	12	27.86	28.00			♂T vs ♀T 0.1812	
	2	61	14	23.69	23.00			♂T vs ♀T 0.1748	
	C	132	50	19.68	19.00	0.99	33.85	♂T vs ♂ 0.2286	<.0001
P. pacificus mated	1	59	18	19.30	19.00	0.62	37.82	♂T vs ♂ 0.8972	0.0027
	2	73	32	19.95	19.00	3.27	30.31	♂T vs ♂ 0.5063	<.0001
	C	172	53	19.48	21.00		120.08	♂ vs ♀ < 0.0001	
P. pacificus control	1	93	12	19.18	20.00		111.05	♂ vs ♀ < 0.0001	
	2	79	41	19.32	21.00		126.81	♂ vs ♀ < 0.0001	
	C	82	32	26.34	30.00	-38.58		♀T vs ♀ < 0.0001	
P. exspectatus mated	1	39	16	26.60	30.00	-34.29		♀T vs ♀ 0.0019	
	2	43	16	26.00	30.00	-40.67		♀T vs ♀ < 0.0001	
	C	50	55	42.88	43.00			♂T vs ♀T < 0.0001	
P. exspectatus control	1	21	11	40.48	43.00			♂T vs ♀T < 0.0001	
	2	29	44	43.82	43.00			♂T vs ♀T 0.0107	

Table 3. Comparison of hermaphrodite and female sibling species lifespans following mating. C is combined data from all trials, and T is treatment (mated or unmated).

z2,3, ablation 20℃		Number		lifespan(days)		%change treatment	%change ♀ vs ♂	Logrank	Cox PH Prob>ChiSq
		death	censored	mean	median				
	C	116	22	34.71	31.00	107.89	-11.83	♂T vs ♂ < 0.0001	<.0001
C. elegans ablated	1	28	4	36.23	38.00	120.18	-15.35	♂T vs ♂ < 0.0001	<.0001
	2	43	9	34.65	31.00	103.14	-10.76	♂T vs ♂ < 0.0001	<.0001
	3	45	9	33.99	28.00	105.28	-10.34	♂T vs ♂ < 0.0001	<.0001
	C	282	18	16.70	18.00		40.63	♂ vs ♀ < 0.0001	
C. elegans control	1	100	1	16.45	18.00		40.56	♂ vs ♀ < 0.0001	
	2	96	3	17.06	18.00		40.60	♂ vs ♀ < 0.0001	
	3	86	14	16.56	15.00		41.16	♂ vs ♀ < 0.0001	
	C	110	14	30.61	32.00	30.34		♀T vs ♀ < 0.0001	
C. inopinata ablated	1	15	0	30.67	32.00	32.60		♀T vs ♀ 0.1410	
	2	45	12	30.92	30.00	28.94		♀T vs ♀ 0.0011	
	3	50	2	30.48	31.00	30.38		♀T vs ♀ < 0.0001	
	C	383	37	23.48	23.00			♂T vs ♀T 0.0003	
C. inopinata control	1	119	16	23.13	23.00			♂T vs ♀T 0.0202	
	2	119	6	23.98	23.00			♂T vs ♀T 0.0436	
	3	145	15	23.38	23.00			♂T vs ♀T 0.0242	
	C	118	20	35.21	35.00	87.21	-3.92	♂T vs ♂ < 0.0001	<.0001
C. tropicalis ablated	1	30	0	29.53	29.50	55.97	18.07	♂T vs ♂ < 0.0001	0.0027
	2	38	16	36.26	35.00	87.72	-1.61	♂T vs ♂ < 0.0001	<.0001
	3	34	20	41.94	47.00	130.90	-25.45	♂T vs ♂ < 0.0001	<.0001
	C	213	41	18.81	18.00		52.46	♂ vs ♀ < 0.0001	
C. tropicalis control	1	70	14	18.93	18.00		49.69	♂ vs ♀ < 0.0001	
	2	68	21	19.32	18.00		46.77	♂ vs ♀ < 0.0001	
	3	75	6	18.16	18.00		61.10	♂ vs ♀ < 0.0001	
	C	129	1	33.83	33.00	17.98		♀T vs ♀ < 0.0001	
C. wallacei ablated	1	31	0	34.87	36.00	23.03		♀T vs ♀ 0.0057	
	2	49	1	35.68	33.00	25.83		♀T vs ♀ 0.0002	
	3	49	0	31.27	32.00	6.86		♀T vs ♀ 0.3265	
	C	386	30	28.67	27.00			♂T vs ♀T 0.1631	
C. wallacei control	1	137	15	28.34	27.00			♂T vs ♀T 0.7572	
	2	122	12	28.35	27.00			♂T vs ♀T 0.7531	
	3	127	3	29.26	25.50			♂T vs ♀T 0.0801	
	C	110	22	30.90	32.00	80.13	8.73	♂T vs ♂ < 0.0001	<.0001
C. briggsae ablated	1	24	5	31.33	39.00	106.39	11.06	♂T vs ♂ < 0.0001	0.0001
	2	49	5	30.26	30.00	80.64	11.99	♂T vs ♂ < 0.0001	<.0001
	3	37	12	31.42	30.00	62.70	5.92	♂T vs ♂ < 0.0001	<.0001
	C	264	12	17.15	18.00		73.08	♂ vs ♀ < 0.0001	
C. briggsae control	1	88	0	15.18	15.00		92.91	♂ vs ♀ < 0.0001	
	2	82	8	16.75	18.00		70.59	♂ vs ♀ < 0.0001	
	3	94	4	19.31	18.00		61.50	♂ vs ♀ < 0.0001	
	C	101	16	33.59	34.00	13.15		♀T vs ♀ 0.0152	
C. nigoni ablated	1	12	2	34.80	37.00	18.82		♀T vs ♀ 0.1412	
	2	38	9	33.88	35.00	18.58		♀T vs ♀ 0.0140	
	3	51	5	33.28	33.00	6.70		♀T vs ♀ 0.6898	
	C	371	49	29.69	29.00			♂T vs ♀T 0.0061	
C. nigoni control	1	120	20	29.29	28.00			♂T vs ♀T 0.9253	
	2	123	12	28.57	29.00			♂T vs ♀T 0.0050	
	3	128	17	31.19	32.00			♂T vs ♀T 0.2840	
	C	138	11	40.23	41.00	64.28	20.50	♂T vs ♂ < 0.0001	<.0001
P. pacificus ablated	1	35	0	43.00	47.00	52.86	-24.98	♂T vs ♂ < 0.0001	<.0001
	2	54	6	40.49	38.00	78.34	21.82	♂T vs ♂ < 0.0001	0.0095
	3	49	5	38.21	35.00	63.55	34.00	♂T vs ♂ < 0.0001	<.0001
	C	236	83	24.49	25.00		76.91	♂ vs ♀ < 0.0001	
P. pacificus control	1	53	54	28.13	31.00		24.55	♂ vs ♀ 0.0002	
	2	90	18	22.71	23.00		86.68	♂ vs ♀ < 0.0001	
	3	93	11	23.36	23.00		122.01	♂ vs ♀ < 0.0001	
	C	169	12	48.47	50.00	11.90		♀T vs ♀ 0.0020	
P. exspectatus ablated	1	17	2	32.26	33.00	-7.93		♀T vs ♀ 0.1298	
	2	74	3	49.33	51.00	16.38		♀T vs ♀ 0.0081	
	3	78	7	51.20	59.00	-1.28		♀T vs ♀ 0.7380	
	C	367	111	43.32	41.00			♂T vs ♀T < 0.0001	
P. exspectatus control	1	125	10	35.04	35.00			♂T vs ♀T 0.0002	
	2	105	50	42.39	41.00			♂T vs ♀T < 0.0001	
	3	137	51	51.87	55.00			♂T vs ♀T < 0.0001	

Table 4. Comparison of lifespans of hermaphrodite and female sibling species following germline ablation. C is combined data from all trials, and T is treatment (z2,3 ablation vs control).

Appendix 2: Videos of yolk venting and egg laying

See videos 1 and 2 attached (on the USB memory stick placed on the inside back cover for the printed version):

Video 1. Representative video of yolk venting by d4 hermaphrodite. A pool of yolk, marked with VIT-2::GFP, is initially visible in the uterus near the vulva. There follow several very small bursts of venting and then one large burst, accompanied by uterine muscle contractions, after which the uterine yolk pool is depleted.

Video 2. Representative video of egg laying venting by d2 hermaphrodite.

Appendix 3: d4 adult-specific and L3 secretome

See excel file 1 attached (on the USB memory stick placed on the inside back cover for the printed version): Mass spectrometry raw data for proteins secreted into the surrounding medium by *C. elegans*.

Appendix 4: Enrichment of proteins with Interpro and GO terms in d4 adult-specific secretome and human milk proteome

See folder 1 attached (on the USB memory stick placed on the inside back cover for the printed version).